Proceedings of the International Conference on Innovative trends in Electronics Communication and Applications (ICIECA 15)

Association of Scientists, Developers and Faculties

Proceedings of the Third International Conference on Innovative trends in Electronics Communication and Applications – ICIECA 2015 held at IITM Research Park, India, Asia between 19th December, 2015 and 20th December 2015.

ASDF

Association of Scientists, Developers and Faculties

www.asdf.international

ISBN : 978-81-929742-6-2

International Conference on Innovative trends in Electronics Communication and Applications 2015

ICIECA 2015

International Conference on Innovative trends in Electronics Communication and Applications 2015

Volume 1

By
ASDF, Chennai, India

Financially Sponsored By
Association of Scientists, Developers and Faculties, India

Innovation and Electronics

19 – 20, December 2015
Indian Institute of Technology Madras – Research Park
Chennai, South India, Asia

Editor-in-Chief
Kokula Krishna Hari K

Editors:

Anbuoli Parthasarathy, S Purushothaman, Saikishore Elangovan

Published by

Association of Scientists, Developers and Faculties
Address: RMZ Millennia Business Park, Campus 4B, Phase II, 6th Floor, No. 143, Dr. MGR Salai, Kandanchavady, Perungudi, Chennai – 600 096, India.
Email: admin@asdf.org.in || www.asdf.org.in

International Conference on Innovative trends in Electronics Communication and Applications 2015 (ICIECA 2015)
VOLUME 1

Editor-in-Chief: **Kokula Krishna Hari K**
Editors: **Anbuoli Parthasarathy, S Purushothaman, Saikishore Elangovan**

Disclaimer:

No responsibility is assumed by the ICIECA 2015 Organizers/Publisher for any injury and/ or damage to persons or property as a matter of products liability, negligence or otherwise, or from any use or operation of any methods, products or ideas contained in the material herein. Contents, used in the papers and how it is submitted and approved by the contributors after changes in the formatting. Whilst every attempt made to ensure that all aspects of the paper are uniform in style, the ICIECA 2015 Organizers, Publisher or the Editor(s) will not be responsible whatsoever for the accuracy, correctness or representation of any statements or documents presented in the papers.

ISBN-13: 978-81-929742-6-2
ISBN-10: 81-929742-1-9

PREFACE

Welcome to the International Conference on Innovative trends in Electronics Communication and Applications – ICIECA 2015 in Indian Institute of Technology – Madras Research Park, Chennai, India, Asia on 19 – 20 December, 2015. If this is your first time to Chennai, you need to look on more objects which you could never forget in your lifetime. There is much to see and experience.

This Conference brought in forward to endeavour a greater height in the Electronics Communication and its implied applications. The present generation runs with a greater speed for communication; with many simplified protocols like Mobile 2G, 3G, 4G and grew 5G communication for voice and data stuffs. Also for the data link, it has grown from the basic terms like Dial-Up to Edge, Wi-Fi, Wi-Max and other advancements.

The innovation in the current trends of the communication systems is growing rapidly without any pause in its development. The human kind is also flexible enough in adapting to the expressive developments which implies the status of the individuals socially as well as economically. Just imagining about the era of 1960's and 2014; what a changeover in all the terms. For a message to be communicated, we have to spend a minimum of 15 days through Postal and transition. Now, it's just 15 seconds and the people love it.

We invite you to join us in this inspiring conversation.

Finally, I thank my family, friends, students and colleagues for their constant encouragement and support for making this type of conference.

-- **Kokula Krishna Hari K**
Editor-in-Chief
www.kokulakrishnaharik.in

TECHNICAL REVIEWERS

- A Amsavalli, Paavai Engineering College, Namakkal, India
- A Ayyasamy, Annamalai University, Chidambaram, India
- A C Shagar, Sethu Institute of Technology, India
- A Kavitha, Chettinad College of Engineering & Technology, Karur, India
- A Padma, Madurai Institute of Engineering and Technology, Madurai, India
- A S N Chakravarthy, JNTU Kakinada, India
- A Tamilarasi, Kongu Engineering College, Perundurai, India
- Abdelbasset Brahim, University of Granada, Spain
- Abdelnaser Omran, Universiti Utara Malaysia, Malaysia
- Abdul Aziz Hussin, Universiti Sains Malaysia, Malaysia
- Abdul Nawfar Bin Sadagatullah, Universiti Sains Malaysia, Malaysia
- Abhay Prabhakar Kulkarni, Director - IICMR
- Abhishek Shukla, U.P.T.U. Lucknow, India
- Aede Hatib Musta'amal, Universiti Teknologi Malaysia, Malaysia
- Ahmed Mohammed Kamaruddeen, Universiti Utara Malaysia, Malaysia
- Ahmed Salem, Old Dominion University, United States of America
- Ali Berkol, Baskent University & Space and Defence Technologies (SDT), Turkey
- Alphin M S, SSN College of Engineering, Chennai, India
- Alwardoss Velayutham Raviprakash, Pondicherry Engineering College, Pondicherry, India
- Anand Nayyar, KCL Institute of Management and Technology, Punjab
- Anbuchezhiyan M, Valliammai Engineering College, Chennai, India
- Ang Miin Huey, Universiti Sains Malaysia, Malaysia
- Anirban Mitra, VITAM Berhampur, Odisha, India
- Ariffin Abdul Mutalib, Universiti Utara Malaysia, Malaysia
- Arniza Ghazali, Universiti Sains Malaysia, Malaysia
- Arumugam Raman, Universiti Utara Malaysia, Malaysia
- Asha Ambhaikar, Rungta College of Engineering & Technology, Bhilai, India
- Ashish Chaurasia, RGPV, Bhopal, Madhya Pradesh
- Asrulnizam Bin Abd Manaf, Universiti Sains Malaysia, Malaysia
- Assem Abdel Hamied Mousa, EgyptAir, Cairo, Egypt
- Aziah Daud, Universiti Sains Malaysia, Malaysia
- B Paramasivan, National College of Engineering, Tirunelveli, India
- Badruddin A. Rahman, Universiti Utara Malaysia, Malaysia
- Balachandran Ruthramurthy, Multimedia University, Malaysia
- Balasubramanie Palanisamy, Professor & Head, Kongu Engineering College, India
- Brahim Abdelbasset, University of Granada, Spain
- C Poongodi, Bannari Amman Institute of Technology, Sathyamangalam, India
- Chandrasekaran Subramaniam, Professor & Dean, Anna University, India
- Choo Ling Suan, Universiti Utara Malaysia, Malaysia
- Cristian-Gyozo Haba, Technical University of Iasi, Romania
- D Deepa, Bannari Amman Institute of Technology, Sathyamangalam, India

- D Gracia Nirmala Rani, Thiagarajar College of Engineering, Madurai, Tamil Nadu
- D Sheela, Tagore Engineering College, Chennai, India
- Daniel James, Senior Researcher, United Kingdom
- David Rathnaraj Jebamani, Sri Ramakrishna Engineering College, India
- Deepali Sawai, Director - MCA, University of Pune (Savitribai Phule Pune University), India
- Dewi Nasien, Universiti Teknologi Malaysia, Malaysia
- Doug Witten, Oakland University, Rochester, United States of America
- Dzati Athiar Ramli, Universiti Sains Malaysia, Malaysia
- Fadhilah Mat Yamin, Universiti Utara Malaysia, Malaysia
- G A Sathish Kumar, Sri Venkateswara College of Engineering, India
- G Ganesan, Adikavi Nannaya University, India
- G Subbaraju, Shri Vishnu Engineering College for Women, India
- Ganesan Kanagaraj, Thiagarajar College of Engineering, Madurai, Tamil Nadu
- Geetha G, Jerusalem College of Engineering, Chennai, India
- Geetha V, Pondicherry Engineering College, Pondicherry, India
- Guobiao Yang, Tongji University, China
- Hanumantha Reddy T, RYM Engneering College, Bellary, India
- Hardeep Singh Saini, Indo Global College of Engineering, Mohali, Punjab
- Hareesh N Ramanathan, Toc H Institute of Science and Technology, India
- Hari Mohan Pandey, Amity University, Noida, India
- Helena Karsten, Abo Akademi University, Finland
- Hidayani Binti Jaafar, Universiti Malaysia Kelantan, Malaysia
- Itebeddine GHORBEL, INSERM, France
- J Baskaran, Adhiparasakthi Engineering College, Melmaruvathur, India
- J Karthikeyan, Anna University, Chennai, India
- J Sadhik Basha, International Maritime College, Oman
- Jebaraj S, Universiti Teknologi PETRONAS (UTP), Malaysia
- Jia Uddin, International Islamic University Chittagong, Bangladesh
- Jinnah Sheik Mohamed M, National College of Engineering, Tirunelveli, India
- John Augustine P, Sri Eshwar College of Engineering, Coimbatore, India
- Julie Juliewatty Mohamed, Universiti Malaysia Kelantan, Malaysia
- K Latha, Anna University, Chennai, India
- K Mohamed Bak, Ilahia School of Science and Technology, India
- K Nirmalkumar, Kongu Engineering College, Perundurai, India
- K P Kannan, Bannari Amman Institute of Technology, Sathyamangalam, India
- K Parmasivam, K S R College of Engineering, Thiruchengode, India
- K Senthilkumar, Erode Sengunthar Engineering College, Erode, India
- K Suriyan, Bharathiyar University, India
- K Thamizhmaran, Annamalai University, Chidambaram, India
- K Vijayaraja, PB College of Engineering, Chennai, India
- Kamal Imran Mohd Sharif, Universiti Utara Malaysia, Malaysia
- Kannan G R, PSNA College of Engineering and Technology, Dindigul, India
- Kathiravan S, Kalaignar Karunanidhi Institute of Technology, Coimbatore, India

- Khairul Anuar Mohammad Shah, Universiti Sains Malaysia, Malaysia
- Khurram Saleem Alimgeer, COMSATS Institute of Information Technology, Islamabad
- Kokula Krishna Hari Kunasekaran, Chief Scientist, Techno Forum Research and Development Center, India
- Konguvel Elango, Dhanalakshmi Srinivasan College of Engineering, Coimbatore
- Krishnan J, Annamalai University, Chidambaram, India
- Kumaratharan N, Sri Venkateswara College of Engineering, India
- L Ashok Kumar, PSG College of Technology, Coimbatore, India
- Laila Khedher, University of Granada, Spain
- Lakshmanan Thangavelu, SA College of Engineering, Chennai, India
- M Ayaz Ahmad, University of Tabuk, Saudi Arabia
- M Chandrasekaran, Government College of Engineering, Bargur, India
- M K Kavitha Devi, Thiagarajar College of Engineering, Madurai, Tamil Nadu
- M Karthikeyan, Knowledge Institute of Technology, India
- M Shanmugapriya, SSN College of Engineering, Chennai, India
- M Thangamani, Kongu Engineering College, India
- M Venkatachalam, RVS Technical Campus - Coimbatore, India
- M Vimalan, Thirumalai Engineering College, Kanchipuram, India
- Malathi R, Annamalai University, Chidambaram, India
- Mansoor Zoveidavianpoor, Universiti Teknologi Malaysia, Malaysia
- Manvender Kaur Chahal, Universiti Utara Malaysia, Malaysia
- Mariem Mahfoudh, MIPS, France
- Marinah Binti Othman, Universiti Sains Islam Malaysia, Malaysia
- Mathivannan Jaganathan, Universiti Utara Malaysia, Malaysia
- Md Haider Ali Biswas, Khulna University, Khulna, Bangladesh
- Md Nur Alam, Pabna university of Science & Technology, Bangladesh
- Mehdi Asadi, IAU (Islamic Azad University), Iran
- Mohamed Saber Mohamed Gad, National Research Center, Egypt
- Mohammad Ayaz Ahmad, University of Tabuk, Saudi Arabia
- Mohammed Ali Hussain, KL University, India
- Mohd Hanim Osman, Universiti Teknologi Malaysia, Malaysia
- Mohd Hashim Siti Z, Universiti Teknologi Malaysia, Malaysia
- Mohd Helmy Abd Wahab, Universiti Tun Hussein Onn, Malaysia
- Mohd Murtadha Mohamad, Universiti Teknologi Malaysia, Malaysia
- Mohd Zulkifli Bin Mohd Yunus, Universiti Teknologi Malaysia, Malaysia
- Moniruzzaman Bhuiyan, University of Northumbria, United Kingdom
- Mora Veera Madhava Rao, Osmania University, India
- Muhammad Iqbal Ahmad, Universiti Malaysia Kelantan, Malaysia
- Muhammad Javed, Cornell University, United States of America
- Mukesh Negi, TechMahindra Ltd, India
- N Rajesh Jesudoss Hynes, Mepco Schlenk Engineering College, Sivakasi, Tamilnadu, India
- N Karthikeyan, SNS College of Engineering, Coimbatore, India
- N Malmurugan, Vidhya Mandhir Institute of Technology, India

- N Meenakshi Sundaram, PSG College of Technology, Coimbatore, India
- N Senthilnathan, Kongu Engineering College, Perundurai, India
- N Shanthi, Nandha Engineering College, Erode, India
- N Suthanthira Vanitha, Knowledge Institute of Technology, India
- Nasrul Humaimi Mahmood, Universiti Teknologi Malaysia, Malaysia
- Nida Iqbal, Universiti Teknologi Malaysia, Malaysia
- Nithya Kalyani S, K S R College of Engineering, Thiruchengode, India
- Nor Muzlifah Mahyuddin, Universiti Sains Malaysia, Malaysia
- Norma Binti Alias, Universiti Teknologi Malaysia, Malaysia
- L Shanmugasundaram, K S R College of Engineering, Thiruchengode, India
- P Dhanasekaran, Erode Sengunthar Engineering College, Erode, India
- P Ganesh Kumar, K. L. N. College of Information Technology, Madurai, India
- P Kumar, K S R College of Engineering, Thiruchengode, India
- P Ramasamy, Sri Balaji Chockalingam Engineering College, India
- P Raviraj, Kalaignar Karunanidhi Institute of Technology, Coimbatore, India
- P Sengottuvelan, Bannari Amman Institute of Technology, Sathyamangalam, India
- P Shunmuga Perumal, Anna University, Chennai, India
- P Sivakumar, K S R College of Engineering, Thiruchengode, India
- P Tamizhselvan, Bharathiyar University, India
- P Thamilarasu, Paavai Engineering College, Namakkal, India
- Pasupuleti Visweswara Rao, Universiti Malaysia Kelantan, Malaysia
- Pethuru Raj, IBM Research, India
- Qais Faryadi, USIM: Universiti Sains Islam Malaysia, Malaysia
- R Ashokan, Kongunadu College of Engineering and Technology, India
- R Dhanasekaran, Syed Ammal Engineering College, Ramanathapuram, India
- R Muthukumar, Shree Venkateshwara Hi-Tech Engineering College, India
- R Nallusamy, Principal, Nandha college of Technology, Erode, India
- R Ragupathy, Annamalai University, Chidambaram, India
- R Sudhakar, Dr. Mahalingam College of Engineering and Technology, India
- R Suguna, SKR Engineering College, Chennai, India
- R Sundareswaran, SSN College of Engineering, Chennai, India
- Radzi Ismail, Universiti Sains Malaysia, Malaysia
- Raghvendra Kumar, LNCT College, Jabalpur
- Rajesh Deshmukh, Shri Shankaracharya Institute of Professional Management and Technology, Raipur
- Rathika P, V V College of Engineering, Tirunelveli, India
- Rathinam Maheswaran, Mepco Schlenk Engineering College, Sivakasi, Tamilnadu, India
- Ravindra W Gaikwad, Pravara Rural Engineering College, Loni
- Razauden Mohamed Zulkifli, Universiti Teknologi Malaysia, Malaysia
- Reza Gharoie Ahangar, University of North Texas, USA
- Roesnita Ismail, USIM: Universiti Sains Islam Malaysia, Malaysia
- Rohaizah Saad, Universiti Utara Malaysia, Malaysia
- Roselina Binti Sallehuddin, Universiti Teknologi Malaysia, Malaysia

- Ruba Soundar K, P. S. R. Engineering College, Sivakasi, India
- S Albert Alexander, Kongu Engineering College, Perundurai, India
- S Anand, V V College of Engineering, Tirunelveli, India
- S Appavu @ Balamurugan, K. L. N. College of Information Technology, Madurai, India
- S Balaji, Jain University, India
- S Balamuralitharan, SRM University, Chennai, India
- S Balamurugan, Kalaignar Karunanidhi Institute of Technology, Coimbatore, India
- S Geetha, VIT University, Chennai, India
- S Jaganathan, Dr. N. G. P. Institute of Technology, Coimbatore, India
- S Natarajan, Karpagam College of Engineering, Coimbatore, India
- S Poorani, Karpagam University, Coimbatore, India
- S Prakash, Nehru Colleges, Coimbatore, India
- S R Kumbhar, Rajarambapu Institute of Technology, India
- S Rajkumar, University College of Engineering Ariyalur, India
- S Ramesh, Vel Tech High Tech Dr.Rangarajan Dr.Sakunthala Engineering College, India
- S Selvaperumal, Syed Ammal Engineering College, Ramanathapuram, India
- S Selvi, Institute of Road and Transport Technology, India
- S Senthamarai Kannan, Kalasalingam University, India
- S Senthilkumar, Sri Shakthi Institute of Engineering and Technology, Coimbatore, India
- S Shahil Kirupavathy, Velammal Engineering College, Chennai, India
- S Vengataasalam, Kongu Engineering College, Perundurai, India
- Samuel Charles, Dhanalakshmi Srinivasan College of Engineering, Coimbatore, India
- Sangeetha R G, VIT University, Chennai, India
- Sanjay Singhal, Founder, Strategizers, India
- Sanjeevikumar Padmanaban, Ohm Technologies, India
- Saratha Sathasivam, Universiti Sains Malaysia, Malaysia
- Sarina Sulaiman, Universiti Teknologi Malaysia, Malaysia
- Sathish Kumar Nagarajan, Sri Ramakrishna Engineering College, Coimbatore, India
- Sathishbabu S, Annamalai University, Chidambaram, India
- Seddik Hassene, ENSIT, Tunisia
- Selvakumar Manickam, Universiti Sains Malaysia, Malaysia
- Shamshuritawati Sharif, Universiti Utara Malaysia, Malaysia
- Shankar S, Kongu Engineering College, Perundurai, India
- Shazida Jan Mohd Khan, Universiti Utara Malaysia, Malaysia
- Sheikh Abdul Rezan, Universiti Sains Malaysia, Malaysia
- Shilpa Bhalerao, Acropolis Institute of Technology and Research, Indore, India
- Singaravel G, K. S. R. College of Engineering, India
- Sivakumar Ramakrishnan, Universiti Sains Malaysia, Malaysia
- Smriti Agrawal, Chiatanya Bharathi Institute of Technology, Hyderabad
- Somasundaram Sankaralingam, Coimbatore Institute of Technology, India
- Subash Chandra Bose Jeganathan, Professional Group of Institutions, India
- Subramaniam Ganesan, Oakland University, Rochester, United States of America
- Suganthi Appalasamy, Universiti Malaysia Kelantan, Malaysia

- Sundar Ganesh C S, PSG College of Technology, Coimbatore, India
- Sunil Chowdhary, Amity University, Noida, India
- Sunita Daniel, Amity University, Haryana
- Suresh Sagadevan, Indian Institute of Science, Bangalore, India
- Syed Sahal Nazli Alhady, Universiti Sains Malaysia, Malaysia
- T Krishnakumar, Tagore Engineering College, Chennai, India
- T Ramayah, Universiti Sains Malaysia, Malaysia
- T Subbulakshmi, VIT University, Chennai, India
- T V P Sundararajan, Bannari Amman Institute of Technology, Sathyamangalam, India
- Tom Kolan, IBM Research, Israel
- Uma N Dulhare, Muffkham Jah College of Engineering & Technology, Hyderabad, India
- Uvaraja V C, Bannari Amman Institute of Technology, Sathyamangalam, India
- V Akila, Pondicherry Engineering College, Pondicherry, India
- V C Sathish Gandhi, University College of Engineering Nagercoil, India
- V E Nethaji Mariappan, Sathyabama University, India
- V Mohanasundaram, Vivekanandha Institute of Engineering and Technology for Women, India
- V Ramesh, Mahatma Gandhi Institute of Technology, Hyderabad
- V Sathish, Bannari Amman Institute of Technology, Sathyamangalam, India
- V Vijayakumari, Sri Krishna College of Technology, Coimbatore, India
- Vaiyapuri Govindasamy, Pondicherry Engineering College, Pondicherry, India
- Veera Jyothi Badnal, Osmania University, India
- Venkatesh MP, Annamalai University, Chidambaram, India
- Vijayalakshmi V, Pondicherry Engineering College, Pondicherry, India
- Vijayan Gurumurthy Iyer, Entrepreneurship Development Institute of India
- Vikrant Bhateja, Shri Ramswaroop Memorial Group of Professional Colleges (SRMGPC), India
- Wan Hussain Wan Ishak, Universiti Utara Malaysia, Malaysia
- Wei Ping Loh, Universiti Sains Malaysia, Malaysia
- Yaty Sulaiman, Universiti Utara Malaysia, Malaysia
- Yongan Tang, Oakland University, Rochester, United States of America
- Yousef FARHAOUI, Moulay Ismail University, Morrocco
- Yudi Fernando, Universiti Sains Malaysia, Malaysia
- Yu-N Cheah, Universiti Sains Malaysia, Malaysia
- Zahurin Samad, Universiti Sains Malaysia, Malaysia
- Zailan Siri, University of Malaya, Malaysia
- Zainuddin Bin Zakaria, Universiti Teknologi MARA, Dungun Campus, Terengganu
- Zamira Zamzuri, Universiti Kebangsaan Malaysia, Malaysia
- Zul Ariff Abdul Latiff, Universiti Malaysia Kelantan, Malaysia

Table of Content

Volume	01	ISBN	978-81-929742-6-2
Month	December	Year	2015

International Conference on Innovative Trends in Electronics Communication and Applications 2015

International Conference on Innovative Trends in Electronics Communication and Applications 2015 [ICIECA 2015]

ISBN	978-81-929742-6-2
Website	icieca.in
Received	02 – April - 2015
Article ID	ICIECA001

VOL	01
eMail	icieca@asdf.res.in
Accepted	15 - November - 2015
eAID	ICIECA.2015.001

LDPC Decoder LLR Stopping Criterion

Janak Sodha[1]
[1]Department of Physics
University of the West Indies
Cave Hill Campus, Barbados

Abstract: *The log-likelihood ratio test on a single check node within the LDPC decoder is monitored to develop a stopping criterion for the decoder that is better than previous stopping criteria, without sacrificing the BER performance. Simulation results are presented for the transmission of the rate* $\frac{1}{2}$ *(288, 576) WiMAX 802.16e LDPC code digits using binary phase shift keying (BPSK) over an AWGN channel.*

Keywords*:* LDPC codes, Stopping Criterion, Decoding Failure, Iterative Decoding

INTRODUCTION

The decoder for a *Low density parity check* (LDPC) code or *Galleger* code [1] will iterate until either a valid codeword has been found or the predefined maximum number of iterations $L_{\max}$ has been reached before stopping. For latency critical applications, the disadvantage is that an LDPC decoder requires many more iterations than a turbo decoder [2], [3], [4], [5]. At low *signal-to-noise ratios* (SNRs), $L_{\max}$ is much larger than the *average number of iterations* $\overline{L}$ required establishing a valid code word under high SNRs. If it could be established that further decoder iterations are unlikely to yield a valid code word, then the decoding latency can be reduced under low SNRs by stopping the decoder early, before $L_{\max}$ iterations. In this paper, a new stopping criterion is presented that out performs the well-known stopping criteria [6], [7], [8] with the added advantage of a much lower implementation complexity.

BACKGROUND

We shall review the iterative log-likelihood decoding algorithm for binary LDPC codes to establish the notation that will simplify the explanation of the stopping algorithm. Let $\mathbf{H}$ represent the LDPC parity check matrix of size $(M \times N)$, which can be viewed as a Tanner graph [1] with N *bit nodes* and M *check nodes*. Let

$$\mathbf{c}^T = \left[c_0, c_1, \cdots, c_n, \cdots, c_{N-1}\right]$$

of $(N \times 1)$ size represent the transmitted code word and let

Cite this article as: Janak Sodha. "LDPC Decoder LLR Stopping Criterion". *International Conference on Innovative Trends in Electronics Communication and Applications (2015)*: 01-08. Print.

$$\mathbf{r}^T = \left[r_0, r_1, \cdots, r_n, \cdots, r_{N-1}\right]$$

represent the corresponding received noisy word, where N is the length of the code word. If after l iterations, the LDPC decoder outputs a valid code word $\widehat{\mathbf{c}}^{(l)}$, then the syndrome $\mathbf{s}$ is given by

$$\mathbf{s} = \mathbf{H}\widehat{\mathbf{c}}^{(l)} = \mathbf{0}$$

where the M syndrome bits within $\mathbf{s}$ correspond to the M check nodes. Using *binary phase shift keying* (BPSK) to transmit the LDPC code digits over an *additive white gaussian noise* (AWGN) channel with a single-sided noise power spectral density N_o W/Hz, the BPSK signal points will have the amplitudes $r_n = \pm\sqrt{E_b R} + n_n$, where E_b is the energy per binary digit, $R = 1 - \frac{M}{N}$ is the code rate and n_n is a zero mean Gaussian random variable with variance $\sigma = \sqrt{\frac{N_o}{2}}$. Let N_m for $m = 0,1,...,M-1$ represent the set of non-zero binary digits on the m^{th} row of $\mathbf{H}$. Furthermore, let $\mathrm{N}_{m,n}$ for $n = 0,1,...,N-1$ represent the set of non-zero binary digits on the m^{th} row of $\mathbf{H}$ excluding n^{th} column or equivalently, the bit nodes connected to the m^{th} check node, except the n^{th} bit node on a Tanner graph. Finally, let Z_n for $n = 0,1,...,N-1$ represent the set of non-zero binary digits on the n^{th} column of $\mathbf{H}$ or equivalently, the check nodes corrected to n^{th} bit node. Let $\lambda_n^{[l]}$ denote the *log-likelihood ratio* (LLR)

$$\lambda\left(c_n \mid \mathbf{r}\right) = \log_e \frac{P\left(c_n = 1 \mid \mathbf{r}\right)}{P\left(c_n = 0 \mid \mathbf{r}\right)}$$

after the l^{th} iteration, where $l = 1,2,\cdots,L_{\max}$, so that

$$\lambda_n^{[l]} = L_c r_n + \sum_{m \in Z_n} \eta_{m,n}^{[l]}$$

where $L_c r_n$ is the *intrinsic* information [9] in which the *channel reliability*

$$L_c = 2\frac{\sqrt{E_b R}}{\sigma^2}$$

and $\eta_{m,n}^{[l]}$ is the extrinsic information on c_n according to the m^{th} check node on the l^{th} iteration of the decoder given by

$$\eta_{m,n}^{[l]} = -2\tanh^{-1}\left[\prod_{j \in \mathrm{N}_{m,n}} \tanh\left(-\frac{\left(\lambda_j^{[l-1]} - \eta_{m,j}^{[l-1]}\right)}{2}\right)\right].$$

The decoding algorithm steps are as follows:

S0 Initialization: Set $\eta_{m,n}^{[0]} = 0$ for all (m,n) with $H(m,n) = 1$

S1 Set $\lambda_n^{[1]} = L_c r_n$

S2 Set the maximum number of decoder iterations $L_{\max}$

S3 For each (m,n) with $H(m,n) = 1$, compute $\eta_{m,n}^{[l]}$

Cite this article as: Janak Sodha. "LDPC Decoder LLR Stopping Criterion". *International Conference on Innovative Trends in Electronics Communication and Applications (2015)*: 01-08. Print.

S4 For $n = 0,1,\cdots N-1,$ compute $\lambda_n^{[l]} = L_c r_n + \sum_{m \in Z_n} \eta_{m,n}^{[l]}$

S5 If $\lambda_n^{[l]} > 0,$ set $\widehat{c}_n = 1,$ otherwise set $\widehat{c}_n = 0$

S6 If $\mathbf{H}\widehat{\mathbf{c}}^{(l)} = \mathbf{0},$ stop decoding, otherwise if $l < L_{\max},$ go to S3, otherwise stop decoding.

The stopping criterion to be presented in the next section will replace step S6 and add a few more steps.

STOPPING CRITERIA FOR LDPC CODES

Typically, l will reach $L_{\max}$ iterations because the extrinsic information $\sum_{m \in M_n} \eta_{m,n}^{[l]}$ oscillates after an initial increase due to a few $\lambda_n^{[l]}$ values distributed throughout $\widehat{c}_n$ that provide overwhelming incorrect evidence in favor of either $\widehat{c}_n = 1$ or $0.$ As in [8], we shall categorize the decoding behavior in terms of $\lambda_n^{[l]}$ as either *convergence*, *stuck* or *oscillation*. In convergence, the average magnitude of the LLRs $\overline{\left|\lambda^{[l]}\right|} = \frac{1}{N}\sum_{n=0}^{N-1}\left|\lambda_n^{[l]}\right|$ increases with each iteration and a valid code word is eventually found. In the stuck case, $\overline{\left|\lambda^{[l]}\right|}$ is stuck on a particular value after a certain number of iterations and a valid code word is not found. Finally in oscillation, $\overline{\left|\lambda^{[l]}\right|}$ oscillates after an initial increase. Although rare, the decoding behavior can change from oscillation to convergence. This behavior is referred to as *slow convergence* [8]. In [6], the stopping criterion is based on monitoring the *variable node reliability* $VNR^{(l)}$ defined by $VNR^{(l)} = \sum_{n=0}^{N-1}\left|\lambda_n^{[l]}\right|,$ which is simply $\overline{\left|\lambda^{[l]}\right|}N.$ At each iteration, the decoder monitors the variation of $VNR^{(l)}$ in relation to a threshold $VNR_{off} = 4N\left(\frac{E_b}{N_o}\right)_{WR},$ where $\left(\frac{E_b}{N_o}\right)_{WR}$ is the *signal-to-noise ratio* (SNR) point near the waterfall region in the bit-error rate (BER) curve for the LDPC code, using the following steps: S1 If $VNR^{(l)} \le VNR^{(l-1)}$ for $l > 1,$ stop decoding; S2 If $VNR^{(l)} > VNR_{off},$ S1 is switched off and further iterations allowed. Thus, if $VNR^{(l)}$ does not change or is less than the previous value, then further iterations are stopped because the stuck or oscillation conditions are assumed to be true. Slow convergence is assumed if $VNR^{(l)} \ge VNR_{off}$ at which point the decoder is allowed to iterate until a valid code word is found or $l = L_{\max}.$

A similar method was adopted by Li *et. al*. [7] in which the average LLR magnitude $\overline{\left|\lambda^{[l]}\right|} = \frac{VNR^{(l)}}{N} = \frac{1}{N}\sum_{n=0}^{N-1}\left|\lambda_n^{[l]}\right|$ is computed at the end of each iteration and utilized as follows: S1 Initialize a counter to zero, set thresholds J and $P.$ Note the symbol λ in [7] has been replaced here by J to avoid confusing it with the LLR symbol $\lambda_n^{[l]}$; S2 If $\left|\frac{VNR^{(l)}}{N} - \frac{VNR^{(l-1)}}{N}\right| < J\left|\frac{VNR^{(l-1)}}{N}\right|$, increase the counter by one. Otherwise reset the counter to zero; S3 If counter reaches P or $l = L_{\max},$ stop decoding. Otherwise proceed to the next iteration. Notice the slight clever modification in comparison to [6], which monitors a factor J increase over the previous value $\overline{\left|\lambda^{[l-1]}\right|}$ over P iterations. It turns out that the optimum value for P is 2 for any LDPC code [7].

Shin *et. al*. [8] proposed a stopping criterion which outperforms the method in [6], but unfortunately, there was no mention of the Li *et. al*. method [7]. The algorithm is based on the *number of satisfied parity-check constraints* $N_{spc}^{(l)}$ given by $N_{spc}^{(l)} = M - 1^T\mathbf{H}\widehat{\mathbf{c}}^{(l)} = M - \sum_{i=0}^{M-1} s_i,$ where 1^T is the all-one column vector of length $M.$ If a valid code word is found, then the syndrome $\mathbf{s} = \mathbf{H}\widehat{\mathbf{c}}^{(l)} = \mathbf{0},$ so that $\sum_{i=0}^{M-1} s_i = 0,$ and $N_{spc}^{(l)} = M.$ Thus, $N_{spc}^{(l)}$ is simply algebraically adding up all the non-zero syndrome bits and taking the total away from the syndrome length $M.$ The stopping criterion employed is to monitor the oscillation of the variable $N_{spc}^{(l)}$ using three thresholds $\theta_d,$ $\theta_{\max}$ and θ_{spc} and a counter c_d as follows: S0 If $l = 1,$ initialize

Cite this article as: Janak Sodha. "LDPC Decoder LLR Stopping Criterion". *International Conference on Innovative Trends in Electronics Communication and Applications (2015)*: 01-08. Print.

$c_d = 0;$ S1 Wait for the test $\mathbf{H}\widehat{\mathbf{c}}^{(l)} = \mathbf{s};$ S2 Compute $N_{spc}^{(l)} = M - \sum_{i=0}^{M-1} s_i;$ S3 If $l > 1,$ compute $d_{spc}^{(l)} = N_{spc}^{(l)} - N_{spc}^{(l-1)}.$ Otherwise go to S1; S4 If $d_{spc}^{(l)} \le \theta_d,$ increase c_d by 1 $(c_d \leftarrow c_d + 1).$ Otherwise reset $c_d = 0$ and go to S1; S5 If $c_d < \theta_{\max}$, go to S1; S6 If $N_{spc}^{(l)} \le \theta_{spc},$ stop decoding. Otherwise reset $c_d = 0$ and go to S1, where c_d counts how long the small increment successively persist. If $c_d \ge \theta_{\max}$, further decoder iterations are stopped if $N_{spc}^{(l)} \le \theta_{spc}.$ If $N_{spc}^{(l)} > \theta_{spc},$ slow convergence is assumed and further iterations are allowed. Clearly this algorithm is monitoring the level of oscillation of $N_{spc}^{(l)}.$ If the oscillations are small and prolonged, further decoder iterations are stopped if the current $N_{spc}^{(l)}$ is not sufficiently large enough ($N_{spc}^{(l)} \le \theta_{spc}$) to indicate the possibility of slow convergence. The disadvantage is that three thresholds $\theta_d,$ $\theta_{\max}$ and θ_{spc} have to be optimized for a given LDPC code. More recently in [10], based once again on $N_{spc}^{(l)},$ a counter was used to only accumulate the evidence in favor of iterating the received noisy word towards a valid code word to slightly outperform the Shin *et. al.* criterion.

PROPOSED STOPPING CRITERION

Gallager [1] proved that for a sequence of K independent binary digits $a_i,$ with a probability p_i for $a_i = 1,$ the probability that the whole sequence contains an even number of binary digits 1's is given by $\left[\frac{1}{2} + \frac{1}{2}\prod_{i=0}^{K-1}(1-2p_i)\right].$ Thus, if we let $\mathrm{N}_{m,n}^{*}$ represent the bit nodes connected to the m^{th} check node, *including* the n^{th} bit node, then to a good approximation the probability $P(s_m = 0 \mid \mathbf{r})$ for the m^{th} check node syndrome is given by

$$P(s_m = 0 \mid \mathbf{r}) = \frac{1}{2} + \frac{1}{2}\prod_{n \in \mathrm{N}_{m,n}^{*}} \left(1 - 2P\left(c_n = 1 \mid \mathbf{r}\right)\right)$$

where

$$P\left(c_n = 1 \mid \mathbf{r}\right) = \frac{e^{\lambda_n^{[l]}}}{1 + e^{\lambda_n^{[l]}}}$$

because the $N_{m,n}^{*}$ bit nodes are sparsely separated. For a given SNR, if the decoder iterations will eventually lead to a valid code word, then $P(s_m = 0 \mid \mathbf{r})$ will gradually increase towards the value 1. To monitor this feature, we shall use the LLR ratio

$$\Lambda = \log_e\left(\frac{P\left(s_m = 0 \mid \mathbf{r}\right)}{1 - P\left(s_m = 0 \mid \mathbf{r}\right)}\right)$$

which will increase to a large value as $P(s_m = 0 \mid \mathbf{r})$ increases towards 1. If the decoder is unable to establish a valid code word, then Λ will be close to zero. To minimize complexity, we shall use only the single M^{th} check node to develop a stopping criterion as follows. After the first $L_{\min}$ iterations, if $\Lambda = \log_e\left(\frac{P(s_{M-1}=0|\mathbf{r})}{1-P(s_{M-1}=0|\mathbf{r})}\right)$ has reduced in comparison to its previous value, then on the next iteration, stop the decoder if the magnitude of the change is less than a step-threshold $T.$ If this change is larger than $T,$ whether it be positive or negative, this would be a good indication that the iteration process is still beneficial and the decoder should be allowed to continue iterating. Further decoder iterations are stopped if the maximum number $L_{\max}$ or until a valid code word has been found, whichever comes first. Let $\Lambda^{[l]}$ represent the current value of $\log_e\left(\frac{P(s_{M-1}=0|\mathbf{r})}{1-P(s_{M-1}=0|\mathbf{r})}\right)$ and $\Lambda^{[l-1]}$ represent its previous value. Let $L_{\min}$ represent the minimum of the decoder iterations before the stopping criterion is activated. In addition to the initialization step S0 of the decoding algorithm, an alert-flag is set to 0 and the following steps are inserted to replace step S6 of the LDPC decoding algorithm presented in section II:

Cite this article as: Janak Sodha. "LDPC Decoder LLR Stopping Criterion". *International Conference on Innovative Trends in Electronics Communication and Applications (2015)*: 01-08. Print.

S6 If $\mathbf{H}\widehat{\mathbf{c}}^{(l)} = \mathbf{0}$ stop decoding, otherwise continue to the next step
S7 If alert-flag = 1, then execute S8, otherwise skip to S9
S8 If $\left|\Lambda^{[l]} - \Lambda^{[l-1]}\right| < T,$ then stop decoding, otherwise set alert-flag = 0
S9 If alert-flag = 0 **and** $\left(\Lambda^{[l]} < \Lambda^{[l-1]}\right)$ **and** $\left(l > L_{\min}\right)$ then set alert-flag = 1

S10 **If** $\left(l < L_{\max}\right)$, **go to S3, otherwise stop decoding.**

WIMAX 802.16E LDPC CODE

The WiMAX 802.16e LDPC code is formed from the expansion of a model matrix H_{bm} of size $\left(m_b \times n_b\right)$, where $n_b = 24$ and $m_b = (1-R)24,$ where R is the code rate. The size of the parity check $\mathbf{H}$ depends on the expansion factor q, with the codeword length $N = qn_b$ and the number of parity checks $M = qm_b$. The values of q range from 24 to 96 in increments of 4 and therefore, the smallest code is of length 576 bits and the largest is 2304 bits. The first $\left(n_b - m_b\right)$ columns represent the systematic bits, with the remaining m_b columns representing the parity bits. Each entry $p(i,j)$ of the base matrix H_{bm} is either a $\left(q \times q\right)$ all zero matrix or a $\left(q \times q\right)$ permuted identity matrix. If the entry is blank or less than zero, it is expanded into the all zero matrix. Otherwise the value represents the circular right shift size of the identity matrix. The base model matrix for rate $\frac{1}{2}$ codes in the WiMAX 802.16e standard is shown in Fig. 1. The shift sizes listed are for the largest code length (N = 2304). For shorter length rate $\frac{1}{2}$ codes, the shift size $s(f,i,j)$ is scaled depending on the expansion factor q_f as follows

$$s(f,i,j) = \left\lfloor \frac{p(i,j) \times q_f}{q_{\max}} \right\rfloor$$

where $\lfloor x \rfloor$ denotes the flooring function applied to x which gives the nearest integer to $-\infty$, $q_{\max}$ is the maximum expansion value of 96 and q_f is one of the 19 expansion values ranging from 24 to 96. For example, the shift size of entry (4,1), which is equal to 61, using an expansion factor of 24 gives $\left\lfloor \frac{61 \times 24}{96} \right\rfloor$, equates to 15. The resulting permutation matrix is shown in Fig. 2. When circularly shifting the identity matrix to the right, the 1 that reaches the last column is brought back to the first column of the same row. This process continues for the total number of shifts. As the bottom row of the identity matrix has a 1 in its last column, shifting it 15 times would result in this 1 being placed at column 15 of that row as shown in Fig. 2. The process of determining the shift size and applying it to the identity matrix is repeated for all nonnegative entries in Fig 1.

-1	94	73	-1	-1	-1	-1	-1	55	83	-1	-1	7	0	-1	-1	-1	-1	-1	-1	-1	-1	-1	-1
-1	27	-1	-1	-1	22	79	9	-1	-1	-1	12	-1	0	0	-1	-1	-1	-1	-1	-1	-1	-1	-1
-1	-1	-1	24	22	81	-1	33	-1	-1	-1	0	-1	-1	0	0	-1	-1	-1	-1	-1	-1	-1	-1
61	-1	47	-1	-1	-1	-1	-1	65	25	-1	-1	-1	-1	-1	0	0	-1	-1	-1	-1	-1	-1	-1
-1	-1	39	-1	-1	-1	84	-1	-1	41	72	-1	-1	-1	-1	-1	0	0	-1	-1	-1	-1	-1	-1
-1	-1	-1	-1	46	40	-1	82	-1	-1	-1	79	0	-1	-1	-1	-1	0	0	-1	-1	-1	-1	-1
-1	-1	95	53	-1	-1	-1	-1	-1	14	18	-1	-1	-1	-1	-1	-1	-1	0	0	-1	-1	-1	-1
-1	11	73	-1	-1	-1	2	-1	-1	47	-1	-1	-1	-1	-1	-1	-1	-1	-1	0	0	-1	-1	-1
12	-1	-1	-1	83	24	-1	43	-1	-1	-1	51	-1	-1	-1	-1	-1	-1	-1	-1	0	0	-1	-1
-1	-1	-1	-1	-1	94	-1	59	-1	-1	70	72	-1	-1	-1	-1	-1	-1	-1	-1	-1	0	0	-1
-1	-1	7	65	-1	-1	-1	-1	39	49	-1	-1	-1	-1	-1	-1	-1	-1	-1	-1	-1	-1	0	0
43	-1	-1	-1	-1	66	-1	41	-1	-1	-1	26	7	-1	-1	-1	-1	-1	-1	-1	-1	-1	-1	0

Fig. 1 The WiMAX 802.16e base model matrix

Cite this article as: Janak Sodha. "LDPC Decoder LLR Stopping Criterion". *International Conference on Innovative Trends in Electronics Communication and Applications (2015)*: 01-08. Print.

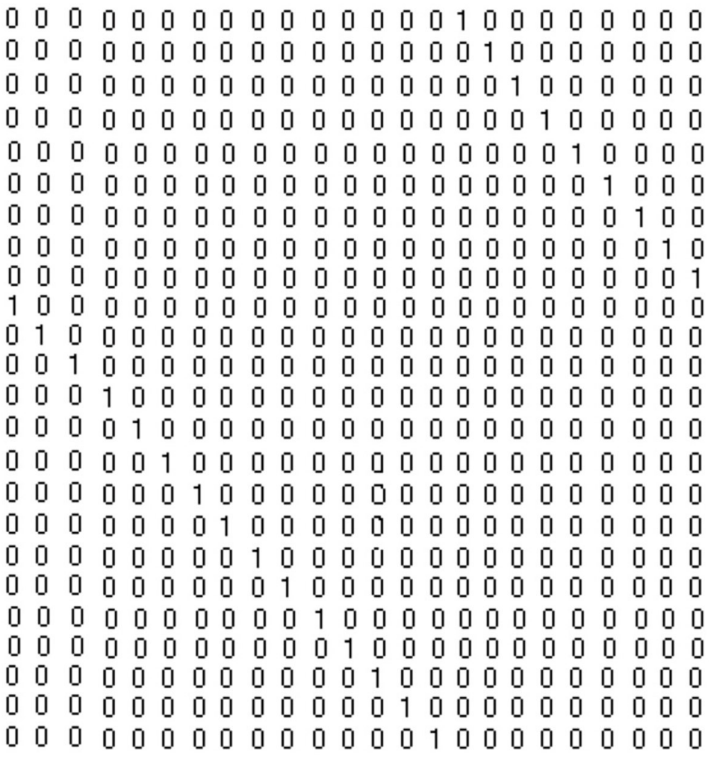

Fig. 2 Permutation matrix formed by circularly right shifting the identity matrix by 15

SIMULATION RESULTS

Using BPSK over an AWGN to transfer the WiMAX [10], 802.16e [IEEE] rate $\frac{1}{2}$ (288, 576) LDPC code digits, simulation results are presented in Figs. 3 and 4 showing the dependence of the *probability of an information binary digit error* P_e and $\overline{L}$ on the step-threshold T over a range of channel SNRs (dB).

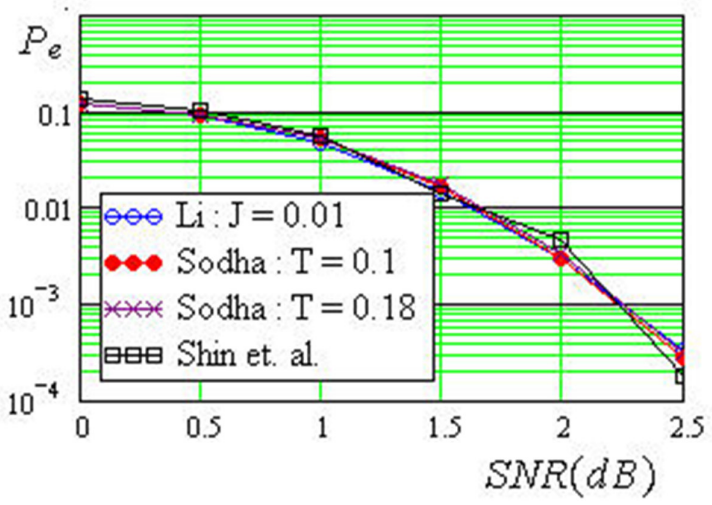

Fig. 3 LDPC decoder performance

Cite this article as: Janak Sodha. "LDPC Decoder LLR Stopping Criterion". *International Conference on Innovative Trends in Electronics Communication and Applications (2015)*: 01-08. Print.

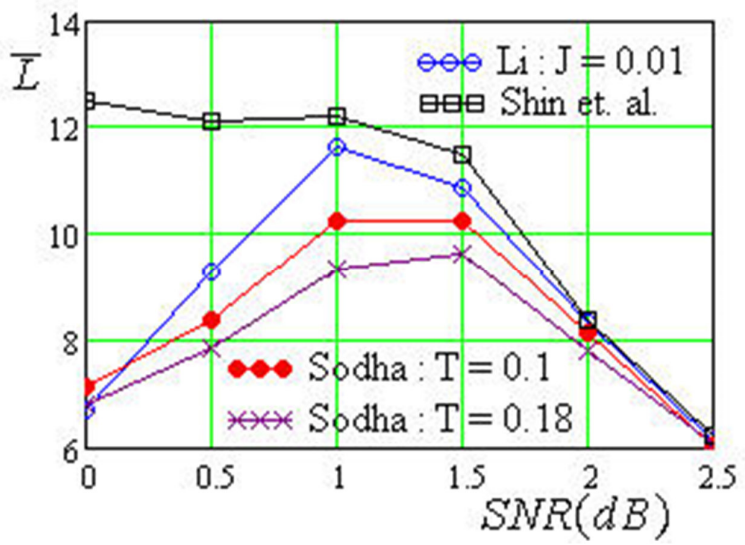

Fig. 4 Average number of iterations

The proposed criterion is compared with previous criteria in these figures ensuring in each case that a given stopping criterion should not significantly impact P_e for a given SNR. The Shin-curve corresponds to θ_d = 8, $\theta_{\max}$ = 6 and θ_{spc} = 260 and the Li-curve corresponds to $P = 2$ and $J = 0.01$. In [7], $J = 0.001$ was recommended in general, but the curve for $J = 0.01$ was selected because the corresponding $\bar{L}$ performance is better. Also, extensive simulations were undertaken to verify as stated in [7] that $P = 2$ is the optimum threshold for any LDPC code. These results have not been shown for brevity. As expected, the stopping criteria curves merge with the $L_{\max} = 15$ (no stopping criteria) curve at high SNRs because of fast convergence. Notice how the proposed stopping criterion outperforms Li and Shin *et. al.*'s algorithm at low SNRs using only a single check node syndrome probability that is calculated using only those bit nodes connected to M^{th} check node. For T larger than 0.18, there is a noticeable increase in P_e that is accompanied with a further reduction in $\bar{L}$. Taking a closer look at the level of complexity involved, specifically for the WiMAX 802.16e rate $\frac{1}{2}$ ($M = 288, N = 576$) LDPC code, the index n of the bit nodes ranges from $n = 0,1,\cdots,575$ and m ranges from $m = 0,1,\cdots,287$. The set of bit nodes connected to the 288^{th} check node are

$$\mathbf{N}^{*}_{287,n} = \{9,135,177,269,288,575\}$$

Given the separation of these bits nodes, the assumption that the probabilities $P(c_n = 1 \mid \mathbf{r})$ at these six nodes are independent is a good approximation to determine

$$P(s_{287} = 0 \mid \mathbf{r}) = \frac{1}{2} + \frac{1}{2} \prod_{n \in \mathbf{N}^{*}_{287,n}} \left(1 - 2 \frac{e^{\lambda_n^{[l]}}}{1 + e^{\lambda_n^{[l]}}} \right)$$

which in turn is used to calculate

$$\Lambda^{[l]} = \log_e \left(\frac{P(s_{287} = 0 \mid \mathbf{r})}{1 - P(s_{287} = 0 \mid \mathbf{r})} \right)$$

at the l^{th} iteration.

Cite this article as: Janak Sodha. "LDPC Decoder LLR Stopping Criterion". *International Conference on Innovative Trends in Electronics Communication and Applications (2015)*: 01-08. Print.

CONCLUSIONS

Using the short-length WiMax 802.16e rate $\frac{1}{2}$ (288, 576) LDPC code, it was shown that the stopping criterion proposed outperforms all the previous algorithms. Specifically, the average number of decoder iterations $\overline{L}$ can be reduced below 10 at the low SNR of 0 dB, instead of the standard 15 required over low SNRs. This can be further improved by increasing the value of the step-threshold T for the penalty of a slight increase in P_e. The stopping criterion proposed reduces the time taken to decode, with a lower complexity than previous methods, to create a latency efficient LDPC decoder.

REFERENCES

[1] R. G. Gallager, Low density parity check codes, *IRE Trans. Information Theory* (8) (1962) 21-28.
[2] C. Berrou and A. Glavieux, Near Optimum Error Correcting Coding and Decoding: Turbo-codes, *IEEE Trans. Commun.* 44 (10) (1996) 1261-1271.
[3] D. J. MacKay and R. M. Neal, Near-Shannon-limit performance of low-density parity-check codes, *Electron. Lett.* 33 (6) (1997) 457-458.
[4] T. J. Richardson, A. Shokrollahi and R. Urbanke, Design of capacity-approaching low-density parity-check codes, *IEEE Trans. Inform. Theory* 47 (2001) 619-637.
[5] J. Sodha and A. Als, Shape nature of error-control codes, *Elsevier Signal Processing Journal* 83 (2003) 1457-1465.
[6] F. Kienle and N. Wehn, Low complexity stopping criterion for LDPC code decoders, Proc. IEEE VTC 2005-Spring, Stockholm, Sweden, June 2005, pp. 606--609.
[7] J. Li, X. You and J. Li (Tiffany), Early Stopping for LDPC Decoding: Convergence of Mean Magnitude (CMM), *IEEE Commun. Letters*, 10 (9) (2006) 667-669.
[8] D. Shin, K. Heo, S. Oh and J. Ha, A Stopping Criterion for Low-Density Parity-Check Codes, *Proc. IEEE VTC2007-Spring*, Dublin, Ireland, April 2007, pp. 1529--1533.
[9] T. K. Moon, Error Correction Coding: Mathematical Methods and Algorithms, John Wiley, NJ, 2005, Chapter 15, pp. 649-652.
[10] IEEE 802.16e. Air interface for fixed and mobile broadband wireless access systems. IEEE Std 802.16e-2005.

Cite this article as: Janak Sodha. "LDPC Decoder LLR Stopping Criterion". *International Conference on Innovative Trends in Electronics Communication and Applications (2015)*: 01-08. Print.

International Conference on Innovative Trends in Electronics Communication and Applications 2015 [ICIECA 2015]

ISBN	978-81-929742-6-2	**VOL**	01
Website	icieca.in	**eMail**	icieca@asdf.res.in
Received	02 - April - 2015	**Accepted**	15 - November - 2015
Article ID	ICIECA002	**eAID**	ICIECA.2015.002

RF Based Online Food Quality Analyser

Shashwat Godhani[1], Revathi S[1]
[1]VIT, Vellore, Tamilnadu, India

Abstract: *Quality of food is determined in terms of food texture, taste and appearance but moisture content (MC) of food is a determination factor of quality & stability of the processed food. Determination of MC in the food product is important economically to big food industries as MC in different food products is measured at various stages of processing and storage. Many techniques have been developed to measure the MC of different food products. Impedance spectroscopy has several advantages over conventional moisture measurement methods and can be used for online moisture measurement. This paper presents the impedance spectroscopy to determine MC of grain samples and reviews the importance of Auto Balancing Bridge (ABB) Circuitry in impedance measurement for moisture analysis. Furthermore, wireless module is also been incorporated for online assessment of MC.*

Keywords*:* Impedance spectroscopy, Auto balancing bridge method, moisture content, food quality

INTRODUCTION

The Food and Agriculture Organization of the United Nations (FAO) gauges that 32 percent of all food delivered on the planet was lost or squandered in 2009. This evaluation is taking into account weight. At the point when changed over into calories, worldwide food misfortune and waste adds up to pretty nearly 24 percent of all nourishment delivered. Basically, one out of each four food calories proposed for individuals is not consumed by them.

Food loss and waste have many negative economic and environmental impacts. Economically, they represent a wasted investment that can reduce farmer's incomes and increase consumer's expenses. Environmentally, food loss and waste inflict a host of impacts, including unnecessary greenhouse gas emissions and inefficiently used water and land, which in turn can lead to diminished natural eco systems and the services they provide.

Quality of the food is determined in terms of food texture, taste and appearance but moisture content of the food is the prime determination factor of quality & stability of the processed food. Moisture content of the food material is important to consider whether the food is suitable before its consumption because moisture content affects the physical and chemical aspect of food which relates with the freshness and the stability for the storage of food for a long period of time. It is vital in deciding the best possible time for harvest and the potential for safe storage. It is also an important factor in determining the market price, because the dry matter of grain has more value than the water it contains and because costs of drying for safe storage must be taken into account. In the processing of grain for flour, other food products, and animal feeds, moisture content of the materials is important information for efficient processing, achieving desired behavior of the materials, and in obtaining high-quality products.

Cite this article as: Shashwat Godhani, Revathi S. "RF Based Online Food Quality Analyser". *International Conference on Innovative Trends in Electronics Communication and Applications (2015)*: 09-19. Print.

Standard methods for determining moisture in grain require oven drying for specific time periods at specified temperatures by prescribed methods. Because such methods are tedious, time consuming, and expensive, they are not suitable for general use in the grain trade, and hence other rapid testing methods have been developed. Most of the modern practical grain moisture testers work on the principle of sensing electrical characteristics of the grain, which are highly correlated with moisture content.

As in [1] the author presented a portable electronic instrument that measures the complex impedance of a parallel plate capacitor with a sample of peanut kernels between its plates. The author used the measured values in empirical equation to estimate the moisture content of the sample which were in good agreement with the values obtained through the standard air oven method. For a similar purpose an impedance analyzer has also been designed [2] that too determines the moisture content in peanuts. These values obtained by the presented design in [2] were also in agreement with the standard air oven method. Similar techniques are presented in [3] where the author presents a low cost instrument to measure the impedance and phase angle along with a parallel plate capacitance system to determine the moisture content in yellow corn. This impedance spectroscopy is highly used in real time applications in measuring moisture content in various packaged food products. Like in cookie dough as in [4] where the author conducted experiments with concentric ring dielectric sensor in frequency range from 10 Hz to 10 KHz. The author calibrated the system with a linear model in which the dependence of capacitance and moisture content is determined. These methods as presented in [2] and [3] are non-destructive methods that provide rapid results and have considerable applications both in drying and storage processes of corn and grain and peanuts products.

Impedance spectroscopy also finds application in paper industry. The fringing field impedance spectroscopy is used in estimating the moisture content in paper pulp. This technique is able to measure moisture concentration in paper pulp at levels as high as 96%. The fringing field impedance method proposed in [6] uses single sided measurements and offers high sensitivity and unlike other methods doesn't require special operating conditions. The problem with all the reported research is that MC of samples highly influence by density, shape of the kernels and air gap between the capacitor plates. This problem can be solved by multi frequency approach. The multi frequency model of impedance spectroscopy is developed for moisture content measurement. This paper presents significance of ABB circuitry in overall design.

METHODOLOGY

Basic Principle

The basic principle behind the impedance spectroscopy is that the dielectric constant of the food sample varies with the moisture content present in it. This principle holds good especially at the lower Radio Frequencies (RF). Hence the variation of the dielectric constant at these frequencies is measured using a portable impedance analyzer and a predictive equation is generated from which the MC of the sample is calculated effectively. Here, we are using ABB for impedance measurement. The ABB method is commonly used in modern LF impedance measurement instruments. Its operational frequency range has been extended up to 110 MHz [10]. The comparison of ABB with other methods is shown in Figure 1[11].

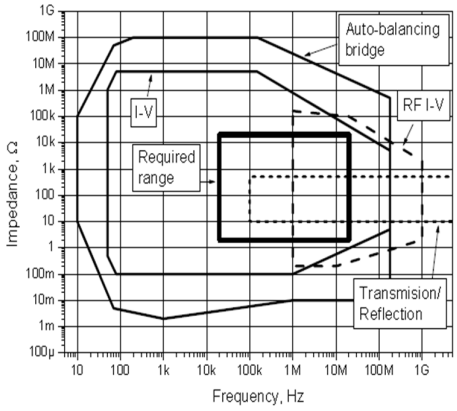

Fig 1. Impedance Measurement Method Characterization

Cite this article as: Shashwat Godhani, Revathi S. "RF Based Online Food Quality Analyser". *International Conference on Innovative Trends in Electronics Communication and Applications (2015)*: 09-19. Print.

Impedance Spectroscopy

Impedance spectroscopy measures dielectric properties of a medium as a function of frequency. The increase in the dielectric constant with MC is found to be more pronounced at the lower frequencies. Hence the variation of the dielectric constant at these frequencies is a useful parameter in estimating the MC. The capacitance of a material is found at two different frequencies. The difference between the two measured capacitances gives a good estimate of the MC, but it gets highly influenced by the size and shape of the sample. Hence two other electrical parameters, which are the dissipation factor D and phase angle θ, are also measured at the two frequencies. Finally combining the values of C, θ, and D at the two frequencies, a predictive equation is generated from which the density independent MC of the sample is calculated effectively. ABB circuitary is crucial in this setup due to high frequency limitation of operational amplifier.

ABB Method

The ABB employs the inverting topology operational amplifier. Basically, in order to measure the complex impedance of the DUT it is necessary to measure the voltage of the test signal applied to the DUT and the current that flows through it. Accordingly, the complex impedance of the DUT can be measured with a measurement circuit consisting of a signal source, a voltmeter, and an ammeter as shown in Figure 2(a). The voltmeter and ammeter measure the vectors (magnitude and phase angle) of the signal voltage and current, respectively.

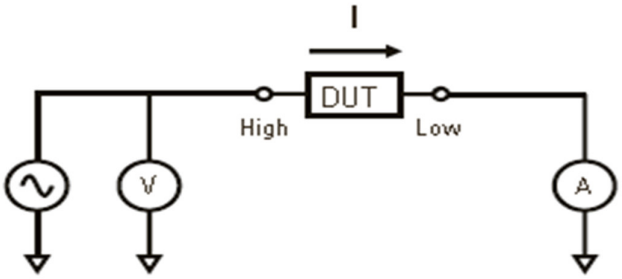

Fig 2(a). The simplest model for impedance measurement

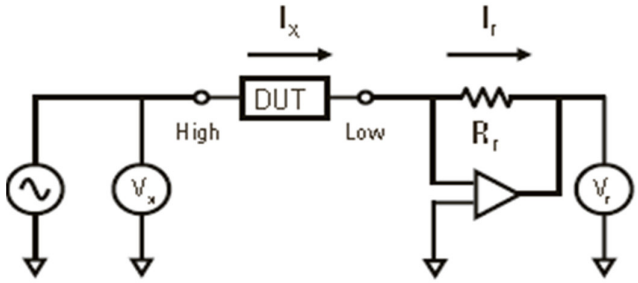

Fig 2(b). Impedance measurement using operational amplifier

The test signal current (Ix) flows through the DUT and also flows into the I-V converter. The operational amplifier of the I-V converter makes the same current as Ix flow through the resistor (Rr) on the negative feedback loop. Since the feedback current (Ir) is equal to the input current (Ix) flows through the Rr and the potential at the Low terminal is automatically driven to zero volts. Thus, it is called virtual ground. The I-V converter output voltage (Vr) is represented by the following equation:

$$V_r = I_r.R_r = I_x.R_r \qquad (2\text{-}1)$$

Ix is determined by the impedance (Zx) of the DUT and the voltage Vx across the DUT as follows:

$$I_x = \frac{V_x}{Z_x} \qquad (2\text{-}2)$$

From the equations 2-1 and 2-2, the equation for impedance (Zx) of the DUT is derived as follows:

Cite this article as: Shashwat Godhani, Revathi S. "RF Based Online Food Quality Analyser". *International Conference on Innovative Trends in Electronics Communication and Applications (2015)*: 09-19. Print.

$$Z_x = \frac{V_x}{I_x} = R_r \cdot \frac{V_x}{Z_x} \qquad (2\text{-}3)$$

The vector voltages Vx and Vr are measured with the vector voltmeters as shown in Figure 2(b).Since the value of Rr is known, the complex impedance Zx of the DUT can be calculated by using equation 2-3. The Rr is called the range resistor and is the key circuit element, which determines the impedance measurement range. The Rr value is selected from several range resistors depending on the Zx of the DUT. The operational amplifier also plays significant role in ABB. The reference resistor Rr and operational amplifier are chosen by performing ABB simulation in TINA Pro Software. For determining impedance magnitude and phase range we have used Agilent 4396B network/spectrum/impedance analyzer with 43961A Impedance test kit and 16092A spring clip fixture. The experimental setup for impedance measurement is shown in fig. 3

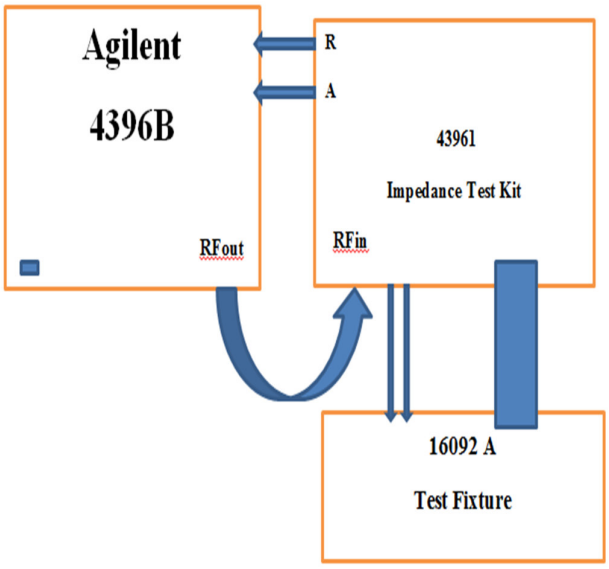

Fig.3 Impedance Measurement Setup

PROPOSED SYSTEM DESIGN

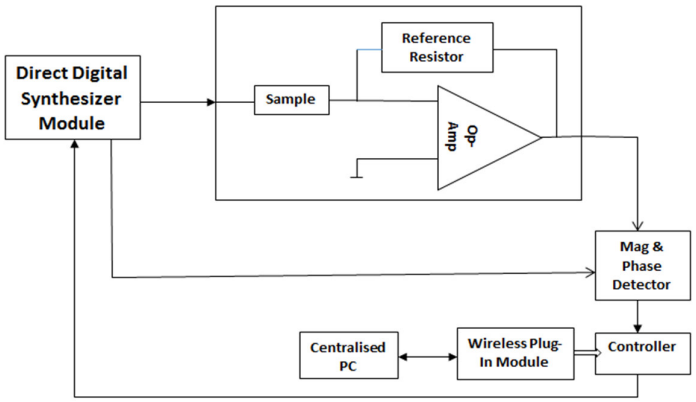

Fig 4. Basic block diagram of proposed module

The DDS module (AD9958) will generate multi frequency RF output based on 32-bit frequency word, which can be load into AD9958 from PIC controller (PIC32MX360F512L). The AD9958 will give 2V analog signal at different frequency, which will apply to ABB circuitry and Gain-Phase detector (AD8302). The op-amp and reference resistor will play important role in ABB arrangement. The op-amp and reference resistor are selected based on simulation result obtained by TINA 7. The output of ABB is measured

Cite this article as: Shashwat Godhani, Revathi S. "RF Based Online Food Quality Analyser". *International Conference on Innovative Trends in Electronics Communication and Applications (2015)*: 09-19. Print.

voltage, which is second input of AD8302. The AD8302 will directly gives voltage ratio and phase difference of applied signal. From these voltage and phase we can compute the impedance of the sample, which can be calibrated further into moisture content. As discussed earlier we are doing multi frequency measurement to nullify the effect of density of the sample, air gap of the parallel plate assembly. Here, we will use Bluetooth plug-in module to provide wireless connectivity.

RESULTS

We have prepared some samples in increment of 2% moisture content ranging from 13% to 29% by following proper procedure. For deciding impedance range we have measured the impedance of lowest and highest moisture sample at two different frequencies. Here, magnitude and phase are are measured using agilent 4396b network/spectrum/impedance analyzer with 43961a impedance test kit and 16092a spring clip fixture. The results obtained are shown in fig5and fig6.

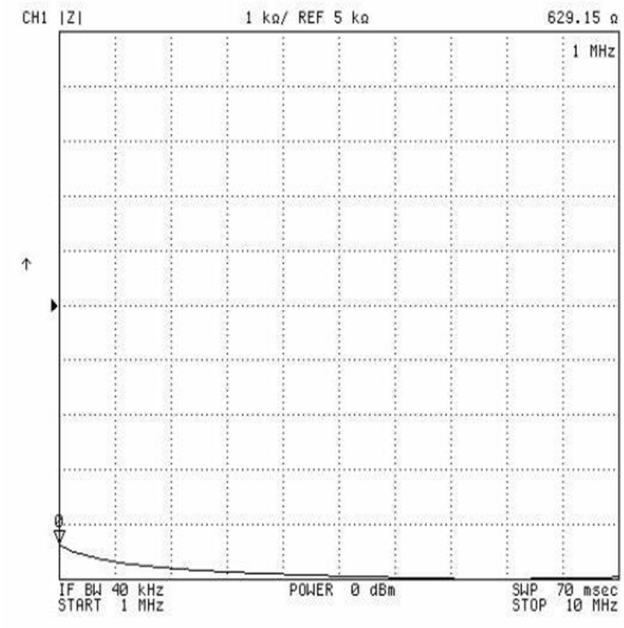

Fig 5a. Impedance mag of 13% sample @1 MHz

Fig 5b. Impedance phase of 13% sample @1 MHz

Cite this article as: Shashwat Godhani, Revathi S. "RF Based Online Food Quality Analyser". *International Conference on Innovative Trends in Electronics Communication and Applications (2015)*: 09-19. Print.

Fig 5c. Impedance mag of 13% sample @10 MHz

Fig 5d. Impedance phase of 13% sample @5 MHz

Cite this article as: Shashwat Godhani, Revathi S. "RF Based Online Food Quality Analyser". *International Conference on Innovative Trends in Electronics Communication and Applications (2015)*: 09-19. Print.

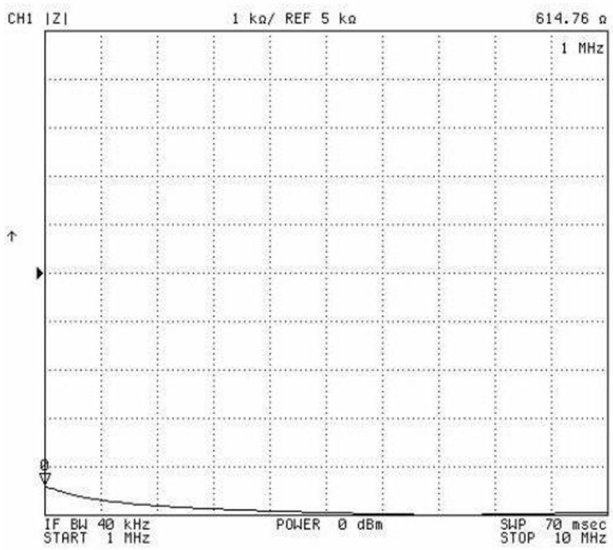

Fig 6a. Impedance mag of 29% sample @1 MHz

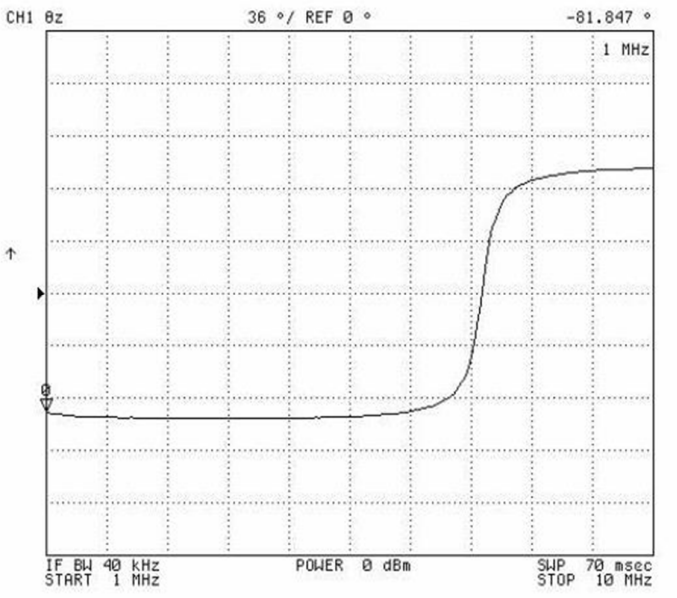

Fig 6b. Impedance phase of 29% sample @1 MHz

Cite this article as: Shashwat Godhani, Revathi S. "RF Based Online Food Quality Analyser". *International Conference on Innovative Trends in Electronics Communication and Applications (2015)*: 09-19. Print.

Fig 6c. Impedance mag of 29% sample @10 MHz

Fig 6d. Impedance phase of 29% sample @10 MHz

So, here we get the impedance magnitude range from 44 to 630 Ω and phase angle range from -82 deg to +86 deg. Now, we have simulated ABB circuit in TINA 7 as shown in fig 7. using different operational amplifier.

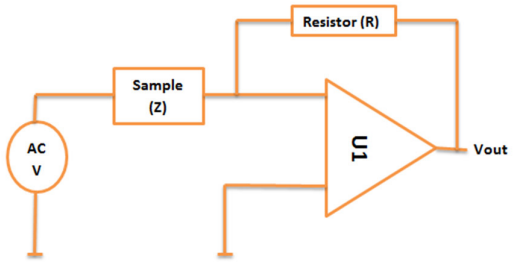

Fig 7. Basic schematic for ABB Circuit

Cite this article as: Shashwat Godhani, Revathi S. "RF Based Online Food Quality Analyser". *International Conference on Innovative Trends in Electronics Communication and Applications (2015)*: 09-19. Print.

Here, we have used 2V ac power supply with frequency ranging from 1MHz to 10MHz. For sample we have taken different lowest and highest values of magnitude and phase. Here, U1 is operational amplifier. Table 1 shows different output voltage at different frequencies. But, we got best result with OPA657 at higher frequencies. Fig.8 shows how OPA 657 gives better spur free output signal than other operational amplifiers. So, we are using OPA657 with operating voltage ±6.5V and reference resistor value 5Ω. So, we get output voltage in terms of mV, which is as per our requirement.

U1	Supply Voltage	Frequency	Vout
AD8001	±5V	1-10 MHz	1.78 V rms to 1.91 V rms
LM318	±6V	1-10 MHz	370.02 mV rms to 1.51 V rms
OPA657	±6.5 V	1-10 MHz	308.77 mV rms to 458.77 mV rms
LTC1052/101	±6.5 V	1-10 MHz	2.34 V rms

Table 1. Op-amp comparison at different frequencies

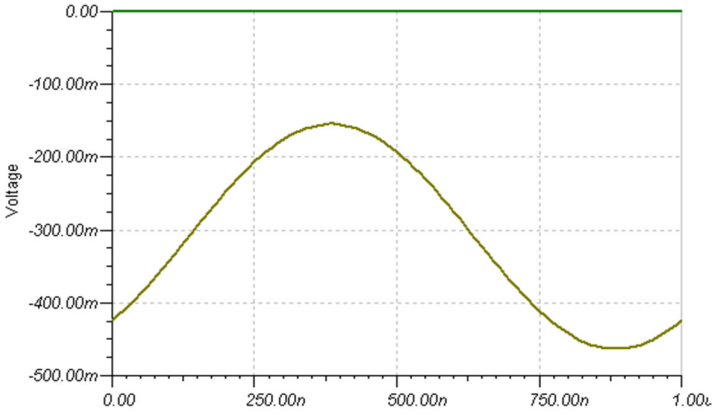

Fig 8a. Vout @1 MHz with OPA657

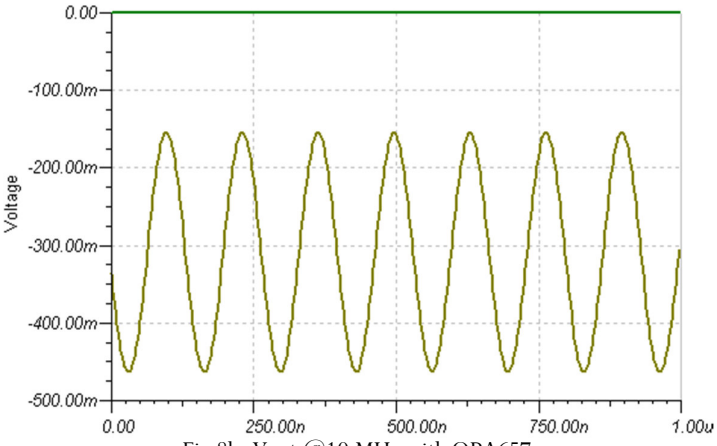

Fig 8b. Vout @10 MHz with OPA657

Cite this article as: Shashwat Godhani, Revathi S. "RF Based Online Food Quality Analyser". *International Conference on Innovative Trends in Electronics Communication and Applications (2015)*: 09-19. Print.

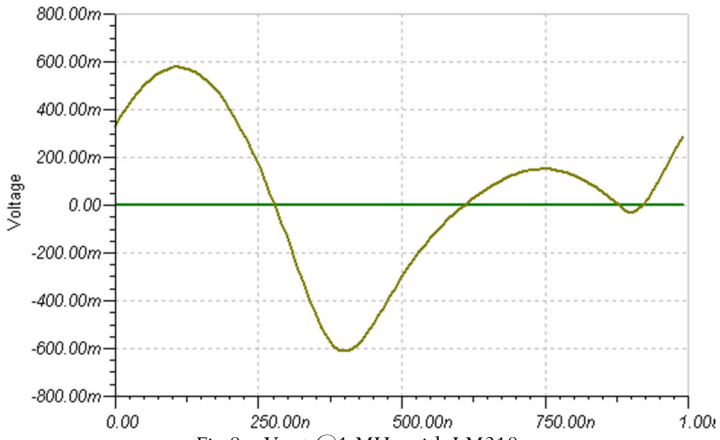

Fig 8c. Vout @1 MHz with LM318

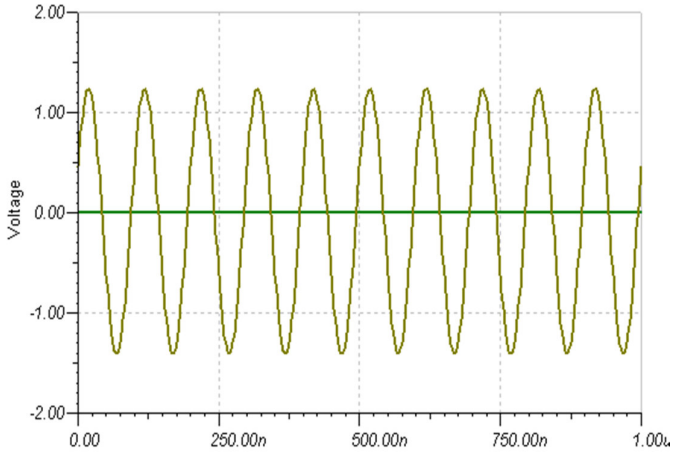

Fig 8d. Vout @10 MHz with LM318

ACKNOWLEDGMENT

Authors are thankful to Director, CSIR-CSIO, Chandigarh for his support and permission to carry out this work.

CONCLUSION

The existence of high correlation between the dielectric properties of grain and amount of water present in the grain at radio frequencies has facilitated the rapid and non-destructive sensing of moisture content. At lower radio frequencies, density-independent moisture content determination is achievable with multiple-frequency measurement. Due to operational amplifier's limitations at high frequencies ABB circuit is very crucial in the proposed circuit. So, we have simulate ABB circuit in TINA & using different operational amplifier and found that OPA657 is best suited for our application as it has very high Gain-BW product 1.66 GHz.

REFERENCES

[1] Chari V. K. Kandala, Chris L. Butts and Stuart O. Nelson, Capacitance Sensor for Nondestructive Measurement of Moisture Content in Nuts and Grain, IEEE TRANSACTIONS ON INSTRUMENTATION AND MEASUREMENT, VOL. 56, NO. 5, OCTOBER 2007

[2] Chari V. Kandala and Chris L. Butts, Design And Performance Of An Impedance Analyzer For Nondestructive Moisture Content Determination Of In-Shell Peanuts, SAS 2008 – IEEE Sensors Applications Symposium Atlanta, GA, February 12-14, 2008

Cite this article as: Shashwat Godhani, Revathi S. "RF Based Online Food Quality Analyser". *International Conference on Innovative Trends in Electronics Communication and Applications (2015)*: 09-19. Print.

[3] Jaya Sundaram and Chari V. Kandala, ESTIMATING THE MOISTURE CONTENT OF GRAIN FROM IMPEDANCE AND PHASE ANGLE MEASUREMENTS, SAS 2009 – IEEE Sensors Applications Symposium New Orleans, LA, USA - February 17-19, 2009

[4] X. Li, A. S. Zyuzin, and A. V. Mamishev, Measuring moisture content in cookies using dielectric spectroscopy, Conference on Electrical Insulation and Dielectric Phenomena, 2003

[5] Kishore Sundara-Rajan, Leslie Byrd and Alexander. V. Mamishev, Moisture Content Estimation in Paper Pulp Using Fringing Field Impedance Spectroscopy, IEEE SENSORS JOURNAL, VOL. 4, NO. 3, JUNE 2004

[6] Ying Zhou, Hanping Mao and Xiaodong Zhang, Hyperspectral Imaging Technology for Detection of Moisture Content of Tomato Leaves, 4th International Congress on Image and Signal Processing, 2011

[7] Stuart O. Nelson, Samir Trabelsi and Andrzej W. Kraszewski, RF Sensing of Grain and Seed Moisture Content, IEEE SENSORS JOURNAL, VOL. 1, NO. 2, AUGUST 2001

[8] Jianwei Qin, Kuanglin Chao, Moon S. Kim, Renfu Lu and Thomas F. Burks, Hyperspectral and multispectral imaging for evaluating food safety and quality, ELSEVIER Journal of Food Engineering, 157–171, 2013

[9] Di Wu and Da-Wen Sun, Advanced applications of hyperspectral imaging technology for food quality and safety analysis and assessment: A review — Part I: Fundamentals, ELSEVIER Innovative Food Science and Emerging Technologies, 1-14, 2013

[10] Impedance Measurement Handbook. Agilent Technologies Co. Ltd. USA.- 2003.

[11] Dumbrava V., Svilainis L. The Automated Complex Impedance Measurement System // Electronics and Electrical Engineering. – 2007. – No. 4(76). – P. 59–62

[12] Svilainis L., Dumbrava V. Measurement of complex impedance of ultrasonic transducers // Ultrasound. – 2007. – No.1(62). – P. 26–29.

[13] L. Svilainis, V. Dumbrava, Test fixture compensation techniques in impedance analysis, Electronics and Electrical Engineering, Vol. 87, Issue 7, 2008, pp. 37-40.

[14] L. Svilainis, V. Dumbrava, Test fixture compensation techniques in impedance analysis, Electronics and Electrical Engineering, Vol. 87, Issue 7, 2008, pp. 37-40.

[15]Linas SVILAINIS, Vytautas DUMBRAVA, Andrius CHAZIACHMETOVAS. Versatile Signal Acquisition System for Ultrasound Equipment Frequency Domain Parameters Estimation. Sensors & Transducers, Vol. 24, Special Issue, August 2013, pp. 7-18

Cite this article as: Shashwat Godhani, Revathi S. "RF Based Online Food Quality Analyser". *International Conference on Innovative Trends in Electronics Communication and Applications (2015)*: 09-19. Print.

International Conference on Innovative Trends in Electronics Communication and Applications 2015 [ICIECA 2015]

ISBN	978-81-929742-6-2	**VOL**	01
Website	icieca.in	**eMail**	icieca@asdf.res.in
Received	02 - April - 2015	**Accepted**	15 - November - 2015
Article ID	ICIECA003	**eAID**	ICIECA.2015.003

Blood Group Detection and Mobile Monitoring System

Nishtha Nagar[1], Aesha Shah[1], Aditya Singh[1], Shreya Akotiya[1]
[1]Ahmedabad Institute of Technology,
Ahmedabad.

Abstract: *Patients at disaster scenes can be greatly benefitted from technologies that continuously monitor their vital status & locations until they are admitted to the hospital. We have tried to design & developed a patient monitoring system that integrates vital signs sensors and transfers the same to allow remote monitoring of patient vital-sign status. This system shall facilitate collaboration between providers at the disaster scene, medical professionals at local hospitals & specialists or experts who might be available for consultation from distant facilities. In modern electronic communications, fiber optic system plays a prominent role. The principle of fiber optics is used in many modern medical electronic fields like endoscopic devices. Mistransfusion of blood will lead to many complications. This project provides an easy and fast means of identification of blood groups. Blood groups differ due to different antigens present in them and these antigens have different optical properties such as absorption and change in optical path length of light. The light from the pulsating LED is passed through the blood sample via an optical fiber cable and the transmitted light is then detected and is converted into voltage. The transmitted light from different blood groups will have different intensities and thereby different voltage levels, based on which, blood groups are classified.*

Keywords*:* Blood Group, Mobile, MEF, Fibre optics

INTRODUCTION

Steady advances in wireless networking, medical sensors, and interoperability software create exciting possibilities for improving the way we provide emergency care. The mobile monitoring system, that is being developed, explores and showcases how these advances in technology can be employed to assist victims and responders in times of emergency. The scope of this project covers a subset of the technologies in mobile patient monitoring system. We have developed a system that facilitates collaborative and time-critical patient care in the emergency response community.

During a mass casualty disaster, one of the most urgent problems at the scene is the overwhelming number of patients that must be monitored and tracked by each first responder. The ability to automate these tasks could greatly relieve the workload for each responder, increase the quality and quantity of patient care, and more efficiently deliver patients to the hospital. Our system accomplishes this through the following technologies:

- Sensors to sense and record vital signs into an electronic patient record database. This dramatically improves the current time-consuming process of manually recording vital signs onto paper pre-hospital care reports and then converting the reports into electronic form for the hospitals.

Cite this article as: Nishtha Nagar, Aesha Shah, Aditya Singh, Shreya Akotiya. "Blood Group Detection and Mobile Monitoring System". *International Conference on Innovative Trends in Electronics Communication and Applications (2015)*: 20-24. Print.

• Pre-hospital patient care software with algorithms to continuously monitor patients' vital signs and alert the first responders of critical changes.

Blood Group Detection Using Fiber Optic Cable

Blood group detection has always played a vital role in the medical field, thus detection of blood group is an essential process. In this report we will be seeing a method by which blood can be categorized into different groups (A, B, O, AB) in a smaller amount of time then the conventional methods.

Transmitter generates the electrical pulses to the LED which converts electrical pulses into optical pulses and this light is then coupled into the optical fiber using optical connector and is made to fall on to the passed blood sample. Some amount of light is absorbed by the blood and the transmitted light is then detected using receiver circuit. Different blood groups will have different voltage levels as detected by the receiver and blood groups are identified.

Blood Groups

Blood mainly consists RBC. This is common in all the groups, the differentiation in the groups occur due to the presence of Antigens in the RBC. For E.g. a group consists of A Antigens and B group consists of B Antigens. The presence and absence of these Antigens helps us in the grouping of blood.

Optical Properties of Blood

The principle behind differentiating the blood groups is due to the variation of the optical properties of different blood groups. When light is passes through different blood groups the amount of absorption differs for each thus the transmitted light intensity also changes. The optical path length for each blood group also changes. This helps in differentiating in the blood groups.

DESIGN

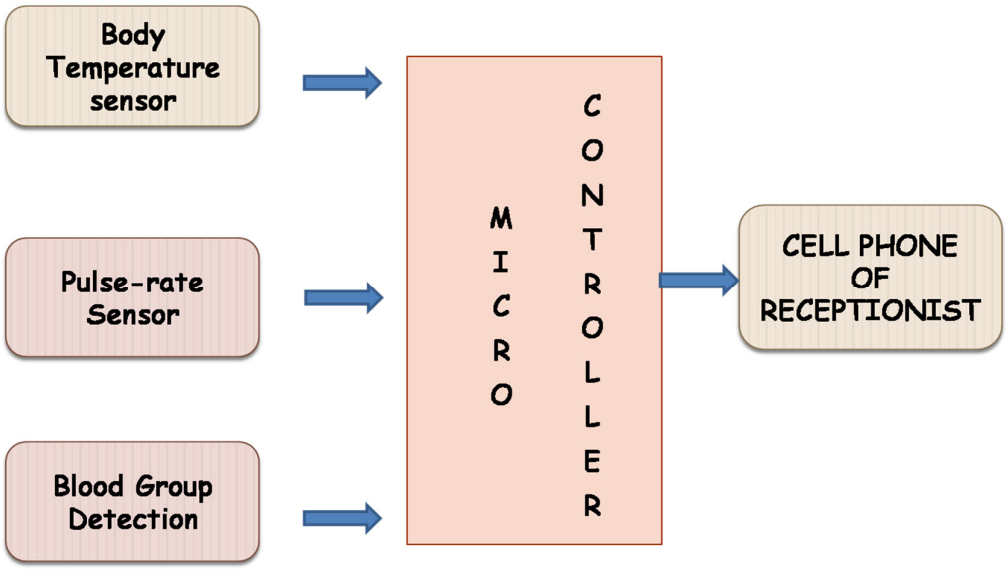

Figure 1. Architecture of patient monitoring system

THE DETAILED DESCRIPTION OF EACH BLOCK

Body Temperature Sensor

The LM35 is an integrated circuit sensor that can be used to measure temperature with an electrical output proportional to the temperature (in °C).

Cite this article as: Nishtha Nagar, Aesha Shah, Aditya Singh, Shreya Akotiya. "Blood Group Detection and Mobile Monitoring System". *International Conference on Innovative Trends in Electronics Communication and Applications (2015)*: 20-24. Print.

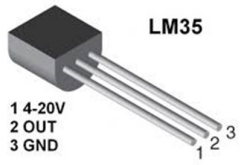

Figure 2. LM35 Body temperature sensor

The temperature sensor is that use substances of various physical properties with temperature variation of the sensor and let the temperature converted to electricity. These regularly change the physical properties of the main body temperature sensor is a core part of the temperature measuring instruments, and a wide variety. In accordance with the measurement method is divided into contact and non-contact two major categories, In accordance with the characteristics of sensor materials and electronic components into the thermal resistance and thermocouple. Used in this experiment is the LM35 temperature sensor.

Pulse-Rate Sensor

Pulse-rate is a very vital health parameter that is directly related to the soundness of the human cardiovascular system. This describes a technique of measuring the pulse rate through a fingertip using Arduino board. While the heart is beating, it is actually pumping blood throughout the body, and that makes the blood volume inside the finger artery to change too. This fluctuation of blood can be detected through an optical sensing mechanism placed around the fingertip. The signal can be amplified further for the microcontroller to count the rate of fluctuation, which is actually the pulse rate. This module detects the light emitted from the IR LED passed through blood and the photodiode detects it.

When your heart pumps the blood and the pressure rises sharply. So the amount of light from the emitter goes to the detector. The detector passes current when it sees more light, which in turn causes voltage drop.

This design uses two consecutive OP-AMPS which amplifies the peak and filters out the noise. Both the OP-AMPS are contained in a single integrated circuit. The IC is LM324 which has four OP-AMPS integrated in it out of which only two OP-AMPs are used in this module. The first OP-AMP will amplify the signal and will pass it on to the next OP-AMP. However, the signal is still weak. This weak signal is the given to the transistor for further amplification. This output is given as input to the Arduino.

Blood Group Detection

In modern electronic communications, fiber optic system plays a prominent role. The principle of fiber optics is used in many modern medical electronic fields like endoscopic devices. The first and foremost thing a doctor does while treating patients met with an accident is to determine patient's blood group. On an average, a doctor takes 10 minutes to find the blood group. In emergency cases, even 10 minutes delay in transfusion of blood may lead to the death of the patient. Hence, determination of blood group of a patient met with an accident, within a very short span of time is a vital factor. So far, blood grouping is done in laboratories or hospitals either by manual method using slide, or tile method or by semi-automated method using gel technology. Whereas all these processes are laborious and time consuming (takes at least 10 minutes). The need for the project is to develop a semi-automated blood grouping device with faster response than any other currently available technologies.

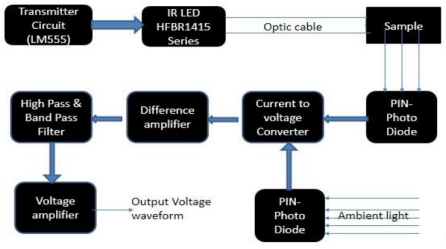

Figure 3. Block diagram of blood group detection system

Transmitter Circuit

The transmitter takes an electrical input and converts it to an optical output from a laser diode or LED. The light from the transmitter is coupled into the fiber with a connector and is transmitted through the fiber optic cable plant. The light from the end of the fiber is coupled to a receiver where a detector converts the light into an electrical signal which is then conditioned properly for use by the

Cite this article as: Nishtha Nagar, Aesha Shah, Aditya Singh, Shreya Akotiya. "Blood Group Detection and Mobile Monitoring System". *International Conference on Innovative Trends in Electronics Communication and Applications (2015)*: 20-24. Print.

receiving equipment. The sources used for fiber optic transmitters need to meet several criteria, it has to be at the correct wavelength, be able to be modulated fast enough to transmit data and be efficiently coupled into fiber.

The 555 timer IC is an integrated circuit (chip) used in a variety of timer, pulse generation, and oscillator applications. The 555 can be used to provide time delays, as an oscillator, and as a flip-flop element. In our project we are using NE555 timer in astable configuration The NE555 parts were commercial temperature range, 0 °C to +70 °C. In astable mode, the 555 timer puts out a continuous stream of rectangular pulses having a specified frequency. Resistor R1 is connected between VCC and the discharge pin (pin 7) and another resistor (R2) is connected between the discharge pin (pin 7), and the trigger (pin 2) and threshold (pin 6) pins that share a common node.

Black Box Design

The black box is designed to hold the sample, the optical cable and the photodiodes. It is divided into two compartments so that light from the optical cable does not fall on the photodiode which is used for ambient light cancellation. The optical cable is placed in a hole of diameter 2cm and the light is made to fall on the sample which is kept in a Slide and cover slip arrangement and the photodiode is kept behind the sample all of which are kept in a straight line to get the maximum result.

Receiver Circuit

The light from optical cable is then passed through the blood sample which is placed in a specially designed wooden box. In the two compartments two photodiodes are placed. Blood sample is placed in the right compartment and light from the optical fiber is passed through the blood sample and the transmitted light is then detected by the photodiode in that compartment.

The other photodiode in left compartment detects only the ambient light. These two photodiodes converts their respective input lights into voltages and these two voltages acts as an input to the instrumentation amplifier. The purpose of the extra photodiode is to eliminate the effect of ambient light on the main diode. The output of the instrumentation amplifier is then given to high pass filter to eliminate any dc in the signal. The resultant signal is then passed through the band pass filter of 8 to 12 kHz and then amplified to remove noises and for better accuracy.

RESULT

Table 1

Blood Group Voltage Levels

BLOOD GROUP	***VOLTAGE LEVELS GAIN=20***
A	*2.20 – 2.29*
B	*2.00 – 2.198*
O	*2.31 – 2.54*
AB	*2.61 – 3.014*

FUTURE SCOPE AND APPLICATION

The device mentioned above has a tremendous potential market in the field of medical sciences. The blood group detection unit is a quick and easy way for determining the blood group and comes as a great help during the times of emergency. The unit can be used otherwise by laboratories and common people for a hassle-free analysis. Moreover, with development in the unit, the Rhesus factor can be determined which will provide a very precise determination of the blood group.

Moreover, the mobile patient monitoring system is a compact and easy to operate device that can be used in ambulances, hospitals, clinics and also at homes. The device can be used by paramedics during the emergency, by doctors at hospitals and can even be installed at homes to continuously monitor terminally-ill patients.

The complete monitoring system that is aimed for development will be providing a wholesome analysis and monitoring of various vital signs of the emergency victims and terminally-ill patients and thus reduces the work of doctors and nurses to a great extent.

Cite this article as: Nishtha Nagar, Aesha Shah, Aditya Singh, Shreya Akotiya. "Blood Group Detection and Mobile Monitoring System". *International Conference on Innovative Trends in Electronics Communication and Applications (2015)*: 20-24. Print.

ACKNOWLEDGMENT

Project work is something that cannot be completed by the blind efforts of an individual but it is a constant inspiration and help of the people you work around. We are extremely thankful to our college, Ahmedabad Institute of Technology, Ahmedabad and our professors for their valuable guidance and providing with excellent working environment. We are also thankful to our family and friends for their support and encouragement.

REFERENCES

[1] G.Keiser, Optical Fiber Communication, McGraw-Hill, 2000.
[2] J.Senior, Fiber optic communication: Principles and Practice, Prentice Hall, 1992
[3] R. Gayakwad, Op-Amp and Linear Integrated Circuits, Prentice Hall of India
[4] Blood Group Detection Using Fiber Optics, T.M. Selvakumari, Armenian Journal of Physics, 2011, vol. 4, issue 3, pp. 165-168
[5] Blood Group Detection Using Fiber Optics Pramod Kakarla, Murari Yashwanth K, Srikanth PVNK, Rishi Kumar R, Pratibha N, Amrita viswa Vidyapeetham, Coimbatore.

Cite this article as: Nishtha Nagar, Aesha Shah, Aditya Singh, Shreya Akotiya. "Blood Group Detection and Mobile Monitoring System". *International Conference on Innovative Trends in Electronics Communication and Applications (2015)*: 20-24. Print.

International Conference on Innovative Trends in Electronics Communication and Applications 2015 [ICIECA 2015]

ISBN	978-81-929742-6-2	**VOL**	01
Website	icieca.in	**eMail**	icieca@asdf.res.in
Received	02 - April - 2015	**Accepted**	15 - November - 2015
Article ID	ICIECA004	**eAID**	ICIECA.2015.004

Sign Language Translating Glove

Ankit Dave[1], Hemang Vaidya[1]
[1]Ahmedabad Institute of Technology, Ahmedabad

Abstract: *A Sign Language Translating Glove is designed by us that takes hand gestures as input and convert them into Text and/or Speech output. The Device contains flex sensors on hand to measure static gestures. The sensors are connected to Arduino to search a library of gestures that generate output signals that can be used to produce written text.*

Keywords: Sign Language, Gestrures, Arduino

INTRODUCTION

A set of 26 unique distinguishable postures makes up the alphabet in ISL used to spell names or uncommon words that are not well defined in the dictionary. Indian Sign Language (ISL) is the native language of some 300,000 to 500,000 people in India. It is, therefore, appealing to direct efforts toward electronic sign language translators.

Linguists have proposed different models of gesture from different points of view, but they have not agreed on definitions and models that could help engineers design electronic translators. Existing definitions and models are qualitative and difficult to validate using electronic systems.

As with any other language, differences are common among signers depending on age, experience or geographic location, so the exact execution of a sign varies but the meaning remains. Therefore, any automatic system intended to recognize signs have to be able to classify signs accurately with different "styles" or "accents". Another important challenge that has to be overcome is the fact that signs are already defined and cannot be changed at the researcher's convenience or because of sensor deficiencies. In any case, to balance complexity, training time, and error rate, a trade-off takes place between the signer's freedom and the device's restrictions.

A sign language translating glove is a device that recognizes hand sign gestures, look it up in database and convert them to text output and voice output.

As the hand gestures are given as input, the sensors will be activated by own and as the letters have already been programmed in microcontroller, it will detect the letter according to sign of hand.

So the output will be shown on LCD display and if also the voice output is activated than the text output will be converted into voice output.

Cite this article as: Ankit Dave, Hemang Vaidya. "Sign Language Translating Glove". *International Conference on Innovative Trends in Electronics Communication and Applications (2015)*: 25-29. Print.

ARCHITECTURE OF SIGN LANGUAGE TANSLATING GLOVE

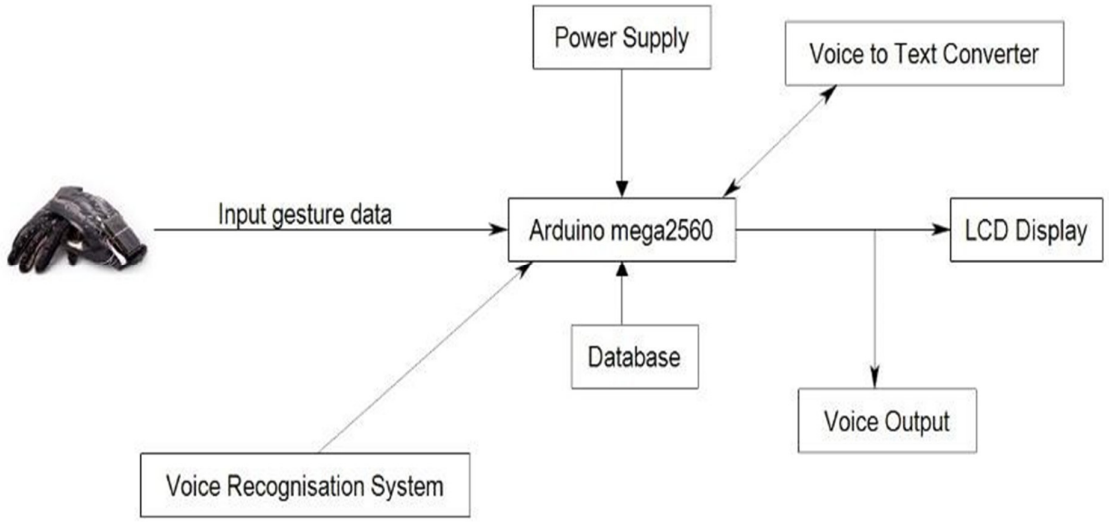

Figure 1 Block Diagram

DATA GLOVE

Data Glove is basically a glove that different components like Resistive Sensors, Accelerometer, ARDUINOATmega2560, LCD display, Speaker, etc. implemented on it. It is to be noted that the figure show below is only conceptual and may differ from the original model.

The Conceptual Image of Data Glove is shown below:

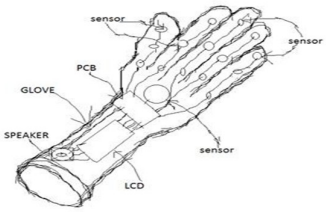

Fig.2 Conceptual Image of Glove

TEXT TO SPEECH CONVERTER

PWM combined with an analog filter can be used to generate analog output signals, i.e. a digital to analog converter (DAC). A digital pulse train with a constant period (fixed base frequency) is used as a basis. To generate different analog levels, the duty cycle and thereby the pulse width of the digital signal is changed. If a high analog level is needed, the pulse width is increased and vice versa.

Averaging the digital signal over one period (using an analog low-pass filter) generates the analog signal. A duty cycle of 50% gives an analog signal with half the supply voltage, while 75% duty cycle gives an analog signal with 75% supply voltage. Examples on filtered output signals are shown at the end of this document.

Cite this article as: Ankit Dave, Hemang Vaidya. "Sign Language Translating Glove". *International Conference on Innovative Trends in Electronics Communication and Applications (2015)*: 25-29. Print.

The analog low-pass filter could be a simple passive RC-filter for instance. The filter removes the high PWM base frequency and lets through the analog signal. The filter crossover frequency must be chosen high enough to not alter the analog signal of interest. At the same time it must be as low as possible to minimize the ripple from the PWM base frequency.

In the AVR, the timer/counters are used to generate PWM signals. To change the PWM base frequency, the timer clock frequency and top counter value is changed. Faster clock and/or lower top value will increase the PWM base frequency, or timer overflow frequency. With full resolution (top value 255) the maximum PWM base frequency is 250 kHz. Increasing the base frequency beyond this frequency will be at the expense of reduced resolution, since fewer step are then available from 0% to 100% duty cycle.

Altering the value of the Output Compare Registers (OCR) changes the duty cycle. Increasing the OCR value increases the duty cycle. The PWM output is high until the OCR value is reached, and low until the timer reaches the top value and wraps back to 0. This is called Fast- PWM.

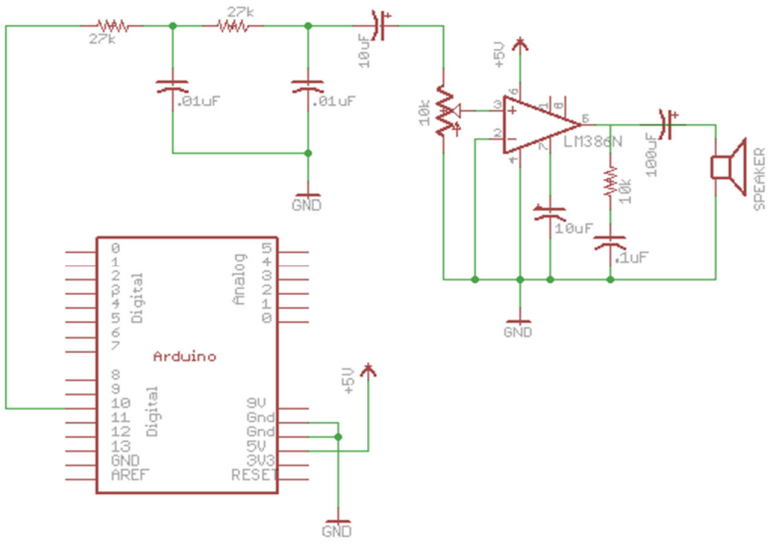

Fig. 3 Circuit Diagram of Amplifier

FLEX SENSOR

They work as variable analog voltage dividers. Inside the flex sensor are carbon resistive elements within a thin flexible substrate. More carbon means less resistance. Usually a flex sensor is used in voltage divider configuration. It is shown below:

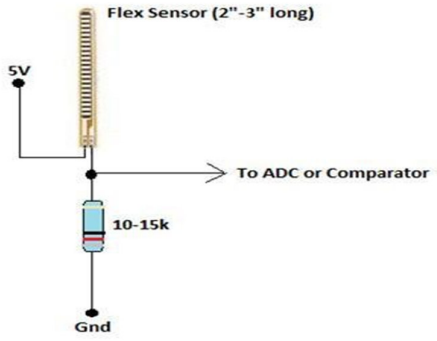

Fig. 4 Circuit Diagram Connection

Cite this article as: Ankit Dave, Hemang Vaidya. "Sign Language Translating Glove". *International Conference on Innovative Trends in Electronics Communication and Applications (2015)*: 25-29. Print.

As shown in figure above the flex sensor is attached in series with a resistor of suitable value, which is taken as reference. The voltages across flex sensor are measured according to the voltage divider rule. As we know that a flex sensor is a type of variable resistor, as the resistance of flex changes, the voltage across it also change. This change in voltage is measured with respect to the bending of the flex sensor.

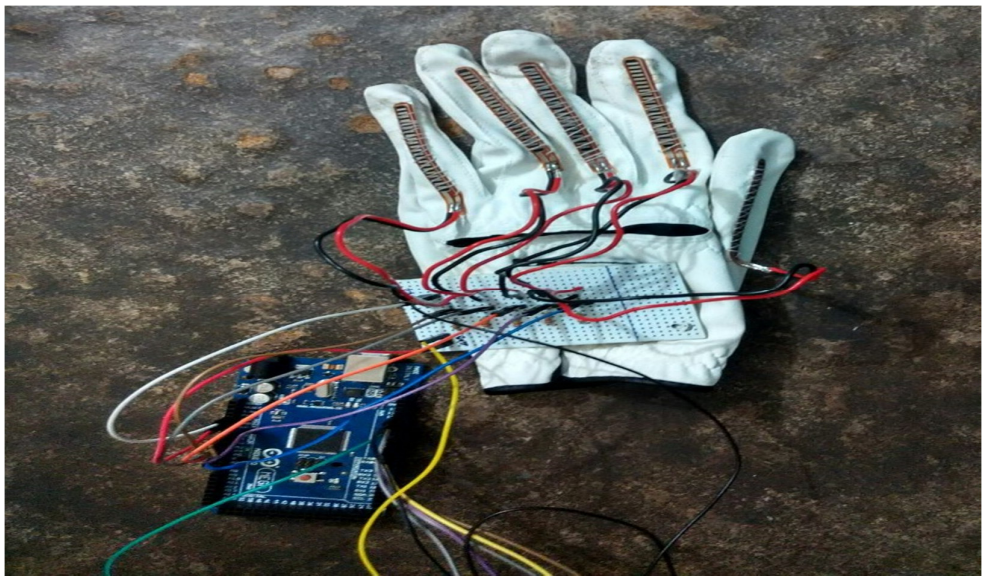

Fig 5 Glove with Flex sensors interfaced to Arduino

The input is taken from between flex sensors and reference resistors to analog pins A0, A1, A2, A3, and A4 of the Arduino board.

SIGN LANGUAGE GESTURES

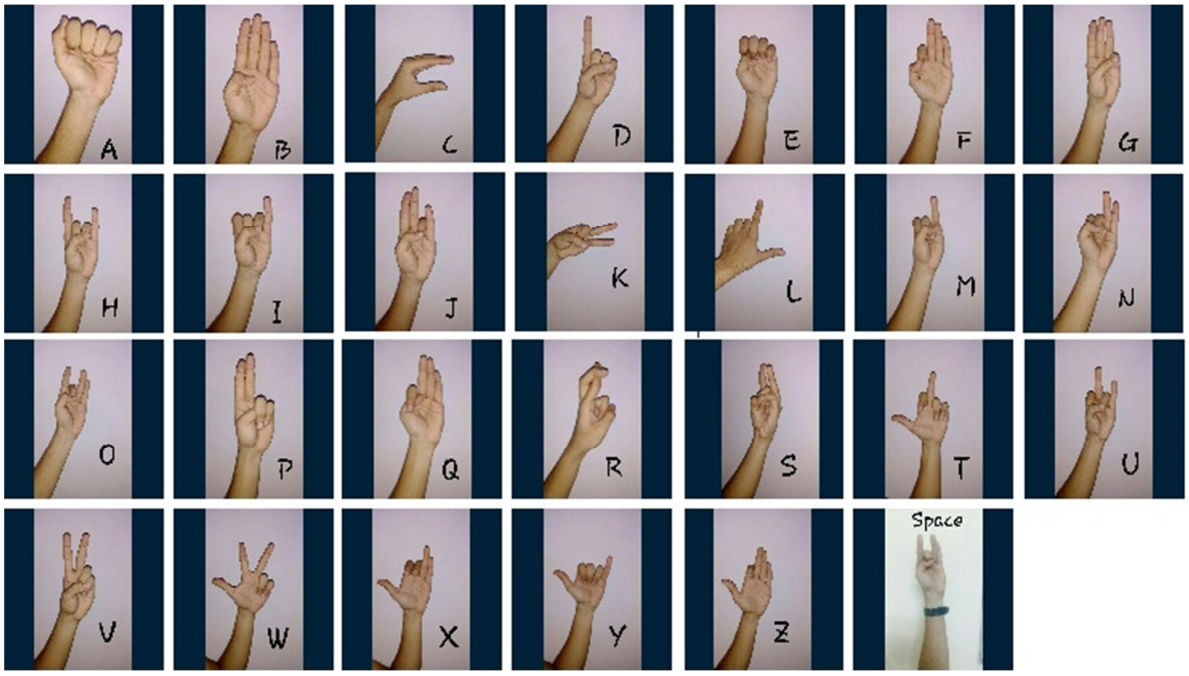

Fig. 6 Sign language gestures

Cite this article as: Ankit Dave, Hemang Vaidya. "Sign Language Translating Glove". *International Conference on Innovative Trends in Electronics Communication and Applications (2015)*: 25-29. Print.

FINAL IMPLEMENTED DEVICE

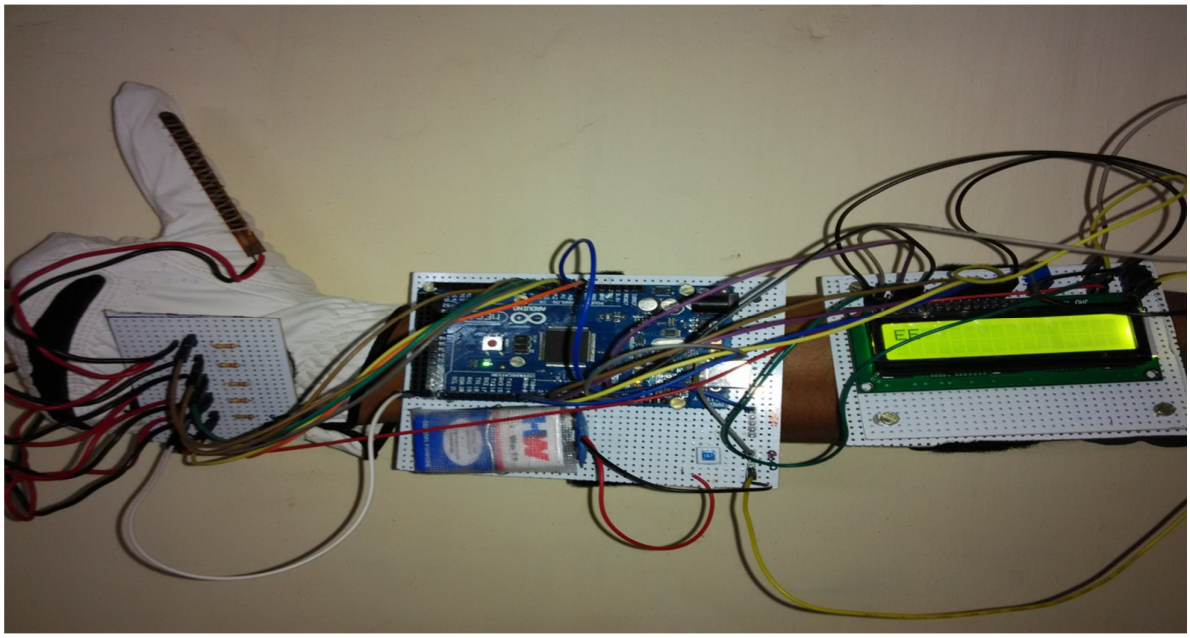

Fig.7 Final Implemented Device

FUTURE SCOPE AND APPLICATION

The main application of this device is for deaf and dumb people. The device will be useful for better communication between deaf/dumb and normal people. We will try to convert the text output into various languages other than English. We will add a voice recognition feature that takes voice input and convert them to text. We will try to advance the device to recognize static as well as dynamic gesture.

ACKNOWLEDGMENT

Project work is something that cannot be completed by the blind efforts of an individual but it is a constant inspiration and help of the people you work around. We are extremely thankful to our college, Ahmedabad institute of technology, Ahmedabad and our professors for their valuable guidance and providing with excellent working environment. We are also thankful to our family and friends for their support and encouragement.

REFERENCES

[1] Muhammad Ali Mazidi, Sarmad Naimi, Sepehr Naimi, *The AVR Microcontroller and Embedded Systems using Assembly and C, Pearson, INDIA, 2011.*

[2] Vision-based Hand Gesture Recognition for Human-Computer Interaction *Computer Science Department, University of Crete Heraklion, Crete, Greece*

[3] HAND GESTURE RECOGNITION: A LITERATURE REVIEW International Journal of Artificial Intelligence & Applications (IJAIA), Vol.3, No.4, July 2012, Rafiqul Zaman Khan and Noor Adnan Ibraheem. Department of Computer Science, A.M.U. Aligarh, India

Cite this article as: Ankit Dave, Hemang Vaidya. "Sign Language Translating Glove". *International Conference on Innovative Trends in Electronics Communication and Applications (2015)*: 25-29. Print.

International Conference on Innovative Trends in Electronics Communication and Applications 2015 [ICIECA 2015]

ISBN	978-81-929742-6-2	**VOL**	01
Website	icieca.in	**eMail**	icieca@asdf.res.in
Received	02 - April - 2015	**Accepted**	15 - November - 2015
Article ID	ICIECA005	**eAID**	ICIECA.2015.005

Virtual Speed Breakers Using Radio Frequency

Aishwarya R[1], Akila P[1], Jayasree V[1], Nivetha E[1]
[1]College of Engineering, Guindy - Anna University

Abstract: *The objective of this presentation is to reduce the number of accidents caused by the conventional speed breakers on the road by slowing the vehicle automatically. This can be achieved by using radio frequency (RF) receiver modules in the future vehicles and use of RF transmitter modules in areas where the speed limitation is required. When the vehicles move into the radiation range of the transmitter the receiver system gets activated and it warns the driver to reduce the speed of the vehicle. This is done unconditionally by limiting the flow of the fuel using ferromagnetic shape memory alloys(FSMA). These alloys come to a different shape upon applying a magnetic field. This technology will prove to be cost effective as it reduces the design cost for the vehicles according to the prevailing road conditions in our country as well as reduce the cost of laying the speed breakers. Above all it prevents the frequent accidents due to the sudden presence of speed breakers. Further this system improves the driving comfort.*

Keywords*:* Speed Breakers, Radio Frequency, FSMA, Magnet.

INTRODUCTION

Today we are in the Age of Technology. The introduction of wireless communication has transcended all barriers and has resulted in making the communication to be almost instant. This phenomenonal achievement has its roots in Radio Frequency. Many applications now use radio frequency to transmit and receive data, provide wireless connectivity among various devices etc. Many new applications can be derived from the existing technology if it is combined and used in a novel method. In this paper, an antenna which makes use of the radio frequency is used as a controlling module to reduce the speed of the four wheeled vehicle. This idea is mainly concentrated for school zones, hairpin bends and U turns where the speed limit is 20km.

DIRECTIONAL ANTENNAE:

Omni directional antennas are employed for this setup. It is a system which radiates power uniformly in one plane and the direction is perpendicular to it. Omni directional antennas have a similar radiation pattern to the dipole antenna. These are used when coverage is required in all directions (horizontally) from the antenna with varying degrees of vertical coverage. Polarization is the physical orientation of the element on the antenna that actually emits the RF energy. This antenna focuses the RF energy in a particular direction. As the gain of aomni directional antenna increases, the coverage distance increases. For directional antennas, the radiation lobes are pushed in a certain direction and little energy is there on the back side of the antenna. Another important aspect of the antenna is the front-to-back ratio. It measures the directivity of the antenna. It is a ratio of energy which antenna is directing in a particular direction, which depends on its radiation pattern to the energy which is left behind the antenna or wasted. The higher the gain of the antenna, the higher the front-to-back ratio is. For this application we require an antenna with a moderate gain. Hence we propose to use the antenna which has a gain of 15 dBi, a front-to-back ratio of 17 dB. This means the gain in the backward direction is 1 dBi. This way the gain is reduced in the opposite direction. Selecting the appropriate gain we could have the antenna set to different range depending upon the width and length of the road.

Cite this article as: Aishwarya R, Akila P, Jayasree V, Nivetha E. "Virtual Speed Breakers Using Radio Frequency". *International Conference on Innovative Trends in Electronics Communication and Applications (2015)*: 30-35. Print.

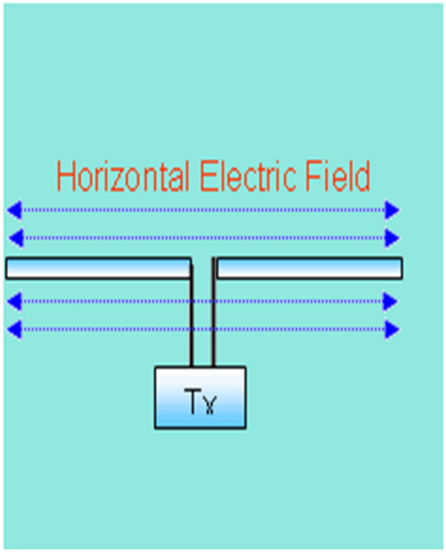

Figure 1. 1 Horizontal Electric field Effect

Figure 1. 2 Omni directional antenna

FERROMAGNETIC SHAPE MEMORY ALLOYS

Ferromagnetic shape-memory (FSM) alloys are materials that exhibit large changes in shape and size in an applied magnetic field. In FSM materials, the magnetic moments of the twin variants play a crucial role in the deformation process: when a sample is exposed to an external magnetic field in the martensitic phase, the magnetic field tends to realign the magnetic moments along the field and, simultaneously, the variant in a favorable orientation with respect to the field grows at the expense of other variants (see Figure 2). The resulting deformation can be as large as 10 %.

The NiMgAl which has Nickel 50%, Magnesium 25%, Aluminium 25% is used as the shape memory alloy. The specialty of this alloy is that it offers immediate response even in the presence of a very small magnetic field. This has the capacity to change shape even in the presence of field of 1 Tesla. This alloy is used in the fuel injection system of the engines. The NiMgAl alloy is casted as a tube and is attached to the common point of the fuel entry into the engine. The alloy is enclosed with a coil to produce a magnetic field on reception of the radiowaves from the antenna. The diameter of the tube is reduced with the increase in magnetic field. This reduces the supply to the engine thus improving the efficiency while saving the fuel during slowing of the vehicle. The FSMA proves to be an efficient system. The property of this alloy is under research and so the alloy may take a few years to come into market for domestic use. Thisalloy can considerably reduce the fuel consumption and also result in efficient fuel management.

Cite this article as: Aishwarya R, Akila P, Jayasree V, Nivetha E. "Virtual Speed Breakers Using Radio Frequency". *International Conference on Innovative Trends in Electronics Communication and Applications (2015)*: 30-35. Print.

Ferromagnetic shape-memory (FSM) alloys are materials that exhibit large changes in shape and size in an applied magnetic field. The key factor behind this phenomenon is martensitic transformation of the crystal lattice below a certain temperature. Regions having typically a tetragonal crystal structure start to form within the parent austenitic, cubic phase, and the resulting strain is accommodated by the formation of strained twin variants (the words "austenitic" and "martensitic" are normally used to describe the different steel variants but they can be also associated with different crystal structures). This behavior is illustrated in Figure 1. The redistribution of these variants, the twin-boundary motion, leads to the macroscopic deformation of the whole element. What differentiates FSM materials from conventional, shape-memory (SM) alloys is that the shape change takes place solely in the martensitic phase. In the case of traditional temperature-driven SM materials, a sample is first cooled, and then deformed to modify the dimensions and shape of the studied sample, and the initial state is retained when the sample is again heated above the martensitic transformation temperature. Some shape-memory alloys exhibit super elasticity, i. e. , an applied stress leads to the martensitic transformation and a large shape change above the transformation temperature. In FSM materials, the magnetic moments of the twin variants play a crucial role in the deformation process: when a sample is exposed to an external magnetic field in the martensitic phase, the magnetic field tends to realign the magnetic moments along the field and, simultaneously, the variant in a favorable orientation with respect to the field grows at the expense of other variants (see Figure 2). The resulting deformation can be as large as 10 times.

For applications, an FSM element has to be biased in a single-variant state in zero field, e. g. , by applying stress. The magnetic field is applied orthogonal to the biasing direction, which leads to the above-mentioned behavior when B > 200-300 mT (at lower fields the magnetic moments just rotate without any structural change taking place). The FSM effect is a reversible process just like the normal SM effect: When the field direction is reversed, the material returns to its original shape.

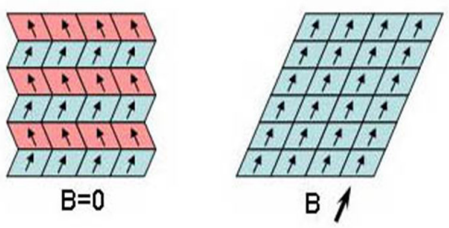

Figure 2. 1 Formation of martensitic regions within the parent austenitic phase.

SYSTEM PRINCIPLE AND WORKING

SYSTEM OVERVIEW

The speed of the vehicle can be controlled by applying clutch, break. To avoid wastage of fuel ferromagnetic shape memory alloys can be used near the place, from which fuel is being injected into the engine. All these actions are performed upon the reception of electromagnetic waves in radio frequency range transmitted by a transmitter installed in the places where speed reduction is required.

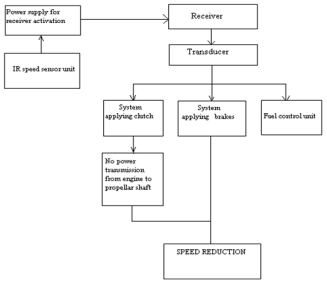

Figure 3. 1 Block diagram of the entire system operation

Cite this article as: Aishwarya R, Akila P, Jayasree V, Nivetha E. "Virtual Speed Breakers Using Radio Frequency". *International Conference on Innovative Trends in Electronics Communication and Applications (2015)*: 30-35. Print.

APPLYING CLUTCH:

The first step in stopping the vehicle is to apply the clutch. This could be done by using a dc motor which is directly connected using a clutch cable to the clutch. The current produced
upon reception of the electromagnetic wave is used to run the motor in a manner that the clutch would automatically be applied so that power transmission from the engine to the propeller shaft is stopped. This system is designed in such a way that the driver has control over the clutch even though the clutch is being applied automatically. This control would enable the driver to start the vehicle even if the engine goes off in the region where electromagnetic wave is being received. For four wheelers the system already present in the automobile is to be used used for applying clutch upon reception of rf waves.

APPLYING BRAKES:

Upon applying clutch the transmission of power from engine to propeller shaft is stopped. The brakes are then applied using a separate breaking system which would be operating along with the breaking system already present in automobiles; the system uses a coil to produce a strong magnetic field. Upon production of magnetic field the system is designed in such a way that the brakes are applied. The production of magnetic depends on the intensity of reception of rf waves which in turn depends on the speed of the vehicle. This magnetic brake system is to be used for four wheelers. For two wheelers a stepper motor is to be used for applying brakes. These stepper motors are supplied with power upon reception of rf waves. The rotation of these motors in steps provides braking through the cables used along with the cables which are used in automobiles for applying brakes. The driver of the vehicle is given control over the brake system so that the driver may stop the vehicle under accidental situations. These actions would retard the speed of the vehicle considerably moving at design speed in the road. The vehicle which is moving at considerably would further be slowed down if the above actions of applying clutch and brake are performed. To overcome this, power required to activate the receiving antenna is supplied from a dynamo which is directly in contact with the rotating wheels of the vehicle. This makes the receiving antenna to be activated only when the vehicle is moving with a speed for which speed retardation is required.

The system which applies brake is to be designed in such a way that the force it would produce upon supplying minimum current is sufficient to reduce the speed of the vehicle which is moving at a design speed in the road.

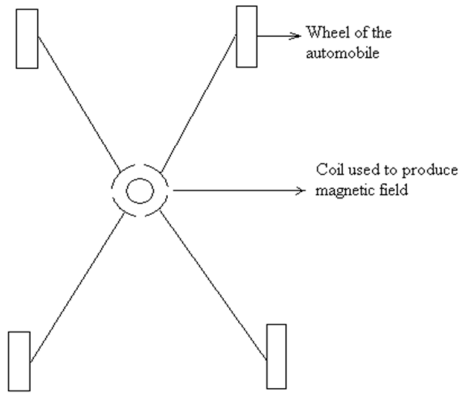

Figure 3. 2 Brake system before applying brake

Cite this article as: Aishwarya R, Akila P, Jayasree V, Nivetha E. "Virtual Speed Breakers Using Radio Frequency". *International Conference on Innovative Trends in Electronics Communication and Applications (2015)*: 30-35. Print.

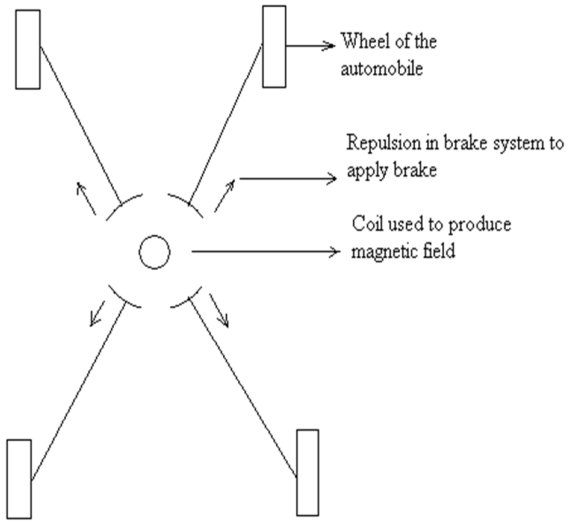

Figure 3. 3 Brake system before applying brake

FUEL CONTROL:

By above actions the speed of the vehicle would be reduced but the fuel supplied to the engine would not be controlled. As power transmission from engine the engine to the propeller shaft has been stopped there is no need that the fuel should continuously be injected into the engine. The fuel supply is to be controlled by using a ferromagnetic shape memory alloy.

The fuel supply can be controlled by reducing the diameter of the pipes from which fuel is being injected into the engine. This is done by using a ferromagnetic shape memory alloy near the point from which fuel is injected into the engine. The current produced upon the reception of a radio waves is supplied to a coil to produce a magnetic field of about 1 tesla at which the diameter of the alloy is reduced .This action would reduce the fuel being supplied to the engine. Ultimately the consumption of fuel upon speed reduction is reduced.

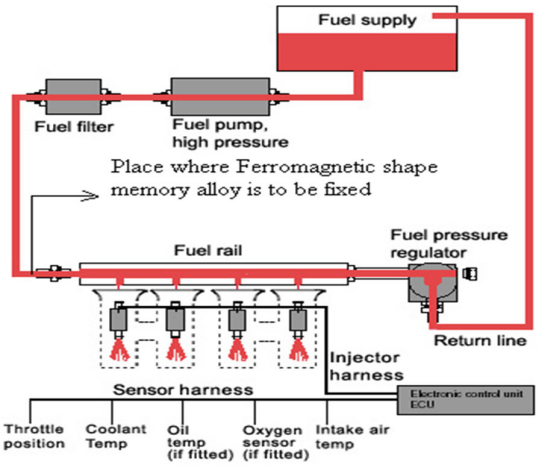

Figure 3. 4 Figure showing the position of ferromagnetic shape memory alloy

Cite this article as: Aishwarya R, Akila P, Jayasree V, Nivetha E. "Virtual Speed Breakers Using Radio Frequency". *International Conference on Innovative Trends in Electronics Communication and Applications (2015)*: 30-35. Print.

SPEED SENSORS

In order to differentiate vehicles coming at a slower speed and those moving at a higher speed, we are going to use a sensor to gauge the speed. It consist of an arrangement of a perforated disc attached to the wheel and an IR light which sends light and the receiver receives it. When the vehicle is moving at a faster pace the light would be available to the sensor continuously. Upon continuous sensing of light the rf receiver would then be activated by supplying power from the unit that supplies power for rf receiver activation. If the vehicle is moving at slower pace the IR light would be available to the wheel speed sensor with continuous interruption. Upon sensing of interrupted IR light the rf receiver would not be activate and the speed will not be controlled by the system provided in the road. This speed sensor system would distinguish between the vehicles moving at slower speed and those moving at higher speed and would control the speed accordingly. The material to be used in the sensor would be chosen in such a way that the RF receiver would be activated if the vehicle is moving at a speed of about 25kmph to 45kmph. For vehicles which are moving at a speed of about 15kmph to 20kmph speed reduction is not necessary and activation of RF receiver would be avoided for vehicles moving at slower pace.

ULTRA LOW POWER RF

Now-a-days even Ultra Low Power RF can also be used by which power consumption can be reduced. ULP wireless connectivity can be added to any portable electronic product or equipment featuring embedded electronics, from tiny medical and fitness sensors, to cell phones, PCs, machine tools, cars and virtually everything in between. Tiny ULP transceivers can bestow the ability to communicate with thousands of other devices directly or as part of a network – dramatically increasing a product's usefulness.

ULP wireless technology differs from Bluetooth technology in that it requires significantly less power to operate. This dramatically increases the opportunity to add a wireless link to even the most compact portable electronic device.

SUGGESTIONS

The significance of the system lies in the use of ferromagnetic shape memory alloy NiMgAl which has a very high sensitivity. It is employed near the nozzle of the fuel injection system so even a slight change can decrease the fuel amount considerably. Also the use of speed breakers may cause congestion in traffic as the vehicles have to come to complete halt. If this system is implemented the vehicle would be moving at a constant rate thereby regulating traffic. Instead of laying big speed breakers near the railway gates, this system can act as an alternative. Nowadays the global trade is increasing though it got hit due to recession. Many cars are imported from foreign countries and our Indian roads are not suitable for those cars as they have a very low base. This system avoids speed breakers and thus suitable for all types of automobiles.

REFERENCES

- http://en.wikipedia.org/wiki/Directional_antenna
- http://www.authorstream.com/Presentation/Ahmedmalaa-92625-fundamental-types-antennas-antenna-electromagnetics-engineering-science-technology-ppt-powerpoint/
- http://www.cisco.com/en/US/tech/tk722/tk809/technologies_tech_note09186a00807f34d3.shtml#topic3
- http://ses.confex.com/ses/2004tm/techprogram/P1155. HTM
- http://depts.washington.edu/cims/publications/pdf/actuators2.pdf
- http://en.wikipedia. org/wiki/Transducer
- http://www.ezlan.net/antennae.html
- http://www.twminduction.com/faq/images/fuel_inj_system. jpg

Cite this article as: Aishwarya R, Akila P, Jayasree V, Nivetha E. "Virtual Speed Breakers Using Radio Frequency". *International Conference on Innovative Trends in Electronics Communication and Applications (2015)*: 30-35. Print.

International Conference on Innovative Trends in Electronics Communication and Applications 2015 [ICIECA 2015]

ISBN	978-81-929742-6-2	**VOL**	01
Website	icieca.in	**eMail**	icieca@asdf.res.in
Received	02 - April - 2015	**Accepted**	15 - November - 2015
Article ID	ICIECA006	**eAID**	ICIECA.2015.006

Intelligent Auto Irrigation System Using ARM Processor and GSM

K Nilson[1], G Sharmila[2], P Praveen Kumar[3]
[2]Assistant Professor and [1, 3]UG scholars, Dr. Navalar Nedunchezhiyan College of Engineering
Cuddalore, Tamilnadu
India

Abstract: *Agriculture is the back bone of India. To make the sustainable agriculture, this system is proposed. In this system ARM 9 processor is used to control and monitor the irrigation system. Different kinds of sensors are used. This paper presents a fully automated drip irrigation system which is controlled and monitored by using ARM9 processor.PH content and the nitrogen content of the soil are frequently monitored. For the purpose of monitoring and controlling, GSM module is implemented. The system informs user about any abnormal conditions like less moisture content and temperature rise, even concentration of CO2 via SMS through the GSM module.*

Keywords*:* Agriculture, Irrigation, ARM Processor, GSM.

INTRODUCTION

In many agricultural cropping systems irrigation is necessary. In semiarid and arid areas, efficient water applications and management are of major concerns [1]. The continuous extraction of water from earth is reducing the water level due to which lot of land is coming slowly in the zones of un-irrigated land. Large amount of water goes waste due to improper planning of water usage. The demand for new water saving techniques in irrigation is increasing rapidly right now [2]. The aim of farmer is to produce "more crop per drop", hence there is need to find the irrigation techniques which consumes less fresh water. These techniques are helpful in the regions where there is a scarcity of fresh water. In the modern drip irrigation systems, the most significant advantage is that water is supplied near the root zone of the plants drip by drip due to which a large quantity of water is saved. At the present era, the farmers have been using irrigation technique in India through the manual control in which the farmers irrigate the land from time to time. This process sometimes consumes more water or sometimes the water reaches late due to which the crops get dried. Water deficiency can be hazardous to plants before wilting becomes visible. This problem can be perfectly solved if automatic controller based drip irrigation system is used in which irrigation will take place only when there is intense requirement of water. Irrigation system uses valves to turn ON or OFF automatically. Automatic Drip Irrigation is a valuable tool for accurate soil moisture control in highly specialized greenhouse vegetable production and it is a simple, precise method for irrigation. It also helps in time saving, removal of human error in adjusting available soil moisture levels and to maximize their net profits. Along with water the other important resources to the crop are the nutrients. If the nutrients are available in the right amount for the growth of crops then the yield of the crops also increases. Thus the productivity can be raised with the proper management of water resources and nutrients.

IRRIGATION

There have been technological advancements in agriculture sector from the last decades and growth of the irrigated areas. But the traditional irrigation methods are still predominant when it comes to try and correct the natural rain distribution [3]. The artificial application of water to the soil for growing crops is called as irrigation. Irrigation is mainly used in dry areas and in periods of rainfall

Cite this article as: K Nilson, G Sharmila, P Praveen Kumar. "Intelligent Auto Irrigation System Using ARM Processor and GSM". *International Conference on Innovative Trends in Electronics Communication and Applications (2015)*: 36-40. Print.

shortfalls to increase crop production. The detail analysis of the conditions must be done while providing irrigation to the land.

Types of Irrigation

1. Surface Irrigation (conventional irrigation)

2. Drip Irrigation

3. Sprinkler Irrigation

The conventional methods of irrigation like sprinklers of overhead type, flood type irrigation systems wets the lower leaves and stem of the plants. When irrigation is done by using such methods the soil surface is often saturated and stays wet for long time after irrigation is completed. These conditions leads to infections by leaf mould fungi. The flood type methods consume large amount of water and the intermediate area between crop rows remains dry and receives water only from incidental rainfall. In order to solve this problem the drip or trickle irrigation is used which is a type of modern irrigation technique that slowly applies small amounts of water to part of plant root zone [4]. Water is supplied frequently, often daily to maintain favorable soil moisture condition and prevent moisture stress in the plant with proper use of water resources.

Figure 1.Drip Irrigation at Root Zone

Drip irrigation at plant's root zone is shown in Figure 1. Its shape depends on soil characteristics. Drip irrigation system saves water because only the plant's root zone receives moisture and helps to conserve water resources. Small amount of water is lost through deep percolation if the proper amount is applied.

SYSTEM ARCHITECTURE

Automation of the irrigation system is gaining importance as there is need to use water resources efficiently and also to increase the field productivity. The system is used to turn the valves ON or OFF automatically as per the water requirement of the plants. The system is used for sensing, monitoring, controlling and for communication purpose. The system block diagram is shown in Figure 2.

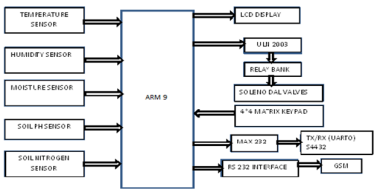

Figure 2.System Block Diagram

Cite this article as: K Nilson, G Sharmila, P Praveen Kumar. "Intelligent Auto Irrigation System Using ARM Processor and GSM". *International Conference on Innovative Trends in Electronics Communication and Applications (2015)*: 36-40. Print.

Different sensors are used to detect the different parameters of the soil like moisture, temperature, humidity, pH of soil and nitrogen content of the soil. Depending upon the sensors output the ARM9 processor will take the necessary action. The moisture sensor output will help to determine whether to irrigate the land or not depending upon the moisture content. Along with moisture sensor the temperature sensor output can also be taken into consideration while irrigating the land. If the moisture content of soil is very low and the temperature is very high then there is need of irrigation for plants, but the time for which irrigation will be provided is different for different temperature range. Because if the temperature is very high then the evaporation rate is also very high and hence we have to provide water for more time in order to attain the proper moisture level in the soil. Hence for different temperature range and moisture content level in the soil the land will be irrigated for different time interval. Soil pH is also detected and measured. pH of the soil is also important factor which will affect the plant growth. Acidic or basic nature of the soil will affect the nutrient availability in the soil. Soil nutrients i.e. macronutrients or micronutrients are helpful for plant growth and there availability depends on the pH of the soil [6]. Hence there is need to measure soil pH. Depending upon the measured pH of the soil, suggestions can be given to the farmer to add various chemicals in order to achieve the desired pH of the soil for good plant growth. Nitrogen is one of the important macronutrient which is required for plant growth. In the system the nitrogen content of the soil is also detected. According to the available nitrogen content in the soil suggestions can be given to the farmer to add the fertilizers containing nitrogen for healthy plant growth. In the system LCD display is used to display various measured parameter of the soil and also the required suggestions. Solenoid valves are used in the system which are controlled through the relay bank. The data is transmitted wirelessly by using Si4432 ISM transceiver and the data is fetched by using PC and which will be used for analyzing purpose. The keypad is used to choose the soil type in which the system will work and accordingly we can set the threshold points. Keypad is also used for manual operation. Thus the system will help to monitor, control and communicate. The system consist of following blocks:

Sensors

Sensors are the device which converts the physical parameter into the electric signal. The system consists of temperature, humidity, moisture, soil pH and soil nitrogen sensor. The output of sensor is analog signal; the signal is converted into digital signal and then fed to the processor. The temperature sensor is used to measure the temperature of the soil. Here LM35 temperature sensor is used. The output voltage of sensor is linearly proportional to the Celsius (Centigrade) temperature. The humidity sensor is used to measure the environment humidity. SY-HS-220 is used as a humidity sensor module. The relative humidity is converted to the output voltage which is the required output. The moisture sensor is used to measure the moisture content of the soil. Copper electrodes are used to sense the moisture content of soil. The conductivity between the electrodes helps to measure the moisture content level. The pH sensor helps to determine the pH of the soil. Electrode is used to measure the pH. The nitrogen sensor is used to measure the nitrogen content of the soil.

ARM 9 Processor

Here ARM9 processor AT91SAM9G45 is used. The ARM926EJ-S based AT91SAM9G45 consist of the combination of user interface functionality and high data rate connectivity. It also consists of LCD Controller, camera interface, audio, resistive touchscreen, Ethernet 10/100 and high speed USB and SDIO. The processor is running at 400MHz and multiple 100+ Mbps data rate peripherals, it has the performance and bandwidth to the network or local storage media to provide an adequate user experience. It supports the latest generation of DDR2 and NAND Flash memory interfaces for program and data storage. It consists of 133 MHz multi-layer bus architecture associated with 37 DMA channels internally, and also a dual external bus interface and distributed memory including a 64-Kbyte SRAM which can be configured as a tightly coupled memory (TCM) sustains the high bandwidth required by the processor and the high speed peripherals. The I/Os support 1.8V or 3.3V operation, and they are independently configurable for the memory interface and peripheral I/Os. The power management controller features efficient clock gating and a battery backup section which minimizes power consumption in active and standby modes.

Features

1. It consists of 32KBytes Data Cache, 32Kbytes Instruction Cache, MMU

2. Peripherals

    1. 2 High Speed Memory Card Hosts are available
    2. For communication Four USARTs are available
    3. It consist of 8-channel 10-bit ADC

3. I/O

    1. It consist of five 32-bit Parallel Input/Output Controllers
    2. It is also having 160 Programmable I/O Lines Multiplexed with up to Two Peripheral I/Os with Schmitt trigger input

Transmitter / Receiver section

ARM9↔ MAX 232↔ Tx/RxSi4432

Fig, 3.Transmitter Section

Cite this article as: K Nilson, G Sharmila, P Praveen Kumar. "Intelligent Auto Irrigation System Using ARM Processor and GSM". *International Conference on Innovative Trends in Electronics Communication and Applications (2015)*: 36-40. Print.

The transmitter section is shown in Fig. 3. It consists of ARM9, MAX 232 and Si4432 ISM transceiver. The soil parameters are sensed by the different sensors in the system. The value of the parameter sensed is stored in the ARM9 processor. The data stored is transmitted further for analyzing purpose. The Si4432 ISM transceiver is used for communication. The receiver section is shown in Fig. 4. It consists of Si4432 ISM transceiver, MAX 232 and PC. The data send by the system is fetched by using PC. The data fetched can be displayed and analyzed by using VB software. Visual Basic i.e VB is used to prepare the graphical user interface(GUI).

PC↔ MAX 232↔ Rx/TxSi4432

Fig. 4.Receiver Section

Si4432 ISM Transceiver

Silicon Laboratories' Si4432 is a highly-integrated, single chip wireless ISM transceiver and it is part of the EZRadioPRO™ family. The EZRadioPRO family includes a complete line of transmitters, receivers, and transceivers which allows the RF system designer to choose the optimal wireless part for their application. It provides advanced radio features. It provides continuous frequency coverage from 240–930 MHz and adjustable output power of up to +20 dBm with the Si4432. The Si4432 provides high level of integration which reduces

BOM cost while simplifying overall system design. The low receive sensitivity (–118 dBm) when coupled with the Si4432's industry-leading +20 dBm output power ensures extended range and improved link performance. The range can be extended by using built-in antenna diversity and through frequency hopping; it also helps to enhance performance. The system link budget is improved by 8-10 dB as antenna diversity is completely integrated into the Si443x which results in substantial increase of range under adverse environmental conditions. The Si4432 receiver uses a single-conversion architecture to convert the 2-level SK/GFSK/OOK modulated receive signal to a low IF frequency. Following a programmable gain amplifier (PGA) the signal is converted to the digital domain by a high performance delta-sigma ADC allowing filtering, demodulation, slicing, error correction, and packet handling to be performed in the built-in DSP, increasing the receiver's performance and flexibility versus analog based architectures.

Features

1. Frequency Range = 240–930 MHz (Si4432/31)
2. FSK, GFSK, and OOK modulation
3. It is having maximum output power of +20 dBm (Si4432)
4. Low Power Consumption-18.5 mA receive transmit -27mA@ +11 dBm
5. It supports data rate from 1 to 128 kbps
6. It requires power supply of 1.8 to 3.6 V
7. It consist of ultra-low power shutdown mode
8. It is having Auto-frequency calibration (AFC) feature
9. It supports TX and RX of 64 byte with FIFOs
10. It comprises of temperature sensor and 8-bit ADC
11. Frequency hopping capability is available
12. It is provided with on-chip crystal tuning

GSM Module

The block diagram of the proposed GSM based system is given in fig. 2. In this system GSM modules is interfaced with the main controller chip. GSM is used for remotely monitoring and controlling the devices via a mobile phone by sending and receiving SMS via GSM network.

SOFTWARE

KEIL µ Vision (IDE)

Keil an ARM company makes C compilers, macro assemblers, real-time kernels, debuggers, simulators, integrated environments, evaluation boards, and emulators for ARM7/ARM9/Cortex-M3, XC16x/C16x/ST10, 251 and 8051 MCU families. When starting a new project simply select the microcontroller you use from the Device Database and the µVision IDE sets all compiler, assembler, linker, and memory options. The Keil ARM tool kit includes three main tools, assembler, compiler and linker. An assembler is used to assemble the ARM assembly program. A compiler is used to compile the C source code into an object file. A linker is used to create an absolute object module suitable for in-circuit emulator. Here visual basic software is used on the PC. The data send by the system is fetched by PC which is used for analysis purpose. The algorithm to view the data is given below.

Algorithm

1. Start

Cite this article as: K Nilson, G Sharmila, P Praveen Kumar. "Intelligent Auto Irrigation System Using ARM Processor and GSM". *International Conference on Innovative Trends in Electronics Communication and Applications (2015)*: 36-40. Print.

2. Open the main form.

3. Select com port of PC.

4. Open wireless data communication.

5. Capture the wireless data.

6. Store the data in database.

7. Show the respective data to user for analysis.

8. End.

ADVANTAGES OF PROPOSED SYSTEM

Relatively simple to design and no man power needed.

1. Reduce soil erosion and nutrient leaching.
2. It consumes less than half of the water needed for a sprinkler system.
3. Fertilizers can also be provided by using the system
4. pH and nitrogen content of the soil is maintained through the suggestions which helps for healthy plant growth.

CONCLUSION

The objective of this paper is to design a fully automated drip irrigation system using GSM and ARM processor. The system provides a real time feedback control module which monitors and controls all the activities of drip irrigation system efficiently. The system valves are turn ON or OFF automatically depending upon the moisture content. This will also provide the efficient information regarding the soil pH and soil nutrients like nitrogen along with the proper suggestions. The data collected by the system can be sending for further analysis purpose. Finally, it is concluded that, with this proposed system one can save manpower and water to improve production which ultimately increases the profit.

REFERENCES

[1] Yunseop(James) Kim et al, "Remote Sensing and Control of an Irrigation System Using a Distributed Wireless Sensor Network", IEEE transactions on instrumentation and measurement, vol.57,no.7, pp.1379- 1387, July 2008.

[2] Mahir Dursun and Semih Ozden," A wireless application of drip irrigation automation supported by soil moisture sensors", Scientific Research and Essays Vol. 6(7), pp. 1573-1582, 4 April, 2011.

[3] Gracon H. E. L. de Lima et al, "WSN as a Tool for Supporting Agriculture in the Precision Irrigation", 2010 Sixth International Conference on Networking and Services, pp.137-142, 2010.

[4] K.Prathyusha1 et al, "Design of embedded systems for the automation of drip irrigation", IJAIEM Volume 1, Issue 2, October 2012.

[5] Yiming Zhou et al, "A Wireless Design of Low-Cost Irrigation System Using ZigBee Technology", IEEE 2009 International Conference on Networks Security, Wireless Communications and Trusted Computing, vol. 1, pp.572 – 575, 2009.

[6] Gayatri Londhe et al, "Automated Irrigation System By Using ARM Processor", IJSRET Volume 3, Issue 2, May 2014.

[7] Vasif Ahmed and Siddharth A. Ladhake; "Design of ultra-low cost cell phone based embedded system for irrigation"; Vol. 55, No. 2 , IEEE Transactions on Consumer Electronics, 2010.

[8] I.F. Akyildiz, W. Su et al, "Wireless sensor networks: a survey", IEEE Transactions on Consumer Electronics, vol. 44, pp. 1291-1297, Aug 2002.

[9] Mahir Dursun, Semih Ozden; "A prototype of PC based control of irrigation" International conference on Environmental Engineering and Applications, vol. 50, pp. s255-258, Nov. 2010.

[10] Ma Shuying et al, "Design of a new measurement and control system of CO2 for greenhouse based on fuzzy control", International Conference on Computer and Communication Technologies in agriculture engineering 2010, pp 128-131, May 2008.

Cite this article as: K Nilson, G Sharmila, P Praveen Kumar. "Intelligent Auto Irrigation System Using ARM Processor and GSM". *International Conference on Innovative Trends in Electronics Communication and Applications (2015)*: 36-40. Print.

International Conference on Innovative Trends in Electronics Communication and Applications 2015 [ICIECA 2015]

ISBN	978-81-929742-6-2	**VOL**	01
Website	icieca.in	**eMail**	icieca@asdf.res.in
Received	02 - April - 2015	**Accepted**	15 - November - 2015
Article ID	ICIECA007	**eAID**	ICIECA.2015.007

A Novel Image Encryption Scheme on the Basis of Genetic Algorithm and Chaos

R Ranjith kumar[1], S Jayasudha[1], S Pradeep[2]
[1]Assistant Professor, [2] UG scholars
Department of ECE, P.A. College of Engineering and Technology, India

Abstract: *This paper focuses on a symmetric image encryption scheme that exploits the basis of genetic algorithm and chaos. The proposed scheme employs only one round encryption to achieve the satisfactory level of security. Plain image is converted into bit stream and the cross over operation in GA is used to perform the modification of pixel in bit level and the population for GA is believed to be the bytes in binary format of the plain image. The key generator [18] that employs chaotic maps increases the sensitivity of the external keys. It is the seed to generate the Random number sequence (RNS) and Mask. RNS is used for crossover operation and Mask is used for breaking correlation among the pixels after crossover. The statistical and experimental results prove the robustness of the proposed scheme.*

Keywords*:* Genetic algorithm, Chaos, Image encryption, Logistic map

INTRODUCTION

The world and the technologies in it are developing in a faster manner, so the threat of secure transmission of the information is essential. The amount of information being transferred in the internet has been increased a lot in these decades. Most of the information is in the form of images. The main question to be asked is that, are these images transferred in a safe manner? The answer for this question is may be or may not be. There is an essentiality that most important information like military and medical images should be transferred with high security. For the transfer of high risk images image processing is a boon. The images have to be modified in a certain way that none could able to access the original information behind it except the sender. This is so called encryption of the image. Many schemes have been proposed in the recent years which are based on many logics. The proposed system is based on GA (Genetic Algorithm) and Chaotic systems.

Genetic algorithms which are commonly called as GA was first developed in order to mimic some of the naturally occurring processes [1]. But in recent days its use has been extended in the processing of images. With the help of GA the encryption of the images can be performed in a better way than many other concepts and it is secure since it is not utilising the natural numbers directly. One of the main notions of the GA is crossover which employs the swapping of data between two points in a byte which is selected by the key given by the user. There are many a type of crossover namely single point crossover, two point crossover, three parent crossover and uniform crossover [2]. The proposed system uses two point crossover techniques, according to which random points are selected and the crossover operation is carried out. Hence the crossover concept of GA plays vital role in the proposed scheme.

The second and the foremost important concept used in the proposed scheme is Chaos [3]. In 1991, thoshiki habutus [4] proposed a system where the cipher image can be obtained by the inverse chaotic mapping concept. Chaos theory has been spread out in many areas where image processing also owns its place [5]-[15] as the system which is built with the chaos has high security and highly sensitive to the conditions which are given at the initial state and the failure of the system is almost rare. Hence the utilisation of the

Cite this article as: R Ranjith kumar, S Jayasudha, S Pradeep. "A Novel Image Encryption Scheme on the Basis of Genetic Algorithm and Chaos". *International Conference on Innovative Trends in Electronics Communication and Applications (2015)*: 41-48. Print.

basis of chaos in the field of image processing keeps on growing. The proposed method combines the elements of GA and Chaos to develop a secure image encryption scheme. It utilizes the key generator [18].The plain image is converted into its binary format and the cross over is performed to modify the pixels in the first stage and the Mask generated from the chaotic maps is applied on the output of the first stage to increase the robustness of the scheme. The proposed system achieves the required level of security in single round [16][17].Different analyses performed on the cipher image proves the randomness and robustness of the cipher. The rest of this paper is managed as follows, section 2 depicts proposed method, and section 3 furnishes the results of various analyses and section 4 is the conclusion.

PROPOSED METHOD

Figure 1 shows the block diagram of proposed method. The plain image of size MxN (8 bpp) is primarily converted into its binary format (I_b) of size (MxN)xn, where n represents the number of bits required for representing a pixel (in this case n=8). Each row of resulting I_b will own a single pixel. I_b is believed as the initial population for the basis of GA. The proposed scheme utilises the crossover operation in GA in order to perform the modification in the initial pixels before the application of the mask. The RNS produces two different random sequences to carry out the crossover among the rows of I_b. After performing the crossover, Modified I_b of size (MxN)xn is then converted into MxN image. This image is then fed into the next section where MxN mask is available for performing the XOR operation. The final image after applying the above process is called as the cipher image. The RNS and Mask obtains the initial seed from the key generator.

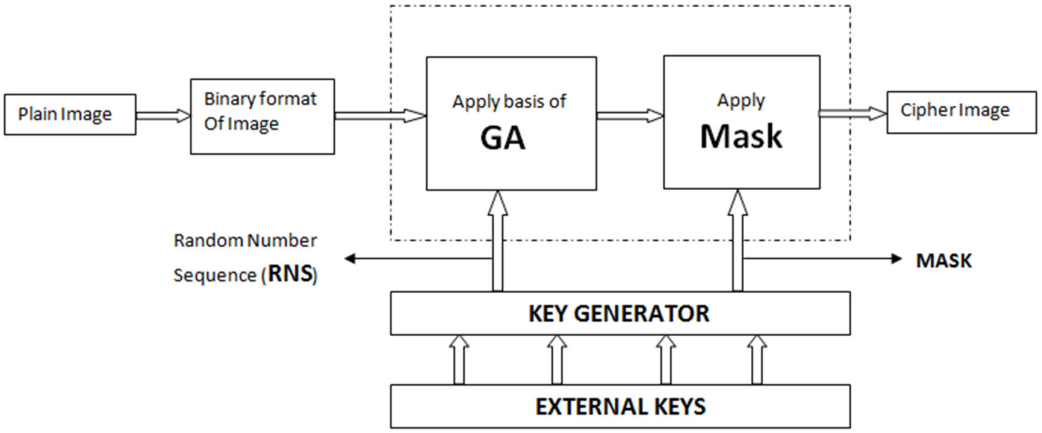

Figure 1 Proposed method

RNS and MASK GENERATION

The proposed system gives rise to 4 keys, each of 53 bits in size. These external keys are fed as the input for key generator [18] in order to increase the sensitivity of keys. The generated external keys are then seeded to generate RNS and apply the mask to it.

RNS

Let the seed from the key generator be X_{il}, then two random number sequence are generated with respect to this seed.

RNSS (random number sequence for selection): This sequence will be in the order of 1 to (MxN).it is generated by chaotic logistic map of the equation,

$$Y_{i+1}=by_i(1-y_i) \quad (1)$$

where b is greater than 3.7 to get chaotic behaviour. RNSS is used for random selection in I_b,

$$RNSS = (Y \times 10^{14} \bmod (MxN)) + 1 \quad (2)$$

RNSS will be a 1x(MxN) vector.Pseudo code 1 shows the procedure for generating RNSS.

RNSCO (random number sequence for crossover): This sequence will be in the range of 2-5, since the cross over is performed on 8 bits. Chaotic tent map is used for the generation of RNSCO,

$$Z_{i+1} = \begin{cases} \mu Zi & Zi \le 0.5 \\ \mu(1-Zi) & Zi > 0.5 \end{cases} \quad (3)$$

where $\mu>1.9$ for chaotic behaviour. The range 2-5 can be achieved by the following equation.

$$RNSCO = (Z \times 10^{14} \bmod 4) + 2 \quad (4)$$

RNSCO will be a 1x((MxN)/2) vector.pseudo code 2 shows this process.

MASK GENERATION

Cite this article as: R Ranjith kumar, S Jayasudha, S Pradeep. "A Novel Image Encryption Scheme on the Basis of Genetic Algorithm and Chaos". *International Conference on Innovative Trends in Electronics Communication and Applications (2015)*: 41-48. Print.

The size of the mask is as same as the size of the plain image (i.e., MxN). The internal key from the key generator X_{i2} is used as the seed for the generation of the mask. The values in the mask are in the range of (0-255). Both the logistic and the tent map are used for the generation of the mask. ie., LT [18] system is used by which the total space is divided into two. For the odd places, the logistic map is used and for the even places, tent map is used.

$$Mask_{i+1} = b \times mask_i \times (1-mask_i), \quad \text{for i= } 1,3,5,7,\ldots\ldots \text{ (MxN)-1}$$

$$Mask_{i+1} = \begin{cases} \mu\, x\, maski & maski \le 0.5 \\ \mu(1-maski) & maski > 0.5 \end{cases} \quad \text{for i= } 2,4,6,8\ldots\ldots\ldots\ldots\ldots\text{(MxN)} \qquad (5)$$

Finally the mask is reshaped from 1x(MxN) to MxN. The generated values are then modified into the range (0-255) using,

$$Final\_mask = (Mask \times 10^{14} \bmod 256) \qquad (6)$$

Refer pseudo code 3 for this process.

BASIS OF GA and MASKING

The 'apply basis of GA' block will perform the cross over operation on I_b. A pair is selected from I_b based on RNSS values and crossover is applied on the selected pair. The modified values will be placed on the locations where the pair was taken. The following steps explain this process.

Step 1: Get RNSS vector of size 1x(MxN) that has values in the range(1 to MxN). For each pair of value in RNSS get the corresponding values of I_b in A and B.

$A = I_b(RNSS(i))$ i.e.. i^{th} row of I_b

$B = I_b(RNSS(i+1))$ i.e.. $i+1^{th}$ row of I_b

Step 2: Get RNSCO vector of size 1x((MxN)/2).Each value in RNSCO determines the cross over point for the pair A,B.

Let A = [0 0 0 0 1 1 1 1] , B = [1 1 1 1 0 0 0 0] and RNSCO = 4

Then cross over is applied as shown below,

A = [0 0 0 0 1 1 1 1] B = [1 1 1 1 0 0 0 0]

A_modified = [0 0 0 0 0 0 0 0] B_modified = [1 1 1 1 1 1 1 1]

Step 3: Replace existing values of A and B in I_b with modified values(i.e.. update I_b).

Step 4: Increment i and repeat step 1 – 3 until i reaches the end of RNSS.

Step 5: Convert the updated I_b into pixels and resize the result to MxN.

Even though this modification of pixels breaks the correlation among the pixels, there is a possibility of unchanged pixels in plain image after the application of GA. If A and B are same then cross over will not modify the value of pixel according to the steps explained above. To completely break the correlation among the pixels, one more technique called masking is employed. The block named 'apply mask' will perform this operation. The Mask generated by the LT system is applied to the output from the GA block. The resulting image is called cipher image which is completely random in nature. Single round is enough for the cipher is enough to attain the required level of security and is proved using various statistical and differential analyses in section 3.

Pseudo code 1:

```
Initialize i =1;
y[i] = X_i1;
// X_i1 is initial seed from key //generator
for i=1: M*N-1
y[i+1] = 4*y[i]*(1-y[i]); // y is a vector of 1 x (MxN)
end
RNSS = mod ( y*10^14 , MxN) + 1
```

Pseudo code 2:

```
Initialize i =1;
z[i] = X_i1;
// X_i1 is initial seed from key //generator
for i=1: M*N / 2
if z[i] <= 0.5
z[i+1] = 2*z[i];
// z is a vector of 1 x (MxN / 2)
else
z[i+1] = 2*(1-z[i]);
end
end
RNSCO = mod ( z*10^14 , 4) + 2
```

Pseudo code 3:

```
Initialize i =1;
Mask[i] = X_i2;
// X_i2 is initial seed from key //generator
for i=1: M*N
if i+1 is even:
if Mask[i] <= 0.5
Mask[i+1] = 2*Mask[i];
// z is a vector of 1 x (MxN)
else
Mask[i+1] = 2*(1-Mask[i]);
end
if i+1 is odd:
Mask[i+1] = 4*Mask[i]*(1-Mask[i])
end
Mask = mod ( Mask*10^14 , 256)
Mask = reshape(Mask,[M N])
```

PERFORMANCE ANALYSIS

KEY SPACE ANALYSIS

A key space of 2^{212} is used in the proposed scheme which is much more sufficient for security. The two important aspects that are contained by the key are exhaustive search that characterise the ability to withstand any type of brute force attack and non-recovery property that specifies how strong the key is infeasible to the attacks. To maintain the system in its high secure state the minimum value of R (number of rounds) can be obtained from the relation [11],

Cite this article as: R Ranjith kumar, S Jayasudha, S Pradeep. "A Novel Image Encryption Scheme on the Basis of Genetic Algorithm and Chaos". *International Conference on Innovative Trends in Electronics Communication and Applications (2015)*: 41-48. Print.

$$R = floor\left[\frac{128}{\log_2 L}\right] + 1 \tag{7}$$

since L = 212 in this system, R = 1.From the NPCR,UACI,NBCR and MAE values which are in Table 2., it can be seen that the system has much more resistance and can withstand any kind of brute-force attacks and requires just an one round encryption

STATISTICAL ANALYSIS

These are the tests which are mainly employed to investigate the robustness of the system which can be calculated by histograms and correlation coefficients of both the plain image and cipher image.

HISTOGRAM ANALYSIS

Histograms are the graphs which are drawn between pixel intensity and their number of occurrences. Each image possesses its own histograms which are widely different from one another. Here image encryption schemes modify the histogram to avoid known plain text attacks. Figure 2 (a) and (b) shows the original image and its corresponding encrypted image. Figure 2(c) and (d) shows their respective histograms. The proposed scheme completely flattens the histogram which shows the encrypted image has pixels that are having approximately equal number of occurrences. It proves the randomness of the cipher image.

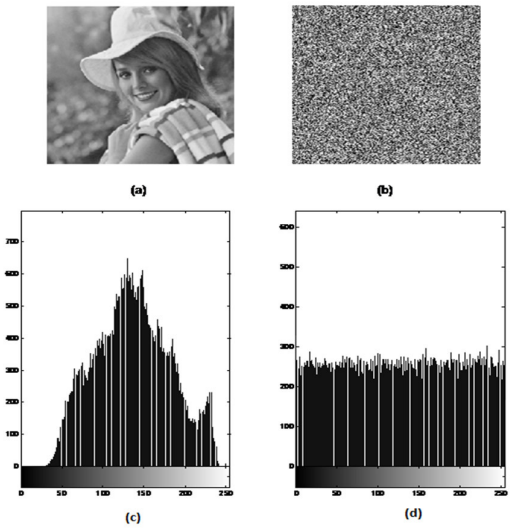

Figure 2 Histogram analysis (a) Plain image (b) Encrypted image (c) Histogram of plain image (d) Histogram of Encrypted image

CORRELATION COEFFICIENT ANALYSIS

Correlation between the pixels of the image must also be analyzed to check the robustness of the system. Generally the correlation between the adjacent pixels in the original images is high but for a good encrypted image it has to me minimised. This analysis is carried out by selecting 10,000 pairs randomly in the manner that they are horizontally, vertically and diagonally adjacent. The correlation can be calculated by using the formula,

$$r_{xy} = \frac{\mathrm{cov}(x, y)}{\sqrt{D(x, y)\sqrt{D(y)}}} \tag{8}$$

where,

$$\mathrm{cov}(x, y) = E\{(x - E(x)) - (y - E(y))\}$$

where, x and y denotes the two adjacent pixels in the image and E(x) and D(y) denotes the mean and standard deviation of corresponding grey levels. Correlation coefficients are compared with different algorithms and tabulated in Table 1.From Table 1, the correlation which is nearly 1 for the plain image is broken nearly to 0 which means that the encrypted image is highly uncorrelated.

INFORMATION ENTROPY ANALYSIS

Cite this article as: R Ranjith kumar, S Jayasudha, S Pradeep. "A Novel Image Encryption Scheme on the Basis of Genetic Algorithm and Chaos". *International Conference on Innovative Trends in Electronics Communication and Applications (2015)*: 41-48. Print.

Information entropy is generally to describe the degree of uncertainty that is present in a system and can be calculated by using the formula,

$$H(m) = \sum_{i=0}^{M-1} p(m_i) \log \frac{1}{p(m_i)} \tag{9}$$

where, m and p (m_i) represents the total number of symbols and probability of occurrence of the symbol respectively. In practical, the information entropy generates random messages but is expected to have a value which is less than ideal one (in this case 8).Entropy must be same as ideal for cipher image so that the enemy cannot guess any part of the image. Table 2 proves the above statement, which the entropy values of the cipher nearly equal to 8 (ideal).

DIFFERENTIAL ATTACK

NPCR and UACI: When a system must resist all kind of attacks it should always be sensitive even a fraction change in the plaintext and key. NPCR and UACI which have been proposed by the NIST [19] are the mostly used methods for testing the sensitivity.

$$NPCR = \frac{1}{n} \| \{ i \mid x_i \neq y_i, i = 0,1,\ldots n-1 \} \| \tag{10}$$

$$UACI = \frac{1}{n} \sum_{i}^{n-1} \frac{| x_i - y_i |}{255} \tag{11}$$

Given two images $x = \{x0, x1, \ldots, xn\text{-}1\}$ and $y = \{y0, y1, \ldots, yn\text{-}1\}$, the NPCR and UACI are defined in Eq.(8) and Eq.(9) [18]. For two random images, the average NPCR is about 0.9961, and the average UACI is about 0.3346 [19]. The NPCR and UACI values for various images are calculated and tabulated in Table 2.

MAE: Mean Absolute Error is an another method to perform the tests on the system against differential attacks[16]. Let C(i, j) and P(i, j) be the gray level of the pixels at the i^{th} row and j^{th} column of a M×N cipher and plain-image, respectively. Then the mean absolute error can be calculated using the formula,

$$MAE = \frac{1}{M \times N} \sum_{j=0}^{N} \sum_{i=0}^{M} | c(i, j) - p(i, j) | \tag{12}$$

The values for various images are calculated and are tabulated in Table 2. Larger value of MAE indicate better security[16].

Strict Avalanche Criterion: The strict avalanche criterion (SAC) is intended to examine the changes in bit-level. According to SAC a single bit change in input will lead to an inundation change in the output. The Number of Bit Change Rate (NBCR) is defined in [20] and is used to measure the SAC performance using Eq.(13).The ideal NBCR is 50% in average [20]:

$$NBCR = \frac{H_m[s_1, s_2]}{L_b} \times 100 \tag{13}$$

$H_m[.]$ calculates the Hamming distance between two encrypted bit streams(s_1 and s_2) obtained by slight difference in the key. L_b is length of the bit stream. The NBCR values listed in Table 2 shows that the system performs efficiently against the differential attacks in bit level.

Randomness test with sp800-22 test suite: The two main strategies which are recommended by the NIST [23] to perform the analysis on the system are checking the P-values that are uniformly distributed over the interval [0, 1] and comparison of the expected value with the value that are calculated from the proportion of the sequence. A large sequence of the binary number has been employed in checking the uniform distribution of the P-value in each test that has been performed. The computation is as follows:

$$\chi^2 = \sum_{i=1}^{10} \frac{(F_i - N/10)}{N/10} \tag{14}$$

Where F_i represents the number of occurrences that the P-value contains in i^{th} interval and N denotes the size of the sample. The P-values can be calculated from the following Eq.

$$P - Value = igamc\left(\frac{9}{2}, \frac{\chi^2}{2}\right) \tag{15}$$

Here, igmac is the incomplete Gamma function. When the P-values are greater than or equal to 0.0001 then it shows that the encrypted image has P-values that are distributed uniformly. The outcomes are tabulated in Table 3. The encrypted image given by the proposed system has passed all the tests and also proved that its distribution is uniform. Hence from the NIST test it can be concluded that the encrypted image from the proposed system is highly random in nature.

Table 1. Comparison of correlation coefficients.

Cite this article as: R Ranjith kumar, S Jayasudha, S Pradeep. "A Novel Image Encryption Scheme on the Basis of Genetic Algorithm and Chaos". *International Conference on Innovative Trends in Electronics Communication and Applications (2015)*: 41-48. Print.

Scheme	Horizontal	Vertical	Diagonal
Original Lena image	0.9882	0.9856	0.9669
AES[19]	0.0770	0.0660	-
Algorithm[21]	0.0845	0.0681	-
Algorithm[22]	0.0965	-0.0318	
Algorithm[18]	-0.0094	-0.0003	-0.0039
Algorithm[17]	0.0015	0.0069	0.0018
Proposed method	-0.0006	-0.0021	0.0022

Table3. NIST Test results

Statistical Test		P-Value	Result
Frequency		0.6065	Success
Block Frequency		0.5502	Success
Runs		0.0852	Success
Statistical test		0.5322	Success
Long runs of one's		1.0000	Success
Binary Matrix Rank		0.4015	Success
Spectral DFT		1.0000	Success
No overlapping templates		0.7312	Success
Overlapping templates		0.9983	Success
Universal		0.6642	Success
Serial	P – Value 1	0.8526	Success
	P – Value 2	0.4029	
Approximate Entropy		0.5816	Success
Cumulative sums		0.5753	Success
Random excursions		0.7725	Success
Random excursions variant		0.4959	Success

CONCLUSION

The proposed encryption scheme utilizes the basis of GA and Chaos to develop a secure image encryption scheme. A mixture of analyses has been carried out to prove the security level of proposed encryption scheme. The proposed method uses crossover operation in GA to perform pixel modification in bit level. Chaotic maps are utilized to generate random number sequences for the assist of crossover and Mask generation. It has a superior sensitivity to the little change in the key due to the structure proposed for key generation and has single round to achieve the necessitated security. The results of various tests like NPCR, UACI, MAE and NBCR proves that the system is robust and can survive against any security attack.

Table 1. Differential and Entropy analysis

Cite this article as: R Ranjith kumar, S Jayasudha, S Pradeep. "A Novel Image Encryption Scheme on the Basis of Genetic Algorithm and Chaos". *International Conference on Innovative Trends in Electronics Communication and Applications (2015)*: 41-48. Print.

S.NO	IMAGE	ENTROPY		NPCR	UACI	MAE	NBCR
		Plain	Cipher				
1.	5.1.09.tiff	6.7093	7.9967	0.9963	0.3335	67.1615	49.8772
2.	5.1.11.tiff	6.4523	7.9971	0.9962	0.3350	85.6294	49.9851
3.	aerial.bmp	6.9940	7.9971	0.9959	0.3339	80.3379	49.9743
4.	airfield.bmp	6.8303	7.9967	0.9960	0.3352	82.1247	50.0040
5.	bananas.png	7.1883	7.9968	0.9966	0.3342	92.985	49.9851
6.	almonds.png	7.3286	7.9965	0.9965	0.3333	77.8629	49.9847
7.	apples.png	7.6688	7.9965	0.9960	0.3328	85.0347	49.8781
8.	baloons.png	7.6934	7.9966	0.9955	0.3347	78.3416	50.0355
9.	barbara.bmp	4.4858	7.9968	0.9959	0.3347	107.439	50.0502
10.	billiard_ball.png	7.8777	7.9971	0.9963	0.3334	86.9552	49.9750
11.	boat..tiff	7.1914	7.9964	0.9960	0.3334	68.4918	49.8974
12.	bridge.bmp	5.7056	7.9972	0.9962	0.3336	80.381	49.8699
13.	building.png	7.4974	7.9967	0.9962	0.3348	81.6513	50.0507
14.	cameraman.bmp	6.9046	7.9969	0.9954	0.3345	88.3031	49.9626
15.	cards.png	7.7015	7.9966	0.9956	0.3339	89.4539	50.0629
16.	carrots.png	7.2489	7.9966	0.9961	0.3341	83.1118	49.9954
17.	chairs.png	7.0077	7.9968	0.9958	0.3343	77.0681	49.8800
18.	clips.png	7.8975	7.9965	0.9963	0.3339	87.1048	50.0389
19.	clown.bmp	5.3684	7.9972	0.9959	0.3338	94.5873	50.1364
20.	coins.png	7.4779	7.9966	0.9964	0.3356	81.8701	50.0628
21.	couple.bmp	7.0572	7.9964	0.9957	0.3331	68.3726	50.1125
22.	crowd.bmp	6.7893	7.9975	0.9959	0.3341	78.1304	50.0637
23.	cushions.png	7.8200	7.9969	0.9961	0.3353	85.7439	50.1371
24.	dollar.bmp	6.9785	7.9967	0.9963	0.3350	85.6641	50.0174
25.	ducks.png	7.7216	7.9968	0.9962	0.3350	76.9442	49.9933
26.	fence.png	7.5103	7.9968	0.9960	0.3340	81.5195	49.9041
27.	finger.bmp	7.1075	7.9970	0.9964	0.3336	71.5721	49.9588
28.	flowers.png	7.9327	7.9966	0.9961	0.3350	84.1959	49.9222
29.	garden_table.png	7.5886	7.9971	0.9956	0.3344	77.1007	49.9699
30.	girlface.bmp	7.0818	7.9968	0.9964	0.3348	82.3625	50.0423
31.	goldhill.bmp	4.5028	7.9971	0.9961	0.3352	107.701	49.9784
32.	guitar_bridge.png	7.2723	7.9970	0.9959	0.3346	84.7575	50.0929
33.	lighthouse.bmp	7.4486	7.9970	0.9960	0.3353	73.0076	49.9535
34.	houses.bmp	7.6548	7.9971	0.9960	0.3350	79.1343	50.0881
35.	trucks.bmp	6.5632	7.9964	0.9964	0.3341	71.2126	49.9289
36.	keyboard.png	6.5977	7.9966	0.9962	0.3355	84.3599	50.0332
37.	kiel.bmp	6.9589	7.9964	0.9961	0.3367	70.2597	50.0151
38.	snails.png	7.6659	7.9970	0.9963	0.3350	86.0029	49.9506
39.	lena.tif	7.4451	7.9967	0.9961	0.3347	68.3637	50.0689
40.	lion.png	7.1707	7.9974	0.9960	0.3348	90.2793	49.9369
41.	livingroom.tif	7.2952	7.9969	0.9962	0.3350	68.4693	50.0715
42.	mandril_gray.tif	7.2925	7.9969	0.9965	0.3350	71.3210	50.0198
43.	mountain.bmp	4.7981	7.9974	0.9966	0.3351	105.637	50.0263
44.	pencils.png	7.8439	7.9968	0.9959	0.3335	79.1839	50.0656
45.	guitar_head.png	7.4193	7.9964	0.9965	0.3338	82.3748	49.9245
46.	woman_blonde.tif	6.9542	7.9964	0.9956	0.3336	70.8953	49.9054

REFERENCES

Cite this article as: R Ranjith kumar, S Jayasudha, S Pradeep. "A Novel Image Encryption Scheme on the Basis of Genetic Algorithm and Chaos". *International Conference on Innovative Trends in Electronics Communication and Applications (2015)*: 41-48. Print.

[1] S. N. Sivanandan, S. N. Deepa, "Introduction to Genetic Algorithm",Springer Verlag Berlin Heidelberg, 2008.
[2] M. Mitchell, "An Introduction to Genetic Algorithms," The MIT Press, Cambridge,USA, 1999.
[3] Jiri Fridrich, "Image Encryption Based on Chaotic Maps", Proceeding of IEEE Conference On Systems, Man, and Cybernetics, pp. 1105-1110, 1997.
[4] Habutsu T et al. "A secret cryptosystem by iterating a chaotic map" Eurocrypt 1991:127-40.
[5] Frank Dachselt and Wolfgang Schwarz, "Chaos and Cryptography", IEEE Transactions on Circuits and Systems I: Fundamental Theory and Applications, Vol. 48, No. 12, pp. 1498– 1509, 2001.
[6] K.W. Wong, "A fast chaotic cryptographic scheme with dynamic look-up table", Physics Letters A, Vol. 298, No. 4, pp. 238–242, 2002.
[7] Wai-kit Wong, Lap-piu Lee and Kwok-wo Wong, "A modified chaotic cryptographic method", Computer Physics Communications, Vol. 138, No. pp. 234-236, 2001.
[8] J. Fridrich, "Symmetric ciphers based on two dimensional chaotic maps", International Journal of Bifurcation Chaos, Vol. 8, No. 6, pp. 1259-1284, 1998.
[9] S. Lian, J. Sun and Z. Wang, "A block cipher based on a suitable use of chaotic standard Map", Chaos, Solitons and Fractals, Vol. 26, No. 1, pp. 117–129, 2005.
[10] Kwok-Wo Wong, Bernie Sin-Hung Kwok, and Wing-Shing Law, "A Fast Image Encryption Scheme based on Chaotic Standard Map", Physics Letters A, Vol. 372, No. 15, pp. 2645– 2652, 2008.
[11] M. Francois, T. Grosges, D. Barchiesi and R. Erra, "A new image encryption scheme based on a chaotic function", Image Communication, Vol. 27, No. 3, pp. 249–259, 2012.
[12] A. Ahmed, Abd El-Latif, Li Li, Tiejun Zhang, Ning Wang, Xianhua Song and Xiamu Niu, "Digital image encryption scheme based on multiple Chaotic systems", Sensing and Imaging, Vol. 13, No. 2, pp. 67–88, 2012.
[13] Yong Wang, Kwok-Wo Wong, Xiaofeng Liao and Tao Xiang, "A block cipher with dynamic S-boxes based on tent map", Communications in Nonlinear Science and Numeric Simulation, Vol. 14, No. 7, pp. 3089–3099, 2009.
[14] Yang Tang, Zidong Wang and Jian-an Fang, "Image encryption using chaotic coupled map lattices with time-varying delays", Communications in Nonlinear Science and Numeric Simulation, Vol. 15, No. 9, pp. 2456–2468, 2010.
[15] T.S. Parker and L.O. Chua, "Chaos: a tutorial for engineers", Proceedings of the IEEE, Vol.75, No. 8, pp. 982–1008, 1987.
[16] Benyamin Norouzi, Sattar Mirzakuchaki, Seyed Mohammad Seyedzadeh and Mohammad Reza Mosavi, "A simple, sensitive and secure image encryption algorithm based on hyper-chaotic system with only one round diffusion process", Multimedia Tools and Applications,Vol. 71, No. 3, pp. 1469-1497, 2014.
[17] R. Ranjith Kumar, B.Saranraj and S.Pradeep, "A new one round image encryption algorithm based on multiple chaotic systems", ICTACT Journal on Image and Video Processing, Vol.5, No. 4, pp. 1017-1023, 2015
[18] R. Ranjith Kumar and M. Bala Kumar, "A New Chaotic Image Encryption Using Parametric Switching Based Permutation and Diffusion", ICTACT Journal on Image and Video Processing, Vol. 4, No. 4, pp. 795-804, 2014.
[19] J. J. Buchholz, "Matlab implementation of the Advanced Encryption Standard", http://buchholz.hs-bremen.de/aes/aes.htm, 2001.
[20] R. Forre, "The strict avalanche criterion: spectral properties of boolean functions and an extended definition", Proceedings on Advances in Cryptology, pp. 450–468, 1990.
[21] Hongjun Liu and Xingyuan Wang, "Color image encryption based on onetime keys and robust chaotic Maps", Computers & Mathematics with Applications, Vol. 59, No. 10, pp. 3320–3327, 2010.
[22] Nooshin Bigdeli, Yousef Farid and Karim Afshar, "A robust hybrid method for image encryption based on Hopfield neural network", Computers and Electrical Engineering, Vol. 38, No. 2, pp. 356–369, 2012. National Institute of Standards and Technology, http://csrc.nist.gov/publications/nistpubs/800-22-rev1a/SP800-22rev1a.pdf.

Cite this article as: R Ranjith kumar, S Jayasudha, S Pradeep. "A Novel Image Encryption Scheme on the Basis of Genetic Algorithm and Chaos". *International Conference on Innovative Trends in Electronics Communication and Applications (2015)*: 41-48. Print.

International Conference on Innovative Trends in Electronics Communication and Applications 2015 [ICIECA 2015]

ISBN	978-81-929742-6-2	**VOL**	01
Website	icieca.in	**eMail**	icieca@asdf.res.in
Received	02 - April - 2015	**Accepted**	15 - November - 2015
Article ID	ICIECA008	**eAID**	ICIECA.2015.008

Impact of GSM Spectrum Auction in 900 & 1800 MHz Band

Somya Agrawal[1], Neelesh Gupta[2], Meha Shrivastava[3]
[1]M-TECH Research Scholar, TIEIT, Bhopal, India
[2]HEAD-EC Dept., TIEIT, Bhopal, India
[3]Asst. Professor, TIEIT, Bhopal, India

Abstract: *Recently Government of India Auctioned 2G spectrums in both 900 MHz & 1800 MHz Band For the GSM operators whose spectrum License is getting over shortly. If an existing 900 MHz band operator receives 1800 MHz band in the New Auction Process, then it will be interesting to learn about the impact on signal coverage of sites at the same location working at different GSM Frequency Band, before and after the new allocated spectrum implementation on field. In order to estimate the signal parameters accurately for mobile system, propagation analysis provides a good initial estimate of the signal characteristics and path loss. The path loss is associated with the design of base stations as this tells us how much a transmitter has radiated to service a given region. Planning tool is used to assist engineers in designing and optimizing wireless networks by providing an accurate and reliable prediction of coverage, which gives RF engineers a state-of-the-art tool to Design wireless networks, Plan network expansions, Optimize network performance & Diagnose system problems. This paper gives an overview of the differences in the propagation losses for 900 MHz and 1800 MHz frequency band using the suitable propagation model and ATOLL tools. It presents a description of the practical propagation modal, their methodology to plot Coverage predictions.*

Keywords*:* GSM, Planning Tool, propagation losses, propagation model

INTRODUCTION

The commercial success of cellular communication, since its initial implementation in the early 1980s, has led to an intense interest among wireless engineers in understanding and predicting radio-propagation characteristics in various urban and suburban areas, and even within buildings. As the explosive growth of mobile communications, it is very valuable to have the capability of determining optimum base-station location, obtaining suitable data rates, and estimating their coverage, without conducting a series of propagation measurements, which are very expensive and time consuming. It is therefore important to develop effective propagation model tools for mobile communication, in order to provide design guidelines for mobile systems.

A very crucial factor in mobile cellular network projects is the ability to make an accurate prediction of propagation path loss within an environment. Propagation models are empirical mathematical formulations to characterize how radio waves behave as a function of frequency, surrounding environment and distance. Several propagation models exist for different link scenarios and these are helpful to service providers for designing and deploying their networks in the best possible way.

By selecting proper Model & loss calculations, a proper RF Planning keeping the future growth plan in mind can reduce a lot of problems that we may encounter in the future and also reduce substantially the cost of optimization. On the other hand a poorly planned network not only leads to many Network problems, it also increases the optimization costs and still may not ensure the desired quality. A planning tool will help by providing an accurate and reliable prediction of coverage

Cite this article as: Somya Agrawal, Neelesh Gupta, Meha Shrivastava. "Impact of GSM Spectrum Auction in 900 & 1800 MHz Band". *International Conference on Innovative Trends in Electronics Communication and Applications (2015)*: 49-58. Print.

Literature Review

Hemant Kumar Sharma et.al. [6] study some propagation model and fading model and also describes two main characteristics of wireless channel path loss and fading. Propagation model depends on the transmitter height, when transmitter height is high Okumara and cost231 wi model are perform better. But when transmitter height is below to roof height prediction of these models is poor. The accuracy of every model in any given Condition will depend on the suitability among parameter required by the model and available terrain, no single model is generally acceptable as the best.

Julie C. Ogbulezie et al. [10] explained Path loss predictions are required for the coverage planning, determination of multipath effects as well as interference and cell calculations. These calculations lead to high level network planning. Drive test measurements were taken along certain routes in Port Harcourt and Enugu, cities in Nigeria. These measurements were compared with calculated values from Okumura- Hata and COST231 Hata models at 900 MHz and at 1800 MHz.

Shewta et al. [21] attempts to investigate the effectiveness of the Okumura-Hata model in a typical Nigerian terrain. A GSM base station operation at 900 MHz band was used for the experiment in a typical sub-urban area within the Northern part of Nigeria. The field measurement results were compared with Okumura-Hata model for rural and sub-urban area. This research thus shows that the Okumura-Hata model for radio wave propagation is very effective for radio wave propagation pathloss prediction in suburban areas in Northern part of Nigeria.

Concepts

A propagation model models how the radio waves react to elevation changes and clutter (e.g., reflection, diffraction, and scattering). Few of the basic definations & concepts of Radio wave propagation is given below.

FREE SPACE PROPAGATION

Path loss (PL) is a measure of the average RF attenuation difference between transmitted signals when it arrives at the receiver, after traversing a path of several wavelengths. It is defined by

$$P_r = (d)\frac{P_t.G_t.G_r.\lambda^2}{(4\pi)^2 d^2 L} \quad P_L(dB) = 10\log\frac{P_t}{P_r} \qquad (1)$$

Where, Pt and pr are the transmitted and received power. In free space, the power reaching the receiving antenna which is separated from the transmitting antenna by a distance d is given by the Friis free-space equation:

$$P_r = (d)\frac{P_t.G_t.G_r.\lambda^2}{(4\pi)^2 d^2 L} \qquad (2)$$

Where, Gt and Gr, are the gain of transmitting and receiving antenna, respectively. L is the system loss factor, not related to propagation. λ is the wavelength in meters.

PROPAGATION MECHANISM

There are some propagation mechanisms that effect propagation in mobile ad hoc network. They are explained as follows.

Absorption: Absorption is a loss that occurs if the signal passes through varying mediums or obstacles in which some of the transmitted signal is converted into another form of energy, usually thermal, and some of it continues to propagate. Any material or atmospheric condition that is non-transparent to electromagnetic signals will result in absorption of the transmitted signal. The conversion of energy occurs at the molecular level, resulting from the interaction of the energy of the radio wave and the material of the medium or obstacle.

Cite this article as: Somya Agrawal, Neelesh Gupta, Meha Shrivastava. "Impact of GSM Spectrum Auction in 900 & 1800 MHz Band". *International Conference on Innovative Trends in Electronics Communication and Applications (2015)*: 49-58. Print.

Refraction: Refraction occurs when a radio wave passes from one medium to another with different refractive indices resulting in a change of velocity within an electromagnetic wave that results in a change of direction.

Reflection: Reflection occurs when a propagating electromagnetic wave impinges upon an object that has very large dimensions compared to the wavelength of the propagating wave. Reflection occurs from the surface of the ground, from walls, and from furniture.

Diffraction: Diffraction losses occur when there is an obstacle in the path of the radio wave transmission and the radio waves either bend around an object or spread as they pass through an opening. Diffraction can cause great levels of attenuation at high frequencies. However, at low frequencies, diffraction actually extends the range of the radio transmission.

Scattering: Scattering is a condition that occurs when a radio wave encounters small disturbances of a medium, which can alter the direction of the signal. Certain weather phenomena such as rain, snow, and hail can cause scattering of a transmitted radio wave. Scattering is difficult to predict because of the random nature of the medium or objects that cause it.

Multipath: Multiple Waves Create "Multipath". Due to propagation mechanisms, multiple waves arrive at the receiver. Sometimes this includes a direct Line-of-Sight (LOS) signal. Multipath propagation causes large and rapid fluctuations in a signal These fluctuations are not the same as the propagation path loss.

Fading: The communication between the base station and mobile station in mobile systems is mostly non-LOS. The LOS path between the transmitter and the receiver is affected by terrain and obstructed by buildings and other objects. The mobile station is also moving in different directions at different speeds. The RF signal from the transmitter is scattered by reflection and diffraction and reaches the receiver through many non-LOS paths. This non-LOS path causes long-term and short term fluctuations in the form of log-normal fading and rayleigh and rician fading, which degrades the performance of the RF channel.

RF PROPAGATION MODALS

Propagation models available in Atoll are listed in the table below along with their main characteristics.

Table 1
Propagation models and characteristics

Propagation model	ITU 370-7 (Vienna 93)	ITU 1546	ITU 526-5	WLL	Standard Propagation Model	ITU 529-3	Erceg-Greenstein (SUI)	COST-Hata Okumura-Hata
Frequency band	100-400 MHz	30-3000 MHz	30-10000 MHz	30-10000 MHz	150-3500 MHz	300-1500 MHz	1900-6000 MHz	150-2000 MHz
Physical phenomena	Free space loss Corrected standard loss	Free space loss + Corrections	Free space loss Diffraction loss	Free space loss Diffraction loss	L(d, H_{Tx}, H_{Rx}, Diff loss, clutter)	L(d, f, H_{Rx}) (per environment) Diffraction loss	L(d, f, H_{Tx}, H_{Rx}) (per environment) Diffraction loss	L(d, f, H_{Rx}) (per environment) Diffraction loss
Diffraction calculation method	-	-	Deygout (3 obstacles) Deygout corrected (3 obstacles)	Deygout (3 obstacles)	Deygout (3 obstacles) Epstein-Peterson (3 obstacles) Deygout corrected (3 obstacles) Millington (1 obstacle)	Deygout (1 obstacle)	Deygout (1 obstacle)	Deygout (1 obstacle)
Profile based on	-	-	DTM	DTM Clutter	DTM Clutter	DTM	DTM	DTM
Profile extraction mode	-	-	Radial	Radial	Radial Systematic	Radial	Radial	Radial
Cell size	Macro cell	Macro cell	Macro cell	-	Macro cell Mini cell	Macro cell Mini cell	Macro cell Mini cell	Macro cell Mini cell
Receiver location	Rooftop	Rooftop	Street	Street Rooftop	Street Rooftop	Street	Street	Street
Receiver	Fixed	Mobile	Fixed	Fixed	Mobile and Fixed	Mobile	Fixed	Mobile
Use	d > 10 km Low frequencies Broadcast	1 < d < 1000 km Land and maritime mobile, broadcast	Fixed receivers WLL	Fixed receivers WLL, Microwave links, WiMAX	1 < d < 20 km GSM, UMTS, CDMA2000, WiMAX, LTE	1 < d < 100 km GSM, CDMA2000, LTE	Urban and suburban areas 100 m < d < 8 km Fixed WiMAX	GSM 900, GSM 1800, UMTS, CDMA2000, LTE

Okumura – Hata Model

This is the commonly employed model for urban and sub-urban areas. This model is the most commonly used for macro-cell coverage planning. This is a combination of the work of Okumura and Hata. Okumura was able to carry out test measurements in Japan. These measurements had a range of clutter type, transmitter height, transmitter power and frequency. He found out that the signal strength decreases at a much greater rate with distance than the predicted free space loss (Medeisis & Kajackas, 2000; Saunders & Hata, 1980; Wilson & Scholtz, 2003).

Hata based his model on Okumura's free test results and predicted various equations for path loss with different types of clutter. The range of tests was carried out from carrier frequency, 150 MHz to 1500 MHz. The distance from the base station ranges from 1km to 20km while the range of the height of the mobile antenna is from 1m to 10 m. Okumura – Hata model is not suitable for micro-cell planning where antenna is below roof height. It is not valid for 1800 MHz and 1900 MHz systems.

Cite this article as: Somya Agrawal, Neelesh Gupta, Meha Shrivastava. "Impact of GSM Spectrum Auction in 900 & 1800 MHz Band". *International Conference on Innovative Trends in Electronics Communication and Applications (2015)*: 49-58. Print.

COST 231 Hata Model

COST is an acronym for European Co-operative for Scientific and Technical research. COST 231 Hata is an extension of the Okumura – Hata model. The COST 231 Hata model and is designed to be used in the frequency range 500 MHz to 2000 MHz. It has correction for urban, suburban and rural (flat) environments. Because of its simplicity and correction factors, it is widely used for path loss predictions at these frequency bands (COST, 1999; Hata, 1981; Okumura, 1968; Wong & Teng, 1997; Wu & Yuan, 1998).

Atoll Standard Propagation Model

SPM is based on the following formula:

$$L_{model} = K_1 + K_2 log(d) + K_3 log(H_{Txeff}) + K_4 \times DiffractionLoss + K_5 log(d) \times log(H_{Txeff}) + K_6(H_{Rxeff}) + K_7 log(H_{Rxeff}) + K_{clutter} f(clutter)$$

(3) Where,

K1: constant offset (dB).

K2: multiplying factor for log(d).

d: distance between the receiver and transmitter (m).

K3: multiplying factor for log(HTxeff).

HTxeff: effective height of the transmitter antenna (m).

K4: multiplying factor for diffraction calculation.

K5: multiplying factor for log(d) x log(HTxeff)

K6: multiplying factor for . HRxeff

K7: multiplying factor for log(HRxeff).

HRxeff : effective mobile antenna height (m).

Kclutter: multiplying factor for f(clutter).

f(clutter): average of weighted losses due to clutter.

Sample Values for SPM Path Loss Formula Parameters

The following tables list some sample orders of magnitudes for the different parameters composing the Standard Propagation

Table 2

Sample Values for Standard Propagation model formula

	Minimum	Typical	Maximum
K1	Variable	Variable	Variable
K2	20	44.9	70
K3	-20	5.83	20
K4	0	0.5	0.8
K5	-10	-6.55	0
K6	-1	0	0
K7	-10	0	0

K1 depends on the frequency and the technology.

Cite this article as: Somya Agrawal, Neelesh Gupta, Meha Shrivastava. "Impact of GSM Spectrum Auction in 900 & 1800 MHz Band". *International Conference on Innovative Trends in Electronics Communication and Applications (2015)*: 49-58. Print.

Table 3

Sample Values for K1 values

Project Type	Frequency (MHz)	K1
GSM900	935	12.5
GSM1800	1805	22
GSM1900	1930	23
UMTS	2110	23.8
1XRTT	1900	23
WiMAX	2300	24.7
	2500	25.4

All K paramaters can be defined by the automatic calibration wizard. Since Kclutter is a constant, its value is strongly dependant on the values given to the losses per clutter classes. From experienced users, the typical losses (in dB) per clutter class are:

Table 4

losses(in db) per Clutter class

Dense urban	From 4 to 5
Woodland	From 2 to 3
Urban	0
Suburban	From -5 to -3
Industrial	From -5 to -4
Open in urban	From -6 to -4
Open	From -12 to-10
Water	From -14 to -12

Proposed Method

Accurate prediction of radio propagation behaviour for the GSM NW is a major task. This paper study & analyze 900 & 1800 band site coverage prediction by the planning tool.A network model designer may be able to capture the necessary RF propagation effects with one of the network simulators, as some applications require higher fidelity modelling of a given RF environment. These can be more general than networking scenarios such as modelling the path loss at a given frequency over three city blocks. These RF propagation simulators are frequently used by network service providers to predict service coverage To achieve results we will use Atoll planning tools present in GSM world to assist a RF planner. We will provide the test case of rural site planning & its verification using Atoll tool present in the market and getting results using its standard propagation model with different

Experimental Results

We have done initial analysis on two sample sites each of 900 & 1800 Mhz band with three sectors respectively.

Cite this article as: Somya Agrawal, Neelesh Gupta, Meha Shrivastava. "Impact of GSM Spectrum Auction in 900 & 1800 MHz Band". *International Conference on Innovative Trends in Electronics Communication and Applications (2015)*: 49-58. Print.

Table 5 site allocation of two different sites

Transmitter	Antenna	Height (m)	Azimuth (°)	ical Downtilt (°)	Power (dBm)	Losses (dB)
1800 site_1	65deg 17dBi 0Tilt 1800MHz	32	10	1	43	3
1800 site_2	65deg 17dBi 0Tilt 1800MHz	32	100	1	43	3
1800 site_3	65deg 17dBi 0Tilt 1800MHz	32	220	1	43	3
900 site_1	65deg 17dBi 0Tilt 900MHz	32	0	1	43	3
900 site_2	65deg 17dBi 0Tilt 900MHz	32	100	1	43	3
900 site_3	65deg 17dBi 0Tilt 900MHz	32	220	1	43	3

900Mhz Band Site Results:

Coverage distribution:

Table 6

Coverage by Signal Level_900

Coverage by Signal Level: SITE_NAME=test 900	KM2
Best Signal Level (dBm) >=-70	1.86
Best Signal Level (dBm) >=-75	3.395
Best Signal Level (dBm) >=-80	5.9
Best Signal Level (dBm) >=-85	10.533
Best Signal Level (dBm) >=-90	17.835
Best Signal Level (dBm) >=-95	28.44
Best Signal Level (dBm) >=-100	40.323
Best Signal Level (dBm) >=-105	44.0,78

Cite this article as: Somya Agrawal, Neelesh Gupta, Meha Shrivastava. "Impact of GSM Spectrum Auction in 900 & 1800 MHz Band". *International Conference on Innovative Trends in Electronics Communication and Applications (2015)*: 49-58. Print.

Prediction:

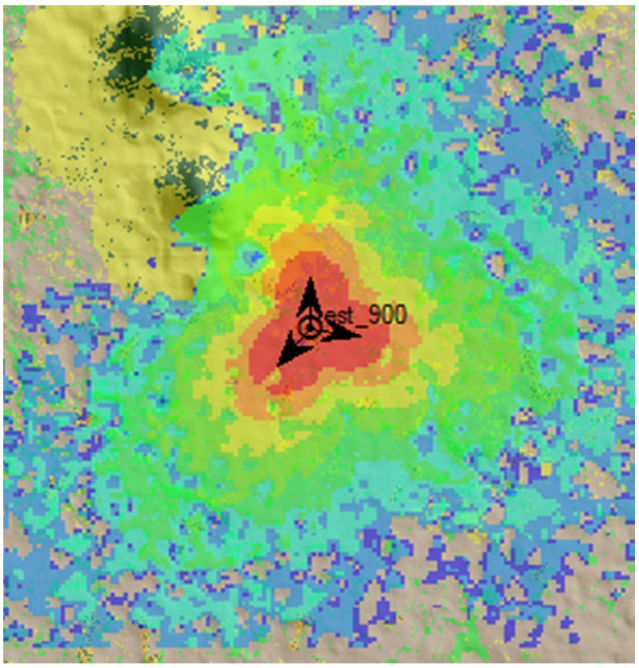

Fig 1:

Covered area by 900 site

Histogram:

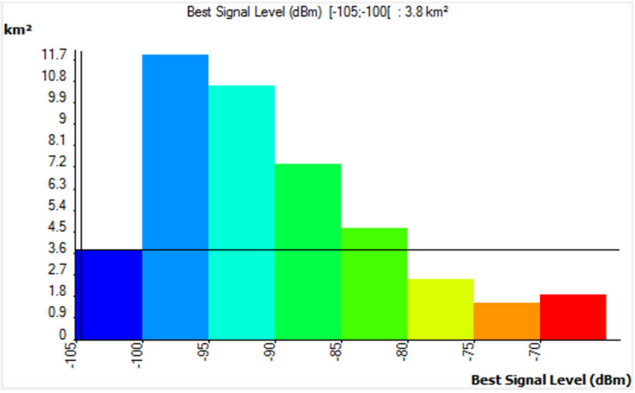

Fig 2:

Histrogram based on Covered Areas in 900

1800 Mhz Band site Results:

Coverage distribution:

Cite this article as: Somya Agrawal, Neelesh Gupta, Meha Shrivastava. "Impact of GSM Spectrum Auction in 900 & 1800 MHz Band". *International Conference on Innovative Trends in Electronics Communication and Applications (2015)*: 49-58. Print.

Table 7

Coverage by Signal Level_1800

Coverage by Signal Level: SITE_NAME=test 1800	KM2
Best Signal Level (dBm) >=-70	0.445
Best Signal Level (dBm) >=-75	1.058
Best Signal Level (dBm) >=-80	2.175
Best Signal Level (dBm) >=-85	4.168
Best Signal Level (dBm) >=-90	7.253
Best Signal Level (dBm) >=-95	13.273
Best Signal Level (dBm) >=-100	21.673
Best Signal Level (dBm) >=-105	26.138

Prediction:

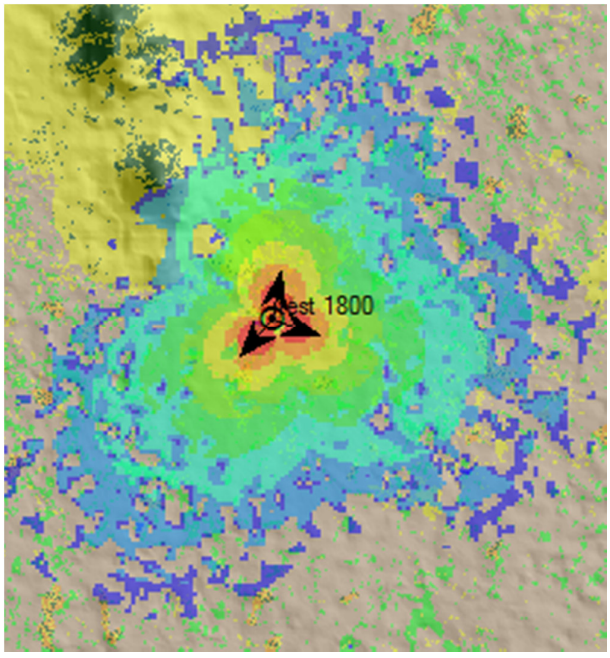

Fig 3:

Covered area by 1800 site

Cite this article as: Somya Agrawal, Neelesh Gupta, Meha Shrivastava. "Impact of GSM Spectrum Auction in 900 & 1800 MHz Band". *International Conference on Innovative Trends in Electronics Communication and Applications (2015)*: 49-58. Print.

Histogram:

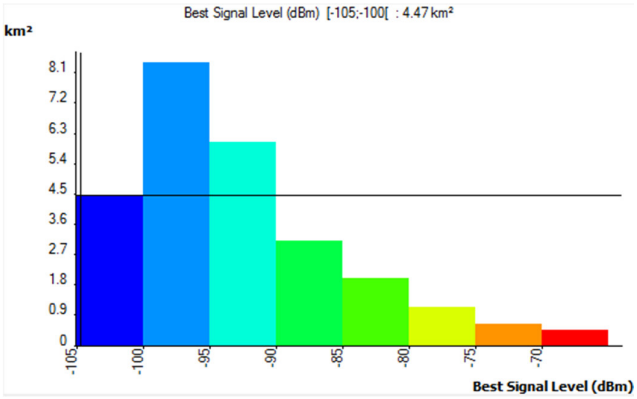

Fig 4:

Histrogram based on Covered Areas in 1800

Conclusion

This analysis of 900 & 1800 band site showing predicated signal strength by the planning tool clearly displays the difference in covered area. It helps us in understanding that 1800 MHz band site covers less area as compared to 900 MHz Band site. And also help in understanding the importance of a good Planning tool. Further, it is also expected that generated coverage prediction will match with the field test results and its verification can be showed in a separate study, if it is considered to replace existing 900 Band Sites with 1800 MHz Band site in a test area.

However, it is out the scope of this work to propose a precise model of the problem, since we use proprietary software which is aware of all these concepts, as well as the consideration of all the existing RF propagation Techniques developed for efficiently using all the possible propagation scenarios.

References

1. A.P.Garcia, "Efect of Terrain on Electromagnetic Propagation in Urban Envioronment on the Andean Region, using The COST-231-Walfisch – Inegami Model and GIS Planning Tools. "
2. Abhishek Keny, "Comparision Between propagation Models for Wireless Application," in 2012.
3. D.D.Dajab and Naldongar Purfait." A Consideration of Propagation Loss Models for GSM during Harmallan in N Djanena (chad)," International Journal of Compauting and ITC Research Vol.4,No 1, pp 43-48 in June 2010.
4. D.D.Dajab and O.E.Ogundapo, "Propagation Loss Models for GSM Macro cell at 900 Mhz in KANO, Nigeria." International Journal of Conference on Engineering and Mathematics ENIMA in 2008.
5. Graziano Cerri, "Appilication of an Automatic Tool for The Planning of Cellular Network in a real Town" IEEE transation on Antennas and Propagation. Vol.5,No.10, Oct 2006.
6. Hemant Kumar Sharma "Survey of Propagation Model in wireless Network." IJCSI International Journal of Computer Science issues,Vol 8,Issuse 3, No 2, may 2011.
7. Ibrahim Khider Eltahir, "The Impact of Different Radio Propagation Models for Mobile Ad hoc Network (NAME) in Urban Area Environment." The 2nd International Conference on Wireless Broadband and Ultra Wideband Communication (Aus Wireless 2007) IEEE.
8. Jingui lu, "Radio Propagation measurments and Modeling in Railway Viaduct Area." Project Supporned by NSFC and The State Key laboratory of Railway Traffic control and Safety Beijing Jiaotong University.

Cite this article as: Somya Agrawal, Neelesh Gupta, Meha Shrivastava. "Impact of GSM Spectrum Auction in 900 & 1800 MHz Band". *International Conference on Innovative Trends in Electronics Communication and Applications (2015)*: 49-58. Print.

9. Julia Andrusenko, "Modeling and Simulation for RF Propagation." The Jonhs Hopkins University Design & Developers Fourm IEEE Globecom 2009.

10. Julie.C.Ogbulerie, "Propagation models for GSM 900 and 1800 Mhz for Port Harcourt and Enagu, Nigeria." Network and communication technologies vol 2, No 3, in 2013.

11. Masaharu Hata, "Empirical Formula for propagation loss in land Mobile radio services" IEEE Trabsaction on Vehicular technology. Vol . VT-29, No. 3, august 1980.

12. Mohd Nazrul Hanif Nordin, "Application of Code Average Method for GSM Coverage Prediction in Different Enviroment" Feb 15-18, 2009 ICACT 2009.

13. Nazar Elfadhil, "Modification of an Open area Okumura- Hata Propagation Model Suitable for OMAN".

14. Nuno cotal, "On the use of Okumura-Hata propagation Model on Railway Communications." ISSN: 1882-5621/13/2013.

15. Ogbulezie, "Site Specific Measurements and Propagation Models for GSM in three Cities in Northern Nigeria." American Journal of Scientific and Industrial Reaearch 2013, 4(2): 238-245.

16. P.R.Ogungbayi, "Propagation Path Loss Characteristics at 900 Mhz in Ilorin, Nigeria ."Epistemics in Science Engineering and Technology Vol.2, No.2, 84-93 2012.

17. Purnima .k.Sharma, "Comparative Analysis of Propagation Path Loss Models with Field Measured Data." International Journal of Engineering Science and Technology Vol.2(6),2010,2008-2013.

18. R.Mardeni, "Optimization of Hata Propagation Prediction Model in Suburban Area in Malaysia." Progress in Electromagnetics Research ,Vol.13,91-106,2010.

19. Reshma Begum Shaik, "Simulation of GSM Mobile networks Planning using ATOLL Planning Tool." International Journal of engineering and Innovative Technology (IJEIT) ISO 9001-2008 Certified Volume. 2, Issue.1, July 2012.

20. Sami A Mawjoud, "Pathloss Propagation model Prediction for GSM N etwork Planning." International Journal of Computer Applications (0975-8887) Volume.84,No.7,December 2013.

21. Shoewn, " Investigation of Radio Waves Propagation Models in Nigerian Rural and Sub-Urban Areas ." American journal of Scientific and Industrial Research 2010.

22. Shveta Sharma, "RF Coverage Estimation of Cellular Mobile System," Intrnational journal of Engineering and Technology Vol.3(60, 398-403,2011-2012.

23. Tapan k. Sarkar, " A survey of Various propagation Models for Mobile Communication." IEEE Antennas and Propagation Magazine Vol.45, No.3, June 2003.

24. Zia Nadir, " Empirical Pathloss characterization for Oman." IEEE 2012.

25. Atoll Wireless Network Engineering Software Version 3.2 Febuary 2013- Geo Data Courtesy of EGS Technology and Geoimages.

26. Atoll RF planning & Optimization Software. Version 2.8.2 AT282-TRG-EO April 2010.

27. Cost Telecommunication cost Action 231 "digital mobile Radio Towards Future Generation Systems.

28. Digital Cellular Telecommunication System Radio Network Planning aspects (GSM 03.30 version 5.0.0) European Telecommunication Standards Institude November 1996.

29. Mentum Planet Delivering more Propagation Wireless access Network.

30. Mentum Planet user Guide Version 4.4 April 2008.TEMS Cell Planner 9.0 ascom December 2009.

Cite this article as: Somya Agrawal, Neelesh Gupta, Meha Shrivastava. "Impact of GSM Spectrum Auction in 900 & 1800 MHz Band". *International Conference on Innovative Trends in Electronics Communication and Applications (2015)*: 49-58. Print.

International Conference on Innovative Trends in Electronics Communication and Applications 2015 [ICIECA 2015]

ISBN	978-81-929742-6-2	**VOL**	01
Website	icieca.in	**eMail**	icieca@asdf.res.in
Received	02 - April - 2015	**Accepted**	15 - November - 2015
Article ID	ICIECA009	**eAID**	ICIECA.2015.009

Analysis of MIMO performance with Beam Forming Algorithms

Emmanuel Nehemiah J[1], Anitha S[1], Banupriya R[1], Vijaya N[1], Susithra G[1]
[1]Wireless Communication Engineering Dept.,
Christ College of Engineering and Technology
Pondicherry, India

Abstract: *The growth of digital wireless communication is marvelous in last few decades. The demand for higher data rate is more and it can be achieved by increasing the bandwidth and channel capacity. Increasing the bandwidth is more challenging, since we are having very limited spectrum. And here capacity is increased to achieve higher data demand through space selectivity. Smart antenna with beam forming algorithm provide higher capacity and higher quality than other system. In this paper the performance of the smart antenna is analyzed with LMS and NLMS algorithm with stimulation results. It is found that the performance of smart antenna is high in NLMS algorithm.*

Keywords*:* MIMO, Beam forming, LMS

INTRODUCTION

The demand in communication capacity is achieved by the employment of the space division multiple access technique. The signal transmitted on the same frequencies can be separated by the smart antenna array and they are separated in spatial domain. Which increase the performance and improved network efficiency of the mobile system.

The features of a wireless channels are thin. Hence for some region the characteristics are zero. Since in spatial domain it varies with DOA. For reducing the bandwidth requirement sparsely spaced element is needed for increasing the convergence rate by reducing the reference training sequence.

The performance of the smart antenna is tested with LMS and NLMS algorithm. Good robustness against execution errors and low computational complexity adds remark to the NLMS. The NLMS having good convergence rate then LMS. Its convergence and computing time are less. For implementation in cost effective way our work is to find the less computing time algorithm.

SYSTEM MODEL

Types of Beamforing Algorithm:

The algorithm of the adaptive antenna is classified based on whether training signal is used and not used [1]. It is classified as blind and non-blind algorithm[2].

Non-Blind Algorithm:

In this algorithm, the training signal is known to both transmitter and receiver the receiver received it from transmitter during training

Cite this article as: Emmanuel Nehemiah J, Anitha S, Banupriya R, Vijaya N, Susithra G. "Analysis of MIMO performance with Beam Forming Algorithms". *International Conference on Innovative Trends in Electronics Communication and Applications (2015)*: 59-64. Print.

period[3] with the training signal the beam former in the receiver can calculate the optimal weight vector.

The data is transmitted after the training period weigh vector which is calculated previously with training signal[4]. For the working of beam former the non-blind algorithm is used in NLMS, LMS and also in steepest-decent.

LMS ALGORITHM

For The property of robust and easy implement, the LMS is having application for equalization, echo cancellation modeling control and beam forming. The antenna is customized to have maximum gain in the direction of desired signal and the gain is low or null in the undesired direction. The beam forming system is show in fig 1.

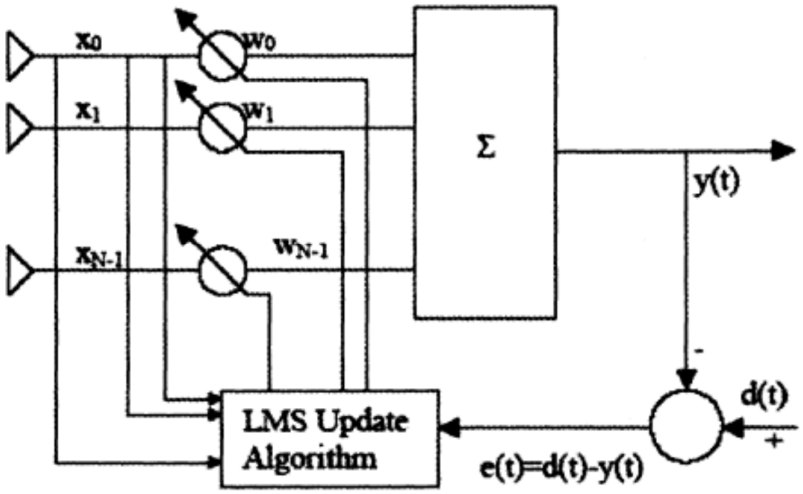

Fig1: LMS beam forming algorithm

The antenna is customizing by combining the output of individual sensors and they are scaled based on the corresponding weight. And with the help of minimum squared error the LMS can compute the weight . Spatial filtering involves the signal estimation in receiver by reducing the error with the help of reference signal d(t)[5]. And it has some correlation with desired signal and beam former output y(t). The solution is obtained by iteration using LMS algorithm.

The phase and amplitude of the incoming signal is adjusted by multiplying the received signal x(t) with the coefficient of the weight vector w. y(t) is the result of the weighted signal. The error e(t)between the desired signal and output y(t) is minimized by employing adaptive algorithm[6]. The output y(n) of the beam forming can be expressed as

$$y(n) = w^H x(n) \quad (1)$$

Where $$w = [w_1, w_2 \ldots, w_k]^H \quad (2)$$

And $$x(n) = [x_{1(n)}, x_2(n) \ldots, x_k(n)] \quad (3)$$

Where H represents the hermitian transpose. The complex vector of weight $w_1, w_2 \ldots, w_k$ adjust the amplitude and phase. The desired beam can be produced by adding together the MMSE weight adaptation with the steepest decent algorithm produces LMS algorithm[7]. For each new samples the weight vectors are updated, this process is called sample by sample techniques. Because of the successive correction the gradient vector leads to the MMSE.

$$\boldsymbol{w}(n+1) = w(n) + \frac{1}{2}U(-\nabla \mathrm{J}(\mathrm{n})) \quad (4)$$

W(n) represents the weight vector at n, W(n+1) represent weight vector at n+1. U represents the step size which control the convergence speed. The value for the gradient vector is calculated through covariance matrix R and cross-correlation r.

Cite this article as: Emmanuel Nehemiah J, Anitha S, Banupriya R, Vijaya N, Susithra G. "Analysis of MIMO performance with Beam Forming Algorithms". *International Conference on Innovative Trends in Electronics Communication and Applications (2015)*: 59-64. Print.

$$\nabla J(n) = -2r(n) + 2R(n)W(n) \quad (5)$$

Where $$\boldsymbol{R}(n) = x(n) * x^h(n) \quad (6)$$

and $$r(n) = x(n) * d^*(n) \quad (7)$$

As we know the error vector $e(n) = d(n) - y(n)$

Substitute the value of gradient vector in the equation number (4) , we get

$$\boldsymbol{w}(n+1) = w(n) + x(n) * d^*(n) - x(n) * x^h(n)w(n) \quad (8)$$

$$\boldsymbol{w}(n+1) = w(n) + x(n)(d^*(n) - x^h(n)w(n)) \quad (9)$$

Sub e(n) $$\boldsymbol{w}(n+1) = w(n) + Ux(n)e^*(n) \quad (10)$$

The gradient value changes randomly as per the input vector. When the rate of convergence U is slow, then it will gives good estimation of large amount of data.

By sending known pilot sequence to the transmitter the knowledge of the transmitter signal is measured, which required by the algorithm[8]. The step size parameter controls the convergence speed. Hence the algorithm depends on the step size. The step size is a positive constant value which control the size of increment applied in one iteration to the next. Three factors determines the response of the LMD algorithm they are

A. Number of weight
B. Step size parameter
C. Eigen value of the correlation matrix

ADVANTAGE: The Main advantage of the LMD is the low computational complexity which is O(L), L is the number of tap weight.

DISADVANTAGE: The main disadvantage is low convergence rate and fluctuation which creates problem in tracking and acquisition.

NLMS ALGORITHM

The NLMS (normalized least mean square algorithm) is used in number of signal processing and control applications. It works by adapting the finite impulse response filters co-efficient. The weight vector can be calculated easily by using NLMS the values are stable and faster in convergence [9]. NLMS is the modification of the LMD algorithm.

The LMS algorithm suffers from the gradient noise amplification problems. The product vector in (10) ($x(n)e^*(n)$) is applied to the weight vector and it is proportional to the input vector x(n). For that $x(n)e^*(n)$ have to be normalized. Hence the final weigh vector of the NLMD algorithm represented by

$$\boldsymbol{w}(n+1) = w(n) + \frac{U}{|x(n)|^2}x(n)e^*(n) \quad (11)$$

The step size of the NLMS algorithm is reduced, which make huge change in weight vector updation. Since the step size varies with respect to input make the convergence faster and more stable[10]. It is shown in equation (11) that step size is divided by the square of the input signal to remove the gradient noise amplification.

Cite this article as: Emmanuel Nehemiah J, Anitha S, Banupriya R, Vijaya N, Susithra G. "Analysis of MIMO performance with Beam Forming Algorithms". *International Conference on Innovative Trends in Electronics Communication and Applications (2015)*: 59-64. Print.

ADVANTAGE: The main advantage of the NLMS algorithm over the LMS algorithm is the faster convergence for correlated[11] and whitened input and the stableness of the output with the varying range of values independent input data[12]. And to implement a shift input of data the NLMS require additional addition, Multiplication and division over the LMS algorithm.

SIMULATION RESULTS

In wireless communication convergence and radiation pattern analysis determine the performance of the algorithm. Matlab14 is used to simulate the training based algorithm. The system of four antennas with ½ wavelength spacing is considered. The BPSK modulation in AWGN radio channel are considered.

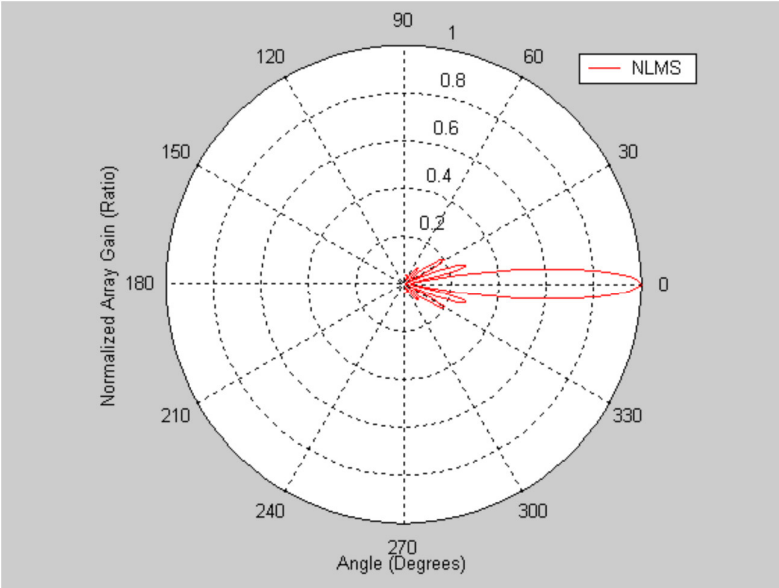

Fig2A: Radiation pattern of NLMS

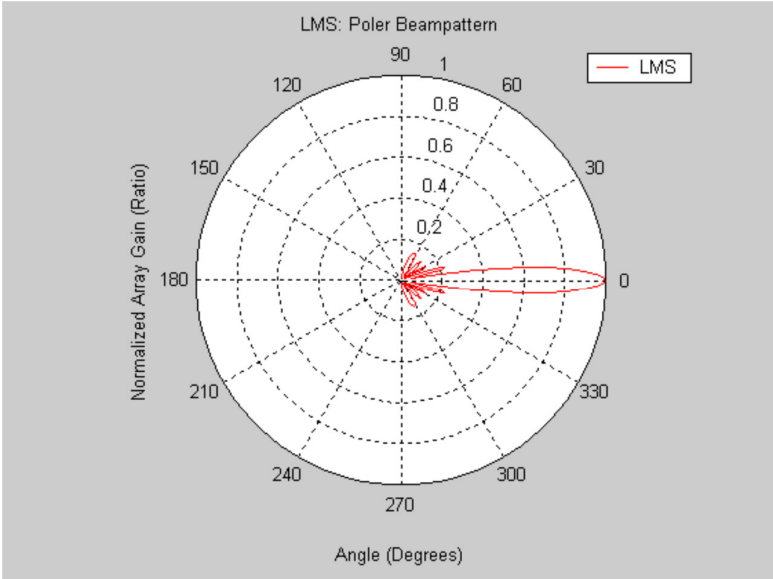

Fig2B: Radiation pattern of LMS and NLMS

Figure 2 shows the comparison of LMS and NLMS. Both the beams are in desired direction where NLMS have length gain and narrow beam width. Also LMS has many lobes while NLS has only two side lobes.

Cite this article as: Emmanuel Nehemiah J, Anitha S, Banupriya R, Vijaya N, Susithra G. "Analysis of MIMO performance with Beam Forming Algorithms". *International Conference on Innovative Trends in Electronics Communication and Applications (2015)*: 59-64. Print.

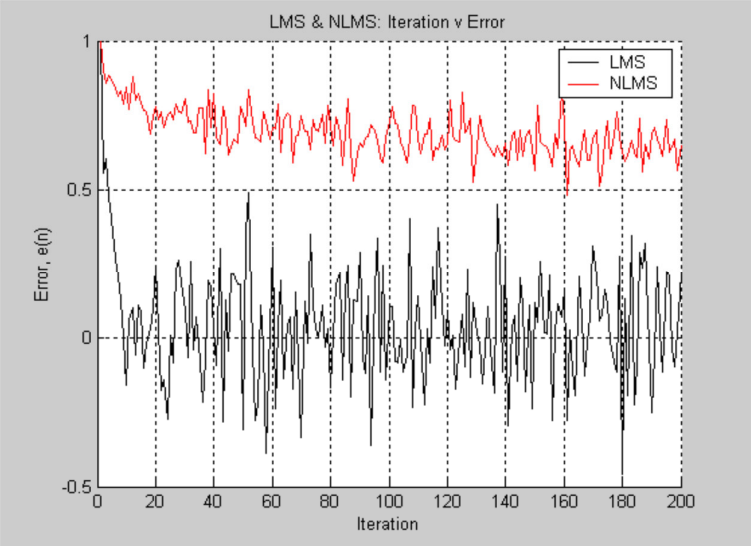

Fig3: Error Convergence of LMS and NLMS algorithms

Figure3 shows the error convergence of both LMS and NLMS. It is found that NLMS is much more stable and less fluctuation for each iteration with optimal step size. NLMS will give good radiation pattern. While the result for LMS shows unstable and low convergence.

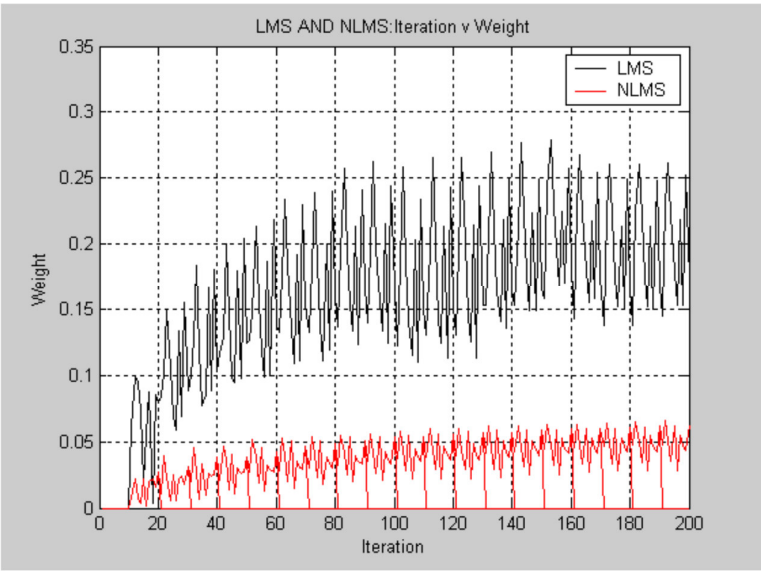

Fig4: Wight vector convergence performed of LMS and NLMS algorithms

The variation for the weight value is high in LMS Algorithm, Hence it is less stable when compared with NLMS. In NLMS also produces some spikes but not that much as compared to the LMS. And also less number of iteration are needed for the converges. Which make the system to converge quickly. With the help of the two results we can conclude NLMS is best in because of being stable and its convergence rate then LMS algorithm.

CONCLUSION

In this paper two non-blind beam forming algorithm- LMS and NLMS are compared on a smart antenna system. It is found that when the number of antenna elements are more the performance of LMS and NLMS would be more. It is analyzed that the error performance of LMS algorithm produce more fluctuations and convergence time is more when compared with the NLMS.

Cite this article as: Emmanuel Nehemiah J, Anitha S, Banupriya R, Vijaya N, Susithra G. "Analysis of MIMO performance with Beam Forming Algorithms". *International Conference on Innovative Trends in Electronics Communication and Applications (2015)*: 59-64. Print.

The radiation pattern and more directional of NLMS out performances LMS. However NLMS is little higher computational cost than LMS. The reason is the extra step size and it is divided by norm of input vector. The result is small and unnoticeable NLM is good algorithm it can be used in applications for slow-noise magnitude variation.

REFERENCES

[1] L. Yun-hui a n d Y. Yu-hang, "A modified multitarget adaptive array algorithm for wireless CDMA system", *Journal Zhejiang Univ SCI*, Vol. 5, No. 11, pp. 1418-1423, 2013.

[2] S. Gazor and K. Shahtalebi, "A new NLMS algorithm for slow noise magnitude variation", IEEE Signal Processing Letter, Vol. 9, No. 11, pp. 338-351, 2011.

[3] M. T. Islam, Z. A. Abdul Rashid, and C. C. Ping,"Performance evaluation of CMA and nCMA blind array algorithm for smart antenna system", *CS-2006-1016,* pp. 1-10, 2006.

[4] M. T. Islam, Z. A. Abdul Rashid, and C. C. Ping, "Comparison between non-blind and blind array algorithms for smart antenna system", *CS-2006-1015*, pp. 1-8, 2006.

[5] J. Zhang, "The adaptive algorithms of the smart antenna system in future mobile telecommunication systems", *IEEE*, pp. 347-350, 2005.

[6] J. Razavilar, F. Rashid-Farrokhi, and K. J. R. Liu, "Software radio architecture with smart antennas: a tutorial on a lgorithms and c omplexity", *IEEE Journal on Selected Areas in Communications*, Vol. 17, No. 4, pp. 662-676, April 1999.

[7] S. C. Douglas and T. Meng, "Normalized data nonlinearities for LMS adaptation", *IEEE Transactions on Signal Processing*, Vol. 42, No. 6, pp. 1352-1365, June 1994.

[8] R. S. Kawitkar and D. G. Wakde, "Smart antenna array analysis using LMS algorithm", *IEEE Int. Symposium on Microwave, Antenna, Propagation and EMC Technologies for Wireless Communications*, pp. 370-374, 2005.

[9] M. Chryssomallis, "Smart antennas", *IEEE Antennas and Propagation Magazine*, Vol. 42, No. 3, pp. 129-136, June 2000.

[10] R. Martínez, A. Cacho, L. Haro, and M. Calvo, "Comparative study of LMS and RLS adaptive algorithms in the optimum combining of uplink W-CDMA", *IEEE*, pp. 2258-2262, 2002.

[11] S. Lim, C. H. Yoo, and S. Kim, "Performance evaluation of beamforming using pilot channel in CDMA2000 reverse link", *IEEE VTC*, pp. 2740-2744, 2001.

[12] Shahera hossain, mohammad tariqul islam and seiichi serikawa, **"**Adaptive Beamforming Algorithms for Smart Antenna Systems", *International Conference on Control, Automation and Systems,* 2008.

Cite this article as: Emmanuel Nehemiah J, Anitha S, Banupriya R, Vijaya N, Susithra G. "Analysis of MIMO performance with Beam Forming Algorithms". *International Conference on Innovative Trends in Electronics Communication and Applications (2015)*: 59-64. Print.

International Conference on Innovative Trends in Electronics Communication and Applications 2015 [ICIECA 2015]

ISBN	978-81-929742-6-2	**VOL**	01
Website	icieca.in	**eMail**	icieca@asdf.res.in
Received	02 - April - 2015	**Accepted**	15 - November - 2015
Article ID	ICIECA010	**eAID**	ICIECA.2015.010

Predicting Muscular Dystrophy through Genetic testing – A Study

Sathyavikasini K[1], Vijaya M S[2]
[1]Research scholar, [2]Associate professor
PSGR Krishnammal College for Women
Coimbatore.

Abstract: *A pathologic condition impairs the normal function or structure of an organ in human beings. In the current genomic era, the identification of the disease is paramount. Genetic diseases are caused by the abnormalities in the inherited genes. Muscular dystrophy is an inherited genetic disorder that is rooted by the huge number of sequence variants found in large sets of genes. There are about 9 major forms in muscular dystrophy and a better understanding is needed to predict this genetic disease. The mutation in the genes causes most of these disorders. There are currently no effective treatments to halt the muscle breakdown in muscular dystrophies. A new approach is to be designed to predict the muscular dystrophy disease subtypes effectively. As the growth of biological data increases, storage and analysis become incredible this in turn increases the processing time and cost efficiency. This paves the way for challenges in computing. The objective of machine learning is to dig out valuable information from a corpus of data by building good probabilistic models. In this paper, a preface to muscular dystrophy, traditional and innovative approaches involved in identifying this disease are discussed.*

Keywords*:* Genes, DNA, Mutation, Codon, Genetic disease, Amino acids, Allele

INTRODUCTION

Muscular dystrophy is a monogenic disease [1] that is caused by mutations in the genes which are in charge of the regular muscle function. Progressive muscle weakness that affects limb, axial and facial muscles are the foremost cause of muscular dystrophy. The other muscles that function in respiratory, cardiac and swallowing are affected in some specific types of muscular dystrophy. In a rare variant, the brain, inner ear, eyes, or skin is impaired by muscular dystrophy disorder [2]. Muscular dystrophy is believed as a genetic ailment flow in a family, even if only one blood relation in the ancestor is affected.

Autosomal recessive, dominant and X-linked are the three patterns of inheritance that causes muscular dystrophy. The recessive pattern of a disease requires two copies of inherited defective genes, one from each parent where both will be carriers of the disease but usually not affected by the disease. The dominant pattern involves, only one copy of the genetic defect to cause the disease. Anyone in the family with the gene mutation can pass the disorder to children. In the case of X-linked, the disease is passed only from mother to their children. In females, two pairs of X chromosomes are present and therefore the daughters turn out into carriers, and generally not affected by the disease. The male comprises of only one X chromosome and gets flawed by muscular dystrophy and hence in most cases the trait is identified in male children. Duchenne, Becker, Emery-Dreifuss, Limb-girdle, Facioscapulohumeral, Myotonic, Spinal, Distal and Charcot Marie tooth disease are the few rare forms of muscular dystrophy [3].

Duchenne muscular dystrophy (DMD) is the X-Linked and most common form of muscular dystrophy is caused by the mutations in the dystrophin gene located on the X chromosome. Dystrophin is the massive human gene that is 2.5MB long and encompasses of 79 exons. The absence of dystrophin gene occurs when a large number of exons are deleted, which is the major cause of DMD [4]. DMD

Cite this article as: Sathyavikasini K, Vijaya M S. "Predicting Muscular Dystrophy through Genetic testing – A Study". *International Conference on Innovative Trends in Electronics Communication and Applications (2015)*: 65-71. Print.

causes out frame deletions that happen in the piece of the codon and the sequence read cannot be done. The patients affected by DMD are diagnosed around children in five years of age when the physical ability deviates obviously from their companion. When untreated, the strength of the muscle strength gets worse, and boys are wheelchair dependent at their early stages of the life. The other complications like respiratory, orthopedic, and cardiac emerge, that shortens the life of the patients [5].

Becker muscular dystrophy (BMD) is the X-Linked caused by the mutations in the dystrophin gene located on the X chromosome. It upholds muscle fiber strength, reduces muscle rigidity and increases sarcolemmal deformability. Less defective mutations in the dystrophin gene result display a much milder dystrophic phenotype in affected patients, known as Becker's muscular dystrophy [4,5]. BMD causes in frame deletions that take place beyond the codons and the sequence still can be read after deletions.

Emery-Dreifuss muscular dystrophy (EMD) can be affected in patients, typically in their childhood and in the early adolescent years with muscle contractures. The symptoms include cardiac conduction defects, muscle weakness and arrhythmias. If the patients left untreated in the early stage, it leads to increasing the risk of stroke and sudden death. The mutations in the Emerin (EMD) and Lamin A/C (LMNA) genes cause Emery- Dreifuss muscular dystrophy. Mutations like point mutations, insertions and deletions in the genes direct to EMD. X-Linked, autosomal dominant and autosomal recessive are three subtypes of EMD muscular dystrophy disease. Each type varies in their prevalence and symptoms.

Limb-girdle muscular dystrophy (LGMD) can be seen in both boys and girls. Nearly mutations in 18 genes are the reason of LGMD. The defects in LGMD show a related distribution of muscle weakness that has an effect on both upper arms and legs. The different patterns of inheritance in LGMD are autosomal and recessive. Missense, insertions and deletion mutations in the genes route to LGMD.

Charcot Marie tooth disease (CMT) includes a number of disorders with an assortment of symptoms grounds damages in peripheral nerves. The disorder affects the peroneal muscle in the lower leg and hence the disease also is known as hereditary motor and sensory neuropathy (HMSN) and peroneal muscular atrophy [6]. CMT causes mild and also severe muscle degeneration, which is dependent on its mutation. There may be mild problems limited to skeletal muscle and also a severe problem like muscle degeneration corresponding with upshot on the brain. More than 30 forms of CMT are noticed and 30 genes are concerned, some may show severe brain malformations, such as lissencephaly and hydrocephalus and hearing loss [7].

The Facioscapulohumeral Muscular Dystrophy (FSHD) is an autosomal dominant neuromuscular disorder. The deletions of D4ZA microsatellite repeats in DUX4 gene on chromosome 4q cause Type 1 FSHD. Mutations such as missense, splice site and small deletions in SMCHD1 gene reflects in Type2 FSHD. The weakness of muscles in the face that slow progress in the shoulder, upper arm muscles and shoulder girdle, down to the stomach and lower limbs [8].

The Myotonic dystrophy is also known as Steinert's disease. The expansion of an unstable CTG trinucleotide repeat in the DMPK gene on chromosome 19 is the basis for this disease. The normal individual has the repeats ranging between 5 and 37. If the repeats exceed 50 then it the cause for myotonic dystrophy. CTG repeat sizes in patients range from 50 to 4000 [9].

Distal muscular dystrophy (DD) also known as Distal myopathy is a group of disorders that mainly affect distal muscles. The distal muscles that are located in the hands, feet, lower arms or lower legs are flawed in this type of muscular dystrophy. There are about eight forms of distal myopathy caused by the defects in various genes.

Spinal muscular atrophy (SMA) is an autosomal recessive neuromuscular disease that results in progressive proximal muscle weakness and paralysis exemplify by degeneration of alpha motor neurons in the spinal cord. On the basis of the age of onset the patients SMA is classified into four types. In the range of the ages lie between Type 1 (0-6 months), Type II (7-18 months), Type III (> 18 months), Type IV (>18 years). The SMN1 gene is responsible for this genetic alteration that results in a reduction of survival motor neuron (SMN) protein [10,11].

Muscular dystrophy is a genetic disorder that is caused by the mutations in a variety of genes. When a mutation occurs in the gene the resultant protein product will be missing or altered. The change of protein in the muscles leads to alteration or malfunction of the muscles that reveal muscular dystrophy.
Muscular dystrophy is progressive and they tend to worsen with time. The factors like age of onset and rate of progression generally fluctuate from one disorder to another. Some these disorders can affect life expectancy. In the summary of all types of muscular dystrophy, the defects in some forms will cause contractures or inflexible joints, and few are accompanied by scoliosis or spinal curvature. Even though the majority muscular dystrophies don't affect the brain, some are accompanied by brain changes that cause learning disabilities that range from slight to severe. Finally, several forms of muscular dystrophy also impinge the heart. It is observed that each disorder has its own special locale of anxiety.

Cite this article as: Sathyavikasini K, Vijaya M S. "Predicting Muscular Dystrophy through Genetic testing – A Study". *International Conference on Innovative Trends in Electronics Communication and Applications (2015)*: 65-71. Print.

DNA MUTATION

Amend in the genetic code that causes a permanent change in the DNA sequence is termed as mutation. DNA mutations perceptibly root to genetic diseases. Single character change in a gene makes an impact on the gene which in turn changes the function of the gene. Muscular dystrophy is a genetic disease caused by the mutations in the genes. A mutation in DNA may do no harm in protein sequences in some of the mutations. Substitution is an exchange of one base to another, such as swapping a base from A to G. Missense mutations are the substitution in a codon that encodes a different amino acid and cause a small change in the protein. For example, missense mutation 347T>C indicates that codon changes CTC-CCC in the dystrophin gene results in DMD, where the protein Leu is altered to Pro [12].

Nonsense mutations are the substitution in a codon that results in premature termination of protein. TAG ("amber"), TAA ("ochre"), TGA ("opal" or "umber") are the three stop codons. For example, a nonsense mutation in the dystrophin gene 433C>T, point out that the codon change CGA-TGA and the protein arg is terminated with amber stop codon and results in BMD [13].

Single character change in a gene makes an impact on the gene which in turn changes the function of the gene. In some cases, a DNA mutation may do no harm in protein sequences. It depends on the sort of DNA mutation and where it is located. A change in codon encodes the same amino acid and causes no change in the protein is called silent mutations [14]. Consider an example, in CAPN3 gene 246G>A specifies CCG-CCA and the protein pro is not misrepresented, but it routes to the LGMD type 2 disease.

During small insertions, a new base is added into the sequence that alters the function of a gene. An increase in the number of the same nucleotides in a location is termed as duplications. For example, EMD disease is caused by the duplications in the emerin gene for the nucleotide change 650_654dupTGGGC [15].

Small deletions occur in the genes when a base is deleted from a sequence that truncates the function of genes. For example, 253delG deletes G in 253 position in the SH3TC2 gene that directs for Charcot-Marie-Tooth disease 4C. Gross insertions and gross deletions occur when the whole number of exons is involved in the insertions are deletions.

Frameshift mutations alters the position of nucleotides in the reading frame, and that forms unrelated amino acids into the protein, generally followed by a stop codon.

For example consider a DNA sequence

Codon: Thr Pro Glu Glu Glu Thr

Sequence: ACT CCT GAG GAG GAG ACT

Missense mutation

Codon: Thr Pro Glu Glu Glu Thr

Sequence: ACT CCT GAG GAG GAG ACT

Sequence: ACT CCT GTG GAG GAG ACT

Codon: Thr Pro Val Glu Glu Thr

In the above noted example, a single nucleotide change from A to T and thus it codes for Val instead of the amino acid Glu.

Nonsense mutation

Codon: Thr Pro Glu Glu Glu Thr

Sequence: ACT CCT GAG GAG GAG ACT

Sequence: ACT CCT GAG TAG GAG ACT

Codon: Thr Pro Val Stop Glu Thr

Silent mutation

Codon: Thr Pro Glu Glu Glu Thr

Sequence: ACT CCT GAG GAG GAG ACT

Cite this article as: Sathyavikasini K, Vijaya M S. "Predicting Muscular Dystrophy through Genetic testing – A Study". *International Conference on Innovative Trends in Electronics Communication and Applications (2015)*: 65-71. Print.

Sequence: ACT CCA GAG GAG GAG ACT

Codon: Thr Pro Glu Stop Glu Thr

In the 6th position the nucleotide changes from T to A with no change in their amino acid. These mutations are termed as Silent mutations.

Frameshift mutations

Sequence: ACTCCTGAGGAGGAGACT

Sequence: ACTCCTCTGAGGAGGAGACT

The base pairs CT are inserted in the 7th position.

Sequence: ACTCCTGAGGAGGAGACT

Sequence: ACTCCTGAGGAAGACT

The base pairs GG are inserted in the 9th position.

MUSCULAR DYSTROPHY DIAGNOSIS

There is no fruitful remedy for muscular dystrophy disorder and the diagnosis of this disease is a tedious process. The disease can be diagnosed with the results of muscle biopsy, electromyography, electrocardiography and DNA analysis.

Serum creatine kinase is a straightforward and economical indicative test for severe forms of dystrophy. The analysis is done by measuring the serum concentration of creatine kinase. The higher concentrations of serum creatinine kinase than normal values suggest a disorder. A specific disorder is not found out by this laboratory analysis. In DMD, serum creatine kinase concentrations are elevated from birth, and the early diagnosis is done by testing in neonates which helps in reduction of disease further in the family. This method does not diagnose all forms of dystrophy [16,17].

Electromyography testing (EMG) is done in two phases. In the first phase a small needle that is gently inserted into the electrical patterns of the muscles in the arm or thigh. The second phase determines how soon the messages are being sent from the brain to nerves by stimulating the nerves of either arm or leg through a small electrical pulse being sent from the brain to the nerves. EMG test is uncomfortable, painful, lengthy procedure. EMG testing is less favored for children and it is mostly performed only on adults for disease identification. EMG tests are done mainly for the investigation in myotonic dystrophy. The performance of EMG is not satisfied for the patients having less creatinine kinase.

Muscle biopsy and DNA testing are widely used tests to predict muscular dystrophies. A muscle biopsy is a surgical practice where a tiny sample of a muscle is extracted and analyzed. The removal of muscle tissue is done using a biopsy needle and microscopic analysis is done to examine the level of the genes that cause muscular dystrophy. A performing muscle biopsy is costly, it is invasive, and at most care should be taken after the surgery. A muscle biopsy might be considered if speedy and trustworthy genetic testing is unavailable.

Genetic testing is an initial step tested on a blood sample to spot the alteration in the genes so as to help in the diagnosis of muscular dystrophy without performing a muscle biopsy. The risk involved in DNA analysis or genetic testing is minimal and the traits can be identified effectively as the disease-causing genes are explicitly known. Carrier mothers, those who may be at risk of passing this disease on to their children are identified by genetic testing and preventive measures can be provided [18]. To find the mutations in the genes for the patients identified through muscle biopsy, the genetic testing is again performed to confirm the diagnosis. However, the muscle biopsy is optional for the patients diagnosed by genetic testing, to distinguish from other phenotypes [19].

APPROACHES TO INFER MUSCULAR DYSTROPHY

General approaches

The clinical diagnosis of DMD is done through the laboratory analysis of dystrophin. The methodologies engage in recent dystrophin diagnostic experiment includes multiplex PCR, Multiplex ligation-dependent probe amplification (MLPA), Southern blot analysis, Detection of virtually all mutations-SSCP (DOVAM-S). The demerits of these technologies are lengthy, painstaking procedure, and not able to detect duplication mutations precisely. In addition, to carry out carrier testing in females the entire family history should be examined [20].

Cite this article as: Sathyavikasini K, Vijaya M S. "Predicting Muscular Dystrophy through Genetic testing – A Study". *International Conference on Innovative Trends in Electronics Communication and Applications (2015)*: 65-71. Print.

The exact mutation in the DMD gene can be analyzed using gene therapy and missense, nonsense, insertions, deletions and splicing mutations are identified through direct sequencing [21, 22]. Molecular diagnostic methods at nucleotide level are required. The direct sequencing analysis is considered to be laborious, expensive and time-consuming. In some cases, the MLPA reports will be negative and point mutation detected by the sanger method requires direct full gene sequencing, and hence the role of direct sequencing in diagnosis of DMD is increased [23].

Polymerase chain reaction (PCR) is now common and often indispensable technique used in medical and biological research labs in the diagnosis of hereditary diseases. PCR has the benefit of being minimally invasive, efficient and very specific for the detection of large gene deletions, The major drawbacks in this approach are a lack of antimicrobial sensitivity data, complexity of the assay, and the price of PCR equipment and kits [24].

Genetic testing is also an option to confirm a Muscular dystrophy disease. As each disease has several subtypes and there are different genes responsible for each subtype, it is important to narrow the possible type of disease as much as possible using the previously mentioned tests. If the gene change can be found and confirmed, this information can then be used to help in testing other family members to determine whether they are carriers of the disease [25].

Computational Approaches

Sequence-based features have significant differences between the sets of genes known to be involved in human hereditary disease and those not known to be involved in disease. These can be examined with the help of cDNA sequences for the OMIM Mendelian disorders [26]. A set of features was chosen from the gene sequences and classification is done with the machine learning techniques [26].

FSHD one form of muscular dystrophy is diagnosed through gene expression profiling. A gene expression data set consists of dozens of samples with more than thousands of genes. The Linear discrminant analysis is done [8]. Some of the limitations of microarray data to classify all forms of muscular dystrophy are (i) the cDNA probes plotted on the microarrays do not cover all of the genes expressed in skeletal muscle, (ii) the properties of probe cDNAs have not been not well-characterized, (iii) homologous genes of each target gene may cross-hybridize with the probes and because relatively large amounts of RNA are required, (iv) each microarray analysis requires pooled RNA samples from several patients [27].

Muscular dystrophy and its subtypes are classified by integrating protein-protein interaction (PPI) network, using interpretable gene set information and mRNA profiling data. Identification of gene sub-networks are done using a distance metric approach named affinity propagation clustering (APC) approach. The biomarkers are identified the functional gene set information is combined. Classification of muscular dystrophy is done with multi-class support vector machines (MSVMs) with the gene set features and subnetworks. Using this approach sub-networks and gene sets are identified that are more relevant to MD [28].

Machine learning techniques have been successfully applied to identifying disease-associated genes [29]. The problem is formulated as a supervised learning problem, where the task is to make the classifiers to learn from training data and the prediction is made from the learned classifier [30].

Schizophrenia is a genetic disease and also a heterogeneous syndrome characterized by perturbations in language, perception, thinking and social relationships [31]. There is no set of symptoms finalized to categorize this disease other than the genetic factors. Disease gene association studies focused on SNP (Single Nucleotide polymorphism) aids in predicting the disease [31]. Twelve machine learning techniques and seven datasets are considered to classify the disease.

Numerous supervised learning techniques and various types of gene or protein annotation data have been used to solve the disease gene classification problem. Supervised algorithms such as k-Nearest Neighbor, Decision tree learning, Artificial Neural Networks, Naive Bayes and Support Vector Machines are compared and their performance is analyzed for predicting the disease.

The classification of muscular dystrophy continues to evolve with the advances in understanding of their molecular genetics. A huge number of muscular dystrophy related defective genes and proteins are identified, but no effective treatments are known for many of its subtypes. At present, there is no effective method to identify and classify all types of muscular dystrophy. The proportion of mutations in deletions, duplications and point mutations differs in each type of disease and to date, no genetic testing has been developed to cover this whole mutational spectrum in a single platform. Large size and number of genes for all types of muscular dystrophy requires considerable effort, cost and time for direct sequencing. The direct sequence analysis of this spectrum involved in all kind muscular dystrophy requires a high level of the laboratory. However, it is more important to know the exact mutation site and type to predict prognosis and, therefore, all the mutation sites should be analyzed effectively.

OBSERVATIONS AND DISCUSSION

From the study, it is observed that few forms of muscular dystrophy are identified through computational methods based on full direct sequencing and microarray data. Usage of microarray gene expression data is convincing when multiple genes involved in a disease and also hereditary traits cannot be detected efficiently. It was observed that the discussed approaches involve more cost for classifying the disease sequences and to predict the type of muscular dystrophy and also accuracy may not be achieved.

Cite this article as: Sathyavikasini K, Vijaya M S. "Predicting Muscular Dystrophy through Genetic testing – A Study". *International Conference on Innovative Trends in Electronics Communication and Applications (2015)*: 65-71. Print.

Tests for only a few types of muscular dystrophy disease are already in clinical use. The apparent benefit of hereditary testing aids in identifying and understanding of risk for a certain type of disease. Predictive hereditary tests for all types of muscular dystrophy need to be done.

The current advancements in gene testing helps in identifying people at a risk of getting a disease in advance in ahead of any symptom appears. An accurate gene test result in finding the disease-related gene mutation.

As the vulnerability of the disease is high the tests helps in detecting the possibility of the disease in carrier mothers so that there is a possibility of finding the disease in carrier son/daughter at the earliest before birth. The traditional method of testing is time consuming and incurs cost overhead.

Identification of genetic factors in complex diseases like muscular dystrophy is a far more difficult task with the standard methods as it is difficult to analyze the data. The complex diseases provide a lot of challenges to standard data analysis techniques.

Therefore, it is essential to model and represent this knowledge in a computational form with minimal loss of biological context through a gene sequences based approach. Disease-gene associations need to be designed and a suitable classification algorithm should be identified to handle this type of data.

With the help of sequence based information, a model can be created based on supervised learning techniques to infer the genetic disease effectively.

CONCLUSION

In this recent survey research on the muscular dystrophy disease identification through computational intelligence is reviewed. This paper elucidates the introduction of DNA mutations, the vulnerability of muscular dystrophy disease and various techniques involved in identifying the disease briefly. From the observations, it is concluded that usage of the available clinical methods is not able to process huge data. Microarray gene expression data and protein-protein interaction methods help in identifying disease when multiple genes involved. Inferring a muscular dystrophy using the mutated gene sequences should be carried out to spot the disease efficiently. To deal with a large number of sequences, new disease identification model should be designed and developed based on the advanced learning techniques like deep learning. A distributed environment should be created with the big data technologies like Hadoop and its components that support in predicting the disease effectively using a large number of mutated gene sequences.

REFERENCES

[1] Preeti Kale1 and Jagannath V Aghav2. Computational Methods to Infer Human Diseases. A Survey.

[2] Eugenio Mercuri, Francesco Muntoni. 2013, Muscular Dystrophies Lancet; 381: 845–60

[3] Jerry Lewis. 2000, Facts About Rare Muscular Dystrophies Congenital (CMD), Distal (DD), Emery-Dreifuss (EDMD) & Oculopharyngeal Muscular Dystrophies (OPMD), Muscular dystrophy foundation. Australia

[4] Alan E H Emery. February 23, 2002, The Muscular Dystrophies THE LANCET • Vol 359 •

[5] Katharine Bushby, Richard Finkel, David J Birnkrant, et.al. November 30, 2009, Diagnosis and management of Duchenne muscular dystrophy, part 1: diagnosis, and pharmacological and psychosocial management Charcot-Marie-Tooth Disease U.S. DEPARTMENT OF HEALTH AND HUMAN SERVICES Public Health Service National Institutes of Health

[6] Agnes Jani-Acsadi, M.D.,1 Karen Krajewski, M.S.,1 and Michael E. Shy, M. D. 2008, Charcot-Marie-Tooth Neuropathies: Diagnosis and Management, Thieme Medical Publisher

[7] Fe′ lix F. Gonza′lez-Navarro, Llu′s A. Belanche-Mun˜ oz, Karen A. Silva-Colo′n. December 13, 2013, Effective Classification and Gene Expression Profiling for the Facioscapulohumeral Muscular Dystrophy, LoS ONE 8(12): e82071. doi:10.1371/journal.pone.0082071

[8] Chris Turner, David Hilton-Jones. December 2008, The myotonic dystrophies: diagnosis and management, Journal of Neurology, Neurosurgery and psychiatry

[9] Mariana T. C. Baioni,1 Celia R. Ambiel. August 2010, Spinal muscular atrophy: diagnosis, treatment and future prospects, Jornal de Pediatria

[10] Adele D'Amico, Eugenio Mercuri, Francesco D Tiziano and Enrico Bertini. November 2011, Spinal muscular atrophy Orphanet Journal of Rare Diseases, Orphanet Journal of Rare Diseases

[11] Kevin M. Flanigan, Diane Dunn, et.al. July 25 2012 Mutational Spectrum of DMD Mutations in Dystrophinopathy Patients: Application of Modern Diagnostic Techniques to a Large Cohort, PMC

[12] Kevin M. Flanigan, Diane Dunn, et.al July 26 2013, Nonsense mutation-associated Becker muscular dystrophy: interplay between exon definition and splicing regulatory elements within the DMD gene, PMC.

Cite this article as: Sathyavikasini K, Vijaya M S. "Predicting Muscular Dystrophy through Genetic testing – A Study". *International Conference on Innovative Trends in Electronics Communication and Applications (2015)*: 65-71. Print.

[13] Krahn M, Bernard R, et.al May 2006 Screening of the CAPN3 gene in patients with possible LGMD2A, Clinical Genetics

[14] Nevo Y, Ahituv S, et.al. June 2001, Novel mutations in the emerin gene in Israeli families, Human Mutation

[15] van Ommen GJB, Scheuerbrandt G. 1993, Workshop report: neonatal screening for muscular dystrophy. Neuromuscul Disord; 3: 231–39.

[16] Bushby K, Hill A, Steele JG. 1999, Failure of early diagnosis in symptomatic Duchenne muscular dystrophy. Lancet; 353: 557–58.

[17] http://evolution.berkeley.edu/evolibrary/article/ mutations_01

[18] Katharine Bushby, Richard Finkel,et.al. 2010, Diagnosis and management of Duchenne muscular dystrophy, part 1: diagnosis, and pharmacological and psychosocial management, Lancet Neurol; 9: 77–93

[19] Madhuri R. Hegde1, Ephrem L.H. Chin1, Jennifer G. Mulle1, David T. Okou1, Stephen T. 2008, Microarray-based mutation detection in the dystrophin gene, Department of Human Genetics, Emory University School of Medicine, Atlanta, Georgia

[20] KN North and KJ Jones.1997, Diagnosing childhood muscular dystrophies. Journal of Paediatrics and Child Health

[21] Roberts et al. March 1992,Point mutations in the dystrophin gene Vol.9 Genetics

[22] Koenig M, Hoffman EP, Bertelson CJ, Monaco AP, Feener C, Kunkel LM. March 1992, Complete cloning of the Duchenne muscular dystrophy (DMD) cDNA and preliminary genomic organization of the DMD gene innormal and affected individuals. Cell 1987;50:509±517

[23] Hyeyoung Lee, Dong Wook Jekarl, Joonhong Park, Hyojin Chae, Myungshin Kim,Yonggoo Kim, and Jong in Lee. 2013, Identification of DMD Mutation in Korean Siblings Using Full Gene Sequencing, Int J Hum Genet, 13(2): 127-130

[24] Masaji Tachikawa, Tatsushi Toda et.al. M.D The Muscular Dystrophies

[25] Euan A Adie, Richard R Adams, Kathryn L Evans, David J Porteous and Ben S Pickard. Speeding disease gene discovery by sequence based candidate prioritization.

[26] Satoru Noguchi1, Toshifumi Tsukahara, Masako Fujita, Rumi Kurokawa, et.al 2003, cDNA microarray analysis of individual Duchenne muscular dystrophy patients Human Molecular Genetics, Vol. 12, No. 6

[27] Chen Wang, Sook Ha et.al September 2012 Computational Analysis of Muscular Dystrophy Sub-types Using A Novel Integrative Scheme Neurocomputing.

[28] Maria Loapez-Bigas and Christos A et.al, 2004, Genome-wide identification of genes likely to be involved in human genetic disease. Ouzounis Nucleic Acids Research, Vol. 32, No. 10

[29] Duc-Hau Le, Nguyen Xuan Hoai, and Yung-Keun Kwon. 2015, A Comparative Study of Classification-Based Machine Learning Methods for Novel Disease Gene Prediction. Advances in Intelligent Systems and Computing,Volume 326, pp 577-588 Aguiar-Pulido, José A. Seoane, Juan R. Rabuñal, Julián Dorado, Alejandro Pazos and Cristian R, Vanessa. Munteanu, 2010. Machine Learning Techniques for Single Nucleotide Polymorphism—Disease Classification Models in Schizophrenia. Molecules, 15, 4875-4889.

Cite this article as: Sathyavikasini K, Vijaya M S. "Predicting Muscular Dystrophy through Genetic testing – A Study". *International Conference on Innovative Trends in Electronics Communication and Applications (2015)*: 65-71. Print.

International Conference on Innovative Trends in Electronics Communication and Applications 2015 [ICIECA 2015]

ISBN	978-81-929742-6-2	**VOL**	01
Website	icieca.in	**eMail**	icieca@asdf.res.in
Received	02 - April - 2015	**Accepted**	15 - November - 2015
Article ID	ICIECA011	**eAID**	ICIECA.2015.011

Robotic Plastic Separator

Alagaraj P[1], Karthik M R[2], Preethi S[2], Pon Rajeswari V[2]
[1]Professor, [2]Student, Department of Electronics & Communication Engineering
Mookambigai College of Engineering
Kalamavur, Tamilnadu, India

Abstract: *Plastic bags are one of the few new chemical materials which pose environmental problem. Plastic bags are used because they are simple and economical to make and they can last a long time. Unfortunately, these same useful qualities can make plastic a huge cleanliness problem. Because the plastic is most economical it gets discarded easily and its persistence in the environment can do great harm. We propose robotic plastic bags separator for separating plastic bags from mixtures, of waste such as paper, fibers, aluminium foil, copper wire chips, sand, and glass. The robotic arm is fitted with an IR sensor and flex sensor to identify the plastic material. The combined output from the IR sensor and flex sensor are processed by the microcontroller and issues commands to sort out the plastic from other materials. Here we use IR sensors and flex sensors to sense the materials for separation. The reflected signal from the IR transmitter can be used to separate the plastic from the waste. The Robot applies some angular displacement to the plastic to confirm before placing in the plastic waste box. This Robot can be used to pick up plastic bags lying by the roadside, playground and all around us. Humans and robots can work alongside to make our planet safe from plastic pollution.*

Keywords*:* Plastic Bags, IR Sensor, Flex Sensor

INTRODUCTION

The purpose of our paper is to present a generalized approach towards a green environment. It describes the development of microcontroller base Robotic separation of non-degradable waste such as plastics from degradable waste. The trend towards economical, miniaturization and high efficiency is by using Infrared sensor and a flex sensor. Here we use an infrared sensor. The Infrared sensor fitted on the robotic arm to sense the materials such as plastic, wood, glass, metal and other materials present in the trash barrel. If the voltage ranges within the limit, the Infrared sensor sends a control signal to the robotic arm through the pre-programmed microcontroller; the robotic arm picks up the plastic material. Now the pre-programmed microcontroller activates the flex sensor and the control signal is sent from the microcontroller to the robotic arm to crush the material, based on the measurements of angular displacement the materials are classified. Finally the non-degradable wastes such as plastics are segregated.

ROBOTIC ARM

In the field of robotics the robotic arm can solve many human limitations. A typical robotic arm is made up of seven metal segments,connected by six joints.The microcontroller controls the movement of stepper motors connected to each joint. The robotic arm uses motion sensor to make sure it moves just the right amount. A robotic arm with six joints closely resembles a human arm, it has equivalent of a shoulder, an elbow and a wrist. The shoulder is mounted to a stationary base. Here we used this robotic arm to pick up the waste materials from the trash barrel.

Cite this article as: Alagaraj P, Karthik M R, Preethi S, Pon Rajeswari V. "Robotic Plastic Separator". *International Conference on Innovative Trends in Electronics Communication and Applications (2015)*: 72-75. Print.

BLOCK DIAGRAM

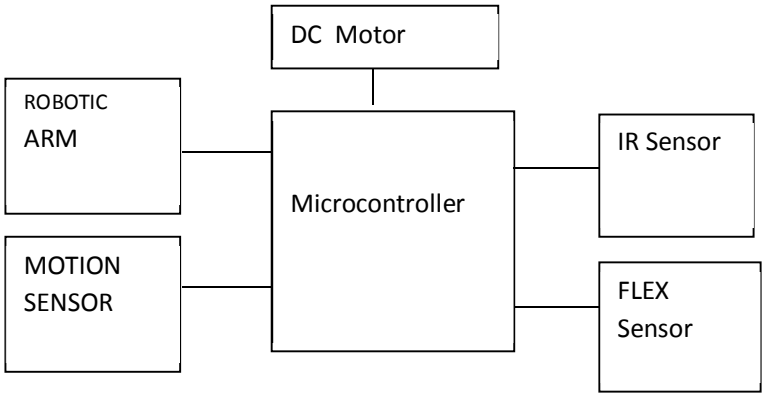

Fig. 1 Block diagram of Plastic Separator

MICROCONTROLLER

A microcontroller is a programmable digital processor with necessary peripherals. It is also known as a small computer on a single integrated circuit containing a processor core, memory and programmable input/output peripherals. It is a complex sequential digital circuit meant to carry out its job, according to the program.It is designed for embedded systems.Analog to digital converter is used to convert the physical quantities like pressure, temperature, etc into the electrical signal (i.e) voltage. A 8-bit ADC has a range of 0-255. The signals which we are getting from our sensor is of analog signal, so the analog signal must be converted to digital signal using analog to digital converter. By converting from analog to the digital, we can begin to use electronics to interface with the analog signal around us. The process flow of analog to digital converter is given below

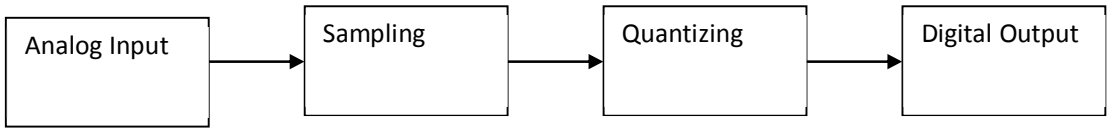

Fig. 2 Block diagram of analog to the digital converter

Infrared sensor

An Infrared sensor is an electronic device. IR sensor consists of an IR transmitter or an IR emitter and an IR detector. The emitter is simply an IR LED and the detector is simply an IR photodiode which is sensitive to IR light of the same wavelength. When IR light falls on the photodiode, the resistances and hence the output voltage change in proportion to the magnitude of the IR light received. Thus the light energy is converted to electrical energy. The IR detector is used in the feedback path of an inverting operational amplifier as shown in Fig.1 below. The output voltage of the op amp is given by

$$vo = \frac{Rf}{Ri}\ vi$$

where vi is negative reference voltage at the input, Rf is the variable resistance of photodiode, the gain of the op amp is gain=$-\frac{Rf}{Ri}$

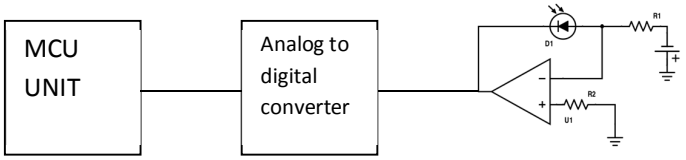

Fig 3. Infrared sensor

Cite this article as: Alagaraj P, Karthik M R, Preethi S, Pon Rajeswari V. "Robotic Plastic Separator". *International Conference on Innovative Trends in Electronics Communication and Applications (2015)*: 72-75. Print.

The output of the op-amp is an analog voltage that varies acording to the light reflected from the plastic materials. The analog output of the op-amp is provided to analog to digital converter whose result is fed to the microcontroller. If the output voltage falls in the range of pre-programmed voltages for plastic, then microcontroller controls the movement of a robotic arm to pick up that material. Here we did a sample experiment to verify the behavior of the voltage for different thickness of plastics in microns.

TABLE I

THICKNESS OF PLASTIC VS VOLTAGE

Microns	Voltage (V)
40	0.2
30	0.4

FLEX SENSOR

Flex sensor has variable resistance that change its resistance depending on the amount of bend on the sensor. They convert meachanical pressure to electrical resistance, the more bend the more the resistance value. The Flat Resistance of flex sensor is 25K Ohms and Bend Resistance ranges fron 45K to 125K Ohms. They are usually in the form of a thin strip from 1"-5" long that vary in resistance.

The output of Infrared sensor is processed by the microcontroller and sends a control signal to the robotic arm to pickup the material. The robotic arm fitted with flex sensor crush the material, depending upon the bend applied to crush the material we can segregate non-degradable waste such as plastics from other metals, wood, glass. The bend radius needed to crush a plastic is high as compared to other materials like metals, wood and glass. The high resistance of the flex senor can be used easily separate plastic from other waste. The basic flex sensor circuit is given below

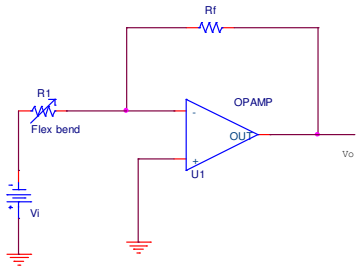

Fig 4. Basic Flex sensor circuit

The flex sensor is connected to an inverting op amp as shown in fig 4. The output voltage is given as

$$vo = \frac{Rf}{Ri}\ vi$$

where Ri is the variable resistance of the flex sensor.

A negative reference voltage vi will give a positive output. The output of Flex sensor circuit is converted to digital before fed to the microcontroller. The microcontroller compares the output voltage with the reference voltages for different grade of plastics stored in the memory to separate plastic from other waste.

CONCLUSION

The awareness of keeping our planet pollution free is increasing rapidly. Engineering always has been a part of development and fulfillment of all needs of Humanity. So here we have just one of the basic experimental solutions for saving our planet from plastic. Further enchancement of this concept can be made by the usage of capacitive proximity sensor instead IR sensors which can reduce time consumption and provide greater accuracy. So, in the future if this may becomes more effective solution to provide green environment and save us from non-degradable plastics. Betterment in cleaning process leads to betterment in life and society which further extends to a better planet to live.

Cite this article as: Alagaraj P, Karthik M R, Preethi S, Pon Rajeswari V. "Robotic Plastic Separator". *International Conference on Innovative Trends in Electronics Communication and Applications (2015)*: 72-75. Print.

REFERENCES

[1] S. KRlMM, C. Y. LIANG, AND G. B. B. M. SUTHERLAND," Infrared Spectra of High Polymers. II. Polyethylene," October 27, 1955
[2] http://www.alldatasheet.com/
[3] http://maxembedded.com
[4] https://www.sparkfun.com/

Cite this article as: Alagaraj P, Karthik M R, Preethi S, Pon Rajeswari V. "Robotic Plastic Separator". *International Conference on Innovative Trends in Electronics Communication and Applications (2015)*: 72-75. Print.

International Conference on Innovative Trends in Electronics Communication and Applications 2015 [ICIECA 2015]

ISBN	978-81-929742-6-2
Website	icieca.in
Received	02 - April - 2015
Article ID	ICIECA012

VOL	01
eMail	icieca@asdf.res.in
Accepted	15 - November - 2015
eAID	ICIECA.2015.012

Invertible Data Embedding By Histogram Modification and Contrast Enhancement

J Kanimozhi[1], P Vasuki[2], K D Karthick[3], M C Arvind kumar[4]

Abstract: *The main aim is to enhance the contrast of a host image by Reversible data hiding algorithm and to improve its visual quality. The highest two bins in the histogram are selected for data embedding so that histogram equalization can be performed by repeating the process. The Reversible data hiding algorithm is used for better preserving the visual quality of contrast enhanced image with increased efficiency. Further, the evaluation result shows that the visual quality can be preserved and also it can be applied to medical and satellite images for better visibility.*

Keywords*:* Data embedding,PSNR,Hiding Capacity

INTRODUCTION

An image is a array, or matrix, of s pixels (picture elements) arranged in columns and rows. Digital image processing is the use of computer computations to perform image processing on digital images. The 2D continuous image is divided into rows and columns. The image can also be a function other variables including depth, color, and time.[1]The input image is first divided into groups based on the optional key. Then RS vector is calculated for each group using flipping function. The RS vector is then compressed and the groups are flipped. Then message bits are included in the flipped groups. This is the resulting Stego image. While extracting the data the Stego image is first divided into groups based on the same optional key. Then RS vector is calculated for each group using the flipping function. The RS vector is then decompressed and the groups are unflipped. Then message bits are obtained from the unflipped groups. Finally the original image is restored. [2]

An image given in the form of a, photograph or ray is first digitized and stored as a matrix of 0,1 digits in computer memory. This digitized image can be displayed on a high-resolution television monitor. For display, the image is stored in a fast-access buffer memory, which refreshes the monitor at a rate of 25 frames per second to produce a visually continuous display. However, the world is in stable motion: stare at something for long enough and it will change in some way. Even a large solid, like a building or a mountain, will change its appearance depending on the time of day (day or night); or various shadows falling upon it. We are concerned with single images. Although image processing can deal with changing scenes, for our purposes, an image is a single picture which represents something. It may be a picture of a person, of people or animals, or of an outdoor scene, or a microphotograph of an electronic component, or the result of imaging. Even if the picture is not immediately recognizable, it will not be just a random blur.

DIGITIZER

Digitizing or digitization is the representation of an object, image, sound, document or a signal (usually an analog signal) by a discrete set of its points or samples. Digital information exists as one of two digits. These are known as bits. An image is digitized to convert it to a form which can be stored in computer's memory or on some form of storage media such as a hard disk. This digitization procedure can be done by a scanner, or by a video camera connected to a frame grabber board in a computer. Once the image has been digitized, it can be operated upon by various image processing operations.

Cite this article as: J Kanimozhi, P Vasuki, K D Karthick, M C Arvind kumar. "Invertible Data Embedding By Histogram Modification and Contrast Enhancement". *International Conference on Innovative Trends in Electronics Communication and Applications (2015)*: 76-84. Print.

Vidicon camer
Photosensitive solid- state arrays.

THE IMAGE PROCESSING SYSTEM

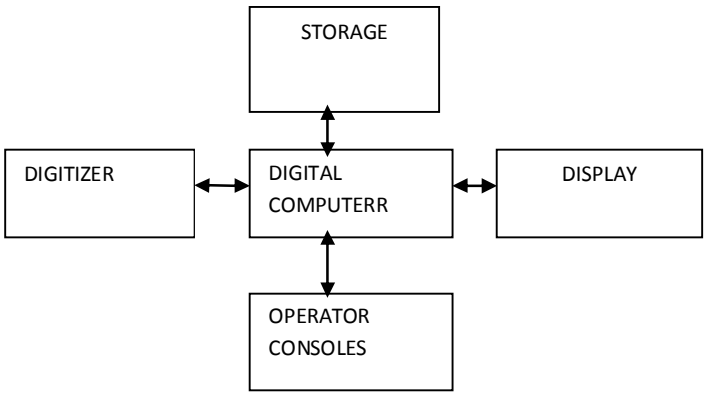

Fig .Block diagram of Image processing system

DIGITAL COMPUTER

A computer is an electronic device that accepts raw data, processes it according to a set of instructions and required to produce the desired result. Mathematical processing of the digitized image such as convolution, averaging, addition, subtraction, etc. are done by the computer.

MASS STORAGE

Mass storage devices used in desktop and most server computers typically have their data organized in a file system. The secondary storage devices normally used are floppy disks, CD ROMs etc.

OPERATOR CONSOLE

The operator console consists of equipment and arrangements for verification of results and for alterations in the software as and when require. The operator is also capable of checking for any errors and for the entry of requisite data.

DISPLAY

Popular display devices produce spots (display elements) for each pixel

- Cathode ray tubes (CRTs).
- Liquid crystal displays (LCDs).
- Printers.

Spots may be binary (e.g., monochrome LCD), achromatic (e.g.,so-called black-and-white, actually grayscale for intensity), pseudo color or false colors (e.g., for intensity or hyper spectral data), or true color (color data displayed as such).

IMAGE PROCESSING FUNDAMENTAL

PIXEL

In order for any digital computer processing to be carried out on an image, it must first be stored within the computing machine in a suitable form that can be manipulated by a computer program. The most practical way of doing this is to divide the image up into a collection of discrete components (and usually small) cells,which are known as *pixels*. Most commonly, the image is divided up into a rectangular grid of pixels, so that each pixel is itself a small rectangle. After this has been done, each pixel is given a value that represents the color of that pixel. It is assumed that the entire pixel is the same color, and so any colour variation that did exist within the area of the pixel before the image was lost. However, if the area of each pixel is very small, then the discrete nature of the image is often not visible to the human eye.

Cite this article as: J Kanimozhi, P Vasuki, K D Karthick, M C Arvind kumar. "Invertible Data Embedding By Histogram Modification and Contrast Enhancement". *International Conference on Innovative Trends in Electronics Communication and Applications (2015)*: 76-84. Print.

Pixel shapes and formations can be used, most notably the hexagonal grid, in which each pixel is a small hexagon. Has some advantages in image processing, including the fact that pixel connectivity is less ambiguously defined than with a squarical grid, but hexagonal grids are not widely used.

PIXEL CONNECTIVITY

The notation of pixel connectivity describes a relation between two or more pixels. For two pixels to be connected they have to fulfill certain criteria on the pixel brightness and spatial adjacency. First, in order of 2 pixels to be connected, their pixel values must both be from the same set of values *V*. A pixel *p* is connected to a pixel *q* if *p* is *4*-connected to *q* or if *p* is *4*-connected to a third pixel which itself is connected to *q*. Or, in other words, two pixels *q* and *p* are connected if there is a path from *p* and *q* on which each pixel is *4*-connected to the next one. A package of pixels in an image which are all connected to each other is called a component. Finding all connected components in an image and marking each of them with a differentiable label is called connected component labeling.

RGB

The **RGB color model** in which red, green and blue light are mixed together in various ways to reproduce a broad array of colors. RGB uses additive color adding and is the basic color model used in television or any other medium that projects color with light. It is the basic RGB model used in computers and for web graphics, but it cannot be used for print production.
The secondary colors of basic model – cyan, magenta, and yellow – are formed by mixing two of the primary colors (**red, green** or **blue**) and excluding the third color.

IMAGE TYPES

There are several ways of encoding the information in an image.

- Binary image
- Grayscale image
- Indexed image
- True color or RGB image

BINARY IMAGE

Each pixel is just blackor white. Since there are only two possible values for each pixel (0, 1), we only need one bitper pixel.

GRAYSCALE IMAGE

Each pixel is a shade of gray, normally from 0 (black) to 255(white). This range means that each pixel can be represented by eight bits, or exactly one byte.

INDEXED IMAGE

An indexed image consists of an array and a color map matrix. The pixel values in the array are direct indices into a color map. By convention, this documentation uses the variable name X to refer to the array and map to refer to the color map.

TRUE COLOR OR RGB IMAGE

Each pixel has a particular color; that color is described by the amount of red, green and blue in it. If each of these components has a range 0–255, this gives a total of 2563 different possible colors. Such an image is a "stack" of three matrices; representing the red, green and blue values for each pixel. This means that for every pixel there correspond 3 values.

METHODOLOGY

IMAGE CONTRAST ENHANCEMENT

CONTRAST ENHANCEMENT:

Contrast defines the difference between lowest and highest intensity level. Higher the value of contrast means more difference between lowest and highest intensity level. Image enhancement is among the simplest and most appealing areas of digital image processing. Basically, the idea behind enhancement techniques is to bring out detail that is obscured, or simply to highlight certain features of interest in an image. It is important to keep in mind that enhancement is a very subjective area of image processing. Improvement in quality of these degraded images can be achieved by using application of enhancement techniques.

Cite this article as: J Kanimozhi, P Vasuki, K D Karthick, M C Arvind kumar. "Invertible Data Embedding By Histogram Modification and Contrast Enhancement". *International Conference on Innovative Trends in Electronics Communication and Applications (2015)*: 76-84. Print.

HISTOGRAM PROCESSING:

Image contrast enhancement employs a partitioning operation over the input histogram to chop it into few histograms so that they have no dominating component in them. Then each sub-histogram goes through the and is allowed to occupy a specified gray level range in the enhanced output image. Thus, a better overall contrast enhancement is acquired by dhe with controlled dynamic range of gray levels and eliminating the possibility of the low histogram components.
The discrete function h(rk)=nk , where rk is the kth gray level in the range of [0, L-1] and nk is the number of pixels having gray level rk.In an image of low contrast, the image has grey levels concentrated in a short band.Define the grey level histogram of an image *h(i)* where :

h(i)=number of pixels with grey level = *i*

NORMALIZED HISTOGRAM

It is p(rk)=nk/n, for k=0,1,…,L-1 and p(rk) can be considered to give an estimate of the probability of occurrence of ray level rk.Each of the two peaks in the histogram is split into two adjacent bins with the similar or same altitude because the numbers of 0s and 1s in the message bits are required to be almost equal. To increase the hiding rate, the highest two bins in the modified histogram are further chosen to be split to all pixels counted in the histogram. The same can be repeated by splitting each of the two peaks into two adjacent bins with the similar heights to achieve the histogram equalization effect.

In this way, data embedding and contrast enhancement are simultaneously performed. Given that the pair number of the histogram peaks to be split is , the added by while the pixels from to 255 are subtracted by in the pre-process (noting L is a positive integer). A location map is generated by assigning 1s to the altered to pixels, and 0s to the others. The location 23 map can be pre-computed and reduced to be firstly embedded into the host image. The value of, the size of the compressed location map, and the previous peak values, incontrary, are embedded with the last two peaks to be split, whose values are stored in the LSBs of the 16 pixels. In the extraction process, the last split peak values are retrieved and the data embedded with them are extracted. After restoring the histogram, the data embedded with the previously split peaks can also be extracted by processing them pair by pair. At last, the location map is obtained from the extracted data to identify the pixel values modified in the image.

REVERSIBLE DATA HIDING USING *HISTOGRAM SHIFTING*

REVERSIBLE DATA HIDING

Reversible Data Hiding (RDH) has been concentrated on a study of Signal processing. The Lossless Data Hiding techniques hide data in a received signal (i.e., an image) which can able to extract the original signal and also with embedded data. It needs two important provisions for data hiding techniques are capacity of embedding should be large and with low distortion. In digital images there are many proposed algorithms to embed invisible data. This method divides the image into pairs of pixels and uses each legitimate pair for hiding one bit of information. So that the capacity is at best 0.5b/pixels. However a compressed location map also needs 0.5b/pixels. To estimate the secret rate and the smudged image quality are the two important metrics watermark within the host signal whileretaining the characteristic of the host untainted.

A technique to embed watermark in the JPEG compressed encrypted images. The algorithm is simple to implement as it is directly performed on the compressed-encrypted domain. it does not require decrypting or partial decompression of the content.. The homomorphism properties of the crypto are exploited, which allows us to detect the watermark after decryption and control the image quality as well. We analyze the relation between payload capacity and quality of the image for different resolutions[5]

NEED FOR REVERSIBLE DATA HIDING:

Reversibility gives the ability to retrieve the exact original input data after extraction process. This is a technique to embed additional message into some distortion not acceptable cover media, such as military or medical images, with a reversible manner so that the original cover content can be restored well after extraction of the hidden message. Reversibility can be used. The lossless embedding highers the size of the original image and lossy embedding process cannot be applied to medical field. Recently, reversible data embedding technique has attracted many attentions. It is also called lossless data hiding

Cite this article as: J Kanimozhi, P Vasuki, K D Karthick, M C Arvind kumar. "Invertible Data Embedding By Histogram Modification and Contrast Enhancement". *International Conference on Innovative Trends in Electronics Communication and Applications (2015)*: 76-84. Print.

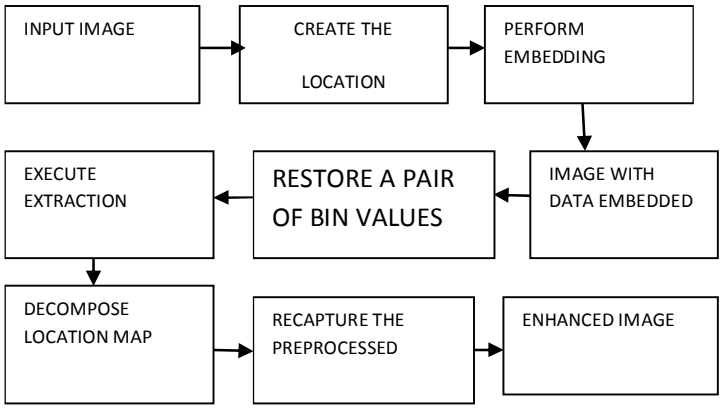

Fig. Block Diagram of RDH Algorithm

.

KEY PARAMETERS OF REVERSIBLE DATA HIDING

Reversible watermarking is a feasible concept due to the fact that the original media usually has a strong spatial or temporary efficiency. Reversibility is guaranteed if enough free space can be found or created to embed the appropriate transform domain by suitable techniques and methods. There are some key parameters are taken care of while trying to increase the embedding capacity at the cost of image quality. A few important ones are briefed below. [3] A joint watermark protocol for the MPML-DRM-A using Chinese remainder theorem. The proposed scheme ensures that only two watermark signals are embedded into the content compared to the embedding of multiple watermark signals into the content with the naive approach. The proposed watermarking protocol involves the entities: an owner levels of distributors a consumer, and a license server. We generate the joint watermark information as the (CRT) solution of a set of congruence's corresponding to each party in the distribution chain. The watermark signal is generated from this joint watermark information using a watermark generation algorithm and then embedded into robust embedding algorithm. The watermark signal is detected using the corresponding watermark detection algorithm. [4] The paper is our response to the call for proposal of the JPEG Security (JPSEC) Working Group. The schemes are very computationally efficient. The schemes are also very secure since they protect 99.15% of the information of an image. Furthermore the schemes are standard compliant which guarantee the inheritance of many nice properties of the un-protected code-streams that have been well built and studied. a JPEG2000 code-stream is structured as a main header followed by a sequence of tile-streams. The code-information should be complete enough stream is terminated by a two-byte marker, EOC (end of code-stream).[6]

FIDELITY

Fidelity is a definition of how far the extracted image resembles the original image in all means. It is an important criterion in bio medical image processing, since even the slightest visual difference cannot be tolerated. A reversible data embedding ensure that there is a perfect balance between quantity of data embedded and the image quality. Fidelity is a term that is concerned with the human visual representation of an image. Fidelity between two pictures are said to be high if the human visual system is not able to detect any visible changes in the modified image.

EFFICIENCY

Efficiency in reversible data embedding depends on the amount of patient information that can be cast into the cover image calculated in bits per pixels (bpp) without affecting the visual quality of the cover image measured in terms of the PSNR.

SECURITY

Security is yet another key factor which deals with the type of encryption and decryption schemes involved in the embedding and extraction procedures, their simplicity in implementation and their strength against hackers. Use of a strong key, number of rounds of encryption is some of the main factors which affect the security of the system. It is a key factor since the patient record in the Hospital storage system should not be tampered with or destroyed on any account.

Cite this article as: J Kanimozhi, P Vasuki, K D Karthick, M C Arvind kumar. "Invertible Data Embedding By Histogram Modification and Contrast Enhancement". *International Conference on Innovative Trends in Electronics Communication and Applications (2015)*: 76-84. Print.

PAYLOAD

Data payload refers to the number of bits a watermark system embeds within a unit of time or within a unit of cover signal. A data embedding scheme that embeds N bits into the cover signal is referred to as an embedded. The required data payload may differ greatly for each application. Copy protection or control applications may require only a few bits of information while broadcast monitoring may require rates three times larger than the previous case, or in case of forensic applications the necessary tobe-embedded to prevent any modification of the content. In medical data management, there cannot be any compromise on the payload content as it has the entire patient information, the doctor‘s diagnosis and subsequent treatment information which cannot be selectively ignore.

PREPROCESSING

In order to reversibly retrieve the original image, a problem must be considered, i.e., overflow and underflow problem (for simplicity, overflow is used to represent either overflow or underflow in the rest of this paper). Therefore, a location map is created to record the locations of pixels which will exceed the permitted value range, gray scale image, after watermark embedding.

The main idea of the median filter is to run through the signal entry by entry, replacing each entry with the median of neighboring entries. The pattern "window", which slides entry by entry, over the entire signal. For one dimension signals, the most obvious window is just the first few preceding and following entries, whereas for 2D (or higher-dimensional) signals such , more complex window patterns are possible (such as "box" or "cross" patterns).The median is simple to define: it is just the middle value after all the entries in the window are sorted numerically.

LOCATION MAP

It is performed by modifying the histogram of pixel values. Firstly, the two peaks in the histogram are found out. The bins between the peaks are not changed while the outer bins are shifted outward so that each of the two peaks can be split into two adjacent bins. To increase the embedding capacity, the highest two bins in the modified histogram can be further to be split, and so on until satisfactory contrast enhancement effect is achieved. To avoid the overflows and underflows due to histogram changes, the bounding pixel values are pre-processed and a location map is generated to memorize their locations. For the recovery of the input image, the location map is embedded into the host image, together with the message bits and other side information. So blind data extraction and complete recovery of the input image are accesed. The proposed algorithm was applied to two set of images.

HISTOGRAM SHIFTING

Algorithm for embedding:

1) Pre-process: The pixels in the range of (0002C255) are processed excluding the first 16 pixels in the bottom row. A location map is generated.
2) Histogram is calculated without counting the first 16 pixels in the bottom row
3) Embedding: The highest two bins in the histogram are split for data embedding. Then the two peaks in the modified histogram are split, and so on until pairs are split. The location map is embedded before the message bits.
4) The finally split peak values are used to replace the LSBs of the 16 excluded pixels to form the marked image.
Algorithm for Extraction and Recovery Process:
1) The LSBs of the 16 excluded pixels are retrieved.
2) The data embedded with the last two split peaks are extracted, the length of the compressed location map, the original LSBs of 16 excluded pixels, and the previously split peak values are known.
3) The recovery operations are carried out by processing all pixels except the 16 excluded ones.
4) The compressed location map is obtained from the extracted binary values and decompressed to the original size.
5) With the decompressed map, those pixels modified in preprocess are identified.
6) A pixel value is subtracted by if it is less than 128, or increased by otherwise. At last, the original image is recovered.

Calculation of PSNR Value:

1)MSE = t1/(row*col);

2)maxval = sum(max(clean));

3)PSNR = 10*log10(maxval/MSE);

Cite this article as: J Kanimozhi, P Vasuki, K D Karthick, M C Arvind kumar. “Invertible Data Embedding By Histogram Modification and Contrast Enhancement”. *International Conference on Innovative Trends in Electronics Communication and Applications (2015)*: 76-84. Print.

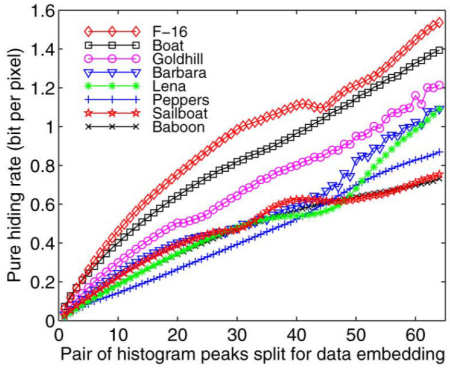

Fig. Pair of Histogram vs Hiding Rate

Matlab is a program that was specifically designed to simplify the implementation of numerical linear algebra routines. It has grown into something much bigger, and it is used to implement numerical algorithms for a wide range of uses. The language used is very similar to standard linear algebra notation, but there are a few extensions that will cause you some problems at first. The input color image is given below By using Reversible Data HidingAlgorithm, Data is embedded in the image.Data is recovered from image but contrast is needed so that the entire image is completely recovered.

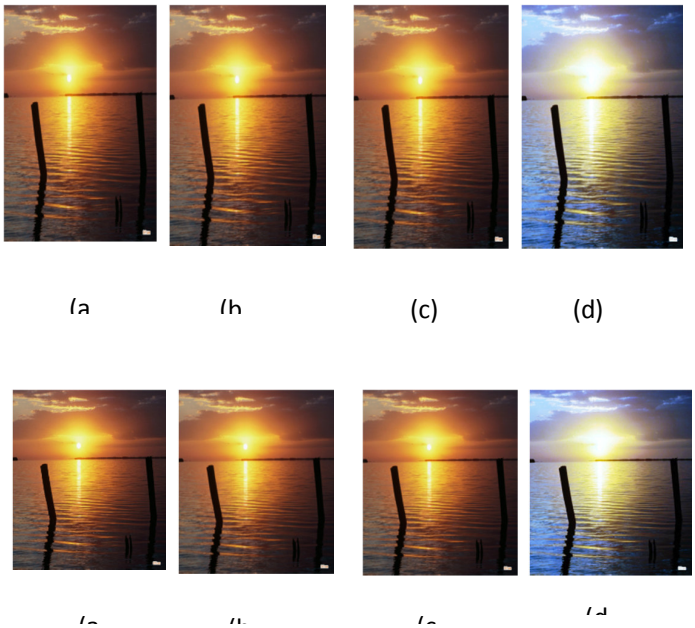

Fig. This is a combination of original image and enhanced image with the high PSNR (a) Original image (b) After applying filter (c) Preprocessed image (d) Enhanced image

Fig. This is a combination of original image and enhanced image with the Low PSNR (a) Original image (b) After applying filter (c) Preprocessed image (d) Enhanced image

Cite this article as: J Kanimozhi, P Vasuki, K D Karthick, M C Arvind kumar. "Invertible Data Embedding By Histogram Modification and Contrast Enhancement". *International Conference on Innovative Trends in Electronics Communication and Applications (2015)*: 76-84. Print.

Table-I

COVER IMAGE	HIDING CAPACITY IN BITS	PSNR (in Decibel)
Sunset	319455	44.95
Blue hill	621669	48.51
Water lilly	315420	44.58
Boat	398344	28.01

Table-II

METHODS	PSNR	MSE	BPP
Difference Expection	18.62	652.56	9.314
Sorting and Prediction	15.49	689.66	5.417
Histogram Shifting	25.3362	642.377	4.8828

CONCLUSION

The algorithm which is used to embed the given data in a image using histogram shifting. The data is embedded into the image by shifting and replacing the bit planes with the values of the data. The embedded data is retrived from the image along with the original image. This algorithm shows high performance compared to the other algorithms such as Difference explansion algorithm. The Bits per Plane value of the proposed algorithm is high compared to the previous algorithm used.

REFERENCES

[1] "Reversible Image Data Hiding With Contrast Enhancement" Author: Hao-Tian Wu, *Member, IEEE*, Jean-Luc Dugelay, *Fellow, IEEE*, and Yun-Qing Shi, *Fellow, IEEE* (2015)

[2] "Lossless Data Embedding New Paradigm in Digital Watermarking" Author: Jessica Fridrich, Miroslav Goljan (2013)

[3] "Reversible Watermarking Techniques: An Overview and a Classification" Author: Roberto Caldelli, Francesco Filippini, and Rudy Becarelli (2011)

[4] "Joint Watermarking Scheme for Multiparty Multilevel DRM Architecture" Author: X. Li, B. Yang, and T. Zeng, (2010)

[5] "Compressed-Encrypted Domain JPEG2000 Image Watermarking" Author: H. Yang, C.-T. Li and R. Xiao (2009)

[6] "Efficient and Secure Encryption Schemes for JPEG2000" Author: J. A. Stark, Y. Yang, X. Sun (2004)

[7] "Composite Signal Representation for Fast and Storage-Efficient Processing of Encrypted Signals" Author: M.-Z.Gao, Z.-G.Wu, and L.Wang (2001)

[8] A. Alavi, R. Link, and S. Kallel, "Adaptive Unequal Error Protectionfor Subband Image Coding," *IEEE Trans. Broadcast.*, vol. 46, no. 3, pp.197–205, Sep. 2000.

Cite this article as: J Kanimozhi, P Vasuki, K D Karthick, M C Arvind kumar. "Invertible Data Embedding By Histogram Modification and Contrast Enhancement". *International Conference on Innovative Trends in Electronics Communication and Applications (2015)*: 76-84. Print.

[9] K. M. Rose and A. Heiman, "Enhancement of One-Dimensional Variable Length DPCM Images Corrupted by Transmission Errors," *IEEE* Trans.Commun., vol. 37, no. 4, pp. 373–379, Apr. 1989.

[10] Z. Zhao,H.Luo,Z.-M. Lu and J.-S. Pan, "Reversible Data Hiding Based on Multilevel Histogram Modification and Sequential recovery," Int. J.Electron. Commun. (AEÜ), vol. 65, pp. 814–826, 2011.

[11] H. T.Wu and J. Huang, "Reversible Image Watermarking on Prediction error By Efficient Histogram Modification," Signal Process., vol. 92, no.12, pp. 3000–3009, Dec. 2012.

[12] Y. Yang, X. Sun, H. Yang, C.-T. Li, and R. Xiao, "A Contrast-Sensitive Reversible Visible Image Watermarking Technique," *IEEE* Trans. Circuits Syst. Video Technol., vol. 19, no. 5, pp. 656–667, May 2009.

[13] J. A. Stark, "Adaptive Image Contrast Enhancement Using Generalizations of Histogram Equalization," IEEE Trans. Image Process., vol. 9,no. 5, pp. 889–896, May 2000.

Cite this article as: J Kanimozhi, P Vasuki, K D Karthick, M C Arvind kumar. "Invertible Data Embedding By Histogram Modification and Contrast Enhancement". *International Conference on Innovative Trends in Electronics Communication and Applications (2015)*: 76-84. Print.

International Conference on Innovative Trends in Electronics Communication and Applications
2015 [ICIECA 2015]

ISBN	978-81-929742-6-2	**VOL**	01
Website	icieca.in	**eMail**	icieca@asdf.res.in
Received	02 - April - 2015	**Accepted**	15 - November - 2015
Article ID	ICIECA013	**eAID**	ICIECA.2015.013

An Efficient Motion Based Video Object Detection and Tracking System

G Sharmila Sujatha[1], V Valli Kumari[1]
[1]Research Scholar, Dept., of CS & SE, College of Engineering (A), Andhra University

Abstract: *In Computer Vision, one of the critical tasks is to detect and track objects. Even today, the issues related to this remain an active area of research. Major limitation of the existing monitoring system for performing the automatic detection of moving objects, is the inability in understanding the narrow variation in brightness between the background and the moving object. Therefore, systems fail to perform the detection of moving target. Subsequently, the results obtained will be full of noise and also the computation time will be increased. Recent advances in multimedia and its associated technologies seek for the processing of video clips database. This research proposes object detection and tracking system in which video segmentation, feature extraction, feature clustering and object detection are combined seamlessly using a single feature. The system is comprised of feature extraction phase and will be followed by tracking of similar video clips for the given query clip. The features such as color, texture, edge density and motion are extracted from each frame. In the feature extraction, initially, the motion feature is extracted using an efficient motion estimation algorithm based on similarity measures followed by other feature extractions.*

Keywords*:* Tracking System, Video Object, Detection**.**

INTRODUCTION

Detection and tracking of moving objects is important in the analysis of video data [5]. Motion is detected using statistical hypothesis testing on difference image between two consecutive frames [2]. Tracking-based approaches for abandoned object detection often become unreliable in complex surveillance videos due to occlusions, lighting changes, and other factors [13]. Video surveillance has been widely used in recent years to enhance public safety and privacy protection. A video surveillance system that deals with content analysis and activity monitoring needs efficient transmission and storage of the surveillance video data. Video compression techniques can be used to achieve this goal by reducing the size of the video with no or small quality loss [12]. A distributed video-surveillance system for the detection of dangerous situations related to the presence of abandoned objects in the waiting rooms of unattended railway stations is presented [1]. Autonomous video surveillance and monitoring has a rich history [10].

In general video surveillance systems uses background estimation and subtraction for the detection and tracking of moving objects. Real world applications can deliver a better performance provided if they are able to tolerate the presence of outliers in the data [7]. In the recent years both in home and business environments for security and management of access points, automatic visual object counting and video surveillance have gained important application [14]. Motion analysis algorithms are based on

Cite this article as: G Sharmila Sujatha, V Valli Kumari. "An Efficient Motion Based Video Object Detection and Tracking System". *International Conference on Innovative Trends in Electronics Communication and Applications (2015)*: 85-97. Print.

processing of multiple-regression pseudo spectrums [15]. Identifying the significant features for performing accurate classification is known as feature selection. The major phases in finding out the feature subset selection system are using best search strategy for finding features. Subsequently, evaluation for testing the significance of these features identified in previous phase [4].In many applications for performing traffic monitoring, human motion capture and also for video surveillance using the moving object detection using background subtraction methods [3].

Detected objects are tracked, and each tracked object has a state for handling occlusion and interference [6]. In the recent past, autonomous video surveillance and monitoring has gained lot of importance as they are able to track human motion in indoor and controlled outdoor environments efficiently [9]. Detection of moving objects is done based on multi-layer lidar that also characterize a zone of interest for reducing the computation complexity of the perception process. Then, fixed frame is used for objects localization and tracking [11]. The Sequence Frame Detection Accuracy (SFDA) is a frame-level measure that penalizes for fragmentations in the spatial dimension while accounting for number of objects detected, missed detects, false alarms and spatial alignment of system output and ground truth objects [8]. Tracking-based approaches for abandoned object detection often become unreliable in complex surveillance videos due to occlusions, lighting changes, and other factors [10].

The rest of the paper is organized as follows. Section II provides various researches conducted in relation to our proposed work. Section III explains about the design strategy and the proposed method. Section IV shows the result and discussion of our proposed method and finally section V concludes our proposed method for video based motion detection and tracking.

Review of recent researches

A numerous researches have been presented in the literature for the detection and tracking of moving object in videos. Almost all existing methods for static suspicious object detection are expected at finding abandoned objects using a static camera in a public place. A brief review of some recent researches is presented here.

Moving objects detection and tracking in video stream were basic fundamental and critical tasks in many computer vision applications. R. Bogush *et al.* [16] proposed an effectiveness increase of algorithms for moving objects detection and tracking. For that, they used additive minimax similarity function. Background reconstruction algorithm was developed. Moving and tracking objects detection algorithms were modified on the basis of additive minimax similarity function.

Vehicle tracking and detection plays an important role in traffic surveillance, still a crucial task in many applications. Template matching was one of the methods used for vehicle detection and tracking. There were several researchers and developers worked on that area. Robust and reliable vehicle detection was a critical step of vehicle recognition. Rajiv Kumar Nath *et al* [17] presented a review of recent template matching methods for detection and tracking of vehicle. Their focus was on systems where the camera was mounted on the vehicle and being fixed such as in traffic/driveway monitoring systems. They discussed the general template matching followed by problem of on-road vehicle detection using template matching.

Shih-Chia Huang [18] has proposed a novel and accurate approach for motion detection in the automatic video surveillance system. In which the methods comprises of modules namely background modelling (BM) module, an alarm trigger (AT) module, and an object extraction (OE) ,which effectively detect the moving objects. In BM module, a novel two phase background approach was adopted which uses a raped matching fallowed by accurate matching for generating optimum background pixels. AT module removes the irrelevant examination of entire background region, thereby facilitates the subsequent OE module to process only the blocks containing moving objects. In last, the OE module was formed as the binary object detection mask for accurate detection of moving objects. The results obtained by the proposed (PRO) method were qualitatively and quantitatively analyzed and compared to the results obtained by other state-of-the-art methods. The observation show that this proposed PRO method outperformed other methods by an F1 metric accuracy rate of up to 53.43%.

Jalil Rasekhi *et al.* [19] has given an detailed explanation of automatic system for airplane detection and tracking using Support Vector Machine (SVM) and the wavelet transform . An experiment was performed to recognize airplane in the opening frame of a video sequence in which 50 airplane images in different situations are used. SVM classifier uses a vector of features for classification of objects pixels and background pixels. Thus the learned model has the ability to detect the airplane in original videos as well as novel images. Therefore, the system acts as a tracker for original videos and as a interpreter for novel images.

After airplane detection in the first frame, the feature vectors of that frame were used to train the SVM classifier. For new video frame, SVM was applied to test the pixels and form a confidence map. Daubechies 4th level of wavelet coefficients corresponding

Cite this article as: G Sharmila Sujatha, V Valli Kumari. "An Efficient Motion Based Video Object Detection and Tracking System". *International Conference on Innovative Trends in Electronics Communication and Applications (2015)*: 85-97. Print.

to input image were used as features. Conducting simulations, it was demonstrated that airplane detection and tracking based on wavelet transform and SVM classification result in acceptable and efficient performance.

YingLi Tian *et al.* [20] have presented a framework for robustly and efficiently detecting abandoned and removed objects based on background subtraction (BGS) and fore-ground analysis with complement of tracking to reduce false positives. In the system background was modelled by three Gaussian mixtures. A person-detection process was also integrated to distinguish static objects from stationary people. They have tested the robustness and efficiency of the proposed method on IBM Smart Surveillance Solutions for public safety applications in big cities and evaluated by several public databases. The test and evaluation had demonstrated that their method was efficient to run on real-time, while being robust to quick-lighting changes and occlusions in complex environments.

Carlos R. del-Blanco *et al.* [21]have proposed an efficient visual detection and tracking framework for the tasks of object counting and surveillance, which meets the requirements of the consumer electronics: off-the-shelf equipment, easy installation and configuration, and unsupervised working conditions. This work was accomplished by a novel Bayesian tracking model that can manage multimodal distributions without explicitly computing the association between tracked objects and detections. It was robust to erroneous, distorted and missing detections.

With the advancement of MEMS technologies, sensor networks have opened up broad application prospects. An important issue in wireless sensor networks was object detection and tracking, which typically involves two basic components, collaborative data processing and object location reporting. The former aims to have sensors collaborating in determining a concise digest of object location information, while the latter aims to transport a concise digest to sink in a timely manner. That issue has been intensively studied in individual objects, such as intruders. However, the characteristic of continuous objects has posed new challenges to this issue. Continuous objects can diffuse, increase in size, or split into multiple continuous objects, such as a noxious gas. Shin-Chih Tu *et al.* [22] proposed a scalable, topology-control-based approach for continuous object detection and tracking. Extensive simulations were conducted, which showed a significant improvement over existing solutions.

Hui Kong *et al*. [23] presented a novel framework for detecting non-flat abandoned objects by matching a reference and a target video sequence. The reference video was taken by a moving camera when there was no suspicious object in the scene. The target video was taken by a camera following the same route and may contain extra objects. The objective was to find these objects. GPS information was used to roughly align the two videos and find the corresponding frame pairs. Based on the GPS alignment, four simple but effective ideas were proposed to achieve the objective: an inter-sequence geometric alignment based on homographies, which was computed by a modified RANSAC, to find all possible suspicious areas, an intra-sequence geometric alignment to remove false alarms caused by high objects, a local appearance comparison between two aligned intra-sequence frames to remove false alarms in flat areas, and a temporal filtering step to confirm the existence of suspicious objects.

Peter Dunne *et al.* [24] presented an approach to localized object detection that was not dependent upon background image construction or object modeling. It was designed to work through camera embedded software using spare processing capacity in a visual signal processor. It used a localized temporal difference change detector and particle filter type likelihood to detect possible trackable objects, and to find a point within a detected object at which a particle filter tracker might be initialized.

Subhabrata Bhattacharya et al. [25] an overview of these problems and the associated limitations of some of the conventional techniques typically employed for these applications. They began with a study of various image registration techniques that were required to eliminate motion induced by the motion of the aerial sensor. Next, they presented a technique for detecting moving objects from the ego-motion compensated input sequence. Finally, they described a methodology for tracking already detected objects using their motion history.

Kalpesh R Jadav, Prof.M.A.Lokhandwal and Prof.A.P.Gharge[29] ,"Vision based moving object detection and tracking", used in video surveillance system. This monitor system cannot find the difference of brightness between the backgrounds and moving object is so small. The accurate moving objet is cannot be achieved. The computation time also increase to heal the noise. The target identified in video clip is on rough area.

PROPOSED METHODOLOGY FOR DESIGNING AN EFFICIENT MOTION BASED VIDEO

Motion Estimation for object detection and tracking

Cite this article as: G Sharmila Sujatha, V Valli Kumari. "An Efficient Motion Based Video Object Detection and Tracking System". *International Conference on Innovative Trends in Electronics Communication and Applications (2015)*: 85-97. Print.

Motion estimation for object detection and tracking has been a major area of research in the recent years. The motion estimation in object tracking and detection plays a major role in estimating the correct object to be tracked. Motion estimation, which generally means the computation of velocity of the moving object in a sequence has been a major problem in image processing and gained more importance in the recent years. However, if the camera is moving, it becomes a difficult task since the image motion is generated by the combined effects of camera motion, structure, and object motion. The intention of moving detection is to extract changing region from image sequence. At present common methods of moving target detection have frame difference, background subtraction, optical flow and motion energy.

Steps involved in our proposed method

The proposed method of motion based video object detection and tracking system consists of the processes such as Video Segmentation, Feature Extraction and Tracking. The first step in our approach is to segment the database video clips into different frames or shots. Next is the Feature extraction step. In our proposed method we extract various features from the segmented image such as color feature, edge density feature and texture feature. Along with these features, motion feature is also extracted which is the major consideration in our proposed approach. The flow diagram for our proposed method shown below,

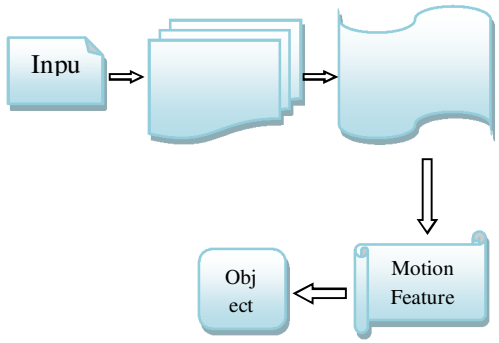

Fig 1: Flow diagram for proposed motion based object detection and tracking

Shot Segmentation

A large amount of digital videos have been generated due to the rapid development of computing and network infrastructures. Normally videos can be represented by a classified structure, while shots are the basis units for constructing high level semantic scenes. The shot boundary recognition is an important preprocessing step for efficient rumination and further content evaluation. A shot consists of succeeding frames which are usually captured by a single camera action. Typically, there are no significant content changes between successive frames in the shot [27]. Once the shot segmentation is done the next step in our process is feature extraction. The shot segmentation is performed with the help of block matching technique which is defined as follows,

Step1. Split the frame into blocks of block size 16.

Step2. First perform block matching for two blocks which are adjacent to eac other.

Step2.1. Then in block matching find the distance of blocks.

Step2.2. Take mean value of distance.

Step3. Repeat these steps for each frame in the video.

Step4. Check whether the mean value is greater than 1.

Step5. The mean value greater than 1 is stored in a variable and these variable and these variable lengths are measured.

Thus the video are shot segmented into various frames with block matching technique.

Cite this article as: G Sharmila Sujatha, V Valli Kumari. "An Efficient Motion Based Video Object Detection and Tracking System". *International Conference on Innovative Trends in Electronics Communication and Applications (2015)*: 85-97. Print.

Segmentation of Shots using Fuzzy C Means Clustering

Cluster analysis is a technique for classifying data, i.e., to divide a given dataset into a set of classes or clusters. The goal is to divide the dataset in such a way that two cases from the same cluster are as similar as possible and two cases from different clusters are as dissimilar as possible. The idea behind cluster repulsion is to combine an attraction of data to clusters with repulsion between different clusters. Here, the distance between clusters and the data points assigned to them should be minimized. Fuzzy c-means (FCM)is a technique of clustering which permits one piece of data to two or more clusters.

The degrees of membership to which a given data point belongs to the different clusters are computed from the distances of the data point to the cluster centers with respect to the size and the shape of the cluster as stated by the additional prototype information. The closer a data point lies to the center of a cluster, the higher is its degree of membership to this cluster. Hence the problem to divide a dataset $D = \{\vec{d}_1, \vec{d}_2, ..., \vec{d}_n\} \subseteq R^P$ into k clusters can be stated as the task to minimize the distances of the data points to the cluster centers and to maximize the degrees of membership.

In probabilistic fuzzy clustering the task is to minimize the objective function:

$$f(D, \delta, \psi) = \sum_{i=1}^{k} \sum_{j=1}^{n} \mu_{ij}^{z} t^2(\vec{\lambda}_i, \vec{d}_j)$$

Where $\mu_{ij} \in [0,1]$ is the membership degree of datum $\vec{d}_j$ to cluster k_i, λ_i is the prototype of cluster k_i , and t $(\vec{\lambda}_i, \vec{d}_j)$ is the distance between datum $\vec{d}_j$ and prototype λ_i . ψ is the set of all k clusters $\vec{\lambda}_1, \vec{\lambda}_2, ..., \vec{\lambda}_k$. $\delta = [\mu_{ij}]$ is called the fuzzy partition matrix and the parameter z is called the fuzzifier.

In possibilistic fuzzy clustering, more intuitive assignment of degrees of membership is achieved by dropping constraint which forces μ_{ij} away from zero for all $i \in \{1,2,...,k\}$. That is, the objective function J is modified to

$$f(D, \delta, \psi) = \sum_{i=1}^{k} \sum_{j=1}^{n} \mu_{ij}^{z} t^2(\vec{\lambda}_i, \vec{d}_j) + \sum_{i=1}^{k} \sigma_i \sum_{j=1}^{n} (1 - \mu_{ij})^z$$

Where, $\sigma_i > 0$.

The first term leads to a minimization of the weighted distances while the second term suppresses the trivial solution by making $\mu_{ij} \neq 0 \; for \, all \; i \in \{1,2,...,k\}$. This approach is called possibilistic clustering, because the membership degrees for one datum resemble the possibility. The formula for updating the membership degrees that is derived from this objective function is:

$$\mu_{ij} = \frac{1}{1 + \left(\frac{t^2(\vec{d}_j, \vec{\lambda}_i)}{\sigma_i}\right)^{\frac{1}{z-1}}}$$

σ is chosen for each cluster separately and can be determined by the equation:

$$\sigma_j = \frac{B}{R_i} \sum_{j=1}^{n} \mu_{ij}^{z} t^2(\vec{d}_j, \vec{\lambda}_i)$$

where usually, B =1 and $R_i = \sum \mu_{ij}$.

After the segmentation process the feature extraction process is performed where various features from the segmented frames are extracted for tracking process.

Feature extraction

When the input data to an algorithm is too large to be processed and it is suspected to be notoriously redundant then the input data will be transformed into a reduced representation set of features. The conversion of input data into a set of features is called feature extraction [26]. Extraction of image features and use of these features to represent image visual content is normally termed as feature extraction. Feature extraction involves reducing the amount of resources required to describe a large set of data accurately.

Cite this article as: G Sharmila Sujatha, V Valli Kumari. "An Efficient Motion Based Video Object Detection and Tracking System". *International Conference on Innovative Trends in Electronics Communication and Applications (2015)*: 85-97. Print.

Color Feature Extraction

The HSV (Hue, Saturation, Value) color components are more related to human perception and hence the color histogram extraction is based on HSV color space. Normally based on S component, the color quantization in HSV color space separate gray bins from others and divides the other equally.Fig 1(a) shows the partition in red SV plane [26]. Inspite of this, the nature of HSV color space is that the colors of low V value looks more alike than colors of high V value with respect to different saturations. In the below example the color similarity between A7 to A9 (normally black) is greater than A4 to A6

The cylindrical HSV space is converted into cone space to solve the above problem.The cylindrical HSV point $A(H_a, S_a, V_a)$ is related to conical HSV point $B(H_b, S_b, V_b)$. The transformation is given by

$$\begin{cases} H_b = H_a \\ S_b = S_a \cdot V_a \\ V_b = V_a \end{cases} \quad \ldots\ldots\ldots \quad (1)$$

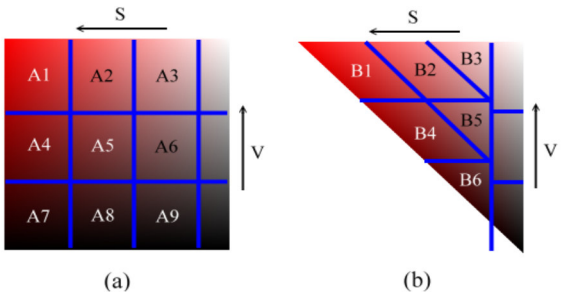

Fig2**:**Color quantization in SV plane (a) Cylindrical space quantization (b) Conical Space quantization

Comparing fig 2(a) and fig2(b), the color of A7 to A9 correspond to B6 and gray bins.This improves the color quantization of dark colors in HSV color space along with the reduction of number of bins used.

Edge density feature extraction

Edge density may be defined as the quality of an image that can point out the regions by means of the magnitude of the edge of the object available in the image. First, the image region is resampled therefore extracting the feature. The resampled regions of the image are administered to gray scaling operation so that each region of the segmented image that is in RGB color space is transformed to grayscale. In our proposed method we have utilized canny edge detection for feature extraction. The Canny algorithm uses an optimal edge detector based on a set of criteria which include finding the most edges by minimizing the error rate, marking edges as closely as possible to the actual edges to maximize localization, and marking edges only once when a single edge exists for minimal response. The canny algorithm consists of various steps like smoothing, finding gradients, non-maximum suppression, double thresholding and edge tracking by hysteresis.

Texture Feature Extraction

The texture features from the image region are extracted by building a colour texture histogram by using a Local Binary Pattern (LBP). To summarize local gray level structure of the image LBP operator can be employed. It is defined as a gray scale invariant texture measure, derived from a common definition of texture in a local neighbourhood

Local Binary Pattern

The local spatial structure of the image texture are characterized by a gray-scale texture operator called Local Binary Pattern (LBP).LBP indicates a magnitude relation between a center pixel and its neighbouring pixels in a micropattern. Given a central pixel in the image, a pattern code is computed by comparing its value with those of its neighborhoods using the expression given below,

Cite this article as: G Sharmila Sujatha, V Valli Kumari. "An Efficient Motion Based Video Object Detection and Tracking System". *International Conference on Innovative Trends in Electronics Communication and Applications (2015)*: 85-97. Print.

$$LBP_{N,R}(x_i, y_j) = \sum_{N=0}^{N-1} F(P_R - P_C)2^N. \quad (4)$$

where P_C is the gray value of the central pixel, P_R is the value of its neighbour, N is the total number of neighbours involved and R is the radius of the neighborhood. The eqn (4) means that the differences in the neighborhood are derived as N bit binary number that results in 2^N distinct value for the LBP code. The texture can thus be described as 2^N discrete distribution given by,

$$T \approx t(LBP_{N,R}(x_i, y_j)) \quad (5)$$

For calculating the LBP feature vector for a given image of size M x N, the central part alone is considered since large neighborhood cannot be used on the borders. The LBP code is calculated for each pixel. The LBP code may be represented as kernel structure index which can be represented as below,

85	75	126
99	95	141
91	91	100

⇨

0	0	1
1		1
0	0	1

Binary: 00111001 Decimal: 57.

Fig 3: An example kernel index structure for LBP.

As per the above kernel the pixels values are being identified and the corresponding decimal values are found out. The LBP feature extraction methods generate the feature descriptor information for each of these images.

Motion feature extraction for motion estimation in video

Generally motion estimation is the process of detecting the motion vectors which forms the transition from one frame to other in a video sequence. The object detection and tracking in any video can be detected based on the motion of the object at consecutive sequences and this can help us in detecting the object. In our proposed method we utilize block matching algorithm for motion estimation process.

Block matching algorithm

The major consideration behind the motion estimation is that the patterns which correspond to objects and background in a frame of video sequence move within the frame to form corresponding objects on the subsequent frame. In block matching proc3ess we divide the current frame into a matrix of 'macro blocks. These macro blocks are then compared with equivalent block and its adjacent neighbors in the previous frame to create a vector that specify the movement of a macro block from one location to another in the previous frame. Thus the motion estimated in the current frame can be obtained by calculating the movements of all macro blocks in a frame. The search area in the macro block is normally reserved upto *P* pixels. This is called the search parameter and this will be larger for larger motion which in turn takes more execution time. Normally the macro block is a square of side 16 pixels and the search parameter *P* is 7 pixels. The general block matching idea is shown in fig 4.

The matching of this macro block is based on the cost function of the various macro blocks. The macro blocks whose output cost function is the least cost is the one that matches closest to the current block. There is various cost function available and the least expensive cost function like Mean Square Error (MSE) is selected for the cost calculation in our method. Based on these MSE values we match the blocks. The expression for the Mean Square Error (MSE) is given the eqn below,

Cite this article as: G Sharmila Sujatha, V Valli Kumari. "An Efficient Motion Based Video Object Detection and Tracking System". *International Conference on Innovative Trends in Electronics Communication and Applications (2015)*: 85-97. Print.

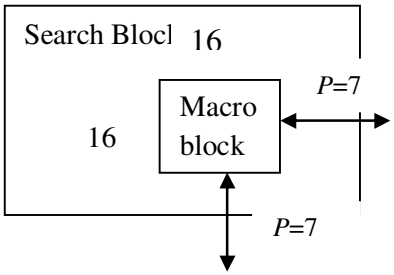

Fig 4: Macro block with side 16 and search parameter P=7

$$\text{Mean Square Error (MSE)} = \frac{1}{N^2}\sum_{p=0}^{N-1}\sum_{q=0}^{N-1}(P_C - P_R)^2. \qquad (7)$$

Here N is the number of sides in macro block, P_C and P_R are the pixels that are being compared from the current block and the reference block

Moving Object Detection and Tracking

From each frame the moving objects are detected. There are different basic methods employed for moving object detection like

- Background Subtraction.
- Temporal Differencing.
- Optical Flow.

The background subtraction method is a straightforward method for moving target detection. In background subtraction method, it is assumed that the background is static so that the background does not change with the number of frames. First the difference between the object P and the background Q is calculated using the formula,

$$D(a,b) = |P(a,b) - Q(a,b)| \qquad (8)$$

Now threshold the difference using the formula given below,

$$Z(a,b) = \begin{cases} 1, D(a,b) > T \\ 0, otherwise \end{cases} \qquad (9)$$

The threshold can be chosen using the gray histogram by taking the bottom value between the two peaks as the threshold[28]. Basically Object tracking is used to find the location of the target in different frames in a sequence of images. The main work of target tracking is to select good target characteristics and use appropriate searching methods. We employ the Image Difference Algorithm for Moving Object Detection and Tracking in our work.

Object Tracking

To achieve a good detection rate on each shot of a video frame, the detection and tracking were combined and some rules are formed to get a complete tracking process. The tracking is of two types,

1) Forward Tracking.
2) Backward Tracking.

Cite this article as: G Sharmila Sujatha, V Valli Kumari. "An Efficient Motion Based Video Object Detection and Tracking System". *International Conference on Innovative Trends in Electronics Communication and Applications (2015)*: 85-97. Print.

Forward Tracking

The forward tracking process is performed on each frame, beginning from frames where the object have been detected. While tracking, same object may be detected many times in a shot which can result in multiple tracking of the object, which may result in over time consumption. Inorder to overcome this problem, some tracking rules are used to identify whether the detected objects are multiplied or not. The rule is generally based on the percentage of overlap between the detected object and the one from the forward tracking in the same frame which is represented as follows, $$\mathrm{F_T} = \max_j \frac{S_{(F_T \cap W_j)}}{\min\left(S_{W_j}, S_{F_T}\right)}$$

(10)

where S_{W_j} is the area of the j^{th} detection and S_{F_T} is the area of the forward tracking. Also $S_{(F_T \cap W_j)}$ represents the area recovered by the detection process.

Backward Tracking

Backward Tracking is performed on each frame to provide an additional set of object being tracked. The backward tracking is very useful in case the object is not detected at the beginning but in the center of the frame. The forward tracking usually represents the object tracking from the detected frame to the end the complete shot while backward tracking gives the unnoticed result from the first frame of the shot to the frame in which the last object detection has performed. Further the backward tracking can also proves to be effective when the forward tracking fails to locate the position of the object in a particular frame. This may be due to occlusion, bad illumination or due to tracker sticks to the background. That is when an object in a frame1 is not tracked correctly and the same object is tracked in frame 5, the information will be propagated back and will provide tracking of the object in the first frame.

Object Tracking Process

In the proposed method, the tracking process is done by comparing the features extracted in the present frame with the extracted features in the previous frame. Suppose we have a total of M number of extracted feature in present frame and N number of feature in the previous frame. Hence a total of M x N matching is required. In this experiment we utilized Euclidean Distance for this matching process. Suppose we consider two feature vectors v_i and vj where $i = 1,2,.....M$ and $j = 1,2,.....N$,then the Euclidean distance is calculated by using the below equation,

$$D(v_i, v_j) = \sqrt{\frac{1}{d}\sum_{m=1}^{i}(v_{im} - v_{jm})^2} \quad (11)$$

Where d is the dimension of the feature vector selected. Once the distances between the features are calculated, the minimum distance object is tracked. This object is the object which we have to be tracked from the video clip. This process is then carried out for different shots and the movements of the object is identified which helps in efficient tracking of the object.

RESULTS AND DISCUSSION

The proposed motion based object detection and tracking system was implemented in the working platform of MATLAB. The detection and tracking process is tested with different frames of video and the upcoming result of the proposed work has been shown below. Initially, the video are segmented to different shots or frames and then features are extracted followed by the detection and tracking process. The results obtained by our proposed method for different frames of the input video is shown below,

This feature extraction provides better outcome when comparetracked image of the object in the first frame. Similarly for different frames the process is repeated and finally the object is tracked. The proposed methodology proved to be more effective and accurate in object detection and tracking.

Cite this article as: G Sharmila Sujatha, V Valli Kumari. "An Efficient Motion Based Video Object Detection and Tracking System". *International Conference on Innovative Trends in Electronics Communication and Applications (2015)*: 85-97. Print.

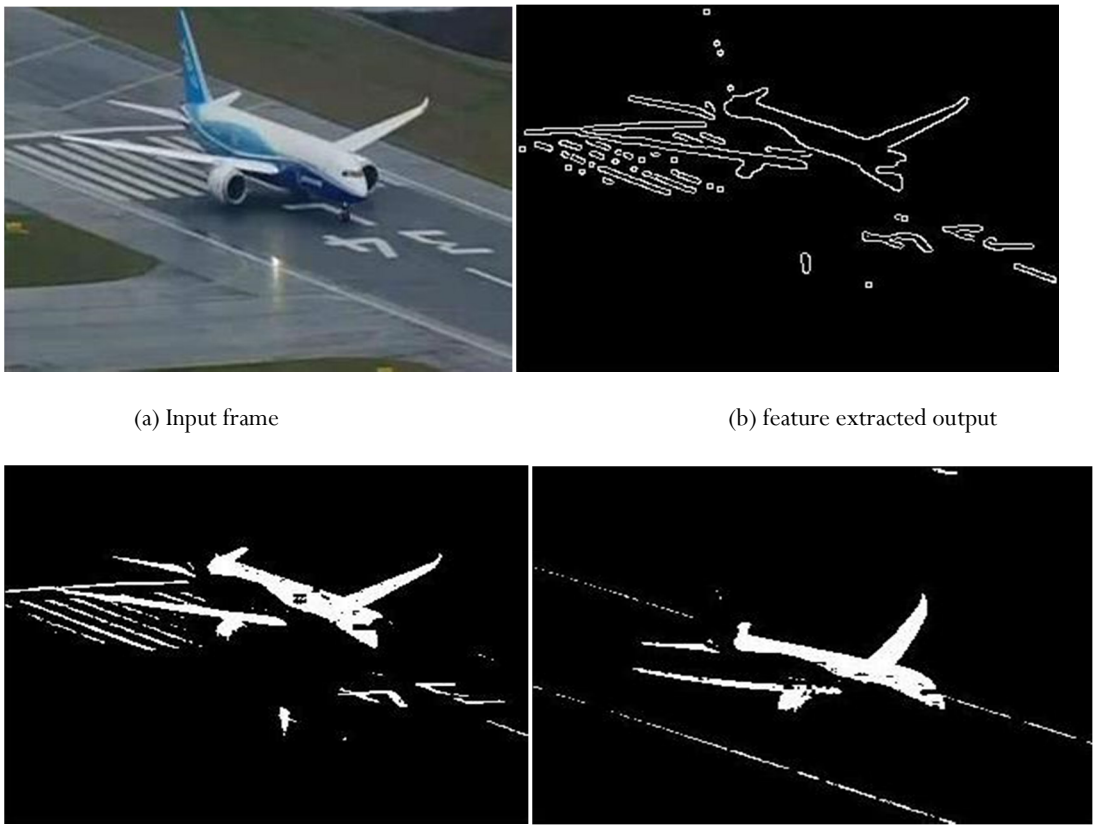

(a) Input frame (b) feature extracted output

(c)Detected object d) Object tracking

Fig 5:Results of object tracking in first frame (Video).

PERFORMANCE ANALYSIS

The values obtained from the calculation are given in Table 1. These values are used for the analysis of performance between the proposed and existing method.

Table1: Precision and Recall for the proposed method

S.No	Performance Analysis				F-Measure	
	Precision		Recall			
	Proposed Method	Existing Method	Proposed Method	Existing Method	Proposed Method	Existing Method
1	0.9988	0.71	1	0.15	0.9993	0.2477
2	0.9995	0.65	1	0.24	0.9997	0.3506
3	0.9995	0.59	1	0.35	0.9997	0.4394
4	0.9935	0.52	1	0.46	0.9967	0.4882
5	0.9925	0.47	1	0.52	0.9962	0.4937

Cite this article as: G Sharmila Sujatha, V Valli Kumari. "An Efficient Motion Based Video Object Detection and Tracking System". *International Conference on Innovative Trends in Electronics Communication and Applications (2015)*: 85-97. Print.

Here the existing method is the previous paper where object detection and tracking using low level features is performed. Each values relating to the methods are entered in the table for comparison and from the table it is clear that our proposed method delivers better precision and recall than the existing method. Here the existing method is the vision based object detection and tracking [29].

The average F-measure value for the proposed and existing method is found out and the corresponding graph is shown in fig 8.

Table 2: Average F-measure for proposed and existing methods

F-measure	Methods	
	Proposed	Existing
Average F-measure	0.9983	0.4039

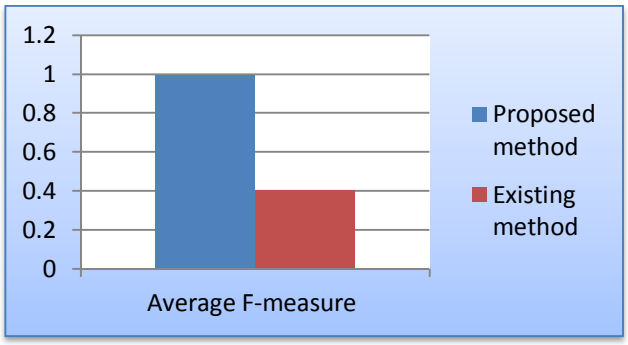

Fig 6: Graphical representation of Average F-measure for proposed and existing method.

CONCLUSION

In this paper we have proposed efficient motion based object detection and tracking system. We developed a unique method using Block matching algorithm and our method proves it is a well-organized method for motion estimation to track and detect the objects in the video. As the results shows the proposed methodology proved to be more efficient and accurate in object detection and tracking than the previous methods. To prove the effectiveness of our proposed method we have compared the precision and recall value along with F-measure of the proposed method with existing method for the object detection and tracking process. As per the performance analysis, it is clear that our proposed method provides better F-measure value when comparing with other method. As a result it can be concluded that our proposed method is efficient in the field of object detection and tracking.

REFERENCES

[1] Claudio Sacchi and Carlo S. Regazzoni, "A Distributed Surveillance System for Detection of Abandoned Objects in Unmanned Railway Environments", IEEE Transactions on Vehicular Technology, Vol. 49, No. 5, September 2000.

[2] Sang Won Hwang, Eun Yi Kim, Se Hyun Park and Hang Joon Kim, "Object Extraction and Tracking Using Genetic Algorithm", IEEE Transactions, 2001.

[3] Rita Cucchiara, Costantino Grana, Massimo Piccardi and Andrea Prati, "Detecting Moving Objects, Ghosts and Shadows in Video Streams", IEEE Transactions on Pattern Analysis and Machine Intelligence, Vol. 25, pp. 1337-1342, October 2003.

[4] Zehang Suna , George Bebisa and Ronald Millerb, "Object detection using feature subset selection", Journal of the Pattern Recognition Society, March 2004.

Cite this article as: G Sharmila Sujatha, V Valli Kumari. "An Efficient Motion Based Video Object Detection and Tracking System". *International Conference on Innovative Trends in Electronics Communication and Applications (2015)*: 85-97. Print.

[5] Chandrika Kamath, Abel Gezahegne, Shawn Newsam and George M. Roberts," Salient Points for Tracking Moving Objects in Video", Image and Video Communications and Processing, 2005.

[6] Masayuki Yokoyama and Tomaso Poggio, "A Contour-Based Moving Object Detection and Tracking", In proceedings of Visual Surveillance and Performance Evaluation of Tracking and Surveillance, 2005.

[7] Codrut Ianasi, Vasile Gui, Corneliu I. Toma, and Dan Pescaru, "A Fast Algorithm for Background Tracking in Video Surveillance, Using Nonparametric Kernel Density Estimation", Electronics and Energetics, Vol. 18, No. 1, pp. 127-144, 2005.

[8] Vasant Manohar, Padmanabhan Soundararajan, HarishRaju, Dmitry Goldgof, Rangachar Kasturi, and John Garofolo, "Performance Evaluation of Object Detection and Tracking in Video", In Proceedings of 7th Asian Conference on Computer Vision, Hyderabad, pp. 151–161, 2006.

[9] Kaiqi Huanga, Liangsheng Wanga, Tieniu Tana, and Steve Maybank, "A real-time object detecting and tracking system for outdoor night surveillance", ELSEVIER Pattern Recognition, Vol. 41, pp. 432-444, 2008.

[10] Limin Liu, Zhen Li, Member, and Edward J. Delp, "Efficient and Low Complexity Surveillance Video Compression Using Backward Channel Aware Wyner-Ziv Video Coding", IEEE Transactions, June 2008.

[11] Sergio A. Rodríguez F, Vincent Frémont, Philippe Bonnifait and Véronique Cherfaoui, " An Embedded Multi-Modal System for Object Localization and Tracking", IEEE Intelligent Vehicles Symposium, 2010.

[12] Sherin M. Youssef, Meer A. Hamza and Arige F. Fayed, "Detection and Tracking of Multiple Moving Objects with Occlusion in Smart Video Surveillance Systems", IEEE Transactions, 2010.

[13] Yuping Lin, Qian Yu and Gérard Medioni, "Efficient detection and tracking of moving objects in geo-coordinates", Machine Vision and Applications, Vol. 22, pp. 505–520, 2011.

[14] Thi Thi Zin, Pyke Tin, Takashi Toriu and Hiromitsu Hama, "A Probability-based Model for Detecting Abandoned Objects in Video Surveillance Systems", Proceedings of the World Congress on Engineering, July 2012.

[15] Boris Vishnyakov, Yury Vizilter and Vladimir Knyaz, "Spectrum-Based Object Detection And Tracking Technique For Digital Video Surveillance", International Archives of the Photogrammetry, September 2012.

[16] R. Bogush, S.Maltsev, A. Kastryuk, N. Brovko and D. Hlukhau, "Motion detection and tracking algorithms in video streams", Journal of Science, Mathematics – Physics, Vol. 25, pp. 143-151, 2009

[17] Jalil Rasekhi, MohammadReza Karami and Mojtaba Bandarabadi, "Wavelet Transform and Supervised Learning Methods for Object Tracking", European Journal of Scientific Research ISSN 1450-216X Vol.41 No.4, pp.626-631, 2010

[18] Shih-Chia Huang, "An Advanced Motion Detection Algorithm with Video Quality Analysis for Video Surveillance Systems", IEEE Transactions on Circuits and Systems For Video Technology, Vol. 21, No. 1, January 2011.

[19] Rajiv Kumar Nath and Dr. Swapan Kumar Deb, "On Road Vehicle/Object Detection And Tracking Using Template", Indian Journal of Computer Science and Engineering, Vol 1 No 2, 98-107, Sept 2010.

[20] YingLi Tian, Rogerio Schmidt Feris, Haowei Liu, Arun Hampapur, and Ming-Ting Sun, "Robust Detection of Abandoned and Removed Objects in Complex Surveillance Videos", IEEE Transactions On Systems, Vol. 41, No. 5, September 2011.

[21] Carlos R. del-Blanco, Fernando Jaureguizar, and Narciso García, "An Efficient Multiple Object Detection and Tracking Framework for Automatic Counting and Video Surveillance Applications", IEEE Transactions on Consumer Electronics, Vol. 58, No. 3, August 2012.

[22] Shin-Chih Tu, Guey-Yun Chang, Jang-Ping Sheu, Wei Li and Kun-Ying Hsieh, "Scalable continuous object detection and tracking in sensor networks", Journal of Parallel and Distributed Computing, Vol. 70, pp. 212-224, 2010

[23] Hui Kong, J. Y Audibert and J. Ponce, "Detecting Abandoned Objects With a Moving Camera", Image Processing, Vol. 19, No. 8, pp. 2201-2210, 2010

Cite this article as: G Sharmila Sujatha, V Valli Kumari. "An Efficient Motion Based Video Object Detection and Tracking System". *International Conference on Innovative Trends in Electronics Communication and Applications (2015)*: 85-97. Print.

[24] Peter Dunne and Bogdan J. Matuszewski, "Histogram-based Detection of Moving Objects for Tracker Initialization in Surveillance Video", International Journal of Grid and Distributed Computing, Vol. 4, No. 3, pp. 71-78, Sept 2011

[25] Subhabrata Bhattacharya, Haroon Idrees, Imran Saleemi, Saad Ali, and Mubarak Shah, "Moving Object Detection and Tracking in Forward Looking Infra-Red Aerial imagery", Machine Vision Beyond Visible Spectrum, Vol. 1, No. 3, pp. 221-252, 2011

[26] J. Fernandeza, R. Guerreroa, N. Mirandaa and F. Piccolia ,"Multi-Level Paralelism In Image Identification,"Mecanica Computational,Vol.28,pp.227-240,Argentina,Nov 2009.

[27] Li Li, Xianglin Zeng,Xi Li,Weiming Hu and Pengfei Zhu ,"Video Shot Segmentation Using Graph-based Dominant-Set Clustering," In.proc.of. First International Conference on Internet Multimedia Computing and Service,New York,USA,2009.

[28] Liang Xiao and Tong-qiang Li,"Research on Moving Object Detection and Tracking,"In.proc.of.Seventh International Conference on Fuzzy Systems and Knowledge Discovery, pp.2324-2327, 2010.

[29] Kalpesh R Jadav, Prof.M.A.Lokhandwala and Prof.A.P.Gharge,"Vision based moving object detection and tracking",National Conference on Recent Trends in Engineering & Technology,May 2011.

Cite this article as: G Sharmila Sujatha, V Valli Kumari. "An Efficient Motion Based Video Object Detection and Tracking System". *International Conference on Innovative Trends in Electronics Communication and Applications (2015)*: 85-97. Print.

International Conference on Innovative Trends in Electronics Communication and Applications 2015 [ICIECA 2015]

ISBN	978-81-929742-6-2	**VOL**	01
Website	icieca.in	**eMail**	icieca@asdf.res.in
Received	02 - April - 2015	**Accepted**	15 - November - 2015
Article ID	ICIECA014	**eAID**	ICIECA.2015.014

Optical Wireless Communication for Underwater Vehicles

C B Gayathri[1]

[1]Asst. Prof of ECE, M. Kumarasamy College of Engineering, Karur

Abstract: *This paper implements and develops a new method of controlling the electric car by employing accelerometer. Generally in the history of evolution of electric cars, there is a lot of changes take place in almost all aspects of the electric car and tremendous advances have been made in the field of electric vehicles. But the basic operation of steering and acceleration system remains the same. So in addition to these advancements, we introduced a new method of controlling electric vehicles, i.e. basic and traditional type of acceleration and steering control is changed. The accelerometer is in-built in the controller which is given to the driver for controlling the vehicle acceleration and steering. The accelerometer in the controller senses the calibrated input from the driver. The controller itself analyses the input and drives the motor and also controls the speed accordingly to it. It gives a feeling of driving a one manned plane. Since there is no need of using legs to drive these vehicle even a paraplegic persons can drive this kind of electric car easily. This new method of controller used in electric vehicles mainly concerned on ease of driving.*

Keywords*:* Integrated optoelectronics, Lighting control, Optical communication equipment, Optical receivers, Optical transmitters

INTRODUCTION

The growing need for underwater observation and subsea monitoring systems has stimulated considerable interest in advancing the enabling technologies of underwater wireless communication and underwater sensor networks. This communication technology is expected to play an important role in investigating climate change, in monitoring biological, biogeochemical, evolutionary, and ecological changes in the sea, ocean, and lake environments, and in helping to control and maintain oil production facilities and harbors using unmanned underwater vehicles (UUVs), submarines, ships, buoys, and divers. However, the present technology of underwater acoustic communication cannot provide the high data rate required to investigate and monitor these environments and facilities. Optical wireless communication has been proposed as the best alternative to meet this challenge. In this paper, optical communication using LEDs is presented as an improvement over acoustic modems for scenarios where high speed, but only moderate distances, is required and lower power, less complex communication system are desired. A ultra-bright blue LED based transmitter system by optimizing it with opt coupler and a enhanced photodiode based receiver system were developed with the goal of transmitting data at high data rates by using On-Off keying technology.

LITERATURE REVIEW

RF waves

The most common way of wireless communication was through Radio waves or RF waves. But unfortunately these waves suffered high attenuation as their propagation underwater was dependent on their frequency and also the salinity of the water. Another loss suffered by the RF waves is due to the refraction that takes place at the air-water interface this phenomenon again leads to loss of information. For the waves to travel a longer distance they need to be of higher frequency but higher the frequency, higher is the

Cite this article as: C B GAYATHRI. "Optical Wireless Communication for Underwater Vehicles". *International Conference on Innovative Trends in Electronics Communication and Applications (2015)*: 98-103. Print.

attenuation which is also directly dependent on the conductivity.

$$\text{Attenuation in dB / metre} = 0.0173 \sqrt{f(conductivity)}$$

f -refers to the frequency of the RF wave used

To overcome this, low frequencies in the range of 10-30 KHz were used but the bit transfer rate using these waves was significantly low.

$$\text{Refraction loss} = -20 \log\{(7.4586 \times 10\text{^}6)/ \sqrt{f} / conductivity$$

This loss can be reduced by connecting an antenna under the sea equipment. The saline content in the water made it a conducting medium and reduced the distance up to which the wave could propagate, therefore this method was not preferred for underwater wireless communication.

Acoustics

ACOUSTICS, they refer to the sound waves. When compared to their speed in air, sound waves travel at a greater speed in the water.

Sound speed in Air-340 m/s

Sound speed in Water-1500 m/s

Acoustics solved the problems posed by the RF communication up to major extent. The data rate achieved by using Acoustic modems underwater measured a data transfer rate of up to few hundred kilobits per second when compared to the RF modems. But as all other modes even Acoustics encountered problems in underwater. The major drawbacks of using Acoustics underwater were that, Speed was directly dependent on temperature, pressure and salinity of water. Presence of thermo clines, haloclines also affected the speed and information carrying capacity of the acoustic waves. As all RF waves here also the data transfer was directly dependent on the frequency of the wave.

Electromagnetic Waves

Here, electromagnetic waves which travel at the speed of light 30,00,00,000 m/s, paving way for a faster communication medium. These waves travel at a speed greater than that of sound waves and were considered as an alternative. But not all waves could travel a longer distance into the water and were attenuated due to absorption and scattering at the air-water interface. Only waves of particular wavelength specifically in the range of 400nm-700nm in the visible spectrum region were attenuated less and could be considered for any communication purpose .Even in this spectrum, wavelength 470nm wavelength-blue light was observed to be attenuated the least and penetrated water the most and could be employed for further applications.

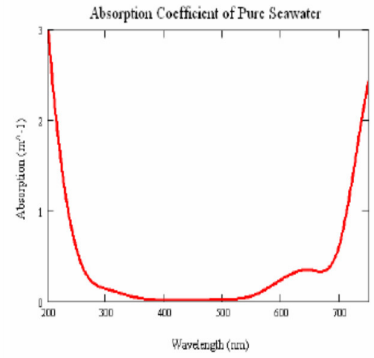

Fig. 1. Absorption coefficient of visible light wavelength

From the above fig 1, it can be inferred that visible spectrum suffered least attenuation. The above figure shows that why blue light was chosen from the visible spectrum. Therefore, from the data we can conclude that blue light suffered least attenuation and could penetrate up to greater depths. Hence it could be employed as the source for transmission underwater.

DESIGN CONSTRAINTS

The main issue that needs to be addressed is that the system has to work in a space-limited vehicle. It has to use minimal power occupy less space and also the system has to work in an environment wherein even though it's not perfectly aligned with the base station it can transmit and receive with least margin of error. More important is that it should be able to support high data rate of communication as

Cite this article as: C B GAYATHRI. "Optical Wireless Communication for Underwater Vehicles". *International Conference on Innovative Trends in Electronics Communication and Applications (2015)*: 98-103. Print.

in >=1Mbps. Therefore, the priorities can be classified as high speed, low power consumption, maximum distance and low complexity of the system.

SYSTEM DESIGN

The key feature that has to be taken care is that of component features and design. As in every communication system it has the transmitter which gets the data either from the computer or microprocessor this electric signal is converted into optical signal by the suitable photon source. Every state in the electric signal must be switched properly during transmission so that receiver can decode the data without any error. On the receiver side, these optical signals are converted back to electrical signals and the data that has been transmitted will be converted back and displayed either on the computer or any display.

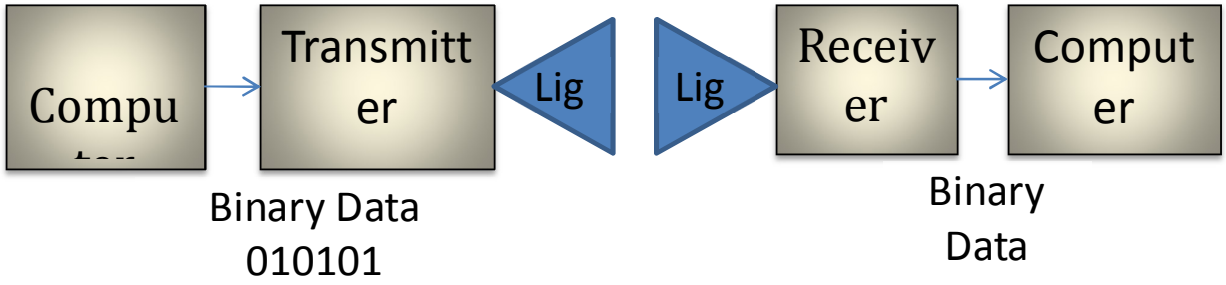

Fig 2 .Wireless optical Communication System Overview

Transmitter

The basic function of transmitter is to convert the data into electric signals and switch this data into optical signals and send it out to the receiver. There is no such special modulation techniques followed during transmission just a simple on-off keying, here ON state represents presence of data and the light glows and OFF represents no data and hence light doesn't glow.

The functional blocks of transmitter can be divided into

- Data from PC
- USB-TTL serial data converter
- Optical driving system
    1. MOSFET Driver
    2. MOSFET
- Photon source

The key design feature is the selection of suitable photon source as the rest of the system drives the photon source. In this design LED was chosen as the photon source from the available sources due to its stability and linearity in the temperature and pressure underwater.

Photon Source

There are many photon sources available anything from a small incandescent bulb to a laser diode can be used as photon source. But, LED's were chosen as they are highly efficient, low-power consumption, more reliable and linear devices.

LED (Light Emitting Diode)

These devices are pn-junction semiconductor devices which emit light when forward biased. It consists of a p-type semiconductor and n-type semiconductor, when forward biased the excited electrons from n-type flow to the p-type junction crossing the energy gap. The wavelength of the light emitted depends upon the band-gap energy between the valence band and conduction band. Unlike, the incandescent bulbs which emit white light consisting of all the wavelengths, LED's are capable of emitting light of specific wavelength as discussed earlier, LED emitting a wavelength of ~470nm was chosen for the design.

The main constraint in choosing the appropriate LED was the recombination time which decides the switching speed of the LED. A recombination time of 1 to 100 ns was chosen as the LED's could reach modulation speeds of several MHz. Moreover, LED's are relatively cheaper and available widely. After deciding upon the photon source, the most suitable LED i.e., ~470 nm has to be selected. For its application as a photo source the LED must emit a minimum luminous flux of 30-60 lumens implying that high power LED's must be chosen. Most of the LED's available emit meager 1-2 lumens. Thereby, a proper LED must be chosen. Here, blue LED

Cite this article as: C B GAYATHRI. "Optical Wireless Communication for Underwater Vehicles". *International Conference on Innovative Trends in Electronics Communication and Applications (2015)*: 98-103. Print.

of 2 Watt- power rating was chosen. High power LED's drawn a current of 500mA-1000mA and requires 2-5 forward voltage drops in series. Though LED's are more efficient even they are very much affected by temperature fluctuations. Therefore, proper heat sinks must be provided to prevent any occurrence of damage.

LED Driver

Once the photon source was decided it has to be driven in accordance with the input binary data from the computer. This data is converted into equivalent voltage levels, these voltage levels have to be converted into equivalent current levels as LED's are mostly current driven devices. For this purpose of current-voltage conversion, MOSFET is preferred as it acts as a switch to control the current flow in the LED's thereby acts as a voltage to current converter.

MOSFET

MOSFET (an electronically controlled switch) is used to switch the current through the LED's. When there is no voltage drop between the gate and the source the resistance between the drain an source is high, thereby MOSFET remains in "off" state .Once a certain voltage drop exists between the gate and the source the resistance between drain and source terminals decreases thereby turning "on" the MOSFET. Essentially, the voltage drop is minimal between the drain and source causing large amount of current to flow through.

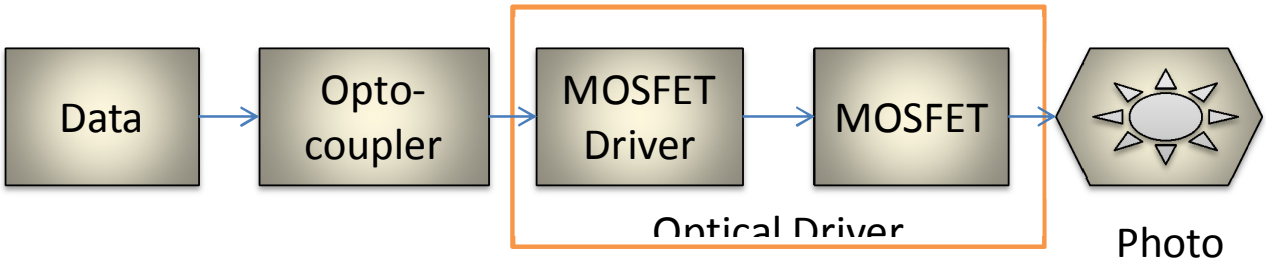

Fig 3. Transmitter System - Overview

SIMULATION TOOL

INTRODUCTION

ASAP (Advanced Systems Analysis Program) 2014 V2 from Breault Research Organization (BRO) is an optical engineering software that is used for optical design and analysis. BRO encourages you to select an operating system that supports optimal performance for ASAP, and uses processor resources intensively for its computation, analysis, and graphical output.

Four-step Process in ASAP

Workflow in ASAP is based on a simple, four-step process that is designed into the UI.

1. Define and verify the system geometry (System)
2. Define and verify the system sources (Rays)
3. Trace
4. Analyze

Communicate with ASAP via its spreadsheet interface, its scripting and macro language, or by important geometry from a computer-aided design (CAD) program.

Software Output

STEP 1 & 2 – Define and verify the system geometry (System)

Cite this article as: C B GAYATHRI. "Optical Wireless Communication for Underwater Vehicles". *International Conference on Innovative Trends in Electronics Communication and Applications (2015)*: 98-103. Print.

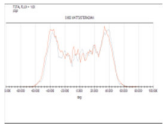

Fig 4. Light LED BB01

STEP 3 - Trace inputs window BB01

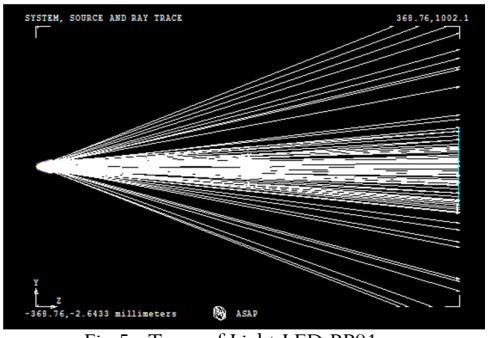

Fig 5. Trace of Light LED BB01

STEP 4 - Analysis window of BB01

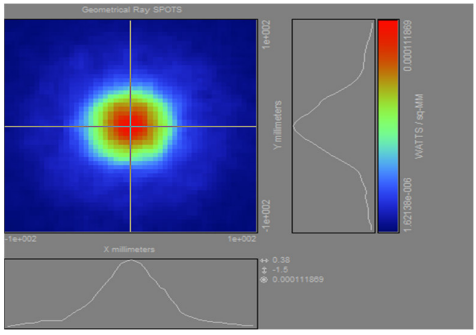

Fig 6. Analysis of Light LED BB01

CONCLUSION

In this paper**,** I had presented a solution to the need for low-power, cost effective, high-speed wireless communication. I had compared possible wireless communication methods, presented an overview of past work, and covered the necessary background information. Then I had presented my design and compared with various LEDs performance on illuminating luminance intensity by doing four step processes and I had analysed the luminance output using ASAP simulation software.

REFERENCES

[1] Brandon Cochenour, Member, IEEE, Linda Mullen, Senior Member, IEEE, and John Muth, Member, IEEE , "Temporal Response of the Underwater Optical Channel for High-Bandwidth Wireless Laser Communications" IEEE JOURNAL OF OCEANIC ENGINEERING, VOL. 38, NO. 4, OCTOBER 2013.

[2] Alexander Vavoulas, Harilaos G. Sandalidis, and Dimitris Varoutas, Senior Member, IEEE "Peer-Reviewed Technical Communication Underwater Optical Wireless Networks: A -Connectivity Analysis" 0364-9059 © 2014 IEEE.

[3] Shijian Tang, *Student Member, IEEE,* Yuhan Dong, *Member, IEEE,* and Xuedan Zhang, *Member, IEEE,"* On Link Misalignment for Underwater Wireless Optical Communications" IEEE COMMUNICATIONS LETTERS, VOL. 16, NO. 10, OCTOBER 2012.

[4] Kwang sub Song, *Senior Member, IEEE,* and Peter C. Chu, "Conceptual Design of Future Undersea Unmanned Vehicle (UUV) System for Mine Disposal" IEEE SYSTEMS JOURNAL, VOL. 8, NO. 1, MARCH 2014.

Cite this article as: C B GAYATHRI. "Optical Wireless Communication for Underwater Vehicles". *International Conference on Innovative Trends in Electronics Communication and Applications (2015)*: 98-103. Print.

[5] Davide Anguita, Davide Brizzolara, Giancarlo Parodi, "VHDL Modules and Circuits for Underwater Optical Wireless Communication Systems" ISSN: 1109-2742, Issue 9, Volume 9, September 2010, WSEAS TRANSACTIONS on COMMUNICATIONS.

[6] N. Farr, A. Bowen, J. Ware, C. Pontbriand "An integrated, underwater optical /acoustic communications system" Woods Hole, MA 02543 USA.

[7] Alok Ranjan, Ashish Ranjan, "Underwater Wireless Communication Network" Advance in Electronic and Electric Engineering , ISSN 2231-1297, Volume 3, Number 1 (2013), pp. 41-46.

[8] P.Vijaya Kumar, S.S.K.Praneeth, Romarsha.B.Narender , "Analysis of Optical Wireless Communication for Underwater Wireless Communication" International Journal of Scientific & Engineering Research Volume 2, Issue 6, June-2011.Sridhara K , "Free space optical communication" *International Journal of Latest Research in Science and Technology* ISSN (Online):2278-5299 *Vol.1,Issue 3 :Page No.202-205 ,September-October (2012).*

Cite this article as: C B GAYATHRI. "Optical Wireless Communication for Underwater Vehicles". *International Conference on Innovative Trends in Electronics Communication and Applications (2015)*: 98-103. Print.

International Conference on Innovative Trends in Electronics Communication and Applications 2015 [ICIECA 2015]

ISBN	978-81-929742-6-2	**VOL**	01
Website	icieca.in	**eMail**	icieca@asdf.res.in
Received	02 - April - 2015	**Accepted**	15 - November - 2015
Article ID	ICIECA015	**eAID**	ICIECA.2015.015

Image Enhancement Using Affine Histogram Equalization Model

J Kanimozhi[1], P Vasuki[1], K G Sowmiyadevi[1], S Padma[1], G L Vijayalakshmi[1]
[1]ECE Department, K.L.N College of Information Technology

Abstract: *Colour image enhancement is complex and challenging task in digital imagery. Preserving the hue of the input image crucial in a wide range of situations. This work aims to develop hue and range (gamut) preservation techniques. The proposed method consists of two stages via range preserving in optimal way enhancement, scaling and shifting colour enhancement. First stage preserves hue in a colour image by the identified affine histogram equalizations method. Second stage preserves the range (gamut)(0 - 1) by scaling and shifting algorithms. The result is compared with the existing method of histogram specification produces the better result.*

Keywords*:* Colour image enhancement, range preserving, scaling and shifting, histogram equalization, histogram specification.

INTRODUCTION

Image enhancement is used to enhance the standard of an image for visual recognition of human beings. It is also used for small grade optics utilization. It is a task in which the set of pixel values of one image is modified to a new set of pixel values so that the new image formed is visually pleasing and is also more suitable for a scrutiny. The main approach for image enhancement such as contrast stretching, slicing, histogram equalization, for grey scale images are discussed in many books. The generalization of these approaches to colour images is not straight forward. Unlike grey scale images, there are some elements in colour images like hue, which need to be properly handled for enhancement.[1] Hue, saturation and intensity are the characteristics of colour. Hue is that characteristic of a colour which decides what kind of colour it is, i.e., a red or an orange. In the spectrum each colour is at the maximum purity (or strength or richness) that the eye can acknowledge, and the spectrum of colours is narrated as fully drenched. If a drenched colour is diluted by being blended with other colours or with white light, its intensity or saturation is decreased. For the purpose of enhancing a colour image, it is to be seen that hue should not alter for any pixel. If hue is changed then the colour gets changed, thereby deforming the image [2].

To enhance the ocular quality of an image without deforming it for image enhancement. Several algorithms are accessible for contrast enhancement in grey scale images, which change the grey values of pixels depending on the criteria for enhancement.

This paper helps to the enormous development in digital colour imaging and display technology. In spite of the major amount of research, colour recognition and colour aspects are still open problems. The demand for fast efficient algorithms improving the colour content of digital images has increased dramatically. The applications of colour image improvement are abundant. They concern for example digital cameras and mobile phone cameras, medical imaging, post-production industry, video reconstruction of old pictures and movies.

Histogram specifications are used in previous methods. Exact histogram specification (HS), which is also known as histogram matching, of single-valued (grey valued) images desire to transform an input image to an output image which exactly fits a prescribed target histogram. Histogram equalization (HE) is a particular instance of HS where the target histogram is uniform. We do not

Cite this article as: J Kanimozhi, P Vasuki, K G Sowmiyadevi, S Padma, G L Vijayalakshmi. "Image Enhancement Using Affine Histogram Equalization Model". *International Conference on Innovative Trends in Electronics Communication and Applications (2015)*: 104-114. Print.

emphasis on the construction of target histograms. Instead, we adopt a simple approach inspired by [4]. For digital image HS is an ill posed problem [5]. The hint to ensuring exact HS is to obtain a *meaningful total strict arrangement* of all pixels in the input digital image. We perform exact HS using the algorithm in [2] which currently provides the best pixel ordering in terms of standard and speed. We perform Recursive Mean Separate Histogram Equalization (RMSHE) using the algorithm in [4]

The extension of histogram methods to colour images is a quite difficult task. The histogram of a gray-value image is single dimensional (1D) while the histogram of a colour image is three dimensional which gives rise to an under-determined problem. For instance, applying HS to each colour channel separately changes the colour content (the hue) of the image. Further it is not easy to produce a colour images that obeys the range constraints. As a central outcome of this paper, we propose a general and optimal hue and range conserving colour allotment methodology [6].

In this paper we deserve to design colour image enhancement methods in the RGB space sharing three important features, namely hue and range (gamut) conservation and low calculation complexity. The hue describes in each area of an image the main colour ingredient that one really recognizes, e.g., red, orange, magenta, yellow and so on .The hue has the nice property of being same under variation of direction and intensity of the incident light [3]. Thus, by preserving the hue and enhancing the brightness, the acquired image will appear more colourful. Normally colour image enhancement consist of two main problems which are Hue preservation, Gamut problem

A colour may displayed on your monitor in RGB may not be printable in the gamut of your cmyk printer. For example a pure red colour only expressed in RGB colour space, that cannot expressed in cmyk colour space.
This is gamut problem. The gamut problem occurred in an enhanced image is rectified by three simple algorithms. This paper proposes three main algorithms which are range preserving in optimal way enhancement,
scaling colour enhancement, shifting colour enhancement

In this paper histogram based methods are selected according to the applications will be effective but selection of fast algorithm will be more efficient. Fast Algorithm is performed by the following steps. Intensity channel of the input RGB image is matched to a particular histogram which gives us the target intensity image.

The RGB colour values are computed based on the target colour space, some methods work directly in the RGB space intensity image so that they satisfy the hue and gamut while others operate in transformed colour spaces. e.g., LHS, constraints in an optimal way. These stages are briefly discussed below.

PROPOSED METHODOLOGY

Histogram equalization is a process of automatically determining the transfer function which produces an output image with a uniform histogram. But histogram equalization is not suitable for some application. In such case, the histogram shape of the output image may be specified. The method used to generate a processed image that has a specified histogram is called histogram matching or histogram specification.
The intensity of a original image W can be defined as

$$f = (1/3)\,(Wr+Wg+Wb) \quad (1)$$

where f is a intensity of the image; Wr,Wg,Wb are intensity of rgb colour;

Similarly from the histogram matched image W1 we can find the intensity as

$$f1 = (1/3)\,(W1(r)+W1(g)+W1(b) \quad (2)$$

where f1 is the intensity of the histogram matched image

In general Affine mapping is defined by

$$W1 = aW + b \quad (3)$$

The equation can be modified for all the RGB components as

$$W1c(x) = a[x]\,W[x] + b[x] \text{ for } c\epsilon\ (r,g,b) \quad (4)$$

Use the intensity of the channels are weights of the R,G,B Channel. To find f^ which is the target intensity of the specified Histogram. its gray value ranges from (0- L-1). The histogram Function does not involve a strict ordering of 'f' which is the Intensity of the original image and f^ is not uniform. This Produces some artifacts…this can be solved by histogram Specification using strict ordering.

Cite this article as: J Kanimozhi, P Vasuki, K G Sowmiyadevi, S Padma, G L Vijayalakshmi. "Image Enhancement Using Affine Histogram Equalization Model". *International Conference on Innovative Trends in Electronics Communication and Applications (2015)*: 104-114. Print.

For intensity fit the equation (2) should be satisfied .this happens if and only if when equation (4) can be modified such that

$$f1[x] = a[x]f[x] + b[x] \quad (5)$$

from equation (5)

$$b[x]=f1[x]-a[x]f[x] \quad (6)$$

sub in equation (4)

$$W1c[x] = a[x] (Wc[x]-f[x]) + f1[x] \text{ for } c\epsilon (r,g,b) \quad (7)$$

By Naik & Murthy algorithm

$$a[x]=(f1[x]/f[x]) \text{ for scaling case(a)}$$

There are two cases by equation (4)

Scaling: for b[x] = 0, equation (7) can be modified as

$$W1c[x]= = (f1[x]/f[x])Wc[x]$$

For c (r,g,b) (8)

Shifting: for a[x] = 1, equation (7) can be modified as

$$W1c[x] =Wc[x]-f[x] +f1[x] \quad (9)$$

These equations are then used for preserving the range, we will use for all x € Xn the magnitudes

$$M[x] = \max \{Wc[x]: c (r, g,b)\}$$

$$m[x] = \min \{Wc[x]: c\epsilon(r,g,b)\} \quad (10)$$

Where M[x] is the maximum and m[x] is the minimum of the RGB components

From algorithm 1, intensity of the original image and the target intensity are computed. The aim is that image has same intensity as target intensity and the hue of the target image and original image is to be matched. The ranges between $0 \leq \omega c \leq L-1$, c{r,g,b}.

First the histogram equalization is applied to the colour image. From the result of histogram equalization of input image it is clear that the histogram is not uniform and its pixel values spread over the entire image. Then the histogram specification is applied to the original image. Here the histogram is uniformly distributed. But the output image of histogram specification consists of problem. The problems occurred in the previous work can be overcome by simple algorithms known as affine histogram equalization model. The model has two simple algorithms. Range preserving in optimal way enhancement, Scaling and Shifting colour enhancement

Here the histogram of the original image having pixels which are not in order once if user want to enhance the input image , should go algorithm 1 after the strict ordering which magnify the dark and bright pixels after that it will be enhanced by using scaling and shifting algorithm. The Following there main algorithms which we have proposed to rectify the hue and gamut problem. The algorithm provided here is the best way to rectify hue. Affine mapping to all pixels for the desired stretching of he gamut problem in [2]. Incase [2] f [i] / f1[i] >> 1 range constraints are not guaranteed. To overcome the problem by switching RGB colour space to CMY colour space and then to transform back to RGB space. This step reads for all c{r,g,b}. This algorithm often used to avoid the range problems. The optimum and gamut problem which are occurred generally in when making image enhancement. the algorithm 2 naik and murthy algorithm gives only gray scale enhancement ,here this paper image enhancement using affine histogram equalization model gives colour image enhancement yet this paper is also suitable for making large size image enhancement and it is assist to tremendous progress in digital colour imaging and display technology. Range preservation in optimal way enhancement:

The gamut problem was removed in a optimal way and the pixel values chosen are closest in the range. This algorithm is a convex combination of scaling and shifting.

AFFINE ALGORITHM TO PRESERVE RANGE

Preserving range is a important parameter. This model is the convex combination of scaling and shifting for T ∈ [0,1]The simplest hue and range preserving method is to apply the range for these components is

Cite this article as: J Kanimozhi, P Vasuki, K G Sowmiyadevi, S Padma, G L Vijayalakshmi. "Image Enhancement Using Affine Histogram Equalization Model". *International Conference on Innovative Trends in Electronics Communication and Applications (2015)*: 104-114. Print.

$$0\ m[x] \leq f(x) \leq M(x)\ L-1 \quad (11)$$

Two types of gamut problem occurs, when maximum of RGB component exceed the range, there occurs upper gamut problem. i.e. L-1

Then M[x] = W1s[x] for s(r, g, b)

For that the best correction of this is to choose pixel values is clearly to choose a[x] in equation (7)

So that the closest value in the range i.e. W1s[x] = L-1 from (11) so

$$L-1=a[x]\ (Wc[x]-f[x]) + f1[x] \quad (12)$$

From (11) for non gray valued pixels

M[x]-f[x] > 0 so that

$$a[x] = \{(L-1-f1[x])/(M[x]-f[x])\} \geq 0$$

Thus for the upper gamut problem the corrected colour values of pixel x is

$$W1c[x]= \{(L-1-f1[x])/(M[x]-f[x])\}(Wc[x]-f[x]+f1[x] \text{ for } c \in (r,g,b) \quad (13)$$

When minimum component m1[x] < 0 then lower gamut problem is occurred. For s (r,g,b) be such that

W1s[x] = m1[x] so that the best correction is W1s[x] = 0,

$$0=a[x]\ (m[x]-f[x])+ f1[x] \quad (14)$$

From (11) for non gray valued pixels f[x] - m[x] > 0 so that

$$a[x] = \{f1[x]/ (f[x] - m[x])\} \quad 0$$

So for the lower gamut problem the corrected colour value is given as

$$W1c[x] = \{f1[x]/ (f[x] - m[x])\}\ (Wc[x]-f[x])+ f1[x] \text{ for c } (r,g,b) \quad (15)$$

This model is the convex combination of scaling and shifting for T [0,1] So combining equation (8) and (9) we get

$$W1c[x] =T\ (f1[x]/f[x]) + (1-T)\ (Wc[x]-f[x]) + f1[x]$$

$$=a[x](Wc[x]-f[x])+f1[x] \quad (16)$$

$$a[x]=T(f1[x]/f[x])+(1-T) \quad (17)$$

We propose a general affine model for image enhancement using affine HS model in the RGB space which gives rise to Algorithm 3. Two simple but key instances of this algorithm are the Multiplicative algorithm 4 and the Additive algorithm 5. We show how the result of Algorithm 3 can be faithfully approximated as a convex mixture of the images obtained by Algorithm 4 and Algorithm 5, which is quite practical. The enhancement performances of our algorithms and the Naik-Murthy algorithm [2] are analyzed in terms of their chromaticity improvement. In all cases, our algorithms clearly exceed the algorithm in [1] recently applied to colour images in [7]. All numerical tests confirm our theoretical outcomes. Our algorithms are simple and fast. They are really efficient when one wishes to give a better clarity of images (not too altered by artifacts) while preserving the original colour ambience.

SCALING AND SHIFTING ALGORITHMS

For T [0,1] the above algorithm yields scaling and shifting algorithms. Observed that from equation (8) , (9) ,(12) and (14)

$$R0m[x] = (m[x]-f[x]) + f1[x] \quad (18)$$

$$R0M[x] = (M[x]-f[x]) + f1[x] \quad (19)$$

$$R1M[x] = (f1[x]/f[x])\ M[x] \quad (20)$$

Cite this article as: J Kanimozhi, P Vasuki, K G Sowmiyadevi, S Padma, G L Vijayalakshmi. "Image Enhancement Using Affine Histogram Equalization Model". *International Conference on Innovative Trends in Electronics Communication and Applications (2015)*: 104-114. Print.

EXISTING ALGORITHMS I & II:

Algorithm I: (Exact Histogram Specification)

Initialization:

u(0)=3f,(β,α):=(0.1, 0.05), and target histogram bh= (bh1, . . ., bhL). Choose K (e.g., K = 6).

For k = 1, . . . ,K compute

3. u(k) = f − η−1(βGTη(Gu(k−1)).

Where η(t) :=t/α + |t| and η−1(y) =αy/1 − |y| and G is a forward difference matrix.

Order the values in according to the corresponding ascending entries of u(K).

HS step: divide the obtained ordered list of indices into L groups and assign gray value 0 to the first bh1 pixels and so on until gray value L − 1 to the last bhL pixels. This provides the target intensity b f. The affine model (8) obeys (a) if and only if

W^c[i] = a[i](wc[i] − f[i]) + f^[i], c {r, g, b}

This algorithm is used to make the pixels strict ordering.

Algorithm II*:* (Naik and Murthy [2])

Compute the intensity f of w and the target intensity b f.

For i in compute

w^c[i] :=(f^[i]/f[i])wc[i] if f[i]/f[i] ≤ 1

w^c[i] :=L − 1 − f^[i]/L − 1 − f[i](wc[i]−f[i]) + f^ [i] if f^ [i]/f[i]>1

Algorithm III: (Range Preserving in Optimal Way enhancement)

Compute the intensity f of W by (1) and the target intensity f1 using histogram matching.

For x Xn compute M[x] and m[x] by 10.if f[x] = 0,

ThenW1[x] = 0.otherwise compute

a[x] = T (f1[x]/f[x])+(1-T)

RTm[x] = a[x] (m[x]-f[x]) + f1[x] (21)

RTM[x] =a[x] (M[x]-f[x]) + f1[x] (22)

For all c (r,g,b):cases

W1c[x]=a[x](Wc[x]-f[x])+ f1[x] if RTm[x]≥ 0 and RTM[x]≤L-1
W1c[x]={(L-1-f1[x])/(M[x]-f[x])} (Wc[x]-f[x]) + f1[x] if RTM[x] ≥L-1
W1c[x]={f1[x]/(f[x]-m[x])} (Wc[x]-f[x]) + f1[x] if RTm[x]<0

The simplest hue range preserving process is to exert the affine mapping to all pixels. By finding the least and largest pixel values compute the average value for all Pixels. It is the desired stretching of pixels. When intensity values are not matched for the original and target, range is not guaranteed .For this cases the solution is to switch from RGB colour space to CMY space and then transform it back to RGB.

The main objective of affine specification model is the intensities of original and target images are to be matched, hue of original and target images are to be coincide, range is in between 0 to L-1.

Cite this article as: J Kanimozhi, P Vasuki, K G Sowmiyadevi, S Padma, G L Vijayalakshmi. "Image Enhancement Using Affine Histogram Equalization Model". *International Conference on Innovative Trends in Electronics Communication and Applications (2015)*: 104-114. Print.

The range is exceeded (L-1) there is occurrence of upper gamut problem. The range is less than 0 there is occurrence of lower gamut problem. These Problems solved in an optimal way doing some pixel correction.

Algorithm IV: (scaling Colour Enhancement)

This algorithm is applied when T = 1.

Compute the intensity f of W by (1) and the target intensity f1 using histogram matching.

For x Xn compute M[x] by10.

if f[x] = 0, then W1[x] = 0.

Otherwise compute

$$R1M[x] = (f1[x]/f[x])M[x] \text{ and for all } c \ (r,g,b) \quad (23)$$

CASES:

$$W1c[x] = = (f1[x]/f[x])Wc[x] \quad (24)$$

if $RTM[x] \leq L-1$

$$W1c[x] = \{(L-1-f1[x])/(M[x]-f[x])\} (Wc[x]-f[x]) + f1[x] \text{ if } RTM[x] \geq L-1 \quad (25)$$

Optimal range preserving algorithm yields two simple scaling and shifting algorithms called additive and multiplicative algorithm. The scaling parameter varies between (0-1). When this parameter is 0 then apply the shifting algorithm. When this is 1 then apply the scaling algorithm

Algorithm V: (Shifting Colour Enhancement)

This algorithm is applied when T = 0.

compute the intensity f of W by (1) and the target intensity f1 using histogram matching.

For x Xn compute M[x] and m[x] by 10.if f[x] = 0,

Then W1[x] = 0.otherwise compute

$$RTm[x] = a[x] (m[x]-f[x]) + f1[x] \quad (26)$$

$$RTM[x] = a[x] (M[x]-f[x]) + f1[x] \quad (27)$$

For all c (r,g,b):cases

$$W1c[x] = a[x] (Wc[x]-f[x]) + f1[x] \quad \text{if } R0m[x] \geq 0 \text{ and } RTM[x] \leq L-1 \quad (28)$$

$$W1c[x] = \{(L-1-f1[x])/(M[x]-f[x])\} (Wc[x]-f[x]) + f1[x] \text{ if } R0M[x] \geq L-1 \quad (29)$$

$$W1c[x] = \{f1[x]/(f[x] - m[x])\} (Wc[x]-f[x]) + f1[x] \quad \text{if } R0m[x] < 0 \quad (30)$$

Instead of applying our Affine Algorithm III for some $\lambda \in [0, 1]$, we can compute the images bw+ by the Shifting Algorithm V and bw× by the Scaling Algorithm IV and build their convex combination for the same $\lambda \in [0,1]$.Our conclusions the scaling colour enhancement algorithm gives the most colourful image. the shifting algorithm yields colour values between those of the scaling and the naik-murthy; it performs better than the last one.

RESULTS AND DISCUSSION

More than 250 images are taken to test the method including Image Database such as CSIQ, Tid 2008, holiday images etc., Three algorithms such as optimal and range preserving, if the range is T=0 then shifting algorithm is applied and if the range is T=1 then scaling algorithm is applied to images after histogram specification and histogram equalization and performance metrics for the images monument.jpg,roping.jpg,1600.jpg,family.jpg, fisher.jpg are shown in Tables 1-4.Table

Cite this article as: J Kanimozhi, P Vasuki, K G Sowmiyadevi, S Padma, G L Vijayalakshmi. "Image Enhancement Using Affine Histogram Equalization Model". *International Conference on Innovative Trends in Electronics Communication and Applications (2015)*: 104-114. Print.

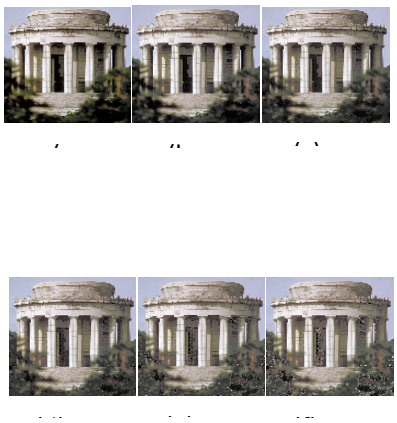

Fig.1. Output of Range preserving in optimal way enhancement using histogram specification .(a)) input image,(b)image when T=0,(c)image when T=0.25,(d) image when T=0.5(e) image when T=0.75(f) image when T=1.(T is a scaling parameter)

Fig .2. Output of Range preserving in optimal way enhancement using histogram equalization is a scaling parameter we already know by algorithm 3.(a)) input image,(b)image when T=0,(c)image when T=0.25,(d) image when T=0.5(e) image when T=0.75(f) image when T=1 (T is a scaling factor).

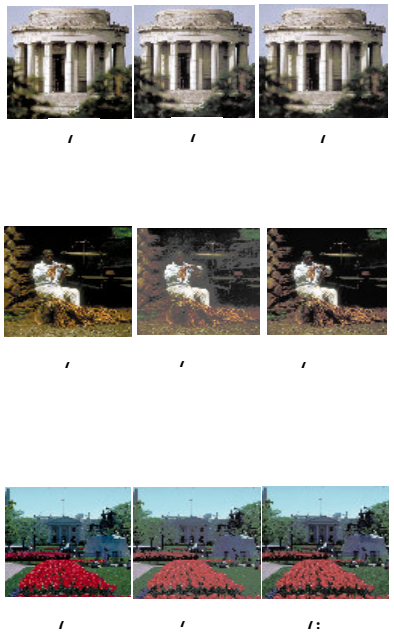

Fig.3. The output of Scaling colour enhancement using histogram specification (middle) and histogram equalization (right corner). If a dark pixel has wrong hue (e.g. due to compression or printing artifacts ,noise,colour cast,etc)the scaling algorithm can magnify the intensity of this wrong colour if the input image contains a lot such pixels, the shifting colour enhancement algorithm can be the better choice

(a,d,g,j,m)=original image.(b,e,h,k,n)=using exact HS (c,f,i,l,o)=using RMSHE (Recursive Mean Separate Histogram Equalization).

Cite this article as: J Kanimozhi, P Vasuki, K G Sowmiyadevi, S Padma, G L Vijayalakshmi. "Image Enhancement Using Affine Histogram Equalization Model". *International Conference on Innovative Trends in Electronics Communication and Applications (2015)*: 104-114. Print.

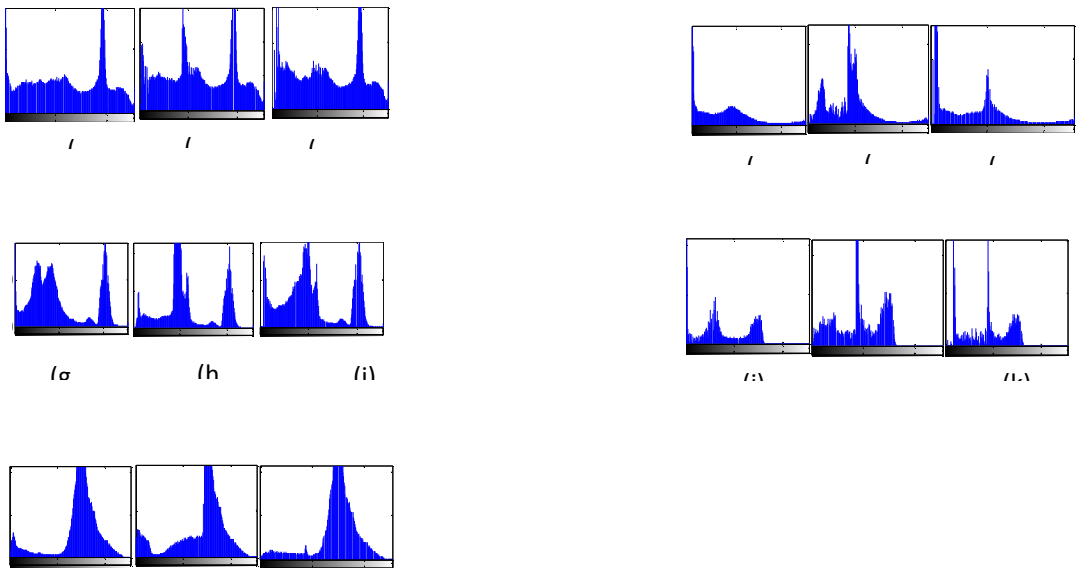

Fig .4. *The histogram output of Scaling colour enhancement using histogram specification (middle) and histogram equalization (right corner). If a dark pixel has wrong hue (e.g. due to compression or printing artifacts, noise, colour cast,etc)the scaling algorithm can magnify the intensity of this wrong colour . if the input image contains a lot such pixels, the shifting colour enhancement algorithm can be the better choice.(a,d,g,j,m)=histogram of original image.(b,e,h,k,n)=histogram of exact HS (c,f,i,l,o)= histogram of RMSHE (Recursive Mean Separate Histogram Equalization).*

Fig5. The output of Shifting colour enhancement. (a,d,g,j,m)=original image.(b,e,h,k,n)=using exact HS (c,f,i,l,o)=using RMSHE (Recursive Mean Separate Histogram Equalization).

The shifting algorithm gives realistic image .we can use this algorithm When this parameter T= 0

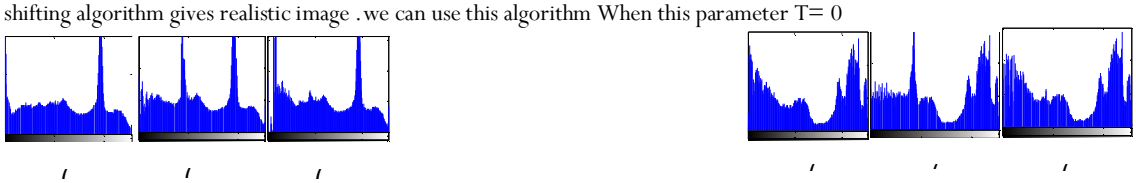

Cite this article as: J Kanimozhi, P Vasuki, K G Sowmiyadevi, S Padma, G L Vijayalakshmi. "Image Enhancement Using Affine Histogram Equalization Model". *International Conference on Innovative Trends in Electronics Communication and Applications (2015)*: 104-114. Print.

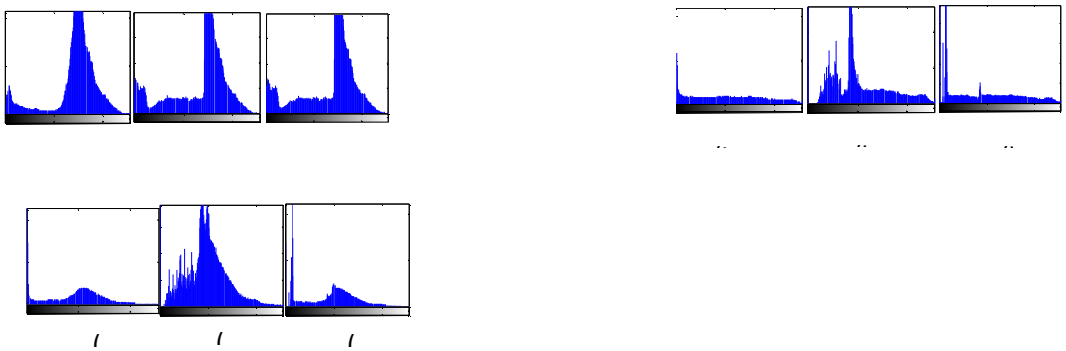

Fig6. The output of Shifting colour enhancement.(a,d,g,j,m)=histogram of original image.(b,e,h,k,n)=histogram of exact HS (c,f,i,l,o)= histogram of RMSHE (Recursive Mean Separate Histogram Equalization).

PERFOMANCE METRICS

The PSNR is commonly used as measure of quality reconstruction of image. High value of PSNR indicates the high quality of image. It is defined via the Mean Square Error (MSE) and corresponding distortion matric, the Peak Signal to Noise Ratio .

$$MSE=1/MN \sum_{m=1}^{} \sum_{n=1} [f(m/n)-f'(m/n)] \quad (x)$$

$$PSNR= 10.\log10 [(255)2/MSE] \quad (y)$$

$$=20.\log10 (255)-10.\log10 (MSE)$$

Here Max is maximum pixel value of image when pixel is represented by using 8 bits per sample. This is 255 bar colour image with three RGB value per pixel.

The RMSE is a frequently used measure of the difference between values predicted by a model or an estimator and the values actually observed

$$RMSE=\sqrt{(1/n\sum_{i=1} (y_i- y_i\hat{})^2)} \quad (z)$$

FOR SCALING ALGORITHM

Table 1 PSNR&RMSE comparison HS Vs HE

S.No	IMAGE	PSNR (HS)	PSNR (HE)	RMSE (HS)	RMSE (HE)
1.	Monument	66.9419	70.7593	0.1147	0.0739
2.	Roping	66.227	71.4759	0.1245	0.0680
3.	1600	65.9193	68.7029	0.129	0.0936
4.	Family	60.9302	69.9982	0.2291	0.0807
5.	Fisher	30.5147	67.2853	7.5999	0.1102

Table 1 shows PSNR comparison for Histogram Specification (HS) and Histogram Equalisation(HE) for images monument.jpg,roping.jpg,1600.jpg,family.jpg, fisher.jpg in which monument.jpg image has the highest PSNR value of 70.7593 for

Cite this article as: J Kanimozhi, P Vasuki, K G Sowmiyadevi, S Padma, G L Vijayalakshmi. "Image Enhancement Using Affine Histogram Equalization Model". *International Conference on Innovative Trends in Electronics Communication and Applications (2015)*: 104-114. Print.

Histogram equalization images compared to HS having 66.94 which is lower by 4dB. For all the images the PSNR value for HE is higher compared to HS applied images.

Table 2 MSE&SSIM comparison HS Vs HE

S.No	IMAGE	MSE (HS)	MSE (HE)	SSIM (HS)	SSIM (HE)
1.	Monument	0.0131	0.0055	0.9992	0.9997
2.	Roping	0.0155	0.0046	0.9789	0.9994
3.	1600	0.0166	0.0088	0.9932	0.9968
4.	Family	0.0525	0.0065	0 .9860	0.9971
5.	Fisher	57.7580	0.0121	0.9979	0.9992

Table 2 shows SSIM comparison for Histogram Specification (HS) and Histogram Equalisation(HE) for images monument.jpg,roping.jpg,1600.jpg,family.jpg, fisher.jpg in which monument.jpg image has the least RMSE value of 0.0680 for Histogram equalization images compared to HS having error of 0.1245 which is higher by 0.6. For all the images the RMSE value for HE is lower compared to HS applied images. Performance metrics table for scaling algorithm proves that Histogram equalization performs better that Histogram specification.

FOR SHIFTING ALGORITHM

Table 3 PSNR &RMSE comparison HS Vs HE

S.No	IMAGE	PSNR (HS)	PSNR (HE)	RMSE (HS)	RMSE (HE)
1.	Monument	65.5686	67.2689	0.1343	0.1104
2.	Bridge	64.844	72.4958	0.146	0.0605
3.	Fisher	29.9339	68.1058	8.1254	0.1003
4.	Snow_leaves	55.8659	69.6058	0.4104	0.0844
5.	Veggies	57.6427	57.8555	0.3345	0.3264

Similarly table 3 also shows the HE applied images performs better than HS applied images.

Table 4 MSE&SSIM comparison HS Vs HE

S.No	IMAGE	MSE (HS)	MSE (HE)	SSIM (HS)	SSIM (HE)
1.	Monument	0.018	0.0122	0.9992	0.9997
2.	Bridge	0.0213	0.0037	0.9989	1.0000
3.	Fisher	66.0228	0.0101	0.9958	0.9996
4.	Snow_leaves	0.1685	0.0071	0.9802	0.9994
5.	Veggies	0.1119	0.1065	0.9799	0.9993

Cite this article as: J Kanimozhi, P Vasuki, K G Sowmiyadevi, S Padma, G L Vijayalakshmi. "Image Enhancement Using Affine Histogram Equalization Model". *International Conference on Innovative Trends in Electronics Communication and Applications (2015)*: 104-114. Print.

Table 4 shows SSIM performance shows the structural similarity of 0.9997 for HE applied monument image. Performance metrics table for shifting algorithm proves that Histogram equalization performs better that Histogram specification.

CONCLUSION AND FUTURE WORK

This paper gives best result for image enhancement. This work provides the first comprehensive and rigorous presentation of the vast family of histogram specification based affine colour assignment models. We have proposed a image enhancement using affine histogram specification model. We analysed the performances of this algorithm and two of its important cases as well as the gamut preserving method. As usual dealing with a topic creates many open questions we have to answer in our future research. Instead of the strength of the input image, we can consider other combinations between the RGB channels that are better adapted to human colour perception and to the image content. Moreover, it may be useful to take the saturation or chromaticity of the input image into account. Finally, a systematic approach to find the target histogram is clearly desirable and topic of future research. Since our algorithms are fast, extensions to video should be envisaged.

REFERENCES

[1] M. Nikolova and G. Steidl, "Fast sorting algorithm for exact histogram specification", Preprint hal-00870501, 2013.

[2] S. F. Naik and C. A. Murthy, "Hue-preserving colour image enhancement without gamut problem", *IEEE Trans. Image Process.*, vol. 12, no. 12, pp.1591–1598, Dec. 2003.

[3] M. Nikolova, Y.-W. Wen, and R. Chan, "Exact histogram specification for digital images using a variational approach", *J. Math. Imaging and Vision*,vol. 46, no. 3, pp. 309–325, Jul. 2013.

[4]S.-D. Chen and A. Ramli, "Contrast enhancement using recursive Mean-Separate histogram equalization for scalable brightness preservation,"*IEEE Trans. On Consumer Electronics*, vol. 49, no. 4, pp. 1301-1309, Nov. 2003.

[5] T. Arici, S. Dikbas, and Y. Altunbasak, "A histogram modification framework and its application for image contrast enhancement", *IEEE Trans. Image Process.*, vol. 18, no. 9, pp. 1921–1935, Sep. 2009.

[6] V. Caselles, J. L. Lisani, J. M. Morel, and G. Sapiro, "Shape preserving local histogram modification", *IEEE Trans. Image Process.*, vol. 8, no. 2, pp.220–229, Feb. 1999.

[7] N. Papadakis, E. Provenzi, and V. Caselles, "A variational model for histogram transfer of colour images," *IEEE Trans. Image Process.*,vol. 20, no. 6, pp. 1682–1695, Jun. 2011.

Cite this article as: J Kanimozhi, P Vasuki, K G Sowmiyadevi, S Padma, G L Vijayalakshmi. "Image Enhancement Using Affine Histogram Equalization Model". *International Conference on Innovative Trends in Electronics Communication and Applications (2015)*: 104-114. Print.

International Conference on Innovative Trends in Electronics Communication and Applications 2015 [ICIECA 2015]

ISBN	978-81-929742-6-2
Website	icieca.in
Received	02 - April - 2015
Article ID	ICIECA016

VOL	01
eMail	icieca@asdf.res.in
Accepted	15 - November - 2015
eAID	ICIECA.2015.016

Rotation Invariant Texture Classification using BRINT and GLCM with SVM Classifier

A Shakin Banu[1], P Vasuki[2], A Glory Sujitha[3], S Amala Deepan[4]

[1,2] KLN College of Information Technology, [3,4] SSM Institute of Science and Technology

Abstract: *Texture classification is one of the four problem domains in the field of texture analysis for the development of effective features to extract from a given textured image. This paper proposes a Binary Rotation Invariant and Noise Tolerant (BRINT) which is a very fast, compact and also more accurate while illumination variations, noise and rotation changes. Here Gray Level Co-occurrence matrix algorithm is used along with BRINT for feature extraction. Texture classification is performed with the SVM classification. The proposed method is compared with the existing K Nearest Neighbourhood algorithm. In our proposed work, snake texture has been taken for processing and the proposed method is quantified with various performance metrics like accuracy, sensitivity, specificity and PSNR performance and found to be greater compared with the existing method.*

Keywords*:* Texture descriptors- local binary pattern (LBP), BRINT, Grey Level Co-occurrence Matrix (GLCM) feature extraction, SVM Classification.

INTRODUCTION

TEXTURE is a fundamental characteristic of the appearance of virtually all natural surfaces and is ubiquitous in natural images. Texture classification, as one of the major problems in texture analysis, has received considerable attention during the past decades due to its value both in understanding how the texture recognition process works in humans as well as in the important role it plays in the field of computer vision and pattern recognition [1].

Typical applications of texture classification include medical image analysis and understanding, object recognition, content based image retrieval, remote sensing, industrial inspection, and document classification.

The texture classification problem is conventionally divided into the two sub problems. It is generally agreed that the extraction of powerful texture features is of more importance to the success of texture classification and, consequently, most research in texture classification focuses on the feature extraction part [1], with extensive surveys [1]. Nevertheless it remains a challenge to design texture features which are computationally efficient, highly discriminative and effective, robust to imaging environment changes (including changes in illumination, rotation, view point, scaling and occlusion) and insensitive to noise. Recently, the Bag-of-Words (Bo W) paradigm, representing texture images as histograms over a discrete vocabulary of local features, has proved effective in providing texture features. Representing a texture image using the Bo W model typically involves the following three steps:

(i) Local texture descriptors: extracting distinctive and robust texture features from local regions;

(ii)Texton dictionary formulation: generating a set of representative vectors (*i.e.,* textons or dictionary atoms) learned from a large number of texture features

Cite this article as: A Shakin Banu, P Vasuki, A Glory Sujitha, S Amala Deepan. "Rotation Invariant Texture Classification using BRINT and GLCM with SVM Classifier". *International Conference on Innovative Trends in Electronics Communication and Applications (2015)*: 115-119. Print.

(iii) Global statistical histogram computation: representing a texture images statistically as a compact histogram over

The learned texton dictionary and instability. In contrast, dense approaches, applying texture descriptors pixel by pixel are more popular. Important dense textures descriptors include Gabor wavelets [8], LM filters [5], MR8 filters [5], BIF features [7], LBP [2], Patch descriptor [6] and RP random features [3] and many others [4].fingerprint matching, visual inspection, image retrieval, biomedical image analysis, face image analysis, motion analysis, edge detection, and environment modeling [8]–[11]. Consequently many LBP variants are present in the recent literature. Although significant progress has been made, most LBP variants still have prominent limitations, mostly the sensitivity to noise , and the limiting of LBP variants to three scales, failing to capture long range texture information. Although some efforts have been made to include complementary filtering techniques , these *increase* the computational complexity, running counter to the computational efficiency property of the LBP method. In this paper, we propose a computationally simple approach, the Binary Rotation Invariant and Noise Tolerant (BRINT) descriptor, which has the following outstanding advantages: It is highly discriminative, has low computational complexity, is highly robust to noise and rotation, and allows for compactly encoding a number of scales and arbitrarily large circular neighborhoods. At the feature extraction stage there is no prelearning process and no additional parameters to be learned.

Proposed Methodology

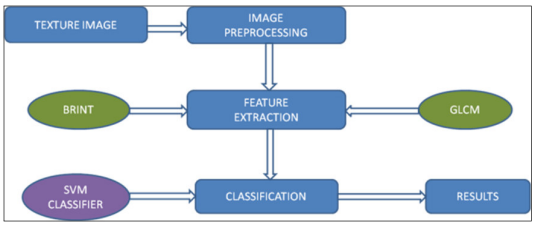

Fig(a) Block Diagram of Proposed Methodology

The input texture image undergoes pre-processing by applying Gaussian filtering to remove the noise from the image. Gaussian filter is windowed filter of linear class, by its nature is weighted mean. The Gaussian Smoothing Operator performs a weighted average of surrounding pixels based on the Gaussian distribution. Then the features are extracted using BRINT and GLCM Feature Extraction methods. Each pixel values are extracted for BRINT as red, green, blue separately. From these values Histograms are generated to analyses the peak values. Similarly same procedure is done for GLCM and the features are extracted successfully from the Image. After the Feature Extraction, Classification is done using SVM (Support Vector Machine) Classifier. Texture classification method involves two phases: the learning phase and recognition phase. In the learning phase, a set of textural feature are extracted for each image. In the recognition phase, the textural features of the sample are compared to those of the training images and the sample is assigned to the category with the best match. If the best match is found, the sample is accepted otherwise it is rejected.

PROPOSED ALGORITHMS - BRINT, GLCM AND SVM

Motivation

The proposed BRINT is based on the concept of local binary pattern (LBP) and Completed Local Binary Pattern (CLBP). LBP operator leading to poor discriminant power and large storage requirements. The LBP operator captures only the very local structure of the texture of database. So it is difficult to collect information from a larger area. CLBP is leading to perform an even higher dimensionality so this system not applicable for storage and reliable classifier learning. These descriptors having one of the noise sensitivity, and information insufficiency. For KNN Algorithm, large value of K gives good performance. But for large K more neighbours are required and hence larger the computing time.

BRINT Algorithm

The BRINT feature vector, in its simplest form, is created in the following manner:

- Divide the examined window into cells (e.g. 16x16 pixels for each cell).
- For each pixel in a cell, compare the pixel to each of its 8 neighbours (on its left-top, left-middle, left-bottom, right-top, etc.). Follow the pixels along a circle, i.e. clockwise or counter-clockwise.
- Where the centre pixel's value is greater than the neighbour's value, write "1". Otherwise, write "0". This gives an 8-digit binary number (which is usually converted to decimal for convenience).
- Compute the histogram, over the cell, of the frequency of each "number" occurring (i.e., each combination of which pixels are smaller and which are greater than the center).

Cite this article as: A Shakin Banu, P Vasuki, A Glory Sujitha, S Amala Deepan. "Rotation Invariant Texture Classification using BRINT and GLCM with SVM Classifier". *International Conference on Innovative Trends in Electronics Communication and Applications (2015)*: 115-119. Print.

- Optionally normalize the histogram.
- Concatenate (normalized) histograms of all cells. This gives the feature vector for the window.

GLCM Algorithm

The algorithm comprises of four main steps, which are

- Decomposition of the gray level image into sub-bands
- Partitioning the textured image into non-overlapping sub-windows
- Extracting co-occurrence features and finally classifying each sub-window as defective or non-defective.
- A histogram is computed from the desired GLCM

SVM Classification Algorithm

Classification using SVM (Support Vector Machine) Classifier is done in the following manner.

- Classify the texture based on the extracted features using SVM classifier.
- In the SVM classifier there are two phases such as train phase and test phase.
- In train phase, train the all dataset features with mentioned label.
- Hyper plane formed with trained features where each hyper plane represented the each group.
- That each grouped train features are labeled at the end of train phase.

RESULTS AND DISCUSSIONS

In pre-processing we are applying Gaussian filtering to our input image. Features are extracted using BRINT and GLCM. Extraction can be done for various noise levels. Each pixel values are extracted for BRINT as red, green, blue separately. From these values Histograms are generated to analyze the peak values. Similarly same procedure is done for GLCM Thus features are extracted successfully from the Image. After the Feature Extraction, Classification is done using SVM (Support Vector Machine) Classifier. Snake Textures have been taken for experimental analysis.

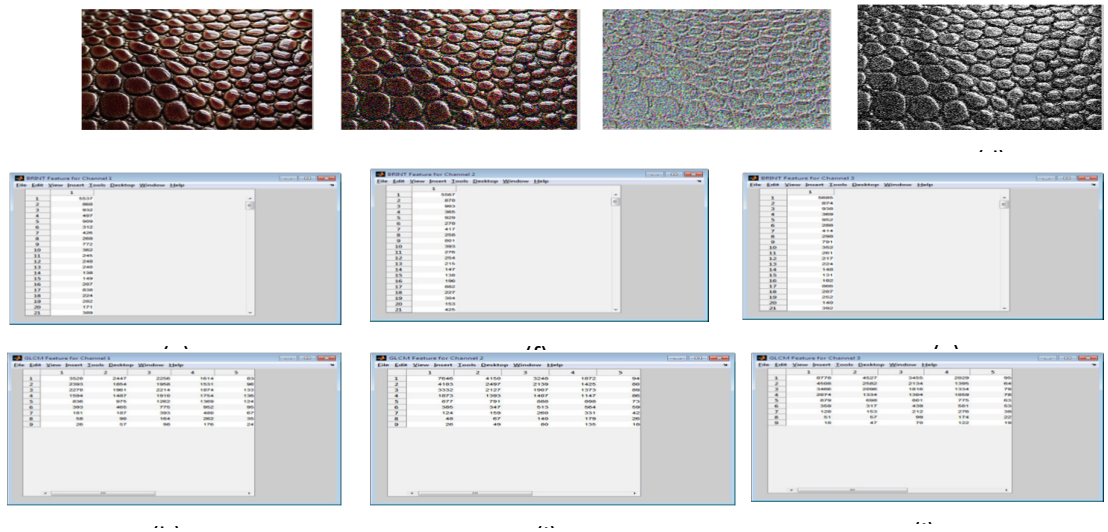

Fig 2:(a) Input Image (b) Filtered Image (c) BRINT Image (d) GLCM Image (e) BRINT Feature Extraction for channel1 (f) BRINT Feature Extraction for channel 2 (g) BRINT Feature Extraction for channel 3 (h) GLCM Feature Extraction for channel 1 (i) GLCM Feature Extraction for channel 2 (j) GLCM Feature extraction for channel 3.

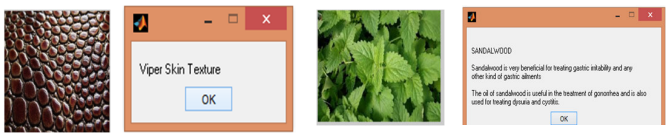

Fig (3) SVM

Cite this article as: A Shakin Banu, P Vasuki, A Glory Sujitha, S Amala Deepan. "Rotation Invariant Texture Classification using BRINT and GLCM with SVM Classifier". *International Conference on Innovative Trends in Electronics Communication and Applications (2015)*: 115-119. Print.

Performance Comparison

The performance of the proposed method is quantified by calculating various performance metrics like Classification Accuracy, Sensitivity, Specificity and PSNR Performance and is compared with existing KNN Algorithm. The performance metrics values are found to be greater compared to the existing method.

The Classification Accuracy A_i depends on the number of samples correctly classified and is evaluated by the formula

$$A_i = \frac{t}{n} * 100 \qquad (1)$$

where t- number of samples correctly classified, n- total number of samples.

The Sensitivity measures the proportion of positives that are correctly identified as such and is defined as

$$S_n = \frac{TP}{TP + FN} \qquad (2)$$

where TP-True Positive, FN-False Negative

The Specificity measures the proportion of negatives that are correctly identified as such and is defined as

$$S_p = \frac{TN}{TN + FP} \qquad (3)$$

where TN-True Negative, FP-False Positive

PERFORMANCE MEASURE	k-NN (%)	SVM (%)
ACCURACY	85	98.889
SENSITIVITY	75	98
SPECIFICITY	70	80.5
PSNR PERFORMANCE	80	85.5

Table 1.Performance Comparison Table

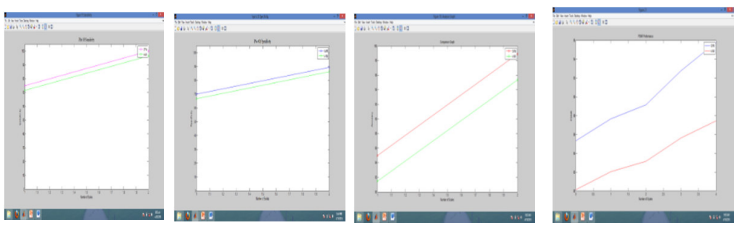

(a) (b) (c) (d)

Fig(4) Performance Comparision Graphs- (a) Plot of Sensitivity (b) Plot of Specificity (c) Plot of Accuracy (d) Plot of PSNR Performance.

Cite this article as: A Shakin Banu, P Vasuki, A Glory Sujitha, S Amala Deepan. "Rotation Invariant Texture Classification using BRINT and GLCM with SVM Classifier". *International Conference on Innovative Trends in Electronics Communication and Applications (2015)*: 115-119. Print.

CONCLUSION

The proposed BRINT descriptor together with GLCM is shown to exploit very good performance on texture databases under both normal conditions and noise conditions. The extracted features undergo SVM Classification. The Proposed method is compared with the existing KNN Algorithm. The performance of the proposed algorithm is quantified by calculating various performance metrics like Classification Accuracy, Sensitivity, Specificity and PSNR Performance. The Classification Accuracy, Sensitivity, Specificity and PSNR Performance are found to be 14%, 23%, 11%, 6% greater respectively compared with the existing KNN Algorithm.

REFERENCES

[1] X. Xie and M. Mirmehdi, "A galaxy of texture features," in *Handbook of Texture Analysis*, M. Mirmehdi, X. Xie, J. Suri, Eds. London, U.K.: Imperial College Press, 2008, pp. 375–406.

[2] T. Ojala, M. Pietikäinen, and T. Mäenpää, "Multiresolution gray-scale and rotation invariant texture classification with local binary patterns," *IEEE Trans. Pattern Anal. Mach. Intell.*, vol. 24, no. 7, pp. 971–987, Jul. 2002.

[3] L. Liu and P. Fieguth, "Texture classification from random features," *IEEE Trans. Pattern Anal. Mach.* Intell., vol. 34, no. 3, pp. 574–586,Mar. 2012.

[4] J. Zhang, M. Marszalek, S. Lazebnik, and C. Schmid, "Local features and kernels for classification of texture and object categories: A comprehensive study," *Int. J. Comput. Vis.*, vol. 73, no. 2, pp. 213–238, 2007.

[5] M.Varma and A. Zisserman, "A statistical approach to texture classification from single images," *Int. J. Comput. Vis.*, vol. 62, nos. 1–2,pp. 61–81, 2005.

[6] M. Varma and A. Zisserman, "A statistical approach to material classification using image patches," *IEEE Trans. Pattern Anal. Mach. Intell.*, vol. 31, no. 11, pp. 2032–2047, Nov. 2009.

[7] M. Crosier and L. D. Griffin, "Using basic image features for texture classification," *Int. J. Comput. Vis.*, vol. 88, no. 3, pp. 447–460, 2010.

[8] B. S. Manjunathi and W. Y. Ma, "Texture features for browsing and retrieval of image data," *IEEE Trans. Pattern Anal. Mach. Intell.*, vol. 18, no. 8, pp. 837–842, Aug. 1996.

[9] L. Liu, B. Yang, P. Fieguth, Z. Yang, and Y. Wei, "BRINT: A binary rotation invariant and noise tolerant texture descriptor," in *Proc. IEEEICIP*, Sep. 2013, pp. 255–259.

[10] S. Lazebnik, C. Schmid, and J. Ponce, "A sparse texture representation using local affine regions," *IEEE Trans. Pattern Anal. Mach. Intell.*,vol. 27, no. 8, pp. 1265–1278, Aug. 2005.

[11] T. Ojala, M. Pietikäinen, and D. Harwood, "A comparative study of texture measures with classification based on feature distributions".

Cite this article as: A Shakin Banu, P Vasuki, A Glory Sujitha, S Amala Deepan. "Rotation Invariant Texture Classification using BRINT and GLCM with SVM Classifier". *International Conference on Innovative Trends in Electronics Communication and Applications (2015)*: 115-119. Print.

International Conference on Innovative Trends in Electronics Communication and Applications 2015 [ICIECA 2015]

ISBN	978-81-929742-6-2	**VOL**	01
Website	icieca.in	**eMail**	icieca@asdf.res.in
Received	02 - April - 2015	**Accepted**	15 - November - 2015
Article ID	ICIECA017	**eAID**	ICIECA.2015.017

New System of Controlling Electric Car Using Concept of Accelerometer

Kavianand G[1], Nivas V M[2]
[1]UG Scholar, Department of Electronics and Communication Engineering,
Anna university affliated Panimalar Engineering College,Chennai, India
[2]UG Student, Department of Mechanical Engineering,
Anna university affliated Panimalar Engineering College, Chennai, India

Abstract: *This paper implements and develops a new method of controlling the electric car by employing accelerometer. Generally in the history of evolution of electric cars, there is a lot of changes take place in almost all aspects of the electric car and tremendous advances have been made in the field of electric vehicles. But the basic operation of steering and acceleration system remains the same. So in addition to these advancements, we introduced a new method of controlling electric vehicles, i.e. basic and traditional type of acceleration and steering control is changed. The accelerometer is in-built in the controller which is given to the driver for controlling the vehicle acceleration and steering. The accelerometer in the controller senses the calibrated input from the driver. The controller itself analyses the input and drives the motor and also controls the speed accordingly to it. It gives a feeling of driving a one manned plane. Since there is no need of using legs to drive these vehicle even a paraplegic persons can drive this kind of electric car easily. This new method of controller used in electric vehicles mainly concerned on ease of driving.*

Keywords: Electric car, Car Controller, Accelerometer, Latest design, Freescale Freedom Board FRDM-Kl25Z

INTRODUCTION

The first electric cars were produced in the 1880s. In early 20th century electric cars were prevalent, when electricity was preferred in automobile propulsion. Advancement in internal combustion technology, and growing petroleum infrastructure, usage of gasoline car increased, which led to the decline of electric propulsion vehicles. But the energy crisis of 1970s and 1980s brought a renewed interest in electric vehicles. Though there is a renewed interest in electric cars, nothing greatly changed in method of controlling the cars acceleration and steering. In this paper, we design and implement a new controller system which can eliminate the present model of accelerator and steering in electric car. Before entering into this model we have to know about the electric car.

The electric vehicle (EV) is propelled by an electric motor, powered by rechargeable battery packs, rather than a gasoline engine. All of their power is derived from the main electricity, supplied to an on board battery which drives an electric motor within the vehicles. The Electric Motor gets its power from a controller and the Controller is powered from an array of rechargeable batteries. The electric vehicle operates on an electric/current principle. It uses a battery pack (batteries) to provide power for the electric motor. The motor then uses the power (voltage) received from the batteries to rotate a transmission and the transmission turns the wheels.

Electric vehicles can able to increase the amount of available power by using a direct motor-to-wheel configuration. Wheels can be used for both propulsion and as braking systems, by connecting multiple motors directly to the wheels and thereby increasing traction. Electric cars are significantly quieter than conventional internal combustion engine propelled automobiles and are typically easy to drive, and perform well. They also do not emit pollutant gases such as greenhouse gas, and giving a large reduction to local air pollution and greenhouse gas.

Cite this article as: Kavianand G, Nivas V M. "New System of Controlling Electric Car Using Concept of Accelerometer". *International Conference on Innovative Trends in Electronics Communication and Applications (2015)*: 120-126. Print.

SYSTEM OVERVIEW

In the proposed system, we suggest to utilize the Freescale freedom board FRDM-KL25Z for accessing the overall four wheeled vehicle control such as Accelerator and Steering. So the new car can be steered with a FRDM-KL25Z kit. Freescale freedom board FRDM-KL25Z is the major electronic unit used in this new method of accelerator and steering control. By using accelerometer MMA8451Q present in an electronic unit we can controls the direction and speed of the battery car. This accelerometer MMA8451Q is capable of detecting changes in orientation, angle of tilt with respect to gravity. With the help of these orientation and tilting angle

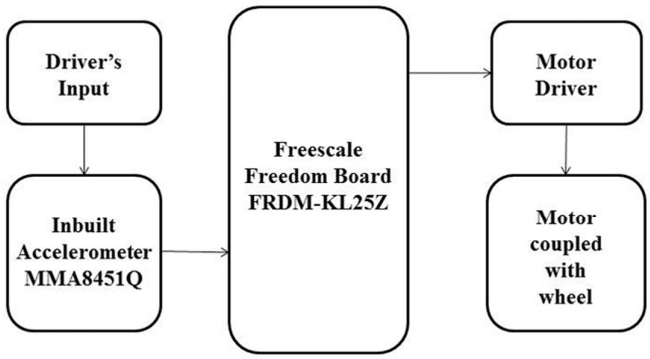

Fig.1 Block Diagram of the System

measurements, we can programme an electronic controller unit, which controls the speed and direction of the car. This method of controlling the electric car will be one of the coolest features of the technology world.

SYSTEM ARCHITECTURE

The construction of this system consists of two parts namely hardware development and software development. Hardware development involved the designing the circuit of the project while the software developments is focused on designing coding to be embedded in the hardware.

Hardware Developement

The new system of controlling electric car includes some of Hardware components. The main hardware components used in the car controller system are Freescale freedom board FRDM-KL25Z which has in-built acceleration sensor MMA8451Q.

Accelerometer MMA8451Q:

The in-built acceleration sensor or accelerometer MMA8451Q is capable of detecting changes in orientation, angle of tilt with respect to gravity. The MMA8451Q is a smart, low-power, three-axis, capacitive, micro machined accelerometer with 14 bits of resolution. This accelerometer is packed with embedded functions with flexible user programmable options, configurable to two interrupt pins. Embedded interrupt functions allow for overall power savings relieving the host processor from continuously polling data. There is access to both low-pass filtered data as well as high-pass filtered data, which minimizes the data analysis required for jolt detection and faster transitions. The device can be configured to generate inertial wakeup interrupt signals from any combination of the configurable embedded functions allowing the MMA8451Q to monitor events and remain in a low-power mode during periods of inactivity. The MMA8451Q is available in a 3 mm x 3 mm x 1 mm QFN package. But we have an in-built accelerometer in the Freescale freedom board itself.

Cite this article as: Kavianand G, Nivas V M. "New System of Controlling Electric Car Using Concept of Accelerometer". *International Conference on Innovative Trends in Electronics Communication and Applications (2015)*: 120-126. Print.

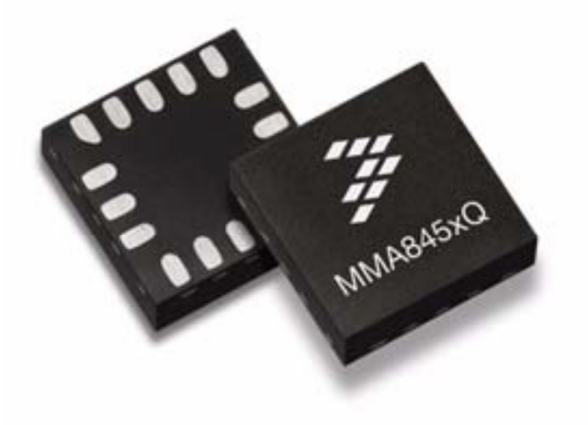

Fig.2 Accelerometer MMA8451Q

Freescale freedom board FRDM-KL25Z:

The main hardware component used is Freescale Freedom board FRDM-KL25Z. Simply saying Freescale Freedom board FRDM-KL25Z itself is the electronic controller unit. The Freescale Freedom KL25Z hardware, FRDM-KL25Z, is a capable and cost-effective design featuring a Kinetis L series microcontroller, the industry's first microcontroller built on the ARM® Cortex™-M0+ core. A Freescale MMA8451Q low-power, three-axis accelerometer is interfaced through an I2C bus and two GPIO signals. It features a KL25Z128VLK, a device boasting a max operating frequency of 48MHz, 128KB of flash, a full-speed USB controller, and loads of analog and digital peripherals.

Fig.3 Freescale Freedom Board FRDM-KL25Z

The FRDM-KL25Z hardware is form-factor compatible with the Arduino™ R3 pin layout, providing a broad range of expansion board options. The on-board interfaces include an RGB LED, a 3-axis digital accelerometer, and a capacitive touch slider. The I/O headers on the FRDM-KL25Z are arranged to allow compatibility with peripheral boards (known as shields) that connect to Arduino™ and Arduino-compatible microcontroller boards.

Software Development

Software development is to develop embedded software required to control hardware development. It is the process of coding computer program which is needed to operate hardware development. The Freescale Freedom board FRDM-KL25Z uses embed c codes. These codes are compiled using online embed c compiler. The code is as follows,

Cite this article as: Kavianand G, Nivas V M. "New System of Controlling Electric Car Using Concept of Accelerometer". *International Conference on Innovative Trends in Electronics Communication and Applications (2015)*: 120-126. Print.

```
#include "mbed.h"
#include "MMA8451Q.h"
PinName const SDA = PTE25;
PinName const SCL = PTE24;
PwmOut m1(PTA4);
PwmOut m2(PTA12);
PwmOut m3(PTC8);
PwmOut m4(PTC9);
#define MMA8451_I2C_ADDRESS (0x1d<<1)
void fwd(float i)
{
        m1=i;
        m2=0;
        m3=i;
        m4=0;
}
void rev(float i)
{
        m1=0;
        m2=i;
        m3=0;
        m4=i;
}
void lft(float i)
{
        m1=i;
        m2=0;
        m3=0;
        m4=i;
}
void rgt(float i)
{
```

Cite this article as: Kavianand G, Nivas V M. "New System of Controlling Electric Car Using Concept of Accelerometer". *International Conference on Innovative Trends in Electronics Communication and Applications (2015)*: 120-126. Print.

```
        m1=0;
        m2=i;
        m3=i;
        m4=0;
}
void stp()
{
        m1=0;
        m2=0;
        m3=0;
        m4=0;
}

int main(void)
{
   MMA8451Q acc(SDA, SCL, MMA8451_I2C_ADDRESS);
   printf("MMA8451 ID: %d\n", acc.getWhoAmI());
   while (true) {
      float x, y, z;
      x = acc.getAccX();
      y = acc.getAccY();
      z = acc.getAccZ();
       wait(0.1f);
      printf("X: %1.2f, Y: %1.2f, Z: %1.2f\n\r", x, y, z);

      if(y>0.3f)
      { rgt(y);}
      else if (y<-0.3f)
      { lft(abs(y));}
      else if (x<-0.3f)
      { fwd(abs(x));}
      else if (x>0.3f)
```

Cite this article as: Kavianand G, Nivas V M. "New System of Controlling Electric Car Using Concept of Accelerometer". *International Conference on Innovative Trends in Electronics Communication and Applications (2015)*: 120-126. Print.

```
    { rev(x);}
    else
    {stp();}

  }
}
```

WORKING

This system of controlling electric cars was mainly based on the principle of measuring the tilting angle and direction. The Freescale Freedom board FRDM-KL25Z senses the tilting angle and its direction by using inbuilt accelerator MMA8451Q. Thus by sensing this tilting angle and direction, it moves the electric car in forward, backward, left and right side almost in all direction with desired speed, based on the input given.

TABLE I
CAR CONTROLLER METHOD BY CONTROLLER TILT DIRECTION

Direction of tilt of controller	Movement of car
Forward	Front
Left	Left
Right	Right
Backward	Reverse

If you tilt the Electronic Controller Unit in forward direction slowly, the car tends to move in forward direction slowly. If you tilt the Electronic Controller Unit in same forward direction suddenly, the car also moves faster. Similarly we can move the electric car in almost all the direction with varying speed with ease. Thus the direction of tilting decides the direction of the car to move and the measure of angle of tilting decides the speed of the car. Since there is no clutch system in the electric car, there is no hindrance for controlling and varying the speed suddenly to our wish.

TABLE II
MOVEMENT OF THE CAR WITH TILTING ANGLE

ANGLE OF TILT	25°	30°	60°	70°	45°
MOTION	Easy Forward	Easy Backward	Maximum Forward	Maximum Backward	Left and Right

RESULTS

In this proposed system, the Freescale freedom board FRDM-KL25Z senses the tilting angle and its direction by using inbuilt accelerator MMA8451Q. Thus by sensing this tilting angle and direction, it moves the electric car in forward, backward, left and right side almost in all direction with desired speed, based on the input given.

If you tilt the controller forward, the electric vehicle moves forward. The angle and speed of tilting determines the speed of the vehicle. Similarly we can drive electric car in all direction and can control the speed of the car using electronic controller unit with ease.

CONCLUSION AND DISCUSSION

Thus we finally designed a four wheeled vehicle with a new controller unit which eliminates the old design of acceleration and steering method of controlling. This system gives the new experience of riding a vehicle such as virtual driving. By implementing this new system of controlling using electronic controller unit can increase the usage of electric cars. We can expand this project to heavy

Cite this article as: Kavianand G, Nivas V M. "New System of Controlling Electric Car Using Concept of Accelerometer". *International Conference on Innovative Trends in Electronics Communication and Applications (2015)*: 120-126. Print.

vehicles in near future. Since there is no need of using legs to drive these kinds of vehicle, even a paraplegic person can drive this kind of electric car easily. This new method of controller used in electric vehicles mainly concerned on ease of driving.

REFERENCES

[1] https://en.wikipedia.org/wiki/Electric_car

[2] Kunal Shrivastava. " electric car "10th Indo-German Winter Academy (2011)

[3] www.freescale.com/FRDM-KL25Z

[4] http://www.farnell.com/datasheets/1884196.pdf

[5] http://www.freescale.com/doc/MMA8451Q

Cite this article as: Kavianand G, Nivas V M. "New System of Controlling Electric Car Using Concept of Accelerometer". *International Conference on Innovative Trends in Electronics Communication and Applications (2015)*: 120-126. Print.

International Conference on Innovative Trends in Electronics Communication and Applications 2015 [ICIECA 2015]

ISBN	978-81-929742-6-2	**VOL**	01
Website	icieca.in	**eMail**	icieca@asdf.res.in
Received	02 - April - 2015	**Accepted**	15 - November - 2015
Article ID	ICIECA018	**eAID**	ICIECA.2015.018

Underwater e-Fish Autonomous Robot

Santosh E[1], Saran S[1], Vinith Kannan A[1], Vishal L[1]
[1]RMK Engineering College
Tamil Nadu
India

Abstract: *Exploration and simulation interfaced with automation is the need of the day in the sphere of intra-vehicular communication. Built on the conception and perception pertaining to internet of things, cloud computing and acoustic sensor networks, our perspective deals with the development of 'Underwater e-fish autonomous robot' with embedded background and interlink it to the simulation process. The significant feature of this vehicle is its self-charging power generation method. The main problem concerned with existing underwater robots and vehicles is the power required to drive the vehicle. To overcome this, we suggest the use of piezo-electric transducers and a thick rubber film cohesively connected by means of a valve and tube. The principle of difference in pressure levels in oceans and seas can be made use of in this technique. On automatic operation, the proposed servo mechanism offers strong electromechanical coupling and large dynamic stresses in bending actuation as well as actuation capability over a range of frequencies for adaptive swimming. The vehicle can be developed for multi-purpose designations based on the application domain under the notion of acoustic sensor networks.*

Keywords*:* e-Fish, Piezo-electric, Robot.

INTRODUCTION

The structure of the 'Underwater e-fish autonomous robot' can be described as an autonomous soft-bodied robot that is both self-contained and capable of rapid, continual body motion. The detailed design, modelling, fabrication, and control of the soft fish focus on enabling the robot to perform rapid escape responses. The robot employs a compliant body with embedded actuators emulating the slender anatomical form of a fish. In addition, the robot has a novel fluidic actuation system that drives body motion and has all the subsystems of a traditional robot on board: power, actuation, processing, and control. At the core of the fish's soft body is an array of fluidic elastomeric actuators. The fish is designed to emulate escape responses in addition to forward swimming because such maneuvers require rapid body accelerations and continuum-body motion. These maneuvers showcase the performance capabilities of this self-contained robot. The kinematics and controllability of the robot during simulated escape response maneuvers are analysed and compared with studies on biological fish. During escape responses, the soft-bodied robot has similar input–output relationships to those observed in biological fish. The major implication of this work is that robots can be both self-contained and capable of rapid body motion. This type of design offers strong electromechanical coupling and large dynamic stresses in bending actuation as well as actuation capability over a range of frequencies for adaptive swimming.

Servo mechanism

The movement of vehicle corresponds to hydraulic technology. By circulation of water through internal body channels with the Futaba servo being attached to the fins, dynamic movement and diving capabilities can be introduced. These innovations enable prolonged fish-like locomotion in three dimensions. The servomotors are controlled by a personal computer with a R/C transmitter and a D/A converter. A control program on the personal computer realizes various motion pattern. This green power, eco-friendly technique can be used to fuel the vehicle in any desired deep sea exploration similar to that of a fish movement and hence, the name e-fish

Cite this article as: Santosh E, Saran S, Vinith Kannan A, Vishal L. "Underwater e-Fish Autonomous Robot". *International Conference on Innovative Trends in Electronics Communication and Applications (2015)*: 127-130. Print.

autonomous vehicle.

Figure 1. Servo mechanism

The autonomous e-fish initially swims straight, and gets kinetic energy. Next, the tail turns to one side, and keeps the posture to the side. This turns by hydrodynamics force. Though real fish turn skillfully using not only tail fin but also pectoral fins or ventral fins, we sketched a structure of the prototype, which turns with only swing of tail fin. As the tail fin is utilized both propulsion and turning, the underwater.

Charging technique

On a statistical analysis, the robots under water last for around six to eight hours and the manual operation of the bots add on to the issues relating to underwater automation. To go by, the significant feature of the 'Underwater e-fish autonomous robot' is its self-charging power generation method.

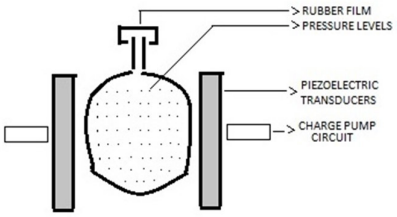

Figure 2. Piezo charging technique - cross sectional view

In this technique, we suggest the use of piezo-electric transducers and a thick rubber film cohesively connected by means of a valve and tube. The principle of difference in pressure levels in oceans and seas can be made use of in this technique. As the pressure changes continuously, the contraction and expansion of rubber film due to difference in pressure makes the related interactions between the piezo-electric transducers. As a result of the intermediate vibrations produced, these could be tapped and used in the circuit consisting of transistors, charge pump storage circuit using CD4093, Schmitt trigger ICs, Schottky diodes, Simple link Wi-Fi interfaced with Tiva TM4C123GH6PM microcontroller. With the knowledge of interfacing of microcontroller with LCD, ADC, control of transistors (as switch), a simple charge pump storage circuit using CD4093 Schmitt trigger IC for interlocking the P-Mosfets switches and programming the Tiva TM4C123GH6PM microcontroller for monitoring and control can be designed.

SENSOR DATA ACQUISITION

To realize underwater applications, many design principles and tools from ongoing, ground-based sensor net research can be made use of. Considering some of the challenges which are fundamentally different, the sensor data acquisition in underwater networks can be established First, radio is not suitable for underwater usage because of extremely limited propagation. While acoustic telemetry is a promising form of underwater communication, off-the-shelf acoustic modems are not suitable for underwater sensor-nets with hundreds of nodes: their power draws, ranges, and price points are all designed for sparse, long-range, expensive systems rather than small, dense, and cheap sensor-nets. Second, the shift from RF to acoustics changes the physics of communication from the speed of light to the speed of sound which offers a difference of order of five in magnitude. While propagation delay is negligible for short-range RF, it is a central fact of underwater wireless. This has profound implications on localization and time synchronization. Finally, energy conservation of underwater sensor-nets will be different than on-ground because the sensors will be larger, and because some important applications require large amounts of data. We are therefore investigating three areas: hardware, acoustic communication with sensor nodes, protocols, underwater network self-configuration, MAC protocol design, time synchronization, and localization and mostly off operation, energy-aware data caching and forwarding.

The Acoustic model refers to the communication with the sound waves. In underwater environment, communicating medium can be either radio, optical or sound (acoustic) waves. But the non-acoustic waves are electromagnetic waves which suffer from high propagation losses as well as scattering problems. These non-acoustic waves do not travel long distances in underwater environment. Radio waves require high transmission power as well as long antennas to communicate and Optical waves suffer from high signal attenuation so it can travel short ranges only. Hence sound is the best communicating medium for underwater networks. Till now and in near future also, the acoustic waves can be seen as the best communication medium for wireless networks.

Cite this article as: Santosh E, Saran S, Vinith Kannan A, Vishal L. "Underwater e-Fish Autonomous Robot". *International Conference on Innovative Trends in Electronics Communication and Applications (2015)*: 127-130. Print.

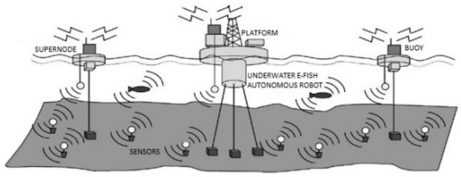

Figure 3. Underwater acoustic sensor network

In the solution put forth in sensor data acquisition, the sensor nodes are present beneath the water level as well as floating on the surface of the water. Under water, nodes are communicating via the acoustic communication and above the surface of water, the nodes are communicating via the radio signals. There can be a master data collector center or an analysis center which can collect the information from these nodes for various purposes. Our perspective is to observe four different types of nodes in the system. At the lowest layer, the large number of sensor nodes is deployed on the sea bed. They collect data through attached sensors and communicate with other nodes through short-range acoustic modems. Several deployment strategies of these nodes are possible; here they are anchored to the sea bed. Tethers ensure that nodes are positioned roughly where expected and allow optimization of placement for good sensor and communications coverage. Node movement is still possible due to anchor drift or disturbance from external effects. Nodes will be able to determine their locations through distributed localization algorithms. At the top layer are one or more control nodes with connections to the Internet. These control nodes may be positioned on an off-shore platform with power, or they may be on-shore; we expect these nodes to have a large storage capacity to buffer data, and access to ample electrical power. Control nodes will communicate with sensor nodes directly, by connecting to an underwater acoustic modem with wires. In large networks, a third type of nodes, called super-nodes, can be deployed. Super-nodes have access to high speed networks, and can relay data to the base station very efficiently. We are considering two possible implementations: the first involves attaching regular nodes to tethered buoys that are equipped with high-speed radio communications to the base station. An alternative implementation would place these nodes on the sea bed and connect them to the base station with fiber optic cables. Super-nodes allow a much richer network connectivity, creating multiple data collection points for the underwater acoustic network.

APPLICATIONS

The vehicle can be developed for multi-purpose designations based on the application domain it is used with. It is built mainly from the Intel, Texas Instruments microcontrollers and ARM products. The most innovative aspect of this vehicle is sought by deploying it to detect the black boxes during airplane crashes. The issue pertaining to the detection of black box or underwater beacon locator is the power supply required to fuel the robotic vehicle for long hours under water and the range it is attributed to. Since, this underwater e-fish autonomous vehicle is driven by a self-charging pump circuit, it can obviously be used for this purpose. The Sentinel XF SONAR is used in this vehicle for detecting the black box and its functionality is empowered with the SONAR acoustic nodes deployed over the surface of water and this acoustic ranging is controlled by means of protocols defined by TDMA and CDMA. The same acoustic ranging node method can be used to resolve the Indian fishermen issue by deploying the autonomous vehicle in the border waters of India and Sri Lanka with alert system application developed for it. Another component is the LMP91050, a programmable integrated sensor used for gas detection in the event of leakages from ships and the radioactive emissions from nuclear plants. Also, the water resistant sick sensors can be used for this purpose. Moreover, for high-resolution sensing of targets like submarines, the LDC1000 inductive sensor along with the SONAR technique is incorporated in this vehicle. The fabricated TMP75B temperature sensor, salinity sensor and the PGA400-Q1 pressure sensor are also embedded to study the nature of underwater flora and fauna. Since the application of GSM modules under water are not well served for many purposes, an acoustic sensor network can be established to monitor the performance of underwater e-fish autonomous vehicle. Once underwater equipment are connected with acoustic sensor networks, it becomes an easy task to remotely control and operate some equipment. The primary differences between modulation techniques lies in the complexity of the receiver, the bandwidth required, and the minimum acceptable received signal-to-noise ratio (SNR). In the acoustic sensor network, all these features are well defined and inter-linked for underwater purposes.

EXPERIMENTAL RESULTS

As a part of the sample working model, a mini autonomous vehicle of length 1.3 meter, weighing approximately 2.6 kg, driven by Futaba S148 with power supply of around 15-20 V can be set up with a cost effective budget of INR 8000. This model can be put into operation with some of the mentioned features integrated into it and introduced underwater along the Indian-Sri Lankan borders to test the working of the same. From the perception of a developer of the 'Underwater e-fish autonomous robot', a prototype to illustrate the practical implementation can be experimentally ascertained. As an paradigm, our team has developed a underwater robot connected by means of Intel Edison with a hybrid application to control the movement so as to observe the various special cases in a real time environment. In the hybrid development spheres, the Ionic framework is used with the capability of linking it to IOT based cloud services.

Cite this article as: Santosh E, Saran S, Vinith Kannan A, Vishal L. "Underwater e-Fish Autonomous Robot". *International Conference on Innovative Trends in Electronics Communication and Applications (2015)*: 127-130. Print.

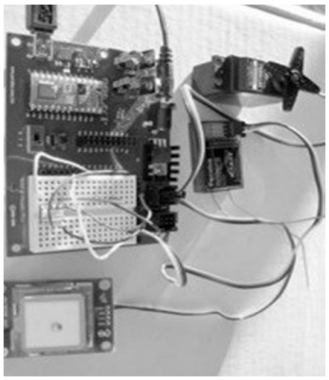

Figure 4.a. Experimental setup

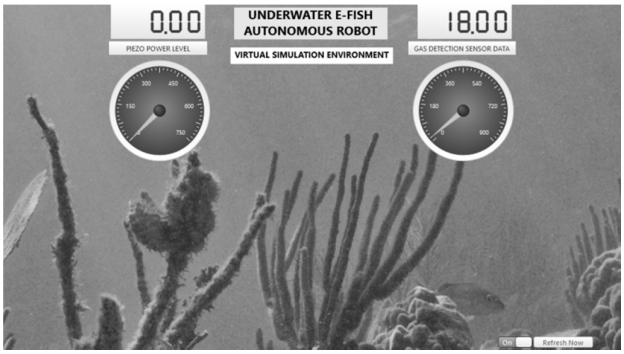

Figure 4.b. ThingWorx virtual simulation environment

On a better and dependable means of using cloud based IOT services, ThingWorx cloud platform is greatly made use of to facilitate the sensor data acquisition. The ThingWorx Composer 5 is utilized taking into account of the quick streaming of driving data in this platform. To bind the values of sensor from nodes, the corresponding application key of the server used in the Arduino IDE code and is then compiled, uploaded into the Intel Edison. In the Figure 4.b, the virtual simulation environment is shown along with the sensor data display widgets. For the data visualization, the wide range of widgets in the composer are used to display the data in mash-up along with e-mail alerts for specific purpose that are used to serve the warning notes by analogously comparing the data obtained through sensors deployed at the particular nodes.

REFERENCES

[1] Benthos, Inc. Fast and Reliable Access to Undersea Data, http: //www.benthos.com/pdf/Modems/ModemBrochure.pdf.

[2] D. Torres, J. Friedman, T. Schmid, and M. B. Srivastava, "Software-defined underwater acoustic networking platform," in Proceedings of the Fourth ACM International Workshop on UnderWater Networks (WUWNet '09), Berkeley, California, USA, November 3 2009, pp. 7:1–7:8.

[3] L. Freitag, M. Grund, S. Singh, J. Partan, P. Koski, and K. Ball, "The WHOI Micro-Modem: An acoustic communications and navigation system for multiple platforms," http://www.whoi.edu/micromodem/, 2005.

[4] F. Guerra, P. Casari, and M. Zorzi, "World ocean simulation system (WOSS): a simulation tool for underwater networks with realistic propagation modeling," in Proceedings of the Fourth ACM International Workshop on UnderWater Networks, ser. WUWNet '09, Berkeley, California, USA, 3 November 2009, pp. 1–8.

[5] R. Masiero, S. Azad, F. Favaro, M. Petrani, G. Toso, F. Guerra, P. Casari, and M. Zorzi, "DESERT underwater: an NSmiraclebased framework to DEsign, simulate, emulate and realize testbeds for underwater network protocols," in Proceedings of IEEE OCEANS 2012, Yeosu, Korea, May, 21–24 2012.

[6] R. Urick, Principles of Underwater Sound. McGraw-Hill, 1983.

Cite this article as: Santosh E, Saran S, Vinith Kannan A, Vishal L. "Underwater e-Fish Autonomous Robot". *International Conference on Innovative Trends in Electronics Communication and Applications (2015)*: 127-130. Print.

International Conference on Innovative Trends in Electronics Communication and Applications 2015 [ICIECA 2015]

ISBN	978-81-929742-6-2	**VOL**	01
Website	icieca.in	**eMail**	icieca@asdf.res.in
Received	02 - April - 2015	**Accepted**	15 - November - 2015
Article ID	ICIECA019	**eAID**	ICIECA.2015.019

Virtualization and Resource Sharing in Optical Clouds using IP-over-WDM Networks with Quality of Service Requirements

Ramasamy Mariappan[1]
[1]Department of Electronics & Communication Engineering
Sri Venkateswara College of Engineering
Tirupati, Andhra Pradesh, India.

Abstract: *Virtualization is an essential concept which plays a major role in Cloud computing for resource sharing on the global internet. This paper proposes the optical cloud virtualization platform (OCVP), as the mediation layer which provides Network as a service (NaaS) to cloud computing by exploiting the functionality provided by optical control plane (CP) enabled IP-over-WDM networks. The optical CVP adopts a different approach that may be called undirected signalling to the optical CP. In fact, an application requests end-to-end network services in terms of end user addresses and perceived QoS parameters such as throughput, transfer delay, blocking probability and the average load share, to the service elements controlling the edge node of the transport network serving its access networks without any knowledge of the transport network infrastructure. The simulation of optical CP on optical CVP shows that the performance of optical cloud is good in terms of end-to-end delay and related QoS parameters.*

Keywords: WDM Optical, Virtualization, Resource sharing.

INTRODUCTION

Cloud computing is a novel paradigm to share resources over the Internet. It is based on the concept of resource virtualization, which enables a transparent access to information and Communication Technology (ICT) services such that the users do not need to know the location and characteristics of the relevant resources. Grid and Cloud Computing [1] models pursue the same objective of constructing large-scale distributed infrastructures, although focusing on complementary aspects. While grid focuses on federating resources and fostering collaboration, cloud focuses on flexibility and on-demand provisioning of virtualized resources. Virtualization provides the ability to run legacy applications on older operating systems, and faster job migration within different virtual machines running on the same hardware. From the security point of view, since virtual machines run isolated in their sandboxes, this provides an additional protection against malicious or faulty codes. Clouds provide access to inexpensive hardware and storage resources through very simple APIs, and are based on a pay-per-use model, so that renting these resources is usually much cheaper than acquiring dedicated new ones. Moreover, people are becoming comfortable with storing their data remotely in a cloud environment. Therefore, scientists are increasingly using clouds, small and medium sized enterprises, and casual users [2], [3].

The rest of this paper is organized as follows. Section II reviews the literature available and section III describes the problem statement with emphasis on QoS requirements. Section IV describes the layered architecture of the proposed system, its approach, design methodology. Section V discusses the implementation and analysis of results obtained. Section VI summarizes our contributions and discusses our future plans.

Cite this article as: Ramasamy Mariappan. "Virtualization and Resource Sharing in Optical Clouds using IP-over-WDM Networks with Quality of Service Requirements". *International Conference on Innovative Trends in Electronics Communication and Applications (2015)*: 131-137. Print.

Related work

Cloud computing [1] is a model generally defined as the clusters of scalable and virtualized resources like distributed computers, storage, system software, etc which makes use of internet to provide on-demand services to the user. The National Institute of Standards and Technology (NIST) has described as, " Cloud computing is a model for enabling convenient, on demand network access to a shared pool of configurable computing resources that can be rapidly provisioned and released with minimal management effort or service provider interaction. This cloud model promotes availability and is composed of five essential characteristics: on demand self service, broad network access, resource pooling, rapid elasticity and measured service."

In cloud computing model, user requires the internet-enabled devices like desktop, smart phone, etc to access the cloud computing services. The service provider is required to maintain various computers, servers, data storage system and high-speed network, etc to provide the computing service. The essential characteristics of clouds are: flexibility, virtualization, scalability, pay-per-use model, and SLAs [1]. The flexibility refers to the easy access to, and the deployment and configuration of the resources used. Scalability is also one of the main drivers for cloud a deployment, exploiting a pay-as-you-grow approach, which leads to cost-effective deployment as well as success of cloud computing .Virtualization, allow the cloud service providers to operate cost-effectively, avoiding over provisioning. This virtualization is a key difference that clouds bring to the table, compared to grids. Virtualization allows them to share resources in a secure manner, facilitating to respect the performance SLAs agreed with their users. Virtualization furthermore enables migration to other servers, both for performance and resilience against failures. Virtualization is the concept exists in WDM optical networks [2] for provisioning and sharing of resources in a logical way as well as for topology reconfiguration. Also, monitoring in clouds is quite challenging, whereas grids [3] apply a different trust model where users, via identity delegation, can access and browse resources at various sites that contain resources. In grids, these resources are typically not that much neither abstracted nor virtualized. The essential characteristics of cloud are described below.

On demand self-service - A customer can access or use the cloud computing services as and when needed without any help or interaction with the cloud services provider. Easy to use intuitive interface enables him to select services as per requirement. The web-based email is an example.

Virtualization- It is an important characteristic of the cloud. User accesses the computing services without being aware about the complexity of the infrastructure. Virtual resources are assigned to the services and need not to be bound to one physical resource. Moving virtual resources from one physical to another does not affect the user.

Access from anywhere - Cloud computing is a network based service. This makes accessibility to the cloud services location independent. The only prerequisite is the use of standard internet enabled devices like low cost desktop computers, mobile handsets etc at client side with high speed network.

Resource pooling- The availability of uninterrupted quality services at customer site requires good planning and resource management by the service provider. In cloud computing, resources are pooled to accomplish the demand of all the consumers using a multi- tenant model, with different physical and virtual resources dynamically assigned and reassigned according to consumer demand. Consumers use the resources like storage, processing, memory, network bandwidth, and virtual machines as per their need.

Rapid elasticity- A consumer can purchase computing power and other available services as per need without worrying about investing in additional resources at site. The service provider on the other hand can monitor the usage of its resources in a dynamically changing scenario. Additional resources can be added or arranged in case of increase in demand and similarity, scaled down or leased to third party when not in use.

Measures services- the usage of cloud computing services is measurable. Based on usage, cloud services are controlled and metered per client on daily, weekly, monthly and annual basis. The service provider uses this measurement for billing, resource optimization, capacity planning and other task. In terms of architectures, the many attempts ([4,5,6]) to classify various cloud paradigms seem to converge to a layered architecture with "everything as a service" (XaaS) taxonomy, comprising the following layers.

Software as a Service (SaaS): This layer provides on demand use of application software running on cloud infrastructure. It comprises all applications that run on the cloud and provide a direct service to the cloud user. This layer can be further subdivided according to the application level offered. On top, we have the actual *Applications* which are basically the final service offered to an end user. Clearly, they can be composed of. a service-oriented approach of lower level services [4] and *Composite Application Services*.

Platform as a Service (PaaS): Computational resources via a platform upon which applications and service can be developed and hosted. Some of the std platforms are OS, database, queuing services and middleware services etc. The PaaS layer can be further decomposed into *Programming Environments* and *Execution Environments*. The former provides programming-language-level environment, whereas the latter offers the run-time execution environment that can take care of automatic scaling and load balancing.

Cite this article as: Ramasamy Mariappan. "Virtualization and Resource Sharing in Optical Clouds using IP-over-WDM Networks with Quality of Service Requirements". *International Conference on Innovative Trends in Electronics Communication and Applications (2015)*: 131-137. Print.

Infrastructure as a Service (IaaS): This lowest level provides the underlying resources, i.e. storage, computing and networking, which PaaS / SaaS rely on. Here, the consumer shares the cloud infrastructure on demand basis but does not manage or controls it, making it appears like a virtual machine to deploy and run arbitrary software. The user has limited control over OS, storage and deployed applications. The "resources" can refer to physical resources, but these often are virtualized. Hence we distinguish both virtual and physical resources. These resources can be further abstracted into what [4] calls "basic infrastructure services" providing higher level functionality than that offered by a typical OS. Offering database functionality is an example of "higher infrastructure services".

The Hardware as a Service (HaaS) [5], refers to providers that offer server infrastructure and take care of operation, management and upgrades of the hardware. On top of SaaS, [4] also introduces an extra human-as-a-service (HuaaS) layer, which rely on interaction and actual data processing by multiple collaborating people. Also, from an architectural perspective, the intermediate layers especially PaaS as well as basic application services in SaaS) can be seen as "cloud middleware", which [6] categorizes in *User Level* and *Core Middleware*. The standard grid technology seems to be situated on this "middleware" layer, which one could position on the PaaS level. The evolution to web-service based access to grids [7] could be seen as more SaaS-like grid offerings. Thus, from a conceptual point of view, it seems that grids are converging to the same layered architecture. While clouds can be seen as an evolution of grids towards high performance computing.

Youssef et al. [5] coin the term "Communication as a Service (CaaS)", as one of the three types of infrastructure, offering dynamic provisioning of virtual overlays for traffic isolation or dedicated bandwidth with QoS guarantees etc. They mainly refer to interfaces for the creation of on-demand communication services or channels. Lower layer virtualization is not addressed there. *Optical Network virtualization* [8, 9] has seen numerous studies and implementations in the form of virtual topology reconfiguration, Virtual Private Networks (VPNs), which connect a number of known end-points over a dedicated communications infrastructure. VPNs create isolated logical networks on a common physical substrate, recent work introduces virtualization in most if not all network elements, such as the switching fabric, the routing and forwarding engine, and the control plane .

IT resources are made up of multiple components such as a central processing unit, storage devices and working memory. *Virtualization of computer systems* [10] results in a virtual machine (VM) that offers all the capabilities of the host resource. These VMs can be instantiated and configured on-demand and introduce a relatively limited overhead. Furthermore, partitioning and aggregating of, for instance, storage resources, leads to the desirable properties of granularity and scalability, respectively.

Only recently, *combined virtualization* of both networking and IT resources has gained widespread attention, mainly due to the popularity of the grid and cloud computing concepts. The idea is to introduce a Logical Infrastructure Composition Layer (LICL) that manages the physical infrastructure consisting of both network and IT resources, and exposes these as virtual resources in a generic way. These, in turn, are combined to form virtual infrastructures that operate independently from each other, and each deploys its own control plane solution as desired. Additional features include dynamic up/down-grading of these infrastructures, as well as guaranteed end-to-end service delivery over diverse resources and complex different technologies.

In parallel, several higher-level cloud management toolkits have been proposed to handle aspects of IT resource virtualization combined with advanced job scheduling, monitoring, storage and user management. The examples of the latter are OpenNebula or Eucalyptus besides several others [11, 12, 13]. These software solutions allow transforming a network of cluster nodes to cooperate in managed cloud network. In general, virtualization can offer a number of *qualitative advantages* over more traditional models, including stricter isolation between users, more flexible enforcement of security policies and higher levels of trust [14]. However, one should not assume these advantages to be implied by virtualization, as careful design remains essential to successfully operate these services. In particular, the study in [15] demonstrates the trade-off inherent to WDM optical network virtualization, and specifically the effect of isolating virtual networks on network dimensions and the control plane scalability. Revisiting the cloud and grid requirements, virtualization mainly caters for *elasticity* and *scalability*, and addresses diversity of applications in terms of *granularity* of their resource needs. The flexibility of on-demand resource provisioning of virtualized resources, due to the less stringent dependence on the availability of a particular physical resource, also enables extra *resilience* opportunities.. To enable on-demand, end-to-end network services across multiple, independent, high-performance transport domains, one solution is based on the Generalized Multi-Protocol Label Switching (GMPLS) protocol suite, which is frequently deployed to bridge the gap between optical transport technology and the IP layer.

OPTICAL CLOUD AND VIRTUALIZATION

This paper proposes the optical cloud virtualization platform (OCVP), which provides Network as a service (NaaS) to cloud computing by exploiting the functionality provided by control plane (CP) enabled networks. The OCVP adopts a different approach that may be called undirected signaling to the CP. In fact, an application requests end-to-end network services in terms of end user addresses and perceived QoS parameters to the service elements controlling the edge node of the transport network serving its access networks without any knowledge of the transport network infrastructure.

Cite this article as: Ramasamy Mariappan. "Virtualization and Resource Sharing in Optical Clouds using IP-over-WDM Networks with Quality of Service Requirements". *International Conference on Innovative Trends in Electronics Communication and Applications (2015)*: 131-137. Print.

A distributed set of service elements collaborates for collecting and correlating network status information about both the transport and the access networks. The collected information is used to map the applications connectivity requests into a set of CP directives. NaaS is composed and orchestrated to provide connectivity on demand to cloud users or to enhance existing cloud services.

Cloud users			
Physical & Virtual network	**Infrastructure service, physical & virtual resources**	**Programming & Execution environments**	**Basic & Composite application services**
NaaS	**IaaS**	**PaaS**	**SaaS**
Virtual Infrastructure Composition Layer (VICL)			
ONVP	**OCVP**	**OSVP**	
Optical Network Control plane (ONCP)			
Network Resources	**Computing Resources**	**Storage Resources**	

Figure 1 Optical Cloud User Interaction with Virtualization platform

The virtualization for cloud computing is done for various Resources such as Network resources, Computing resources and Storage resources. The resources are shared through optical Cloud Virtualization platform (OCVP), Network Virtualization Platform (ONVP) and Storage Virtualization Platform (SVP). The network connectivity to various virtualization platforms are done through IP based logical connection i.e. virtual connection. In turn, the virtualization platforms provide NaaS, IaaS, PaaS and SaaS to the cloud user on shared resource basis. The cloud user interaction through different virtualization platforms is depicted in the layered architecture shown in figure 1. The user QoS requirements are satisfied through these virtualization platforms in terms of higher network Utilization, higher throughput, lower latency, lower transfer delay, reduced message overhead and the guaranteed bit rate.

RESOURCE VIRTUALIZATION

The virtualization of resources of optical cloud involves the interaction between different logical layers as shown in figure 2.

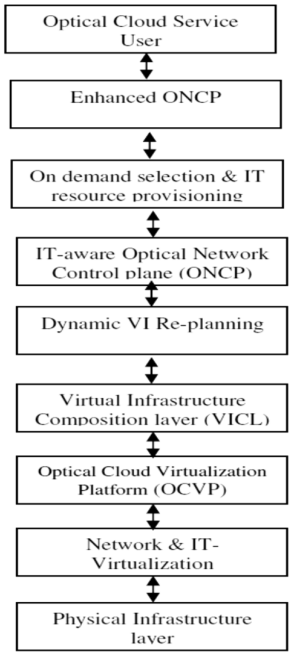

Figure 2 Virtualization of Resources in Optical Cloud

The physical infrastructure layer has physical resources such as WDM channels, network elements, topology and IT resources such as CPU, storage elements, etc. The network resources and IT resources are virtualized to access them logically anywhere. The virtualized resources are brought to the global internet through a common infrastructure called optical cloud virtualization platform

Cite this article as: Ramasamy Mariappan. "Virtualization and Resource Sharing in Optical Clouds using IP-over-WDM Networks with Quality of Service Requirements". *International Conference on Innovative Trends in Electronics Communication and Applications (2015)*: 131-137. Print.

(OCVP). The resources under OCVP are accessed and managed through virtual infrastructure composition layer (VICL). Any updates in the physical or IT resources are then done through dynamic re-planning layer. Pay per use as well as on demand provisioning and selection of IT resources to the cloud users are deployed through optical network control plane (ONCP) and enhanced ONCP. The functions of Optical network control plane include collecting routing information, distributing the optical network topology (physical) information, calculation of optimal path, etc. The routing protocols used by optical clouds:

i. Link state routing: OSPF,IS-IS
ii. Distance vector routing: RIP, IGRP

The ONCP calculates optimal path using hierarchical Path computing element protocol (PCEP), which is scalable for large number of optical nodes in the cloud. The network resources are reserved through the use of resource reservation protocol RSVP. Multi-domain optical cloud uses hierarchical PCEP on the enhanced NCP, which deploys Generalized Multi-Protocol Label Switching (GMPLS), which is using the traffic engineering (TE) with OSPF routing protocol for dynamic resource allocation. It also applies this GMPLS over optical data plane between inter-domain TE for multi-domain optical clouds. Topology aggregation for the optical cloud uses star mesh aggregation by assigning the length of shortest path as link weight. It also uses full mesh topology aggregation for comparing the performance.

Optical Link weight = Shortest path distance / WDM wavelength availability

RESULTS AND DISCUSSION

In this section, we describe the performance measurement of WDM optical cloud using simulation environment. The following assumptions are made to make the evaluation simpler.

i. All nodes are assumed to have full wavelength conversion.
ii. Each traffic demand requires 20 servers with one wavelength channel.
iii. The resource provisioning select the resource based on the shortest distance and minimum load to balance the load between the cloud servers.

Simulation parameters:

i. 3 domains, 21 nodes, 2 data centers
ii. Intra-domain: 16 wavelengths
iii. Inter-domain: 32 wavelengths
iv. 50 servers per data center

With the chosen input parameters, the following QoS parameters of the optical cloud network are analysed.

i. End to end delay
ii. Packet delivery ratio
iii. Packet loss ratio

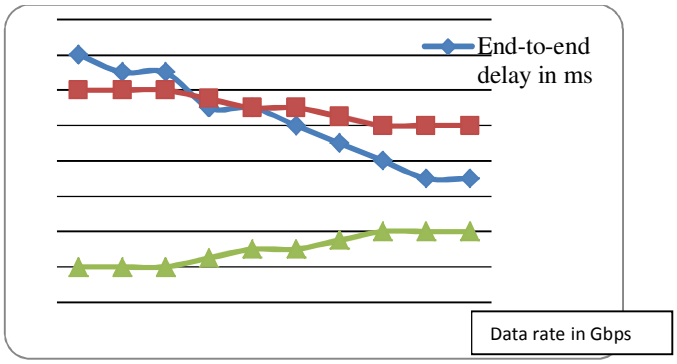

Figure 3 Data rate versus QoS parameters

It is observed from the figure 3 that while increasing ehe data upload / download rate, the end-to-end delay is varying within a limit of 0.5ms, packet delivery ratio is confined within 80% with the loss ratio of 20% maximum. These values are lying within the tolerance level of the WDM optical network, not affecting its QoS performance.

Parameters for measuring QoS performance of Optical cloud are:

i. Path compute time (τ)
ii. Number of control messages (m)
iii. Blocking probability (ρ)
iv. Ave Cloud Resource load (l)

Cite this article as: Ramasamy Mariappan. "Virtualization and Resource Sharing in Optical Clouds using IP-over-WDM Networks with Quality of Service Requirements". *International Conference on Innovative Trends in Electronics Communication and Applications (2015)*: 131-137. Print.

By varying the network load / server, we measured the above performance parameters as tabulated in Table 1. It is observed that the path computation time is limited within a fraction of second, even for the maximum load. This is due to the hierarchical PCE protocol, with the expense of little overhead messages.

TABLE I
LOAD VS QOS PARAMETERS

Load / server in Erlangs	**QoS Parameters**			
	τ ms	*m*	ρ	*l* %
2	347	152	0.0001	07
4	383	175	0.0001	11
6	422	190	0.0001 3	17
8	455	215	0.0003	23
10	498	242	0.0004 3	39
12	521	263	0.0006 1	51
14	570	290	0.0008	60
16	613	315	0.0009 2	72
18	635	337	0.0015	81
20	657	345	0.0018	92

The blocking probability is also restricted to the maximum value of 0.0018. This is due to efficient topology aggregation and hence the virtualization of the topology and network resources. Since the blocking probability is much less, the average cloud resource load attains upto 92% when the load per cloud server is maximum. This shows that the optical cloud resources are efficiently used. It also shows that the load is distributed in such a way that the cloud servers are balanced. This is due to the WDM physical topology aggregation and distribution of routing information to all nodes and cloud servers. Thus, cloud users are sharing the resources of the cloud with maximum efficiency.

CONCLUSION

In this paper, we propose optical cloud virtualization platform (OCVP) to deploy on demand provisioning and selection of IP-over-WDM optical network resources as well as IT resources in an efficient way with the help of enhanced optical network control plane (ONCP) which makes easier access and management of cloud resources. The performance of the WDM optical cloud and QoS parameters were studied through simulation setup.The simulation results show that the proposed virtualization platform for the WDM optical cloud is achieving good performance values satisfying its QoS requirements. The end-to-end delays observed as well as the packet loss ratio are within the tolerance of the WDM network. This is evident from the QoS parameters measured respectively path computation delay, blocking probability, message overhead and average cloud load. These QoS parameters are achieving the required performance for sharing of resources of IP-over-WDM optical cloud, managed through optical NCP by making use of virtualization of its resources with optical CVP. In future, the interaction between optical control plane and data plane, energy efficient sharing of resources can be dealt out.

ACKNOWLEDGMENT

The authors would like to acknowledge the Management and Principal of Sri Venkateswara College of Engineering, Tirupati for having given the facilities to do this research work.

REFERENCES

[1] Foster I, Yong Zhao, Raicu I, Lu S (2008) Cloud computing and grid computing 360- degree compared. In: Grid computing environments workshop, 2008. GCE '08, Austin Convention Center, Austin, 12-16 Nov. 2008

Cite this article as: Ramasamy Mariappan. "Virtualization and Resource Sharing in Optical Clouds using IP-over-WDM Networks with Quality of Service Requirements". *International Conference on Innovative Trends in Electronics Communication and Applications (2015)*: 131-137. Print.

[2] Audouin et al (2009) CARRIOCAS project: an experimental highbit rate optical network for computing-intensive scientific and industrial applications. TridentCom 2009, Washington, DC, 6-8 April 2009

[3] Lehman T, Sobieski J, Jabbari B (2006) DRAGON: a framework for service provisioning in heterogeneous grid networks. Communications Magazine IEEE 44(3):84-90

[4] A. Lenk, M. Klems, J. Nimis, S. Tai, and T. Sandholm, "What's inside the cloud? an architectural map of the cloud landscape," in *Proc. 2009 ICSE Workshop on Software Engineering Challenges of Cloud*

[5] L. Youseff, M. Butrico, and D. Da Silva, "Toward a unified ontology of cloud computing," in *Proc. Grid Computing Environments Workshop (GCE 2008)*, Austin, TX, USA, 16 Nov. 2008, pp. 1-10.

[6] C. Vecchiola, S. Pandey, and R. Buyya, "High-performance cloud computing: A view of scientific applications," in *Proc. 10th Int. Symp. Pervasive Systems, Algorithms, and Networks (I-SPAN 2009)*, Kaohsiung, Taiwan, 14-16 Dec. 2009, pp. 4-16.

[7] N. McKeown, T. Anderson, H. Balakrishnan, G. Parulkar, L. Peterson, J. Rexford, S. Shenker, and J. Turner, "OpenFlow: enabling innovation in campus networks," *ACM SIGCOMM Comput. Commun. Rev.*, vol. 38, no. 2, pp. 69-74, Apr. 2008.

[8] N. M. K. Chowdhury and R. Boutaba, "A survey of network virtualization," *Comput. Netw.*, vol. 54, no. 5, pp.

[9] Y. Wang, Y. Jin, W. Guo, W. Sun, and W. Hu, "Virtualized optical network services across multiple domains for grid applications," *IEEE Commun. Mag.*, vol. 49, no. 5, pp. 92-101, May 2011.

[10] T. Takeda, D. Brungard, D. Papadimitriou, and H. Ould-Brahim, "Layer 1 virtual private networks: driving forces and realization by GMPLS," IEEE *Commun. Mag.*, vol. 43, no. 7, pp. 60-67, Jul. 2005.

[11] P. Sempolinski and D. Thain, "A comparison and critique of Eucalyptus, OpenNebula and Nimbus," in *Proc. 2nd IEEE Int. Conf. Cloud Computing Technology and Science*, Indianapolis, IN, USA, 30 Nov.-3 Dec. 2010.

[12[[Online]. Available: http://www.openstack.org

[13] C. Baun and M. Kunze, "The KOALA cloud management service: a modern approach for cloud infrastructure management," in *Proc. 1st Int. Workshop on Cloud Computing Platforms (CloudCP 2011)*, Salzburg,

[14] D. Owens, "Securing elasticity in the cloud," *Commun. ACM*, vol. 53, pp. 46-51, Jun. 2010.

[15] M. De Leenheer, J. Buysse, C. Develder, and B. Mukherjee, "Isolation of virtual optical networks," in *Submitted to Int. Conf. on Computing, Networking and Communications (ICNC 2012)*, Maui, Hawaii, USA, 30 Jan. - 2 Feb. 2012.

Cite this article as: Ramasamy Mariappan. "Virtualization and Resource Sharing in Optical Clouds using IP-over-WDM Networks with Quality of Service Requirements". *International Conference on Innovative Trends in Electronics Communication and Applications (2015)*: 131-137. Print.

International Conference on Innovative Trends in Electronics Communication and Applications 2015 [ICIECA 2015]

ISBN	978-81-929742-6-2	**VOL**	01
Website	icieca.in	**eMail**	icieca@asdf.res.in
Received	02 - April - 2015	**Accepted**	15 - November - 2015
Article ID	ICIECA020	**eAID**	ICIECA.2015.020

Simulink Modelling of the Majority Pseudo-noise Sequence Acquisition Method for Multi-Carrier CDMA

F Khisamov[1], A Zolotuev[1], D Sobachkin[1], M Bobilev[1]
[1]Krasnodar High Military School, Krasnodar
Russia

Abstract: *In this article we propose majority pseudo-noise sequence (PNS) acquisition method for multi-carrier direct sequence code division multiple access (MC-DS-CDMA) communication systems, that allows for low hardware requirements and able to operate in low-quality channels. We research this method using specially developed Simulink model. The proposed method may find application in military and public communication systems.*

Keywords: Simulink Modelling, CDMA, Pseudo-noise Sequence (PNS).

INTRODUCTION

Increase in the volume of the transmitted traffic in mobile wireless networks caused by intensive integration of telecommunication technologies in many areas of human life has encouraged the development of wireless broadband access (WBA) technologies. For example, next generation 5G networks will in near future come in place of the recently deployed 4G networks. Prospective development area of the WBA networks recently became multi-carrier communication systems based on OFDM (orthogonal frequency division multiplexing) [1], [2], in which data transmission is carried out in parallel on several orthogonal subcarriers. Fourth generation standards, such as Wimax and LTE were designed based on this method, in addition to 802.11 standard family and also digital video broadcasting DVB. High spectral efficiency and multipath resistance are primary advantages of the OFDM.

Modulation method MC-DS-CDMA (multi-carrier direct sequence code division multiple access) is one of the directions of development of OFDM-oriented communication systems. MC-DS-CDMA or MC-CDMA [3] can be used in the military communication systems for data transmission with the simultaneous enemy station jamming by means of transmitting a powerful noise signal on one of the subcarriers [4].

Using the aperiodic pseudo-noise sequences (PNS) in the MC-DS-CDMA for signal modulation means the necessity of guaranteeing reliable PNS synchronization or PNS acquisition. So in this paper a majority PNS acquisition algorithm is proposed, that offers high efficiency in low-quality channels and low hardware complexity. Article covers the experimental analysis of this algorithm using the computer model developed in Simulink.

Known PN Acquisition Methods

Basic PNS acquisition methods are serial search, sequential search, parallel acquisition and matched filter correlators method [5], [6], [7]. The multicarrier nature of modulation methods or multiple access methods in MC-CDMA / MC-DS-CDMA systems is what had defined the characteristic features of the PN acquisition methods. For instance, it is possible to treat the PN acquisition in them as a combination of some basic methods. For example, study [8] looks at PN acquisition method using a serial search system on parallel subcarriers. Key elements of it are non-coherent correlators and equal gain combining scheme. In paper [9] a modification of a parallel acquisition of PN sequences of MC-CDMA systems is suggested. In the proposed method the search region of each searcher is

Cite this article as: F Khisamov, A Zolotuev, D Sobachkin, M Bobilev. "Simulink Modelling of the Majority Pseudo-noise Sequence Acquisition Method for Multi-Carrier CDMA". *International Conference on Innovative Trends in Electronics Communication and Applications (2015)*: 138-142. Print.

modified so that it overlaps with that of other searches. Acquisition scheme [9] is based on non-coherent correlators. The main disadvantage of many acquisition techniques is high enough complexity of hardware. Let's also point out that most studies look at acquisition methods for public communication systems that do not suffer from jamming [4]. This article looks at majority PN acquisition algorithm that is suitable for military communication systems, with multicarrier signals, and offers low hardware complexity [10].

Principle of the Method

By treating the maximum length sequence as a cyclic code (2^k-1, k), one can make a parity equation system and a corresponding parity matrix, which in turn could be modified to look like [10]:

$$H'=[IP^T], \quad (1)$$

where: I is an identity submatix.

By writing out H' (1) in expanded form, it could be seen that the last row shows a relation between the different phases of the PNS with some initial phase φ_0. Then the majority method can be presented as [10]:

$$\varphi_0 = \varphi_l \left[\alpha^{-l} \alpha^{-l+1} \dots \alpha^{-l+k-1}\right], \quad (2)$$

where: α^{-l+l} is a matrix column vector.

Fig. 1 shows a diagram representing a device that implements said synchronization algorithm. It consists of: α field element generator, receiver φ_l-phase register, "AND" element blocks, XOR block, switch, "K" counters with threshold switches, PNS detector, control block, time-shift module, correlator and a resolver. For each work cycle of a receiver φ_l-phase register the α field element generator should process"κ" cycles, which creates a sequence of the $a_1, a_2, \dots, a_k$ symbols. In fact, if for the first "κ" symbols we assume that the field generator state is α^0, then by shifting it to the right we get $\alpha^1, \alpha^2, \dots, \alpha^{k-1}$, which, including α^0 will produce the following sequence in the adder register: $a_1, a_2, \dots, a_k$. After receiving the following symbol the filed generator state would be at α^1, which would produce a_1 as an adder output, and by shifting the generator to the right we would get $a_2, \dots, a_k$. Threshold elements, in turn would accumulate the a_i values, and after passing the set threshold value the decision on the initial state φ_0 is made (fig. 1).

MC-DS-CDMA systems use the same PNS to widen the spectrum on every subcarrier, and that's why during the acquisition process, it is reasonable to use the majority algorithm for acquisition purposes, since every subcarrier is processed separately in ODFM. Therefore, the solver present in the diagram on fig.1, as well as the decoding in the purposed scheme works using the majority algorithm, making the decision by using the majority of the received PNS symbols on every subcarrier.

PNS synchronization is achieved by time shifting the signal on the delay equal to the time needed to determine the phase of the received segment, which is always known on the receiving end, and by confirming the correct acquisition by using the correlation method.

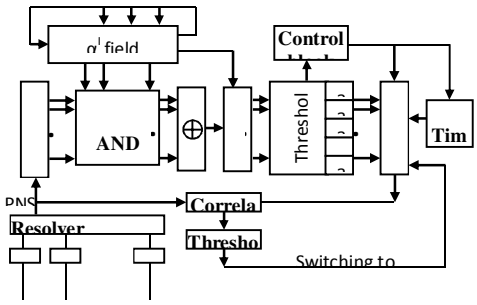

FIGURE 1. PNS ACQUISITION METHOD DIAGRAM

SIMULINK MODEL

To experimentally evaluate the proposed acquisition method, a model was created using the Simulink [11] package, that implements an acquisition system that has the PNS transmitted over parallel subcarriers. The model allows for an experimental evaluation of the probability characteristic of the proposed device and is essentially equivalent to the MC-DS-CDMA systems. Flowchart of the system is present in the fig. 2. Key elements of the model are: PNS generator [11], repeat block (serial/parallel), that does the serial to parallel signal transformation, depending on the number of the subcarriers, that are used to transmit the PNS, majority receiver, binary symmetric channel block, and a majority decoder, flowchart of which is present in fig. 3.

Cite this article as: F Khisamov, A Zolotuev, D Sobachkin, M Bobilev. "Simulink Modelling of the Majority Pseudo-noise Sequence Acquisition Method for Multi-Carrier CDMA". *International Conference on Innovative Trends in Electronics Communication and Applications (2015)*: 138-142. Print.

It should be pointed out that the main difficulties during the model development stage have been met while attempting to save the initial system state and the intermediate states in the majority decoder subsystem. For example, in the initial implementation the in-built Simulink tools for memory read and write: *Data Store Memory* [11] have been used, but they have caused random memory "read" and "write" processes, which led to data corruption. The *Memory* [11] blocks have been used instead, (see fig. 3) and that had caused extra complication in the model because of the necessity to add new blocks that were required for the correct function of the system. This approach has allowed for the decoder to function correctly. Also, due to peculiarities in the developed subsystems and in the in-built Simulink blocks a lot of counters had to be used in the final model, to control the fill up of the *Discrete Shift Register,* fill up of the resolver counters, control over the length of the treated PNS segment, etc.(see fig. 3).

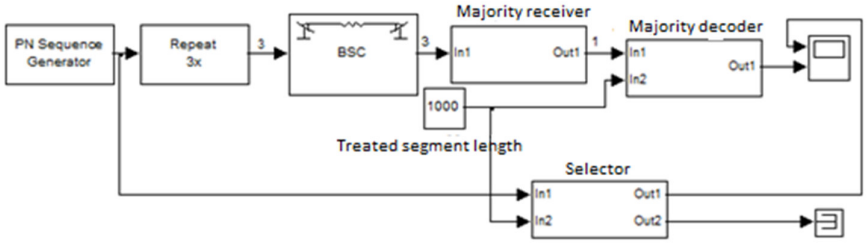

Figure 2. Simulink model diagram

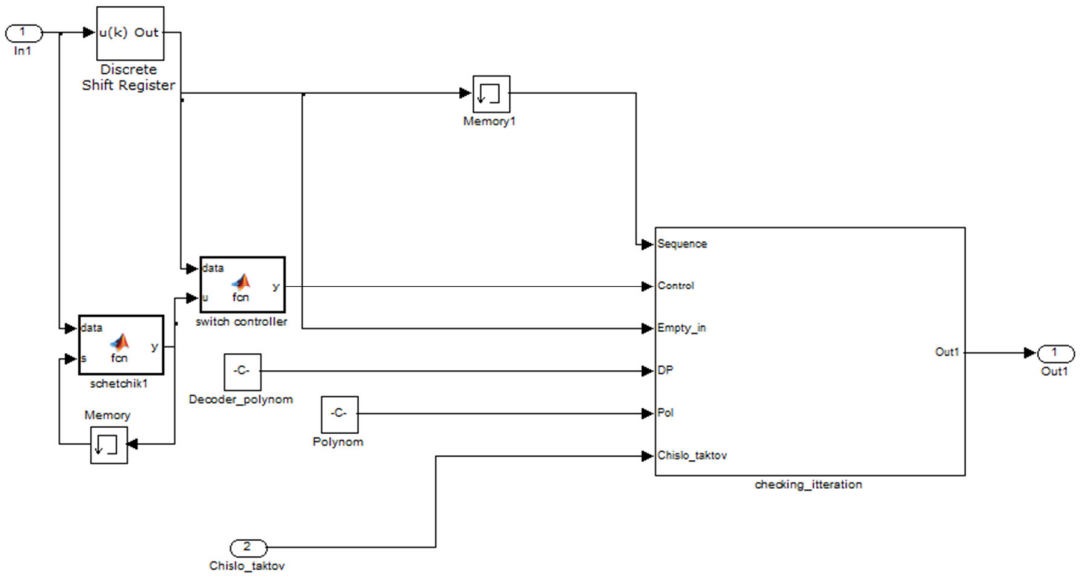

Figure 3. Majority decoder subsystem diagram

EXPERIMENTAL RESEARCH

Majority acquisition algorithm experimental research is performed by measuring medium bit error rate BER of majority decoder output for different system parameters, which presented in table 1. Besides model of majority algorithm authors have developed using Simulink a simple model of sequential search method to compare it with proposed acquisition algorithm. Diagram of sequential search model is shown in figure 4.

TABLE I
SYSTEM PARAMETERS

Parameter	Value
Polynom	k=20 [20 17 0] ($x^{20} + x^{17} + 1$) k=29 [29 27 0] ($x^{29} + x^{27} + 1$)

Cite this article as: F Khisamov, A Zolotuev, D Sobachkin, M Bobilev. "Simulink Modelling of the Majority Pseudo-noise Sequence Acquisition Method for Multi-Carrier CDMA". *International Conference on Innovative Trends in Electronics Communication and Applications (2015)*: 138-142. Print.

Parameter	Value
Sample time	16e-5/2/1
Data type	Double
Received PN-sequence segment length	1) N=127 2) N=1000
Subcarrier number	1) Nc=3 2) Nc=5

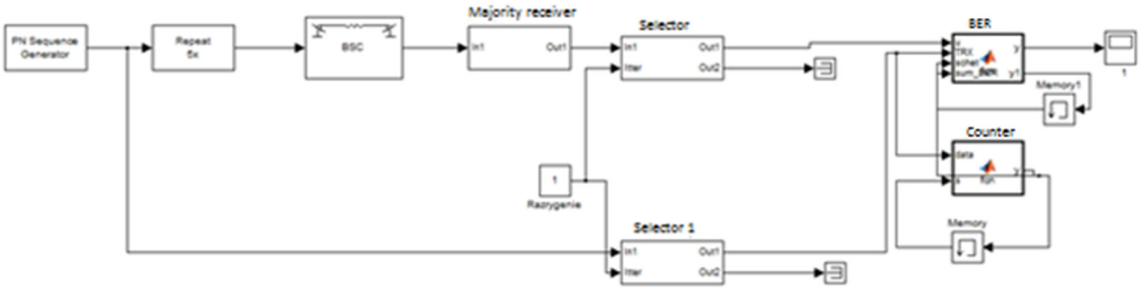

Figure 4 – Sequential search acquisition model diagram

Table 2 shows results of BER measuring for majority acquisition and sequential search models, obtained experimentally. So increasing the number of subcarriers N_c from 3 to 5 in channel with subcarrier error probability $P=0.2$ reduces majority acquisition algorithm *BER* almost five times and allow to be synchronized communication systems faster in contrast to the sequential search method, where the bit error rate is reduced by two orders of magnitude, but still remains high ($BER=5.75*10^{-2}$). As expected, increasing the length of the linear recurrent shift register k degrade performance of the acquisition system. Increasing the length of the treated segment N on the contrary is improves the accuracy of PN-sequence acquisition.

In fig. 5 is presented relation of *BER* against subcarrier error probability *P*, experimentally obtained for majority acquisition algorithm and sequential search method for system parameters: Nc=3, N=127, k=29.

Obtained results allow us to conclude that majority acquisition methods are very efficient in low-quality channels in comparison with sequential search method and permit faster synchronization in the communication system.

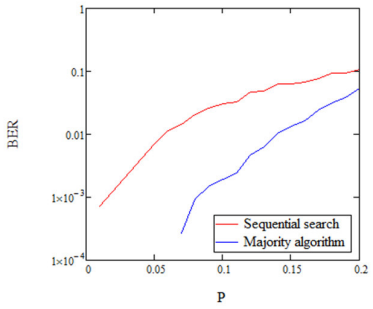

Figure 5.*BER* against of subcarrier error probability *P*

TABLE II
EXPERIMENTAL RESULTS

BER / P	Sequential search	Majority
Nc=3, N=127, k=29		

Cite this article as: F Khisamov, A Zolotuev, D Sobachkin, M Bobilev. "Simulink Modelling of the Majority Pseudo-noise Sequence Acquisition Method for Multi-Carrier CDMA". *International Conference on Innovative Trends in Electronics Communication and Applications (2015)*: 138-142. Print.

BER / P	Sequential search	Majority
0.01	0.001	0
0.1	$3.36*10^{-2}$	$1.3*10^{-3}$
0.2	$11.04*10^{-2}$	$5.24*10^{-2}$
Nc=5, N=127, k=29		
0.01	0	0
0.1	0.01	0
0.2	$5.75*10^{-2}$	$1.37*10^{-2}$
Nc=5, N=127, k=20		
0.01	0	0
0.1	$0.1*10^{-2}$	0
0.2	$5.62*10^{-2}$	$0.85*10^{-2}$

CONCLUSION

In this paper majority pseudo-noise acquisition algorithm for multi-carrier-based telecommunication systems MC-DS-CDMA was experimentally researched. Studies were conducted using developed in Simulink acquisition algorithm computer model. Key elements of the developed model are majority decoder and resolver (majority receiver). Experimental results show high efficiency of majority PN-sequence acquisition algorithm for MC-DS-CDMA system in low-quality channels and that it can be used in military communication systems.

REFERENCES

[1] K. Fazel, S. Kaiser, *Multi-carrier and spread spectrum systems: from OFDM and MC-CDMA to LTE and WiMAX,* 2nd ed. John Wiley & Sons Inc., 2008.

[2] R. Prasad. *OFDM for wireless communications systems,* Boston: Artech House, Inc., 2004.

[3] T. Ilavarasi, N. Kumaratharan, K. Rasadurai, "MC-CDMA based SDR for Next Generation Wireless Communications", *International Journal of Computer Applications*, vol. 73, no. 13, pp. 12-19, Jul. 2013.

[4] H. Wang, Y-D. Yao, R. Wang, L. Shen, Coordinated jamming and communications in an MC-CDMA system. Available: http://www.personal.stevens.edu/~hwang38/paper/CJamCom.pdf

[5] C.Regazzoni, Course acquisition and tracking in DS/SS systems. Available: http://www.isip40.it/resources/Dispense/Radio/05_PN_ACQUISITION.pdf

[6] W. S. Waseem, J. Al-Zubiady, H. M. Al-Zubiady, "Search strategies for the acquisition of DS spread spectrum signals", *Int. J. Electronics*, vol. 84, no. 2, 1998, pp. 83-104.

[7] P. Schafer, M. Nakagawa, "Direct-Sequence Multi-Carrier CDMA Parallel Acquisition in a Multipath Fading Channel" in IEEE International Conference on Communications, June 23-27, 1996, pp. 1503-1507.

[8] L-L. Yang, L. Hanzo, "Serial acquisition performance of single-carrier and multi-carrier DS-CDMA over Nakagami-m fading channels", *IEEE Transactions on wireless communications*, Oct. 2002, vol. 1, no. 4, pp. 692-702.

[9] J. Moon, Y-H. Lee, "Parallel acquisition of PN sequences in Rayleigh fading channel and the application to the multi-carrier CDMA systems," in 12th IEEE International Symposium on Personal, Indoor and Mobile Radio Communications. Sep. 30 - Oct. 3, 2001, no. 2. pp. G6-G10.

[10] I. A. Novikov, V. N. Nomokonov, A. A. Shebanov. i dr., "K voprosu o mazhoritarnom dekodirovanii M-posledovatel'nostey," *Voprosi Radioelektroniki*. no. 5, 1976.O. Beucher and M. Weeks, *Introduction to MATLAB & SIMULINK A Project Approach,* 3rd ed. Hingham, Massachusetts, 2008.

Cite this article as: F Khisamov, A Zolotuev, D Sobachkin, M Bobilev. "Simulink Modelling of the Majority Pseudo-noise Sequence Acquisition Method for Multi-Carrier CDMA". *International Conference on Innovative Trends in Electronics Communication and Applications (2015)*: 138-142. Print.

International Conference on Innovative Trends in Electronics Communication and Applications 2015 [ICIECA 2015]

ISBN	978-81-929742-6-2	**VOL**	01
Website	icieca.in	**eMail**	icieca@asdf.res.in
Received	02 - April - 2015	**Accepted**	15 - November - 2015
Article ID	ICIECA021	**eAID**	ICIECA.2015.021

Location Based Routing Protocol in Manet Using Alert

R Gayathri[1]
[1]Assistant Professor, Department of Computer Science and Engineering,
Aalim Muhammed Salegh College of Engineering, Chennai, Tamilnadu, India

Abstract: *Mobile Ad Hoc Networks (MANETs) use anonymous routing protocols that hide node identities and/or routes from outside observers in order to provide anonymity protection. However, existing anonymous routing protocols relying on either hop-by-hop encryption or redundant traffic either generate high cost or cannot provide full anonymity protection to data sources, destinations, and routes. The high cost exacerbates the inherent resource constraint problem in MANETs especially in multimedia wireless applications. To offer high anonymity protection at a low cost. I propose an Anonymous Location-based Efficient Routing proTocol (ALERT). For anonymity ALERT hides mainly source and destination identity using pseudonym which changes frequently. And ALERT also hide route between source and destination. With this ALERT also having stratergy against intersection attacks. I show that ALERT achieves better route anonymity protection and lower cost compared to other anonymous routing protocols. Also, ALERT achieves comparable routing efficiency to the GPSR geographical routing protocol.*

Keywords*:* Mobile ad hoc netwI.

INTRODUCTION

Now a day's using mobile Ad-hoc Network, numerous wireless applications can be developed and these are used in much number of areas like mainly in military, education, commerce, entertainment.

MANET- MANET's basic features are self-organizing and independent infrastructure. All the nodes in the network are mobile and use wireless communications to communicate with other nodes. But as perspective of security of MANET, these networks get easily broken their security. Mainly data get lost or stolen by tampering and analyzing data and traffic analysis eavesdropping method or attacking routing protocol. For this security issue one solution is to use anonymous routing in the network that cannot be identified by any other nodes or attacker or observer. Although this anonymous routing is not required in general application .but it is very essentitial in Military, Banking like application, where security of communication is main purpose.

Anonymous routing provides secure communication between two nodes by hiding nodes original identity and prevents these nodes from traffic analysis attacks of adversaries.

In this paper the main task of anonymous routing is to hide identity and location of data sources (i.e sender, receipent) and route.so attacker cannot easily identify identity and location in network of nodes.

Existing anonymity routing protocols in MANETs can be mainly classified into two categories: hop-by-hop encryption [9], [12], [2], [6], [1] and redundant traffic [11], [7], [4],[10], [14], [13], [3]. Most of the current approaches are limited by focusing on enforcing anonymity at a heavy cost to precious resources because public-key-based encryption and high traffic generate significantly high cost. In addition, many approaches cannot provide all of the aforementioned anonymity protections. For example, ALARM [6] cannot protect the location anonymity of source and destination, SDDR [16] cannot provide route anonymity, and ZAP [3] only focuses on destination anonymity. Many anonymity routing algorithms [3], [2], [3], [6], [1], [14], [10] are based on the geographic routing protocol (e.g.,

Cite this article as: R Gayathri. "Location Based Routing Protocol in Manet Using Alert". *International Conference on Innovative Trends in Electronics Communication and Applications (2015)*: 143-152. Print.

Greedy Perimeter Stateless Routing (GPSR) [17]) that greedily forwards a packet to the node closest to the destination. However, the protocol's strict relay node selection makes it easy to reveal the source and destination and to analyze traffic.

In order to provide high anonymity protection (for sources, destination, and route) with low cost, I propose an Anonymous Location-based and Efficient Routing proTocol (ALERT). ALERT dynamically partitions a network field into zones and randomly chooses nodes in zones as intermediate relay nodes, which form a non-traceable anonymous route. Specifically, in each routing step, a data sender or forwarder partitions the network field in order to separate itself and the destination into two zones. It then randomly chooses a node in the other zone as the next relay node and uses the GPSR [17] algorithm to send the data to the relay node. In the last step, the data is broadcasted to k-nodes in the destination zone, providing k-anonymity to the destination. In addition, ALERT has a strategy to hide the data initiator among a number of initiators to strengthen the anonymity protection of the source. ALERT is also resilient to intersection attacks [19] and timing attacks [19]. I theoretically analyzed ALERT in terms of anonymity and efficiency. I also conducted experiments to evaluate the performance of ALERT in comparison with other anonymity and geographic routing protocols.

Motivation and Contribution

The motivation of this paper is to ALERT can be used in different network models with node movement patterns. Such as random way point model and group mobility model. Generally ALERT provides unpredictable and dynamic routing path, which having no. of dynamically selected intermediate nodes.

1. First ALERT partitions given network area into two zones as horizontally (or vertically).

2. Then again split every partition into two zones as vertically (or horizontally). This process called as hierarchical zone partition.

3. After partitioning ALERT randomly select a node in each zone at each step as an intermediate relay node ,in this way ALERT provide dynamically creating an unpredictable routing path

Related Work

Anonymous routing schemes in MANETs have been studied in recent years. By the different usage of topological information, they can be classified into on-demand or reactive routing methods [7], [15], [8], [11], [12], [2], [14], [10], [3], and proactive routing methods [5]. Also there are anonymous middleware working between network layer and application layer [4]. Since topology routing does not need the node location information, location anonymity protection is not necessary.

TABLE 1: Summary of Existing Anonymous Routing Protocols

Category			Name	Identity anonymity	Location anonymity	Route anonymity
Reactive	Hop-by-hop encryption	Topology	MASK [32]	source	n/a	yes
			ANODR [33]	source, destination	n/a	yes
			Discount-ANODR [34]	source, destination	n/a	yes
		Geographic	Zhou *et al.* [3]	source, destination	source, destination	no
			Pathak *et al.* [4]	source, destination	source, destination	no
			AO2P [10]	source, destination	source, destination	no
			PRISM [6]	source, destination	source, destination	no
	Redundant traffic	Topology	Aad [8]	destination	n/a	yes
		Geographic	ASR [11]	source, destination	source, destination	no
			ZAP [13]	destination	destination	no
Proactive	Redundant traffic	Topology	ALARM [5]	source, destination	source	no
Middleware	Redundant traffic	Geographic	MAPCP [9]	source, destination	n/a	yes

HELPFUL HINTS

Figures and Tables

Table 1 shows the classification of the methods along with their anonymity protection. To clearly show the featured anonymity protection in different reactive routing methods, the table provides a finer classification of different anonymity methods, including hop-by-hop encryption [7], [15], [8], [11], [12], [11], [14], [10] ,and redundant traffic routing [7], [14], [3].

In hop-by-hop encryption routing, a packet is encrypted in the transmission of two nodes en route, preventing adversaries from tampering or analyzing the packet contents to interrupt the communication or identify of the two communicating nodes. Hop-by-hop encryption routing can be further divided into onion routing and hop-by-hop authentication. In onion routing, packets are encrypted in the source node and decrypted layer by layer (i.e., hop by hop) along the routing path. It is used in Aad [7], ANODR [15] and Discount-ANODR [8] topological routing. Aad [7] combines onion routing, multicast, and uses packet coding policies to constantly change the packets in order to reinforce both destination and route anonymity. The onion used in ANODR [15] is called trapdoor

Cite this article as: R Gayathri. "Location Based Routing Protocol in Manet Using Alert". *International Conference on Innovative Trends in Electronics Communication and Applications (2015)*: 143-152. Print.

boomerang onion (TBO), which uses a trapdoor function instead of public key-based encryption. ANODR needs onion construction in both route discovery and return routing, generating high cost. To deal with this problem, the authors further proposed Discount-ANODR that constructs onions only on the return routes

ALARM [6] uses proactive routing, where each node broadcasts its location information to its authenticated neighbours so that each node can build a map for later anonymous route discovery. However, this map construction leaks destination node locations and compromises the route anonymity. Different from all other studied methods. MAPCP [4] is a middleware between network and application layers, in which every hop in the routing path executes probabilistic broadcasting that chooses a number of its neighbours with a certain probability to forward messages.

Mix zones [13] and GLS [20] are zone-based location services. Mix zones are an anonymous location service that unveils the positions of mobile users in a long time period in order to prevent users' movement from being tracked. Each location aware application that can monitor nodes' locations on top of Mix zones is only allowed to monitor the nodes that are registered to it. Therefore, by letting each node associate with some zones but stay unregistered, these users' location changes are untraceable in unregistered zones. Although GLS also uses hierarchical zone partition-ing, its use is for location service while in ALERT, its use is for anonymous routing. ALERT is also different from GLS in the zone division scheme. A zone in ALERT is always divided into two smaller rectangles, while GLS divides the entire square area into four sub squares and then recursively divides these into smaller squares. The zone division in ALERT occurs when selecting a next forwarding node, so the zones are formed dynamically as a message is being forwarded. In contrast, the zone division and hierarchies in GLS are configured in advance and the location servers are selected based on the different hierarchies

Organization

The rest of this paper is organized as follows. I introduce the preliminary work in Section II. I give the formal model of ALERT in Section III. An efficient ALERT scheme is proposed in Section IV. I analyse the proposed scheme in Section V. Finally, the conclusions are given in Section VI.

PRELIMINARIES

For ease of illustration, I assume the entire network area is generally a rectangle in which nodes are randomly disseminated. The information of the bottom-right and upper left boundary of the network area is configured into each node when it joins in the system. This information enables a node to locate the positions of nodes in the entire area for zone partitions in ALERT.

ALERT features a dynamic and unpredictable routing path, which consists of a number of dynamically deter-mined intermediate relay nodes.

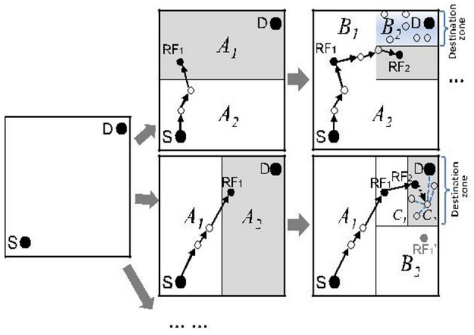

Fig. 1. Examples of different zone partitions.

As shown in the upper part of Fig. 1, given an area, I horizontally partition it into two zones A_1 and A_2. I then vertically partition zone A_1 to B_1 and B_2. After that, I horizontally partition zone B_2 into two zones. Such zone partitioning consecutively splits the smallest zone in an alternating horizontal and vertical manner. I call this partition process hierarchical zone partition. ALERT uses the hierarchical zone partition and randomly chooses a node in the partitioned zone in each step as an intermediate relay node (i.e., data forwarder), thus dynamically generating an unpredictable routing path for a message.

Fig. 2 shows an example of routing in ALERT. I call the zone having k nodes where D resides the destination zone, denoted as Z_D. k is used to control the degree of anonymity protection for the destination. The shaded zone in Fig. 2 is the destination zone. Specifically, in the ALERT routing, each data source or forwarder executes the hierarchical zone partition. It first checks whether itself and destination are in the same zone. If so, it divides the zone alternatively in the horizontal and vertical directions. The node repeats this process until it until it and Z_D are not in the same zone

Cite this article as: R Gayathri. "Location Based Routing Protocol in Manet Using Alert". *International Conference on Innovative Trends in Electronics Communication and Applications (2015)*: 143-152. Print.

It then randomly chooses a position in the other zone called temporary destination (TD), and uses the GPSR routing algorithm to send the data to the node closest to TD. This node is defined as a random forwarder (RF). Fig. 3 shows an example where node N_3 is the closest to TD, so it is selected as a RF. ALERT aims at achieving k-anonymity [18] for destination node D, where k is a predefined integer. Thus, in the last step, the data are broadcasted to k nodes in Z_D, providing k-anonymity to the destination.

Fig. 2. Routing among zones in ALERT

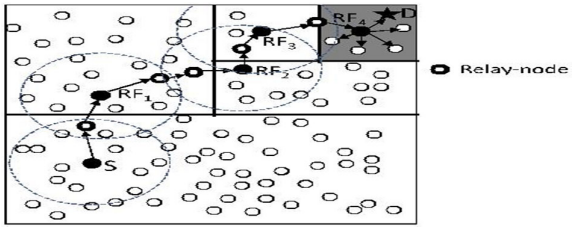

Given an S-D pair, the partition pattern in ALERT varies depending on the randomly selected TDs and the order of horizontal and vertical division, which provides a better anonymity protection. Fig. 1 shows two possible routing paths for a packet pkt issued by sender S targeting destination D in ALERT. There are also many other possible paths. In the upper routing flow, data source S first horizontally divides the area into two equal-size zones, A_1 and A_2, in order to separate S and Z_D. S then randomly selects the first temporary destination TD_1 in zone A_1 where Z_D resides. Then, S relies on GPSR to send pkt to TD_1. The pkt is forwarded by several relays until reaching a node that cannot find a neighbor closer to TD_1. This node is considered to be the first random-forwarder RF_1. After RF_1 receives pkt, it vertically divides the region A_1 into regions B_1 and B_2 so that Z_D and it are separated in two different zones. Then, RF_1 randomly selects the next temporary destination TD_2 and uses GPSR to send pkt to TD_2. This process is repeated until a packet receiver finds itself residing in Z_D, i.e., a partitioned zone is Z_D having k nodes. Then, the node broadcasts the pkt to the k nodes.

The lower part of Fig. 1 shows another routing path based on a different partition pattern. After S vertically partitions the whole area to separate itself from Z_D, it randomly chooses TD_1 and sends pkt to RF_1. RF_1 partitions zone A_2 into B_1 and B_2 horizontally and then partitions B_1 into C_1 and C_2 vertically, so that itself and Z_D are separated. Note that RF_1 could vertically partition A_2 to separate itself from Z_D in two zones but may choose a TD further away from the destination than the TD that resulted from the horizontal partition. Therefore, ALERT sets the partition in the alternative horizontal and vertical manner in order to ensure that a pkt approaches D in each step.

As GPSR, we assume that the destination node will not move far away from its position during the data transmission, so it can successfully receive the data. In this design, the tradeoff is the anonymity protection degree and transmission delay. A larger number of hierarchies generate more routing hops, which increases anonymity degree but also increases the delay. To ensure the delivery of packets, the destination sends a confirmation to the source upon receiving the packets. If the source has not received the confirmation during a predefined time period, it will resend the packets.

FORMAL MODEL OF ALERT

In this section, I give the formal Algorithm and Routing method of ALERT.

Pseudonym and Location of Node: Dynamic pseudonym is another name or identity given to node. In ALERT pseudonym used as node identifier with replacement of its real MAC address. Nodes MAC addresses can be used to trace nodes existence in the network. Therefore replacing MAC address with pseudonym is the main advantage of ALERT protocol. This pseudonym is the combination of MAC address and Current time stamp. But if this information is known by attacker then it is easily find out the node. Therefore, to prevent this time stamp can be randomly selected. This pseudonym is not permanent; it expires after a specific time period so that attacker cannot associate the pseudonym with nodes. With this pseudonym there is one problem is changing pseudonym frequently create routing uneasy. Therefore these pseudonym changes frequently should be appropriately determined.

The ALERT Routing: Generally ALERT provides unpredictable and dynamic routing path,which having no.of dynamically selected intermediate nodes.

1. First ALERT partitions given network area into two zones as horizontally (or vertically).
2. Then again split every partition into two zones as vertically (or horizontally). This process called as hierarchical zone partition.
3. After partitioning ALERT randomly select a node in each zone at each step as an intermediate relay node ,in this way ALERT provide dynamically creating an unpredictable routing path.

Cite this article as: R Gayathri. "Location Based Routing Protocol in Manet Using Alert". *International Conference on Innovative Trends in Electronics Communication and Applications (2015)*: 143-152. Print.

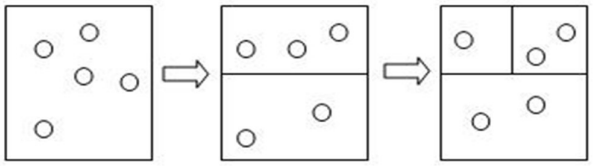

Fig. 1 Horizontal Partitioning

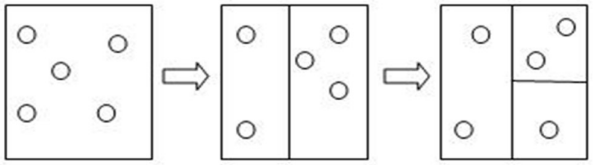

Fig. 2 Vertical Partitioning

Above fig. shows both partitioning, here we generally network considered in rectangle form. In this rectangle circle consider as nodes. Consider one example of routing in ALERT .Following fig shows this

Fig 3. Zonal Routing of Nodes

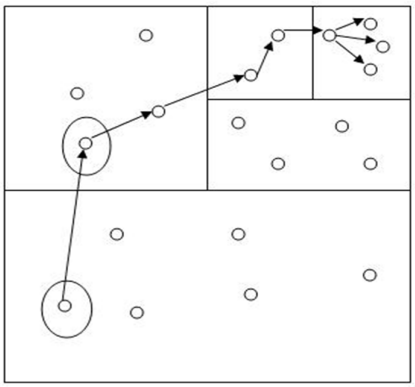

In this example I first horizontally partition network then vertically and so on. While this partitioning each data source of forwarder node checks whether itself and destination nodes are not in same zone. If it is not then partitioning continues. In above fig where the destination node locates that zone is called as destination zone denoted as ZD and that zone having k nodes, which is used to control the degree of anonymity.

While in routing first source node randomly chooses a node in other zone known as temporary destination (TD) and then uses GPSR routing algorithm to send the data to node close to TD. This process continues to reach data to destination node. A node closer to TD known as Random Forwarder (RF) .But in destination zone data is broadcasted in ZD to k nodes which provides k anonymity i.e attacker or observer does not known at destination node.

Here one assumption is taken that destination node with not leave the destination zone during the data transmission to it. So it can successfully receive the full data without any loss. For successful completion of data transmission destination node send a confirmation to source node. If source node not receives to confirm during predefined time period, it will resend packets. As a large no. of hierarchies generated they create more routing hops which increases anonymity degree but also increase the delay.

Location of Destination Zone: Zone position is made from the upper left and bottom right coordinates of a zone. It is used by each packet forwarder to check whether it is separated from destination zone or not, To calculate zone position we have H denotes total no. of partitions in order to produce ZD and no .of nodes i.e k and node density ρ ,

$$H = \log2(\rho.G/k) \quad eq(1)$$

Cite this article as: R Gayathri. "Location Based Routing Protocol in Manet Using Alert". *International Conference on Innovative Trends in Electronics Communication and Applications (2015)*: 143-152. Print.

Where as G=size of entire network area Using H and G the position (0,0) & (Xg , Yg) of entire network area and position of destination node d the source can calculate the zone position of ZD.

Packet Format: For successful routing between source and destination some information is needed, which is embeds in the packet by source and each packet forwarder node. For ALERT following packet format is use.

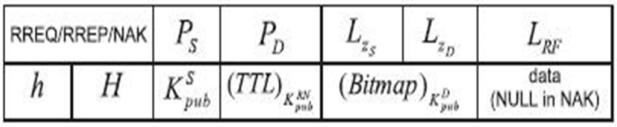

Fig.4 ALERT Packet Format

RREQ/RREP/NAK- use to acknowledge the loss of packet.

P_s- Pseudonym of a source.

P_d – pseudonym of a destination.

Lzs & Lzd – are the position of Hth partitioned source zone and destination zone.

h- Number of divisions.

H – Maximum number of division allowed.

In this paper, I use two different network models, random way point model [17] and group mobility model [18]. With the random way point model as the default setting, I also compare the performance of ALERT in the group mobility model. In the group mobility model, we set the movement range of each group to 150 m with 10 groups [6] and to 200 m with five groups.

Anonymity Protection: The main goal of ALERT is to provide identity and location anonymity of source and destination in MANET. For this ALERT dynamically and randomly chooses relay node for forming route between source and destination. So due to this intruder cannot observe a stastical pattern of transmission. Anonymous path between source and destination ensures that a node on the path does not know where the endpoints are. Unlinkability is major strength of privacy protection i.e source and destination cannot be associated with the packets in their communication by adversaries.

Strategy against Intersection Attacks: Intersection attack, in which an attacker can determine communicating nodes using observation of routing between them and collecting information about them Active Users To counter intersection attack ALERT proposes a strategy. In this it broadcasted the packets in destination zone ZD. So that attacker confuse who is destination .This broadcasting is done in two steps. In first step packet is broadcasted but not reach to destination node. In second step nodes who receive the packets then forward packets to remaining node who yet not receive in this destination node is present so it receive the packet. In this situation attacker get confused and can't concentrate in their observation

ANALYSIS OF THE SCHEME

In this section, I theoretically analyze the anonymity and routing efficiency properties of ALERT. I analyze the number of nodes that can participate in routing that function as camouflages for routing nodes. I estimate the number of RFs in a routing path, which shows the route anonymity degree and routing efficiency of ALERT. I calculate the anonymity protection degree of a destination zone as time passes to demonstrate ALERT's ability to counter intersection attacks. In this section, I also use figures to show the analytical results to clearly demonstrate the relationship between these factors and the anonymity protection degree

Security

In this analysis scenario, I assume that the entire network area is a rectangle with side lengths l_A and l_B and the entire area is partitioned H times to produce a k-anonymity destination zone. For the parameters of results in the figures, unless otherwise indicated, the size of the entire network zone is 1000 mX1000 m and the number of nodes equals 200. I set H = 5 to ensure that a reasonable number of nodes are in a destination zone.

Cite this article as: R Gayathri. "Location Based Routing Protocol in Manet Using Alert". *International Conference on Innovative Trends in Electronics Communication and Applications (2015)*: 143-152. Print.

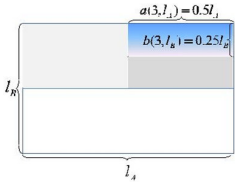

Fig. 5. The side lengths of the 3rd partitioned zone.

I first introduce two functions to calculate the two side lengths of the hth partitioned zone:

$a(h,I_A)=1_A/2^{(h/2)}$, eq(2)

$b(h,I_B)=I_B/22^{[h/2]}$ eq(3)

The side lengths of the destination zone after H partitions are $a(h,I_A)$and $b(h,I_B)$. Fig. shows an example of three partitions of the entire network area. The side lengths of the final zone after the three partitions are

$a(3,I_A)=1_A/2^{[3/2]}$,$=0.5I_A$ eq(4)

and

$b(3, I_B)= I_B /2^{[3/2]})'=0.25I_B$ eq(5)

The Number of Possible Participating Nodes: The intention of his analysis is to characterize how many possible nodes are able o participate in one S-D routing. The number of these nodes shows how many nodes can become camouflages in a routing path. These possible participating nodes include RFs and the relay nodes between two RFs using GPSR. The nodes that actually conduct the routing are not easily discovered among the many possible participating nodes, thus making the routing pattern undetectable. Because the positions of both S and D affect the number of possible participating nodes in routing, the positions influence routing anonymity. I first calculate the probability that partitions are needed to separate S and D denoted as $p_s(\sigma)$-1. I use to denote the closeness between S and D. $p_s(\sigma)$ actually is the probability that D is located in a position that can be separated from a given S using σ partitions. I can get

$p_s(\sigma) = 1/2\,\sigma \quad 0< \sigma<=H$ eq(6)

I use $Ne(\sigma)$ to denote the expected number of nodes that possibly take part in routing based on a given closeness

$Ne(\sigma) = a(\sigma,I_A),b(\sigma,I_B)$ eq(7)

where p denotes the density of nodes. By considering different closeness σ I arrive at the final expected number of possible participating nodes from a S to any D:

$Ne =\Sigma^{H}_{\sigma=1} Ne(\sigma)\, p_s(\sigma)= \Sigma^{H}_{\sigma=1} a(\sigma,I_A),b(\sigma,I_B)\, p\ \ 1/2^{\sigma}$ eq(8)

I set the total number of nodes in the network to 100, 200, and 400, respectively, and use (5) to calculate the number of possible participating nodes.

The Number of Random-Forwarders: The number of RFs determines the length of the routing path in ALERT. Therefore, it reflects the energy efficiency and degree of anonymity of ALERT. From the anonymity view, for a network with a fixed number of nodes, more RFs offer higher anonymity but will reduce the number of nodes in the destination zone, and consequently reduce the anonymity protection of destination node. Therefore, the number of RFs should be carefully determined to ensure a sufficient number of nodes located in the destination zone. For a pair of S-D with closeness σ, we define $p_i(\sigma ,i)$ as the probability that an S-D routing path has i RFs. The number of RFs is determined by the zone partition pattern.

Destination Anonymity Protection: Destination anonymity is determined by the number of nodes in the destination zone, which is related to node density and the size of the destination zone. According to the work in [13], the probability that a node with a moving speed *v* remains in the destination zone, which is a circular area with radius r, after time period t, denoted by $p_r(t)$, is exponentially distributed:

Where $p_r(t) = e^{-t/\beta(r)}$ eq(9)

$\beta(r) = \Pi r/2v$ eq(10)

Cite this article as: R Gayathri. "Location Based Routing Protocol in Manet Using Alert". *International Conference on Innovative Trends in Electronics Communication and Applications (2015)*: 143-152. Print.

In order to apply (9) and (10) to my method, I assume the Hth partitioned destination zone is a square that can be approximated by a circle covering approximately (see fig:6) the same area. This assumption is feasible, which only requires a square for the entire network area (i.e., $l_A = l_B$) and an even number of partitions (i.e., $a(H, l_A) = b(H, l_A)$). I use 2r' to denote the side length of the destination zone. Hence, we can calculate the radius of this approximate circle as below:

$$\Pi r2 = (2r')2 \rightarrow r = 2r' / \Gamma\Pi \qquad \text{eq(11)}$$

For ALERT to be usable, I need to ensure that the pseudonym and location exchange cost is low compared with regular communication messages. Let N, N_L, f, F, and T denote the total number of nodes, the number of location servers, the frequency of pseudonym, and location updates and the frequency of regular communication messages, respectively. The number of messages exchanged between location servers within time T is N_L x (N_L 1) x f x T, the number of messages for pseudonym updates is N x f x T. The number of communication messages in the network is N x F x T. Therefore, if the location servers incur only a small fraction of messages, we need to make sure that N_L x (N_L-1) x f x T/ N x F x T <<1.Regular communication frequency should be much higher than update exchange messages. thus ,f << F, so that N x f x T./ N x F x T <<1.Therefore

$$\frac{N_L \times (N_L-1) \times f \times T + N \times F \times T}{N \times F \times T} << 1$$

$$\frac{N_L \times (N_L-1) \times f \times T}{N \times F \times T} << 1$$

$$\frac{N_L \times (N_L-1) \times f}{N \times F} << 1$$

which can be satisfied if N_L is comparable to ΓN. This is reasonable when the transmission range of nodes is modest so that only a small number of location servers are needed.

Performance

In this section, I provide experimental evaluation of the ALERT protocol, which exhibit consistency with my analytical results. Both prove the superior performance of ALERT in providing anonymity with low cost of overhead. Recall that anonymous routing protocols can be classified into hop-by-hop encryption and redundant traffic. I compare ALERT with two recently proposed anonymous geographic routing protocols: AO2P [10] and ALARM [6], which are based on hop-by-hop encryption and redundant traffic, respectively. All of the protocols are geographic routing, so we also compare ALERT with the baseline routing protocol GPSR [1] in the experiments. In GPSR, a packet is always forwarded to the node nearest to the destination. When such a node does not exist, GPSR uses perimeter forwarding to find the hop that is the closest to the destination. In ALARM, each node periodically disseminates its own identity to its authenticated neighbors and continuously collects all other nodes' identities. Thus, nodes can build a secure map of other nodes for geographical routing. In routing, each node encrypts the packet by its key which is verified by the next hop en route. Such dissemination period was set to 30s in this experiment. The routing of AO2P is similar to GPSR except it has a contention phase in which the neighboring nodes of the current packet holder will contend to be the next hop. This contention phase is to classify nodes based on their distance from the destination node, and select a node in the class that is closest to destination. Contention can make the ad hoc channel accessible to a smaller number of nodes in order to decrease the possibility that adversaries participate, but concurrently this leads to an extra delay. Also, AO2P selects a position on the line connecting the source and destination that is further to the source node than the destination to provide destination anonymity, which may lead to long path length with higher routing cost than GPSR

Simulation

In this section I discuss about the simulation of network model.

Cite this article as: R Gayathri. "Location Based Routing Protocol in Manet Using Alert". *International Conference on Innovative Trends in Electronics Communication and Applications (2015)*: 143-152. Print.

The tests were carried out on NS-2.29 simulator using 802.11 as the MAC protocol with a standard wireless transmission range of 250 m and UDP/CBR traffic [21] with a packet size of 512 bytes. The test field in our experiment was set to a 1000 m x 1000 m area with 200 nodes moving at a speed of 2 m/s, unless otherwise specified. The density was set to 50, 100, 150, and 200 nodes per square meters. The duration of each simulation was set to 100 s unless otherwise indicated. The number of pairs of S-D communication nodes was set to 10 and S-D pairs are randomly generated. S sends a packet to D at an interval of 2 s. The final results are the average of results of 30 runs. The confidence interval can be thus calculated from different runs and are shown when necessary. The confidence interval information is drawn along with the average point (in a "I" shape) on those figures.

For encryption, the symmetric encryption algorithm is AES and the public key encryption is RSA. Data are generated randomly according to the packet size specified in the paper. Packets are encrypted whenever needed. The encryption algorithm is single threaded, running along with other parts of the experiment on a 1.8 Ghz processor. A typical symmetric encryption costs several milliseconds while a public key encryption operation costs 2-3 hundred milliseconds.

I use the following metrics to evaluate the routing performance in terms of effectiveness on anonymity protection and efficiency:

1. **The number of actual participating nodes**. These nodes include RFs and relay nodes that actually participate in routing. This metric demonstrates the ability of ALERT's randomized routing to avoid routing pattern detection.
2. **The number of random forwarders**. This is the number of actual RFs in a S-D routing path. It shows routing anonymity and efficiency.
3. **The number of remaining nodes in a destination Zone**: This is the number of original nodes remaining in a destination zone after a time period. A larger number provides higher anonymity protection to a destination and to counter the intersection attack. We measure this metric over time to show effectiveness on the destination anonymity protection.
4. **The number of hops per packet**. This is measured as the accumulated routing hop counts divided by the number of packets sent, which shows the efficiency of routing algorithms.
5. **Latency per packet**. This is the average time elapsed after a packet is sent and before it is received. It includes the time cost for routing and cryptography. This metric reflects the latency and efficiency of routing algorithms.
6. **Delivery rate**. This is measured by the fraction of packets that are successfully delivered to a destination. It shows the robustness of routing algorithms to adapt to mobile network environment.

In this Paper, I conclude that Existing anonymous routing protocols, depend on either hop- by-hop encryption or redundant traffic which generate high cost. And some protocols are not provide complete source, destination, and route anonymity protection. ALERT is distinguished by its low cost and anonymity protection for sources, destinations, and routes. It uses dynamic hierarchical zone partitions and random relay node selections to make it difficult for an intruder to detect the two endpoints and nodes en-route. ALERT further strengthens the anonymity protection of source and destination by hiding the data initiator/receiver among a number of data initiators/ receivers. In addition, ALERT has an efficient solution to counter intersection attacks. It can also achieve comparable routing efficiency to the base-line GPSR algorithm. Like other anonymity routing algorithms, ALERT is not completely bulletproof to all attacks. Future work lies in reinforcing ALERT in an attempt to thwart stronger, active attackers and demonstrating comprehensive theoretical and simulation results.

References

[1] K.E. Defrawy and G. Tsudik, "PRISM: Privacy-Friendly Routing in Suspicious MANETs (and VANETs)," Proc. IEEE Int'l Conf. Network Protocols (ICNP), 2008

[2] V. Pathak, D. Yao, and L. Iftode, "Securing Location Aware Services over VANET Using Geographical Secure Path Routing," Proc. IEEE Int'l Conf. Vehicular Electronics and safety (ICVES), 2008

[3] X. Wu, J. Liu, X. Hong, and E. Bertino, "Anonymous Geo-Trans. Parallel and Distributed Systems, vol. 19, no. 10, pp. 1297-1309, Oct. 2008.

[4] C.-C. Chou, D.S.L. Wei, C.-C. Jay Kuo, and K. Naik, "An Efficient Anonymous Communication Protocol for Peer-to-Peer Applica-tions over Mobile Ad-Hoc Networks," IEEE J. Selected Areas in Comm., vol. 25, no. 1, pp. 192-203, Jan. 2007.

[5] K.C. Lee, J. Haerri, L. Uichin, and M. Gerla, "Enhanced Perimeter Routing for Geographic Forwarding Protocols in Urban Vehicular Scenarios," Proc. IEEE GlobeCom Workshops, 2007

[6] K.E. Defrawy and G. Tsudik, "ALARM: Anonymous Location- Aided Routing in Suspicious MANETs," Proc. IEEE Int'l Conf. Network Protocols (ICNP), 2007.

[7] I. Aad, C. Castelluccia, and J. Hubaux, "Packet Coding for Strong Anonymity in Ad Hoc Networks," Proc. Secure comm and Workshops, 2006

[8] L. Yang, M. Jakobsson, and S. Wetzel, "Discount Anonymous On Demand Routing for Mobile Ad Hoc Networks," Proc

Cite this article as: R Gayathri. "Location Based Routing Protocol in Manet Using Alert". *International Conference on Innovative Trends in Electronics Communication and Applications (2015)*: 143-152. Print.

Secure communications and Workshops, 2006

[9] Sk.Md.M.Rahman,Mambo,A.Inomata,and E. Okamoto, "An Anonymous On-Demand Position-Based Routing in Mobile Ad Hoc Networks," Proc. Int'l Symp. Applications on Internet (SAINT), 2006

[10] X. Wu, "AO2P: Ad Hoc On-Demand Position-Based Private Routing Protocol," IEEE Trans. Mobile Computing, vol. 4, no.4, 335-348, July/Aug. 2005.

[11] Y.-C. Hu, A. Perrig, and D.B. Johnson, "Ariadne: A Secure On- Demand Routing Protocol for Ad Hoc Networks," Wireless Networks, vol. 11, pp. 21-38, 2005.

[12] Z. Zhi and Y.K. Choong, "Anonymizing Geographic Ad Hoc Routing for Preserving Location Privacy," Proc. Third Int'l Work-shop Mobile Distributed Computing (ICDCSW), 2005.

[13] A.R. Beresford and F. Stajano, "Mix Zones: User Privacy in Location-Aware Services," Proc. IEEE Second Ann. Conf. Pervasive Computing and Comm. Workshops (PERCOMW), 2004

[14] B. Zhu, Z. Wan, M.S. Kankanhalli, F. Bao, and R.H. Deng, "Anonymous Secure Routing in Mobile Ad-Hoc Networks," Proc. IEEE 29th Ann. Int'l Conf. Local Computer Networks (LCN), 2004

[15] J. Kong, X. Hong, and M. Gerla, "ANODR: Anonymous on Demand Routing Protocol with Untraceable Routes for Mobile Ad Hoc Networks," Proc. ACM MobiHoc, pp. 291-302, 2003

[16] K. El-Khatib, L. Korba, R. Song, and G. Yee, "Anonymous Secure Routing in Mobile Ad-Hoc Networks," Proc. Int'l Conf. Parallel Processing Workshops (ICPPW), 2003.

[17] S. Ratnasamy, B. Karp, S. Shenker, D. Estrin, R. Govindan, L. Yin, and F. Yu, "Data-Centric Storage in Sensornets with GHT, a Geographic Hash Table," Mobile Network Applications, vol. 8, no. 4, pp;427-442, 2003

[18] L. Sweeney, "k-Anonymity: A Model for Protecting Privacy," Int'l J. Uncertainity Fuzziness Knowledge-Based Systems, vol. 10, no. 5, pp. 557-570, 2002

[19] J. Raymond, "Traffic Analysis: Protocols, Attacks, Design Issues, and Open Problems," Proc. Int'l Workshop Designing Privacy Enhancing Technologies: Design Issues in Anonymity and Unobserva-bility (WDIAU), pp. 10-29, 2001

[20] J. Li, J. Jannotti, D.S.J. De, C. David, R. Karger, and R. Morris, "A Scalable Location Service for Geographic Ad Hoc Routing," Proc. ACM MobiCom, 2000

[21] The Network Simulator - ns-2," http://www.isi.edu/nsnam/ns

Cite this article as: R Gayathri. "Location Based Routing Protocol in Manet Using Alert". *International Conference on Innovative Trends in Electronics Communication and Applications (2015)*: 143-152. Print.

International Conference on Innovative Trends in Electronics Communication and Applications 2015 [ICIECA 2015]

ISBN	978-81-929742-6-2	**VOL**	01
Website	icieca.in	**eMail**	icieca@asdf.res.in
Received	02 - April - 2015	**Accepted**	15 - November - 2015
Article ID	ICIECA022	**eAID**	ICIECA.2015.022

Realization of LBT for Co-existence of U-LTE with Wi-Fi using Cognitive Radio

A C Sumathi [1], M Priya [1], R Vidhyapriya [2]
[1]Department of Computer Science and Engineering, SNS College of Engineering, Coimbatore, Tamilnadu, India
[2] Department of Information Technology, PSG College of Technology, Coimbatore, Tamilnadu, India

Abstract: *The advanced cellular network, Long Term Evolution (LTE) which presently operates in licensed spectrum has been extended to Unlicensed LTE (U-LTE) by Qualcomm and Ericsson to improve data rate and spectral efficiency by utilizing unlicensed spectrum. Carrier Aggregation of 3GPP LTE-A supports the aggregation of licensed and unlicensed spectrum in small and femto cells to provide better user experience. The recently evolved intelligent technology viz. Cognitive radio which supports the efficient spectrum utilization is applied in the proposed system model to detect the white spaces in unlicensed spectrum to accomplish Listen-Before-Talk (LBT) regulatory requirement of radio communication in U-LTE. Another major goal of U-LTE to co-existence along with WiFi users in a non-interference style is also accomplished by the use of Cognitive radio. Based on the above concepts, it is attempted to enhance the unlicensed spectrum utilization and to address the coexistence issues in U-LTE.*

Keywords*:* LTE, U-LTE, Cognitive Radio, Carrier Aggregation, Coexistence issues, Spectrum Utilization.

INTRODUCTION

Need for U-LTE

A rapid increase of mobile data usage and emergence of new applications such as Multimedia Online Gaming (MMOG), Mobile TV, Web 2.0 streaming contents have motivated the 3rd Generation Partnership Project (3GPP) to work on the LTE on the way towards fourth-generation (4G) mobile. 4G LTE is one of several competing 4G standards along with Ultra Mobile Broadband and WiMax (IEEE 802.16). The leading cellular providers have started deploying 4G technologies, with Verizon and AT&T launching 4G LTE networks and Sprint utilizing its new 4G WiMax network. The main goal of LTE is to provide a high data rate, low latency and packet optimized radio-access technology, supporting flexible bandwidth deployments. Same time its network architecture has been designed with the goal to support packet-switched traffic with seamless mobility and great quality of service. However, the supply of (licensed) frequency spectrum allocated to cellular operators is very limited; operators have been feeling the crunch.

Qualcomm, Huawei and Ericsson lobbied the 3GPP standards committee to allow LTE service to run on the 5 GHz band. That band is one of two unlicensed bands that are typically used by Wi-Fi service. 5 GHz is the U-NII (Unlicensed National Information Infrastructure) band and since it is relatively less congested, when compared the common 2.4 GHz ISM band and because new software has been developed to make the various signals play nice within a shared spectrum band, U-LTE in the 5GHz band is winning acceptance. 5 GHz band has a shorter communication range due to higher path loss but has wider available bandwidth. Fig. 1 shows the unlicensed spectrum layout in several different main regions at 5 GHz band [1].

Cite this article as: A C Sumathi , M Priya , R Vidhyapriya. "Realization of LBT for Co-existence of U-LTE with Wi-Fi using Cognitive Radio". *International Conference on Innovative Trends in Electronics Communication and Applications (2015)*: 153-158. Print.

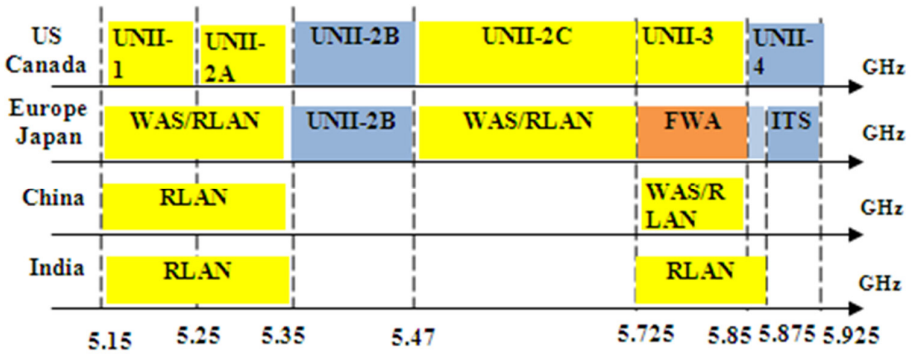

Fig. 1 Unlicensed Spectrum in different regions

Carrier Aggregation in U-LTE

The first design principle of U-LTE is the integration with licensed spectrum [2]. The integration between unlicensed and licensed carriers both operating LTE is the key operating mechanism. The Carrier Aggregation (CA) mechanisms defined in LTE Rel-10 to Rel-12 can serve this purpose in target scenarios. CA is a key feature of LTE-Advanced (LTE-A) that enables operators to create larger "virtual" carrier bandwidths for LTE services by combining separate spectrum allocations. CA is the primary feature deployed by operators with commercial LTE-Advanced service. The need for CA in LTE-Advanced arises from the requirement to support bandwidths larger than those currently supported in LTE (up to 20 MHz) while at the same time ensuring backward compatibility with LTE. The benefits of this aggregation include higher peak data rates and increased average data rates for users. CA enables the combination of up to five LTE Release 8 (Rel-8) compatible carriers [3]. The licensed LTE carriers are Primary carriers and unlicensed carriers are Secondary carriers. Since the secondary carriers are under the control of primary in situations like load shifting and channel adaption the security and service QoS are ensured. Moreover, control plane messages are always transmitted on the licensed band and thus QoS is ensured. The user-plane data can be transmitted on either licensed or unlicensed carriers.

Coexistence Features

Due to non-exclusive usage nature of unlicensed spectrum by U-LTE, there are two main challenges. The foremost challenge of design of U-LTE is its coexistence with Wi-Fi systems on a fair and friendly basis. The Wi-Fi systems are the user deployed systems and they are the incumbent users or primary users of the unlicensed band. The PHY/MAC implementation differences between LTE transmissions and Wi-Fi, hinders the direct implementation of U-LTE transmissions as it can generate continuous interference to Wi-Fi systems. Second is the coexistence with different other U-LTE operators in the same unlicensed band. The operation in unlicensed band also needs to factor in the regulatory requirements of a given region. In some markets, like Europe and Japan, a specific waveform requirement on supporting LBT (Listen-Before-Talk) at milliseconds scale is required which would need changes in LTE air interface. In other markets, like US, Korea and China, there are no such requirements. In [4] without modifying PHY/MAC standards, three mechanisms are adopted to behave U-LTE as a good neighbor. Channel selection enables the small cells in U-LTE to select cleanest channel for SDL (Supplemental Downlink) carrier transmissions. In case of dense usage of Wi-Fi and U-LTE small cells, where no clean channel can be found, Carrier-Sensing Adaptive Transmission (CSAT) algorithm is used in Time Division Multiplexing (TDM) transmissions. Final alternative method is to restrict the use of unlicensed band for SDL transmissions in case of lightly loaded small cells.

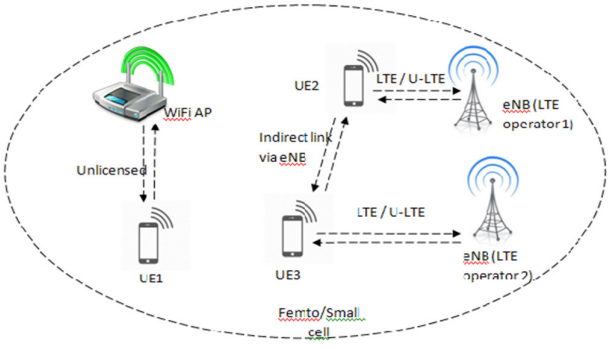

Fig. 2 Deployment Scenario of U-LTE with WiFi users

In Fig 2, the deployment scenario of U-LTE along with WiFi users is shown. User Equipments (UEs), by communicating with Wi-Fi Access Point (AP) using the unlicensed spectrum, form a *femto cell* and become primary users. During their communications with

Cite this article as: A C Sumathi , M Priya , R Vidhyapriya. "Realization of LBT for Co-existence of U-LTE with Wi-Fi using Cognitive Radio". *International Conference on Innovative Trends in Electronics Communication and Applications (2015)*: 153-158. Print.

eNodeB (eNB), UEs form *a small cell* and try to utilize the unlicensed spectrum and become secondary users. As mentioned earlier, U-LTE operates in two modes: Supplemental Downlink (SDL) and Time Division Duplex (TDD). In SDL mode, the unlicensed spectrum is used only for downlink traffic, thereby eNB performs most of the necessary operations to ensure reliable communications, including checking whether the intended unlicensed channel is free from other use [5]. For TDD mode, the unlicensed spectrum is used for both uplink and downlink, resulting additional implementation complexity in UEs for LBT feature. Latest release of 3GPP LTE standard Rel.13 supports usage of unlicensed spectrum in both operating modes [6].

In summary, it may be arrived that besides Qualcomm and Huawei, the coexistence issue for U-LTE and Wi-Fi has not been addressed extensively by researchers. Hence, in this work the usage of Cognitive Radio (CR) in small cells is proposed. In this context, the following sections discuss the fundamentals of CR, the present usage of CR in LTE, and the proposed deployment of CR in U-LTE.

COGNITIVE RADIO NETWORKS

Features of CRN

The Federal Communication Commission (FCC) defined Cognitive radio (CR) as the radio that can change its transmission parameters based on interaction with the environment in which it operates [7]. The Wireless communication has been increased and requirement of high data rate has also been increased. The licensed spectrum space remains idle at most of the times [8] due to inefficient allocation of frequencies and the cellular bands are overloaded. To meet the spectrum demands and to utilize the spectrum, FCC revisited the problem of spectrum management [9]. This inventiveness focused on CR. The IEEE 802.22 is the standard for cognitive wireless regional area networks (WRANs). The main goal of CR is to identify the unused licensed spectrum for secondary users (SU) without causing interference to the Primary User (PU). This method of sharing is often called Dynamic Spectrum Access (DSA).

Sensing Techniques

Spectrum sensing is the ability to measure, sense and be aware of the parameters related to the radio channel characteristics, availability of spectrum, transmit power, interference, noise and radio's operating environment [10]. Spectrum sensing in Cognitive Radio Networks (CRN) is done for two purposes. One is to identify the spectrum opportunities (white spaces), other to detect the interference in the spectrum. White space detection is done by Non-cooperative approach (also known as Primary transmitter method) and Cooperative/collaborative approach. Non-cooperative approach includes match filter based detection, energy based detection, covariant based detection, cyclostationary based detection, waveform based detection, etc. In Cooperative/collaborative approach, information from multiple Cognitive radio users is incorporated for primary user detection. This approach includes either centralized access to the spectrum coordinated by a spectrum server or distributed approach [11]. Interference based sensing approaches includes (i) interference temperature detection where the secondary users coexist with primary users and are allowed to transmit with low power and are restricted by the interference temperature level so as not to cause harmful interference to primary users and (ii) primary receiver detection where the interference and/or spectrum opportunities are detected based on primary receiver's local oscillator leakage power.

Channel switching Techniques

In order to improve the spectrum occupancy and also to reduce the disruption rate to primary users the secondary users schedule their spectrum usage [12]. The mechanisms used for channel switching are predictive channel switching, random channel switching and optimal channel switching. Predictive channel switching mechanism calculates the remaining idle time of each channel and the channel with the largest remaining idle time is selected for switching. Random channel switching makes the selection in random manner when the interference occurs [13]. In optimal channel switching scheme the channel that is free and offers longer remaining idle time is selected for switching. The channel selection is made either in a reactive or proactive manner. In Reactive method the secondary user opts for channel switching only after collision with the primary user. In Proactive method secondary user predicts the collision and switches the channel before it occurs.

RELATED WORKS

In [14] authors have studied the Type 2 sensing (interference detection) for single-input single-output system of LTE-Advanced network. Cognitive radio technology is applied to sense the spectrum by using the conventional method of energy detection. In [15], the effect of distance between the macro user and femto cell on Signal-interference noise ratio(SINR), Path-loss(PL) and Throughput(THR) with changing bandwidth in LTE-A environment using Cognitive radio was analysed. In [16], the authors have focused on improving resource efficiency in LTE network by considering CR Device to Device (D2D) communication links. In [17, 18], the QoS (Quality of Service) maximization requirement for secondary users in CRN built upon 3GPP LTE platform was experimented.

Cite this article as: A C Sumathi , M Priya , R Vidhyapriya. "Realization of LBT for Co-existence of U-LTE with Wi-Fi using Cognitive Radio". *International Conference on Innovative Trends in Electronics Communication and Applications (2015)*: 153-158. Print.

In summary, all the above works have focused only on LTE and LTE-A networks along with CR. However, no attempt is made in U-LTE with CR, despite CR's basic nature in exploiting white spaces efficiently. Hence, a detailed analysis has been made in this work for efficient spectrum unitization of unlicensed band for U-LTE using CR technique.

COGNITIVE RADIO IN U-LTE

System Model

The proposed system is so modelled to utilize the attributes of the CR to optimally operate U-LTE in U-NII band (5 GHz). As LBT feature is mandatory in regions like Europe, Japan and India, an efficient mechanism is to be devised to share the unlicensed spectrum with Wi-Fi, the primary users of the specified band in a non-interference basis. The extensive use of U-LTE by both primary and secondary users restricts the availability of clean channels and Qualcomm, by applying CSAT algorithm in TDM fashion, attempted to provide a solution for it. In this context, in this work, it is proposed to incorporate CR for effective spectrum sharing between U-LTE and Wi-Fi as well as between different U-LTE operators.

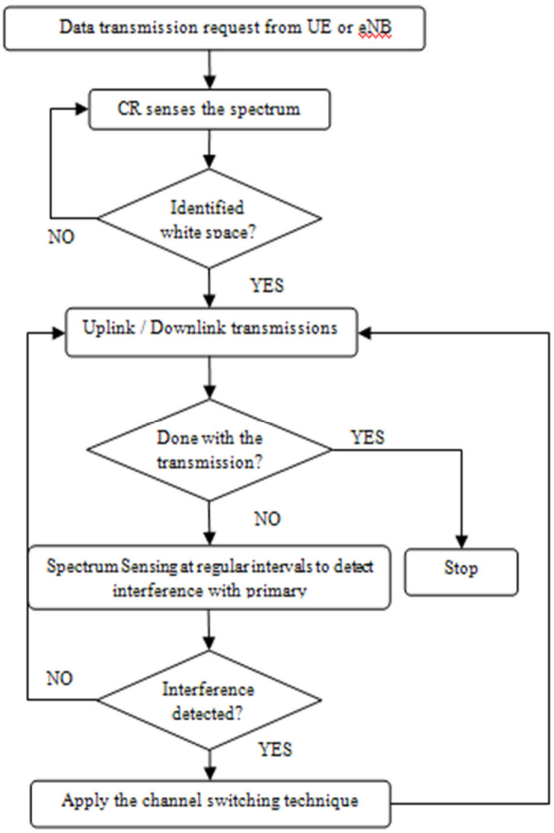

Fig. 3 System Model

Fig.3 depicts the system model of applying Cognitive radio features in U-LTE. The request of data transmission from either UE or eNB triggers the CR to sense the spectrum to identify the white space or the clean channel. Once the clean channel is identified, uplink or downlink transmissions will occur. To meet out the coexistence of U-LTE with Wi-Fi users in a non-interference basis, the CR senses the spectrum at regular intervals. Whenever the CR foresees the presence of Wi-Fi transmissions, channel switching is applied to switch the U-LTE transmissions to another clean channel. The deployment scenario of U-LTE shown in Fig.2 is enhanced with Cognitive radio devices only at eNBs for SDL mode and at UEs along with eNBs in TDD mode.

Spectrum Sharing

The major objective of the proposed work is to extend the capabilities of CR to identify the white space as well as to avoid interference with incumbent Wi-Fi users in a typical U-LTE. As stated in Section 2.2, various approaches, such as match filter based detection, energy based detection, covariant based detection, cyclostationary based detection, waveform based detection etc., can be used for white space detection by CR. Out of these techniques, it was observed by the authors that the cyclostationary methods yields better

Cite this article as: A C Sumathi , M Priya , R Vidhyapriya. "Realization of LBT for Co-existence of U-LTE with Wi-Fi using Cognitive Radio". *International Conference on Innovative Trends in Electronics Communication and Applications (2015)*: 153-158. Print.

results through their previous work [19]. When CR foresees the requirement of the spectrum under usage by an incumbent user, it uses one of the channel switching mechanisms to shift the current transmission to some other clean channel. As discussed in Section 2.3, the channel switching mechanisms presently available are predictive channel switching, random channel switching and optimal switching and the selection of the switching mechanism is left to the nature of the application and the designer.

SIMULATION RESULTS

The system model is simulated incompliance to Rel. 10/11 3GPP LTE standards using Matlab 2012(b) showing the coexistence of LTE and Wi-Fi in 5 GHz band ranging from 5.0 to 5.3 GHz, 6 channels each with assumed bandwidth of 20MHz. The first phase of simulation is attempted without LBT feature i.e. without the application of CR. In the non-LBT feature, LTE occupies the available free channel and their transmissions will long last according to the usage. Since Wi-Fi systems adopt a contention based medium access control (MAC) protocol with random back off mechanism, it finds the medium busy most of the time, resulting in high back off rate. The above scenario is simulated with entries of multiple LTE and Wi-Fi systems into the spectrum in a random fashion and their occupancy in the available free channel. The success rate of LTE and Wi-Fi systems are studied for repeated iterations of simulation run. The simulation results prove the non-friendly and unfair sharing nature of LTE in the unlicensed band by occupying the spectrum most of the time, causing interference and denying the space for the incumbent Wi-Fi users. In Fig. 4, the performance graph shows the average success rate of LTE appears higher than Wi-Fi systems.

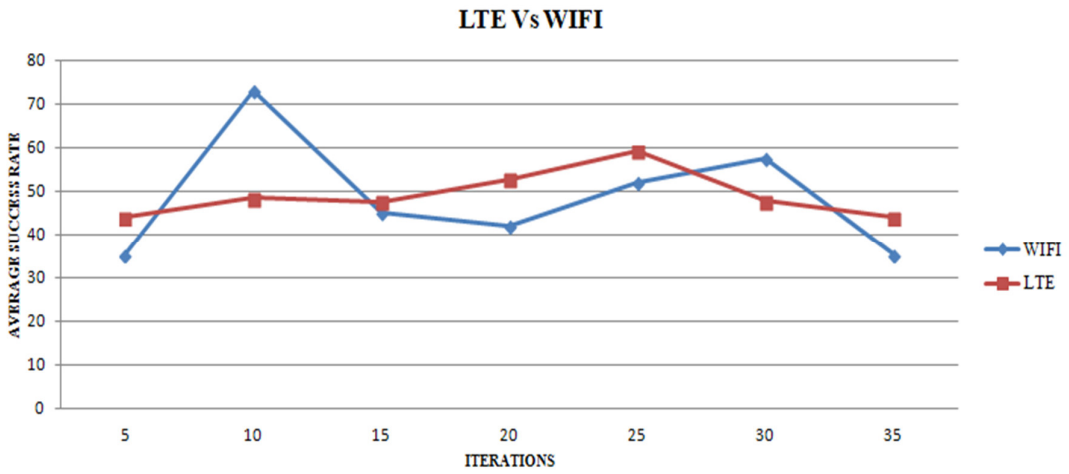

Fig. 4 Success rate of LTE and Wi-Fi systems

The second phase of simulation, inclusion of CR for the realization of LBT feature is under progress and yet to be completed.

CONCLUSION AND FUTURE WORK

The spectrum utilization of radio frequencies is gaining momentum due to the invasion of wireless equipments in every field of human life. In this regard, there is a change over from licensed LTE to U-LTE in view of the evident advantages of latter in terms of speed, cost etc. An improved method is proposed in this work to include CR in U-LTE for effective utilization of the white spaces in the radio spectrum. The basic attributes of channel searching and channel switching are utilized in this work to optimize the functionality of U-LTE in terms of clean channel searching and co-existence of secondary users with primary users. The Phase I simulation results of coexistence of U-LTE and Wi-Fi in unlicensed 5 GHz band in non-LBT fashion proved the unfair sharing of spectrum between them. The Phase II simulation with application of CR features to improve the effective spectrum sharing between U-LTE and Wi-Fi is under progress for the future publications.

REFERENCES

[1] 3GPP RP-140808, "Review of Regulatory Requirements for Unlicensed Spectrum", Alcatel-Lucent, Alcatel-Lucent Shanghai Bell, Ericcson, Huawei, HiSilicon, IASEI, LG, Nokia, NSN, Qualcomm, NTT Docomo, June 2014.

[2] Huawei, "U-LTE: Unlicensed Spectrum Utilization of LTE",available at http://www.huawei.com/ilink/en/download/hw-327803, February 2014.

[3] 4g America, "LTE Carrier Aggregation Technology Development and Deployment Worldwide" (white paper), available at https://www.4gamericas.org/files/8414/1471/2230/4G_Americas_Carrier_Aggregation_FINALv1_0_3.pdf, October 2014.

Cite this article as: A C Sumathi , M Priya , R Vidhyapriya. "Realization of LBT for Co-existence of U-LTE with Wi-Fi using Cognitive Radio". *International Conference on Innovative Trends in Electronics Communication and Applications (2015)*: 153-158. Print.

[4] Qualcomm,"Qualcomm Research LTE in Unlicensed Spectrum: Harmonious Coexistence with Wi-Fi", available at https://www.qualcomm.com/media/documents/files/lte-unlicensed-coexistence-whitepaper.pdf, June 2014.
[5] Nokia, "Nokia LTE for Unlicensed Spectrum", June 2014.
[6] 3GPP Website: http://www.3gpp.org/release-13
[7] S. Haykin, "Cognitive radio: brain-empowered wireless communications," IEEE J. Select. Areas Commun. Vol 23 (2), Feb. 2005, pp. 201– 220.
[8] Deepa Das, Susmita Das, "Primary User Emulation Attack in Cognitive Radio Networks: A Survey", IRACST, Vol.3, No3, June 2013.
[9] Carl R. Stevenson, Gerald Chouinard, "IEEE 802.22: The First Cognitive Radio Wireless Regional Area Network Standard", IEEE Communications Magazine, January 2009.
[10] Tulika Mehta, Naresh Kumar, Surender S Saini, "Comparison of Spectrum Sensing Techniques in Cognitive Radio Networks", International Journal of Electronics & Communication Technology Vol. 4, Issue Spl - 3, April - June 2013
[11] Anita Garhwal and Partha Pratim Bhattacharya,"A Survey on Spectrum Sensing Techniques in Cognitive Radio", International Journal of Computer Science & Communication Networks,Vol 1(2), 196-206
[12] Marko Hoyhtya, Sofie Pollin, and Aarne Mammela, "Improving the performance of cognitive radios through classification, learning, and predictive channel selection", Advances in Electronics and Telecommunications, Vol 2, No. 4, December 2011.
[13] Yoonchul Baek, Joon-ho Lee, Seok Lee and Hyung Seok Kim, "Predictive channel scanning and switching algorithm for the coexistence of Ieee 802.15.4 and wifi", International Journal of Innovative Computing, Information and Control Volume 9, Number 7, July 2013.
[14] Prasanth Karunakaran, Thomas Wagner, Ansgar Scherb and Wolfgang Gerstacker, "Sensing for Spectrum Sharing in Cognitive LTE-A Cellular Networks", IEEE Wireless Communications and Networking Conference (WCNC), 2014
[15] Mahmoud Nagieb, Mona Shokair, "Improvement of Coverage and Mobility in LTE-A Femto-cell based on Cognitive Radio Network", International Journal of Computer Applications (0975 – 8887) Volume 86 – No.11, January 2014.
[16] Gurwinder Singh, Puneet Mehta, "Review on Analysis of LTE and Cognitive Radio Network using OFDM Signal", International Journal on Recent and Innovation Trends in Computing and Communication Volume: 2 Issue: 8.
[17] Alia Asheralieva, Kaushik Mahata, "A Two-Step Resource Allocation for LTE-based Cognitive Radio Network", Computer Networks 59 (2014) 137–152.
[18] Alia Asheralieva, Kaushik Mahata, "Resource Allocation for LTE-based Cognitive Radio Network with Queue Stability and Interference Constraints", Physical Communication 14 (2015) 1–13.A.C.Sumathi and Dr.R.Vidhyapriya, " Detection of Malicious Secondary User Using Spectral Correlation Technique in Cognitive Radio Network", Australian Journal of Basic and Applied Sciences, 9(5) March 2015, Pages: 185-191

Cite this article as: A C Sumathi , M Priya , R Vidhyapriya. "Realization of LBT for Co-existence of U-LTE with Wi-Fi using Cognitive Radio". *International Conference on Innovative Trends in Electronics Communication and Applications (2015)*: 153-158. Print.

International Conference on Innovative Trends in Electronics Communication and Applications 2015 [ICIECA 2015]

ISBN	978-81-929742-6-2	**VOL**	01
Website	icieca.in	**eMail**	icieca@asdf.res.in
Received	02 - April - 2015	**Accepted**	15 - November - 2015
Article ID	ICIECA023	**eAID**	ICIECA.2015.023

Wireless Sensor Network for Forest Conservation using Energy Efficient Protocol

S Divya Bharathi[1], P Vimalarani [2], K Saraswathi[3]
[1,3]UG Student, ECE Department, KLN College of IT
[2]PhD Student, CSE Department, TCE
Madurai, Tamilnadu.
India

Abstract: *One of the biggest threats to humanity and nature in recent times is the change in climate such as the Global warming that is caused by the excess emissions of carbon to the atmosphere. Apart from these there are also other notable climate changes that affect nature. The major cause for Global warming is deforestation even though factors such as industrial effluents, automobile exhaust also contribute a little to this catastrophe. Many serious measures have been taken by the Government of various countries to keep in control of the rustlers involved in Deforestation. Some of these methods include fixing of a large number of cameras in certain areas of the forest spread over a wide range, awareness programs including public awareness, automatic alarm testing, use of satellites to provide images of forests, etc. Some of the issues to be considered when implementing such schemes are hugs cost and power consumption. Also the lifetime of the materials and hardware used should be considered. In this paper, an efficient wireless sensor networking algorithm is proposed that can be used to prolong the life time of the network by using the Heterogeneous - Hybrid Energy Efficient Distributed Protocol (H-HEED).*

Keywords*:* Wireless Network, Sensor nodes, Network Lifetime, Sensors.

INTRODUCTION

The major cause for the global climatic changes in many areas is the deforestation and the release of a large amount of CO_2 into the atmosphere. Not just the CO_2 but other greenhouse gases have been sent into the atmosphere. Forests have been destroyed due to many reasons such as forest fire which is a natural cause. But apart from this other activities such as logging and land conversion for agriculture were also done. So to avoid global climate changes, the deforestation and degradation of forests should be reduced. Many statistics and survey have been conducted to record such destruction. The overall statistics results show that more than 15 million hectares of forests have been lost every year globally. Due to this every year more than 15% of greenhouse gases and CO_2 is emitted globally. Deforestation occurs mostly in the tropical regions where there are large forests and tons of trees. The record stands at 87% of global deforestation occurring in these tropical countries such as Brazil, Indonesia, etc. Carbon and CO_2 emission is more in these areas and more than 210 GT (Giga Tons) of carbon has been emitted. So there is a need to keep these activities under control for the wellbeing of our planet and ourselves.

One such solution to detect these problems is by using sensors and wireless detectors. A wireless sensor network (WSN) is used to sense and monitor both physical and environmental conditions by using various interconnected sensors. These sensors are spatially distributed over an area and contain autonomous sensors that coordinate with each other or send signals. The environmental conditions denote the various conditions of the atmosphere or environment such as the pressure, temperature, vibrations, sound, etc. Each node in the WSN is also equipped with a radio transmission device called the radio transceiver and other wireless communication devices to enable communication and signal transmission. A small microcontroller is embedded inside each node to control them and

Cite this article as: S Divya Bharathi, P Vimalarani, K Saraswathi. "Wireless Sensor Network for Forest Conservation using Energy Efficient Protocol". *International Conference on Innovative Trends in Electronics Communication and Applications (2015)*: 159-165. Print.

the nodes are running using an energy source such as a battery.

At first the development and implementation of the WSN was used for surveillance of battlefield during wars and for other military operations. Most of the military applications comprise of various sensors for various needs. But in recent time they are also being used in industrial areas and public areas as well. They include monitoring the industrial processes, healthcare, environment monitoring, traffic control, habitat monitoring, etc. Other than these sensors have been used in places such as in homes, offices, banks and also in other economical areas.

Many researches have been done in the WSN in recent times but most of them focused mainly on the internal issues such as the MAC, the routing protocols used for transmission, energy saving and other issues related to the lifetime of the nodes. In some areas research also focus on the architecture of the gateways that connect the WSN and the rest of the world. Here the lifetime of a node or the node's life time is an important factor and increasing the node's life time is a good research focus.

This can be done by using the Hybrid Energy Efficient Distributed (HEED) protocol as discussed in [4]. It is a clustering protocol that uses the available residual energy as the primary parameter and network topology features such as the distance to nearby nodes and node degree are used as the secondary parameters. The secondary parameters are used to break the ties between various candidate cluster heads during cluster selection for load balancing. Here all nodes in the WSN are taken to be homogeneous nodes where all the nodes contain the same initial energy.

In this paper, the study focuses on the impacts of heterogeneity in case of energy of the nodes. That is the impact of varying energies within the nodes should be studied. So an assumption is made where we take some percentage of the nodes to have more energy than the other nodes within the same network. As the lifetime of the WSN is limited it keeps degrading and the energy should be refilled by adding new nodes to the network. These nodes are added with more energies than the energies available in the nodes that are within the network. This way again the heterogeneity is preserved [15] and the study can be continued.

STATE-OF-ART IN FOREST MONITORING

Forest monitoring have been done to prevent deforestation and to sense any activities that will endanger the environment of the forest. Apart from forests, other areas of the planet have also been sensed for other activities. Remote sensing is an essential method that can make observations over a large area of the surface of the Earth more than possible by normal ground based observations. The remote sensing makes use of a large number of resources to accomplish this task. A number of cameras and multi-spectral scanners are used for capturing and sensing the places. RADARs are mounted over the air-borne and space-borne platforms. The remote sensing can take aerial photographs and satellite images as well and also yield LiDAR datasets. The data available from remote sensing varies in resolution and quality depending on the method that is used for image capturing. To capture images over a single province of a country or over a large geographical area, the aerial photography, satellite imaging, LiDAR are used and high resolution satellite sensors such as IKONOS and Quickbird are used. The regional datasets of specific regions are captured at regular intervals from satellites such as SPOT, Landsat, etc. and the lower resolution data are captured across the entire planet everyday using satellites like MODIS. By comparing and analyzing the image data with respect to the extent of the forest and its texture, it is possible to identify the areas of the forest that have been illegally poached or extinguished due to forest fire or other causes.

Another existing sensor and notification system is the Automatic Alarm System. The system provides an alarming mechanism to the main monitoring system by making use of various sensors and the MSP430 controller and the Chipcon CC2420. The system is embedded with the Zigbee protocol for operations. The major disadvantage in this system is that the lifetime of the sensors Is very short due to large power consumption.

NEED FOR HEED PROTOCOL

The remote sensing method explained above can cover over a large area of the planet or a forest alone specifically. Due to this the officials will not be able to identify the specific place where the forest poaching happened. The change in terrain and texture of the forests can be seen but not the exact location unless they can go and confirm. Also this method demands the use of a large amount of money for the RADARs and satellites. In case of the Automatic Alarm System as said before the power or energy consumption of the sensors is large and so the refilling of energy should be done often. So there is a need for increasing the lifetime of a sensor node.

This can be achieved by implementing clustering mechanism using the Hybrid Energy Efficient Distributed (HEED) protocol. Using this protocol, the exact locations of the poaching or any other activities in a forest can be identified by enhancing the lifetime of a sensor node in a cost effective manner. By improving the lifetime the sensors can be used for a longer duration that will help the system to identify specific areas. The proposed method requires a two-step simulation process; (1) the first step describes the formation of clusters using the HEED protocol and also explains about the heterogeneous HEED protocol (H-HEED protocol) and (2) the second step shows the performance of the performance of the H-HEED protocol obtained from the simulation and it is compared with the performance of the original HEED protocol.

Cite this article as: S Divya Bharathi, P Vimalarani, K Saraswathi. "Wireless Sensor Network for Forest Conservation using Energy Efficient Protocol". *International Conference on Innovative Trends in Electronics Communication and Applications (2015)*: 159-165. Print.

PROPOSED SYSTEM

The HEED Protocol

The HEED protocol is implemented in MATLAB by creating a simulation of sensor nodes connected in a WSN. Let us consider there are a total of N sensor nodes in the WSN and that they are dispersed in various locations randomly over a square region of 100*100 square meters. This is shown below in Figure 1 as simulated in MATLAB. Certain assumptions have been made for the clustering algorithm for the clustering of the given network model. The basic assumptions are:

1) The nodes in the WSN are quasi-stationary
2) The locations of all the nodes are not known.
3) All nodes are similar in characteristics such as processing, communication and performance.
4) The nodes are left unattended after they are deployed into the network.

The cluster heads are the center nodes for each of the clusters within the network and the selection of cluster heads are primarily defendant on the amount of energy left in each node, which is the residual energy of the nodes. Every time a node involves itself in activities such as sensing, processing or communication then a little bit of energy is consumed for such activities. So the consumed energy is kept noted for each activity and the residual energy or the remaining energy of each of the nodes is calculated based on this.

During the clustering process, sometimes there may be a tie between two cluster head when a sensor node falls within the range of both these cluster heads. In such cases a secondary parameter is used to identify the cluster head to which it should be assigned. This parameter is the intra cluster communication cost. The intra cluster communication cost is the energy needed or consumed when the node wants to communicate with other nodes in other clusters. The ties are broken and the node which yields less intra cluster communication cost is favoured. This intra cluster communication cost parameter (C) is a function two things: (1) the properties of the cluster such as cluster size and (2) the fact if varying power levels are permitted for intra cluster communication or not. This is the power level (P) used for the intra cluster communication.

If this power level is fixed for all the sensor nodes and the requirement is to distribute the load among various cluster heads then:

$$C \propto Node\ Degree$$

That is the cost is directly proportional to the Node Degree in this case. And if the power level is fixed for all nodes and the requirement is to create dense clusters then:

$$C \propto \frac{1}{Node\ Degree}$$

That is the cost is inversely proportional to the Node Degree. This means that a particular node will join a cluster head with minimal node degree if the priority is to maintain or distribute loads with all cluster heads and it will join a cluster head with maximal node degree if the priority is to create a dense cluster with more nodes.

Each of the nodes in the network performs a neighbor discovering phase where they detect their neighboring nodes and then broadcast their communication cost to them. This way the other nodes will know how much it costs to communicate with the other nodes. Similarly each of the nodes maintains a probability value for itself that say how much probability is there for that node to become a cluster center. The probability value CH_{prob} is given as below:

$$CH_{prob} = \max\left(C_{prob} * \left(\frac{E_{residual}}{E_{max}}\right), P_{min}\right) \quad (1)$$

Here,

C_{prob} – Initial percentage of cluster heads probability for the N nodes (set to 0.05)

E_{max} – Maximum energy of a node

$E_{residual}$ – Residual energy of a node

P_{min} – Threshold value for probability

The cluster head formation of the network in the MATLAB simulation is shown below in Figure 1.

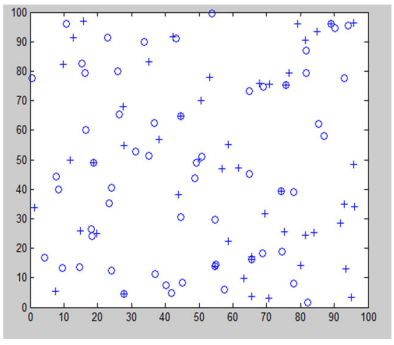

Figure 1. Cluster head formation in HEED network

Cite this article as: S Divya Bharathi, P Vimalarani, K Saraswathi. "Wireless Sensor Network for Forest Conservation using Energy Efficient Protocol". *International Conference on Innovative Trends in Electronics Communication and Applications (2015)*: 159-165. Print.

Heterogeneous HEED Protocol

The Heterogeneous HEED protocol or model uses varying energy levels for the nodes. The H-HEED protocol makes use of two or three types of nodes based on the needs and they are called the 2-level H-HEED protocol and the 3-level H-HEED protocol respectively. First let us take a look at the 2-level H-HEED protocol.

The 2-level Heterogeneous HEED protocol uses two types of sensor nodes in the network such as the (1) Normal nodes and (2) Advanced nodes. Consider a network that contains a total of N sensor nodes out of which the faction of advanced nodes is m. So the total number of advanced nodes is:

$$N_{adv} = N * m \quad (2)$$

The total fractions of number of normal nodes are given as $(1 - m)$ and the number of normal nodes is given as:

$$N_{norm} = N * (1 - m) \quad (3)$$

Let the initial energy of all the normal sensor nodes be E_{norm} and the initial energies of all the advanced nodes be kept higher than that of the normal nodes. The advanced nodes have α times more energy than the normal nodes. So the initial energies of the advanced nodes is given by:

$$E_{adv} = E_{norm} * (1 + \alpha) \quad (4)$$

The total initial energy of the whole network [9] combining the normal nodes and advanced nodes is then given as below:

$$E_{total} = (N_{norm} * E_{norm}) + (N_{adv} * E_{adv})$$
$$= [N * (1 - m) * E_{norm}] + [N * m * E_{norm} * (1 + \alpha)]$$
$$E_{total} = N * E_{norm} * (1 + \alpha * m) \quad (5)$$

From the above equation it is known that the 2-level H-HEED network has $(\alpha * m)$ time more energy than the normal HEED networks for the same number of sensor nodes. So the advanced nodes with higher energies can be used for special activities such as detecting specific locations of forest fire or forest poaching activities that will take more time than usual

The 3-level Heterogeneous HEED protocol uses three types of sensor nodes in the network such as the (1) Normal nodes, (2) Advanced nodes and (3) Super nodes. Same as in the 2-level H-HEED network consider a network that contains a total of N sensor nodes out of which the faction of advanced nodes and super nodes combined is m and the fraction of super nodes from this fraction m is m_0. So the total number of normal, advanced and super nodes is given as below:

$$N_{sup} = N_{norm} * m_0 \quad (6)$$
$$N_{adv} = N_{norm} * (1 - m_0) \quad (7)$$
$$N_{norm} = N * (1 - m) \quad (8)$$

Here also let the initial energies of the normal nodes be E_{norm} and the initial energies of the advanced and super nodes are higher than the normal nodes. Let the initial energy of the advanced nodes be α times more than the normal nodes and the initial energy of the super nodes be β times more than the normal nodes. Thus the initial energies of the advanced and super nodes are given as:

$$E_{adv} = E_{norm} * (1 + \alpha) \quad (9)$$
$$E_{sup} = E_{norm} * (1 + \beta) \quad (10)$$

The total initial energy of the whole network [13] [14] combining the normal nodes, advanced nodes and the super nodes is then given as below:

$$E_{total} = (N_{norm} * E_{norm}) + (N_{adv} * E_{adv}) + (N_{sup} * E_{sup})$$
$$= [N * (1 - m) * E_{norm}] + [N * m * (1 - m_0) * E_{norm} * (1 + \alpha)] + [N * m * m_0 * E_{norm}(1 + \beta)]$$
$$E_{total} = N * E_{norm} * [1 + m * (\alpha + m_0 * \beta)] \quad (11)$$

From the above equation it is seen that the 3-level H-HEED network has $(m * (\alpha + m_0 * \beta))$ time more energy than the normal HEED networks for the same number of sensor nodes.

In the multi-level Heterogeneous HEED protocol the initial energy value of each of the sensor nodes in the network is randomly distributed over the closed set range as given below:

$$[a_{min}, a_{max}] = [E_{norm}, E_{norm} * (1 + a_i)]$$

Here a_{min} and a_{max} are the upper bound and lower bound values of the range and they represent the minimal and maximal energies respectively. A node N_i is assigned with an initial energy that is a_i time higher than the normal initial energy E_{norm} and it is given as below:

$$E_i = E_{norm} + (1 + a_i) \quad (12)$$

The total initial energy of the whole network [11] is then given as below:

$$E_{total} = \sum_{i=1}^{N} E_{norm} * (1 + a_i)$$
$$= E_{norm} * (N + \sum_{i=1}^{N} a_i) \quad (13)$$

During the cluster formation phase each node has its own maximum energy level value defined by E_{max} and this is only in cases of heterogeneity HEED networks.

Cite this article as: S Divya Bharathi, P Vimalarani, K Saraswathi. "Wireless Sensor Network for Forest Conservation using Energy Efficient Protocol". *International Conference on Innovative Trends in Electronics Communication and Applications (2015)*: 159-165. Print.

SIMILATION RESULTS

The simulation is done using the MATLAB environment. A heterogeneous sensor network is considered with a total of $N = 100$ sensor nodes that are randomly distributed over the square area of 100*100 square meters. The base station of the whole network is assumed to be positioned in the center of the square area at position $(50,50)$. Initially the parameter values for the cluster head probabilities are set as below:

$$P_{min} = 0.0001$$
$$C_{prob} = 0.05$$

The energy consumed for transmitting message from or to the radio should also be calculated during the simulation. The energy consumed by the radio for transmitting a $k - bit$ message over a total distance of D is given as below:

$$E_{Tx}(k, D) = E_{Tx-elec}(k) + E_{Tx-amp}(k, D) \quad (14)$$

$$E_{Tx-amp}(k, D) = \begin{cases} kE_{fs}D^2 \\ kE_{mp}D^4 \end{cases} \quad (15)$$

$$E_{Tx-elec}(k) = kE_{elec} \quad (16)$$

Similarly the energy consumed by the radio to receive a message of $k - bit$ over a total distance of D is given as below:

$$E_{Rx}(k) = E_{Rx-elec}(k) = kE_{elec} \quad (17)$$

Here,

E_{elec} – Electronics energy

$E_{fs}D^2$ *and* $E_{mp}D^4$ – Amplification energies

The electronics energy constitutes to the energy consumption activities such as the coding and decoding of messages, modulation, filtering, sending and receiving signals, etc. The amplification energy constitutes to factors such as the distance of transmission and the error rate of the message that is transmitted. Apart from these the other external factors such as noise are ignored.

In the simulation process the various parameters such as the number of sensor nodes and their initial energies are defined at the start. The parameters for the different types of HEED protocol that is used for the experimentation is as below in Table 1:

TABLE 1
PARAMETERS FOR EXPERIMENTATION

Protocol	**Parameters**
HEED	$N = 100, P_{min} = 0.0001, C_{prob} = 0.05$
2-level H-HEED	$m = 0.25,\ N_{adv} = 25,\ N_{norm} = 75,\ E_{norm} = 100\%,\ \alpha = 1.25,\ E_{adv} = 125\%$
3-level H-HEED	$m = 0.30,\ m_0 = 0.4,\ N_{norm} = 70,\ N_{adv} = 18,\ N_{sup} = 12,\ E_{norm} = 100\%,\ \alpha = 1.25,\ \beta = 2.5,\ E_{adv} = 125\%,\ E_{sup} = 250\%$
Multi-level H-HEED	$a_{min} = 0.25,\ a_{max} = 2.5$

The simulation is executed in MATLAB for the designed HEED network by using 100 sensor nodes in the 100*100 square meters area. During the simulation each of these nodes form clusters by implementing the above discussed 4 types of HEED protocols and finally a comparison is made between these algorithms. At the time of simulation after forming clusters the sensor nodes keep communicating with each other and also send data packets to the base station (located in the center) about the various sensing activities. The energies of the nodes are consumed over the round and after the normal nodes lose their energy completely then they are refilled again to start the next round. At the start of next round again the nodes are cluster with new cluster heads. The performance of the HEED protocol is tested by taking three analyses as given below:

1) By calculating the number of alive nodes at each round.
2) The total remaining energy in each round.
3) The number of packets sent to the base station in each round.

Figure 2 below shows the comparison of the number of alive nodes at each round. In case of HEED since all the nodes are normal they die fast after consuming the energy. But in case of the 2-level and 3-level H-HEED networks the advanced and super nodes live for longer duration of time and so such nodes stay alive even after the round completes. In the multi-level H-HEED the sensor nodes die at random time due to their random energies. On average the multi-level H-HEED provides good performance here.

Figure 3 below shows the total amount of energy remaining after the end of each round. This is the sum of residual energies of all the nodes in the network except the base station. If the residual energy or remaining energy is high then after the sensing round is over this

Cite this article as: S Divya Bharathi, P Vimalarani, K Saraswathi. "Wireless Sensor Network for Forest Conservation using Energy Efficient Protocol". *International Conference on Innovative Trends in Electronics Communication and Applications (2015)*: 159-165. Print.

energy can be used to send many data packets to the base station as review of the sensing. From the figure it is seen that the 3-level H-HEED and the multi-level H-HEED networks have more residual energy lef.t compared to that of the normal HEED and 2-level H-HEED networks. This way the forest poaching and sudden forest fires can be alerted to nearby base stations easily and faster by using the residual energy left after sensing.

Figure 4 below shows the total number of packets sent to the base station at each round. The performance is said to be high if the number of packets is also high since more packets means more reports and sensing information have been shared. This depends directly on the residual energy left because nods having more residual energy have higher probability to become the cluster head and more energy will help the nodes to send more packets. From the figure it is clear that the 3-level H-HEED and the multi-level H-HEED networks have a really high packet delivery ration compared with the other two methods.

By comparing all the results from above it is evident that the multi-level H-HEED protocol and the 3-level H-HEED protocols are more efficient and can be used for the sensing of activities and forest poaching in various areas. This way the energy consumption is reduced and the overall lifetime of the sensor nodes are increased so they can keep sensing for more information and can send more amounts of data packets and reports back to the base station or the officials.

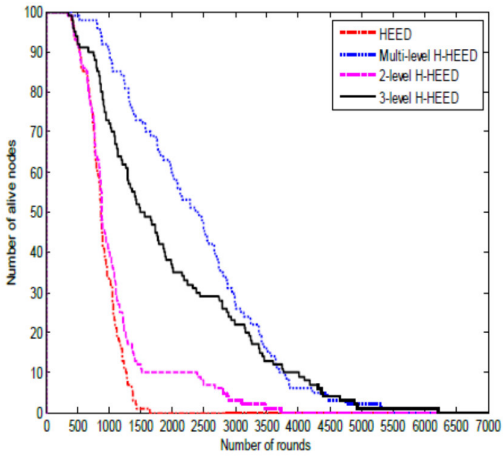

Figure 2. Comparison of number of nodes alive at each round in HEED networks

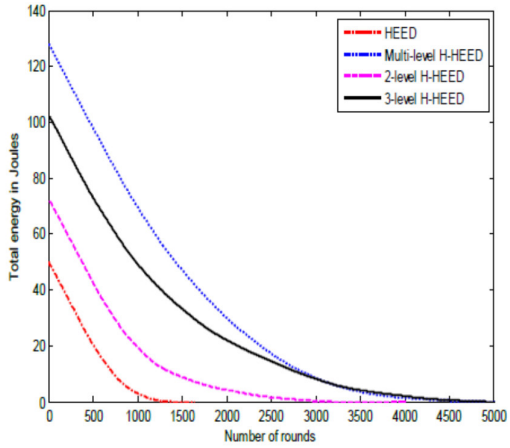

Figure 3. Comparison of total remaining energy at each round in HEED networks

Cite this article as: S Divya Bharathi, P Vimalarani, K Saraswathi. "Wireless Sensor Network for Forest Conservation using Energy Efficient Protocol". *International Conference on Innovative Trends in Electronics Communication and Applications (2015)*: 159-165. Print.

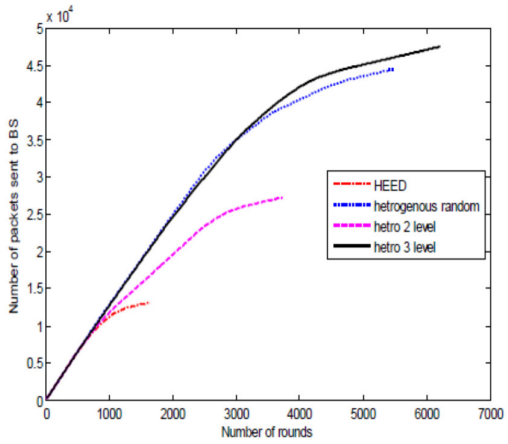

Figure 4. Comparison of number of packets sent to base station in HEED networks

CONCLUSIION

The lifetime of a sensor node is an important factor in any WSN. By increasing the lifetime it is possible to achieve many tasks in sensing and monitoring. In this paper the lifetime of sensor nodes are increased by implementing the heterogeneous HEED protocol or the H-HEED protocol. Different levels of heterogeneity were used in the proposed system such as the 2-level, 3-level and multi-level in terms of the energy of the sensor nodes. By improving the lifetime of the sensor nodes, the officials and the government were able to monitor the poaching activities and other activities in the forest easily.

REFERENCE

[1] Vieira, M.A.M; Coelho, C.N; da Silva, D.C., Jr.; da Mata, J.M; "Survey on Wireless Sensor Network Devices", IEEE Conference on Emerging Technologies and Factory Automation, Volume 1, pp. 537-544, September 2003.

[2] Raghunathan, V; Schurgers, C; Sung Park; Srivastava, M.B; "Energy-aware Wireless Micro-sensor Networks", IEEE Signal Processing Magazine, Volume 19, Issue 2, pp. 40-50, March 2002.

[3] Akyildiz, I.F; Weilian Su; Sankarasubramaniam, Y; Cayirci, E; "A Survey on Sensor Networks", IEEE Communication Magazine Journal, Volume 40, Issue 8, pp. 102-114, August 2002.

[4] Ossama Younis; Sonia Fahmy; "Distributed Clustering in Ad-hoc Sensor Networks: A Hybrid, Energy-Efficient Approach", Twenty-third Annual Joint Conference of the IEEE Computer and Communications Society (INFOCOM), March 2004.

[5] Heinzelman, W.R; Chandrakasan, A; Balakrishnan, H; "Energy-Efficient Communication Protocol for Wireless Micro-sensor Networks", Proceedings of the 33rd Hawaii International Conference on System Sciences (HICSS), January 2000.

[6] Lindsey, S; Raghavendra, C.S; "PEGASIS: Power-Efficient Gathering in Sensor Information Systems", IEEE Aerospace Conference Proceedings, Volume 3, pp. 1125-1130, 2002.

[7] Arati Manjeshwar; Agarwal, D.P; "TEEN: A Routing Protocol for Enhanced Efficiency in Wireless Sensor Networks", In Proceedings of the 15th International Parallel and Distributed Processing Symposium, pp. 2009-2015, April 2000.

[8] Arati Manjeshwar; Agarwal, D.P; "APTEEN: A Hybrid Protocol for Efficient Routing and Comprehensive Information Retrieval in Wireless Sensor Networks", In Proceedings of the International Parallel and Distributed Processing Symposium (IPDPS) with Abstracts and CD-ROM, pp. 195-202, April 2001.

[9] Georgios Smaragdakis; Ibrahim Matta; Azer Bestavros; "SEP: A Stable Election Protocol for Clustered Heterogeneous Wireless Sensor Networks. 2nd International Workshop on Sensor and Actor Network Protocols and Applications (SANPA), 2004.

[10] Mao Ye; Chengfa Li; Guihai Chen; Jie Wu; "EECS: An Energy Efficient Clustering Scheme in Wireless Sensor Networks", 24th IEEE International Performance, Computing and Communications Conference, pp. 535-540, April 2005.

[11] Li Qing; Qingxin Zhu; Mingwen Wang; "Design of a Distributed Energy Efficient Clustering Algorithm for Heterogeneous Wireless Sensor Networks", Computer Communications Journal, Volume 29, Issue 12, pp. 2230-2237, August 2006.

[12] Heinzelman, W.B; Chandrakasan, A.P; Balakrishnan, H; "An Application-specific Protocol Architecture for Wireless Micro-sensor Networks", IEEE Transactions on Wireless Communications, Volume 1, Issue 4, pp. 660–670, October 2002.

[13] Trilok C. Aseri; R. B. Patel; Dilip Kumar; "EEHC: Energy Efficient Heterogeneous Clustered Scheme for Wireless Sensor Networks", International Journal of Computer Communications, Elsevier, Volume 32, Issue 4, pp. 662-667, March 2009.

[14] Yingchi Mao; Zhen Liu; Lili Zhang; Xiaofang Li; "An Effective Data Gathering Scheme in Heterogeneous Energy Wireless Sensor Network", International Conference on Computational Science and Engineering (CSE), Volume 1, pp. 338-343, August 2009.Sakthi, A; Jeyalakshmi, R; Dr. Hariharan, K; "A Novel Wireless Sensor Network for Forest Conservation", CII INNOVATOR '11 Magazine, 2011.

Cite this article as: S Divya Bharathi, P Vimalarani, K Saraswathi. "Wireless Sensor Network for Forest Conservation using Energy Efficient Protocol". *International Conference on Innovative Trends in Electronics Communication and Applications (2015)*: 159-165. Print.

International Conference on Innovative Trends in Electronics Communication and Applications 2015 [ICIECA 2015]

ISBN	978-81-929742-6-2
Website	icieca.in
Received	02 - April - 2015
Article ID	ICIECA024

VOL	01
eMail	icieca@asdf.res.in
Accepted	15 - November - 2015
eAID	ICIECA.2015.024

FPGA Digital Data Acquisition with Rate Buffering for X-ray Sensor for XSM payload of Chandrayaan-2

Priyanka D Goswami[1]
[1]Instrumentation and Control Engineering,
Institute of Technology, Nirma University
Ahmedabad, Gujarat

Abstract: *The XSM is one of the proposed sensors for the Chandrayaan-2 satellite. It measures the X-ray spectrum of solar x-ray. The paper discusses a UART based digital data acquisition system that consists of three modules: the clock generator block, the ADC interface block that converts the 16 bit data to 8 bit data and the UART module that transmits the data In serial form using RS232 protocol with start and stop bits. The programming is done using Verilog language in Libero IDE software. The testing is done using ModelSim. The UART has been developed in the Actel ProAsic 3 FPGA.*

Keywords*:* XSM, Chandrayaan-2, ModelSim.

INTRODUCTION

Solar X-ray Spectrometer (XSM) is one of the proposed sensors for the Chandrayaan-2 satellite (orbiter), which will be launched in the near future by ISRO, India. This sensor will provide measurement of X-ray spectrum of solar X-rays in the energy range of 1- 20 keV with energy resolution of approximately 200eV at 5.9 keV. XSM instrument will be made up of the sensor package and the electronics package. The detector analog output will be pre-processed for event detection, and then converted to digital form using 10 bit ADC, which will be processed further in a FPGA (Field Programmable Gate Array) [1]. The digital data stream will be transferred to the satellite data transmission electronics for sending it to Earth stations.

Here I describe a FPGA based Digital Data Acquisition Subsystem (DDAS), which receives the XSM ADC digitized word stream, provides a simple rate buffering and then an output serial stream with UART format. All components of the DDAS, including the UART convertor are designed, developed and implemented within a Pro-ASIC Actel FPGA.

XSM Instrument- Brief

The X-ray radiation will be detected by a silicon drift detector, which provides a very fast response and a wide dynamic range. The detector will have a suitable window and cover to provide the threshold limit for high energy X-rays up to 1 keV. It will be also covered with a aluminum cap, very close, which will provide it a wide field of view. Additionally protection covers from intense and sudden solar X-ray bursts will be incorporated. This sensor module will be mounted on a bracket outside the satellite. Signals from the sensor will be brought out, and transferred to the XSM electronics module, in the satellite. Temperature of the sensor module is maintained using a temperature controller. Electronics processing circuits include sensor signal pre-processing using pre-amplifiers, peak detection and Analog to Digital conversion (10 bit). The raw data rate from the ADC, is such that after the post processing, the instrument will generate 1024 channel energy spectrum information per second[1] .The processed digital data is formatted and transferred to the payloads data processing unit.

Cite this article as: Priyanka D Goswami. "FPGA Digital Data Acquisition with Rate Buffering for X-ray Sensor for XSM payload of Chandrayaan-2". *International Conference on Innovative Trends in Electronics Communication and Applications (2015)*: 166-169. Print.

FPGA DIGITAL DATA ACQUISITION SYSTEM

FPGA Digital Data Acquisition System

A system for acquiring the raw SDD digitized (10bit) data, with a simple computer interface is required, during the development and testing of the XSM sensor. The raw data rate is higher than the final sensor data rate and it can be of the variable rate. Further it should have the minimum devices and simple operation. Hence the design of the DDAS was carried out such that, it could be incorporated within the Actel Pro-Asic FPGA device that was used to interface with the ADC circuit board. The output was required on a commonly available I/O port in any desktop computer, with minimum wiring connections, and with default software drivers on the computer. To meet with these, the DDAS was designed with a front end data buffering register set with the control signals driven by the ADC, a serial to parallel convertor with direct formatting for UART/RS-232c serial format connected to a buffered output pin of FPGA to drive the serial data to a computer RS-232 port.

This design does not require any external UART or USB interface device, and thus reduces the complexity, while also removing the need to provide FPGA logic, required to initialize and control such special devices, which also requires involved HDL programming, special UART device control/programming lines . At the same time, it only provides that RS-232 functionality subset which is required for this application. The goal is continuous data acquisition with the above scheme by selecting a UART transmission rate at least two times faster than the input data rate.

Design and Implementation Method

Design and HDL coding was carried out using Verilog, using the Libero project environment, natively used for the Actel Pro-Asic devices. The code simulation and verification was done using Modelsim (in built in Libero). The Steps followed for the design, development and simulation of DDAS are shown in figure.1.

Some of the features and facilities in Libero, used to implement the project were:

- Project and design flow management
- Synplify Pro ME synthesis which optimizes Actel FPGA device performance and area utilization.
- Modelsim ME VHDL or Verilog behavioral, post-synthesis and post-layout simulation.
- Physical design implementation and I/O pin layout.
- Interface for device programmer.

Modular approach was followed for DDAS design, with each module implementing a specific function and connected to other modules with defined electrical and timing interfaces. This resulted in ease of simulation and testing the DDAS. The modules are (1) Clock generator (2) ADC interface and register set for initial rate buffering (3) Parallel word to serial and UART formatting along with serial output.

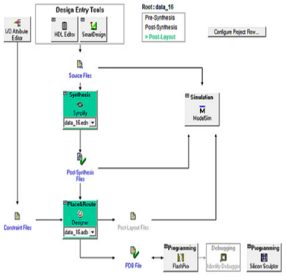

Figure.1. Flowchart showing steps of project development in Libero IDE

Each module is briefly described,

- Clock Generator was created to give the desired clock rate to the UART block. The block would use the 40MHz FPGA clock as the input and using a frequency divider reduce the clock frequency to standard frequency required by the UART for data transmission.

Cite this article as: Priyanka D Goswami. "FPGA Digital Data Acquisition with Rate Buffering for X-ray Sensor for XSM payload of Chandrayaan-2". *International Conference on Innovative Trends in Electronics Communication and Applications (2015)*: 166-169. Print.

- The ADC Interface module took the input, 16 bit data from the ADC (Analog to Digital Convertor). This data is divided into two 8 bit words (MSB and LSB) and transmitted over to the UART block, along with necessary timing signals This is required as UART can send maximum 8 bit data (excluding start and stop bits) in one cycle.
- UART module in which the 8 bit parallel data received from the above block is transmitted serially and the output can be taken from the assigned I/O pin of the FPGA and given to the RS232 port of PC for data transmission. Hence this block will basically act as a parallel to serial data convertor with the ADC 8 bit byte (part of the Word) inserted into the UART work register at the required bit locations. The output data packet for each input byte will be of 11 bits (1 start bit, 8 bit data, and 2 stop bits) and this will be transmitted serially.

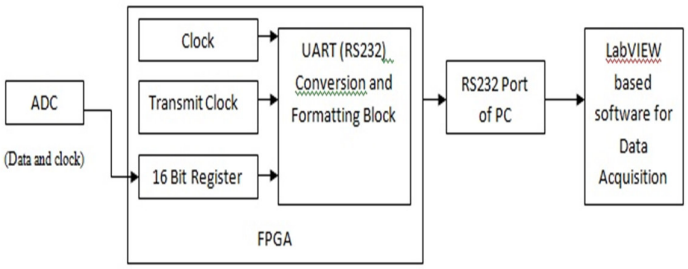

Figure.2. Block Diagram of DDAS module

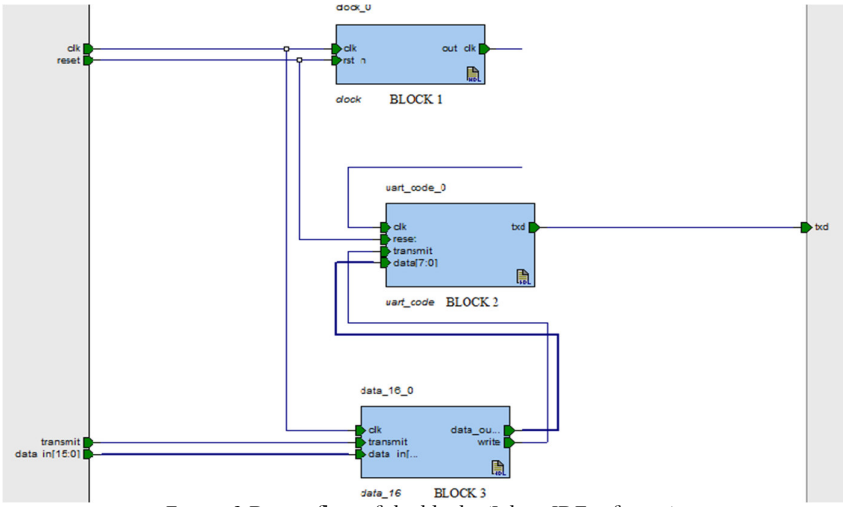

Figure.3 Design flow of the blocks (LiberoIDE software)

Simulation and Testing

Each block was created compiled and simulated in th Libero IDE software using tools such as HDL Editor, SySnplify and ModelSim. The simulation was carried out fofor different UART bit rates like 76 kbits and 115 kbits. Microsemi FlashPRO module was used to load the HDL code in the FPGA and the output was observed on the DSO.

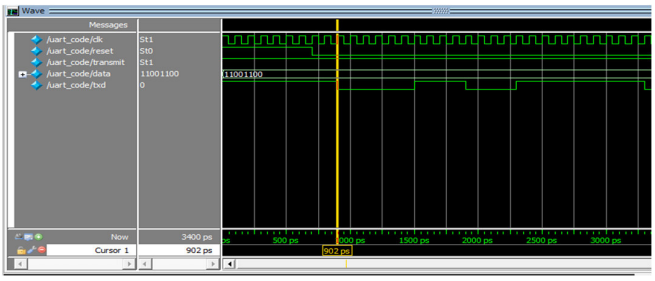

Figure.4. Output waveforms of UART using ModelSim

Cite this article as: Priyanka D Goswami. "FPGA Digital Data Acquisition with Rate Buffering for X-ray Sensor for XSM payload of Chandrayaan-2". *International Conference on Innovative Trends in Electronics Communication and Applications (2015)*: 166-169. Print.

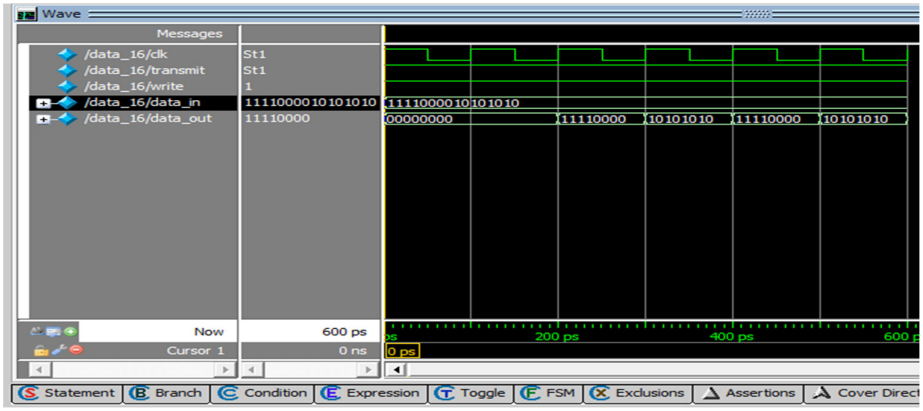

Figure.5.Output waveforms of 16 bit to 8 bit convertor using ModelSim

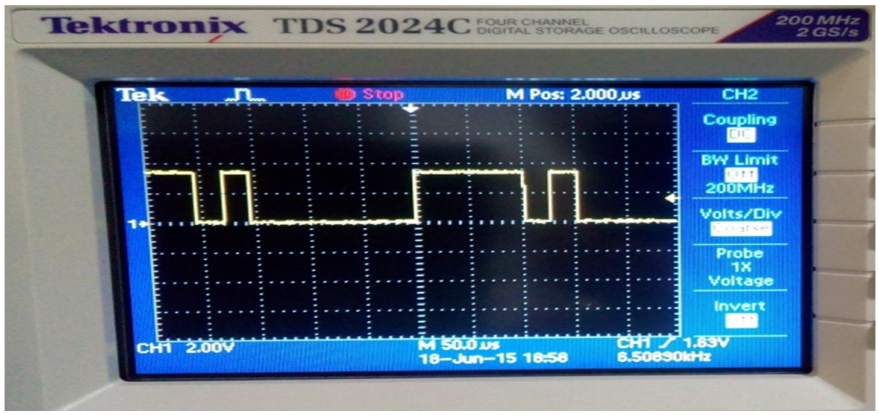

Figure.6. Waveform of 11 bit serial output for 8 bit parallel input data given to UART (as seen on DSO)

CONCLUSION

The DDAS with a UART serial data interface, compatible with the XSM detector digitized data stream was designed, developed and tested with the Actel Pro-Asic FPGA.

ACKNOWLEDGMENT

I would like to convey my gratitude to Mr. M Shanmugam, Sr. Scientist,PRL,DOS, for providing me with the opportunity to work at the PLANEX laboratory, and for guiding me throughout the project. I would also like to thank Mr. Arpit Patel, Mr.Tinkal Ladiya and the other staff members for helping me, guiding me and providing the required resources for the successful completion of the project. I am also thankful to the Dean, Physical Research Laboratory, DOS, and Ahmedabad for granting me the opportunity to work at this prestigious institution.

REFERENCES

[1] Real World FPGA Design with Verilog by Ken Coffman, Prentice Hall PTR
[2] M. Shanmugam, S. Vadawale, Y. B. Acharya, S. K. Goyal, Arpit Patel, Bhumi Shah and S. V. S. Murty "Solar X-ray Monitor (XSM) on-board Chandrayaan-2 orbiter" 43rd Lunar and Planetary Science Conference, March 2012, LPI Contribution No. 1659, id.185
[3] Computer Arithmeic and Verilog HDL Fundamentals by Joseph Cavanagh, CRC Press
[4] Actel ProAsic [Online] www.microsemi.com

Cite this article as: Priyanka D Goswami. "FPGA Digital Data Acquisition with Rate Buffering for X-ray Sensor for XSM payload of Chandrayaan-2". *International Conference on Innovative Trends in Electronics Communication and Applications (2015)*: 166-169. Print.

International Conference on Innovative Trends in Electronics Communication and Applications 2015 [ICIECA 2015]

ISBN	978-81-929742-6-2	**VOL**	01
Website	icieca.in	**eMail**	icieca@asdf.res.in
Received	02 - April - 2015	**Accepted**	15 - November - 2015
Article ID	ICIECA025	**eAID**	ICIECA.2015.025

Design of Multiband Microstrip Patch antenna with I-shape slot for wireless applications

Nilima Arun Bodhaye[1], Prasanna L Zade[2]
[1]Electronics and Telecommunication Department, Priyadarshini College of Engineering, Nagpur, India
[2]Electronics and Telecommunication Department, Yashwantrao Chavan college of Engineering, Wanadongri

Abstract: *In this paper a new structure of multiband micro strip patch antenna is designed and analysed. The proposed micro strip patch antenna is designed with H-shaped slot. The proposed micro strip patch antenna with H-shape slot is results in dual frequency band Ist band at 2.42Ghz and another at 3.59Ghz. The proposed patch antenna is further modified by introducing double I shaped slots. The modified antenna results in three frequency bands Ist at 2.44Ghz, IInd at 3.54Ghz and IIIrd at 5.37Ghz. Also the radiation characteristics, such as, return loss, VSWR, input impedance, radiation patterns and the surface current densities have been introduced and discussed. The proposed and modified micro strip patch antenna is designed on FR4 substrate that having dielectric constant 4.4. of thickness 1.50mm. Design results are obtained by a HFSS (High Frequency Structure Simulator) which is used for simulating microwave passive components.*

Keywords*:* Microstrip, slot, return loss, VSWR, dielectric, radiation pattern.

INTRODUCTION

Antennas play a very important role in the field of wireless communications. Different types of antennas are Parabolic Reflectors, Patch Antennas, Slot Antennas, and Folded Dipole Antennas. All type of antenna is good in their own properties and usage. Hence antennas are almost everything in the wireless communication without which the world could have not reached at this advance age of technology

In today's world the role of microstrip patch antennas is a very significant in the field of wireless communication systems. Construction of a microstrip patch antenna [1] is very simple using a conventional Microstrip fabrication technique. Microstrip patch antennas with rectangular and circular patch are most commonly used antnnas. These patch antennas are used as simple and for the widest and most demanding applications. Dual characteristics, circular polarizations, dual frequency operation, frequency agility, broad band width, feed line flexibility, beam scanning can be easily obtained from these patch antennas. The Microstrip antennas are very popular based on their applications. This antenna has some Merits and De-merits as any other. The merits of these antennas have some similarities as of the conventional microwave antennas, as these cover a broader range of frequency from 100 MHz to 100 GHz, same is the case with these Microstrip antennas. Some merits of these Microstrip antennas are Low weight, low volume and thin profile configurations which can be made conformal [1]. Low fabrication cost, readily available to mass production. Linear and circular polarizations are possible. Easily integrated with microwave integrated circuits. Capable of dual and triple frequency operations. Feed lines and matching network can be fabricated simultaneously. These are widely used in the handheld devices (wireless) such as pager, mobile phones, etc.

A number of microstrip patch antennas with multiband property have been proposed, and various techniques have been used to achieve the multiband operation [2][3]. The mainly used methods are etching slots and slits on the patch or on the ground plane, for

Cite this article as: Nilima Arun Bodhaye, Prasanna L Zade. "Design of Multiband Microstrip Patch antenna with I-shape slot for wireless applications". *International Conference on Innovative Trends in Electronics Communication and Applications (2015)*: 170-178. Print.

examples S-shaped slot [2], U-shaped slot [4], C-shaped slot [5]etc.

Most of the previous researches have been adapted for multi-band design; few researches have been focused on dual-bands design. Dual-bands antennas designs have been explained in the papers [6]–[8].In these above papers the dual- band have been achieved by adding the proper slits in the near of radiating patch element and the ground plane, by the inserting of slit, the desired two rejected bands have been obtained.

In this paper a multiband microstrip patch antenna is proposed. This proposed microstrip antenna is designed on a FR4 substrate which is having dielectric constant of 4.4. On the substrate a rectangular shape patch is introduced. A H- shaped slot on the top of radiating patch and by using the probe feed line the dual bands are achieved. For increasing the resonance frequency, new double I-shaped slots are used on the radiating patch and the bandwidth of antenna is also increased by using these slots. However, these antennas are not fulfilling the complete requirement of multiband operation for wireless technology. These antennas are small in size and compact. These structures are designed and simulated with microstrip technology and suitable for multiband wireless communication.

The paper is organized as follows. In Section 2, basic design of proposed microstrip patch antenna is described. In Section 3, the modified structure of microstrip patch is presented for tetra-band operation. In Section 4, the simulated results of proposed dual band and tri-band antenna design are presented and compared. Finally, the paper is concluded in Section 5.

DESIGN AND MODELING

This section, we will introduce the design of our antenna. First the three essential parameters for the design of a rectangular Microstrip Patch Antenna are:

• Frequency of operation (f_o): The resonant frequency of the antenna must be selected appropriately. The resonant frequency selected for design is 2.4 GHz.

• Dielectric constant of the substrate (ε_r): The dielectric the dielectric substrate is selected as 1.6 mm. material selected for design is glass epoxy which has a dielectric constant of 4.4.

• Height of dielectric substrate (h): For the microstrip patch antenna to be used in cellular phones, it is essential that the antenna is not bulky. Hence, the height of the conventional patch antenna is selected as 1.6mm.

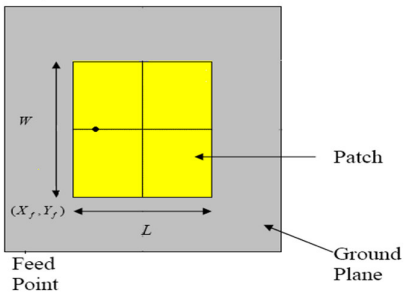

Figure 1: Rectangular microstrip antenna

The initial calculation starts from finding the width of the patch which is given as:

Step 1: Calculation of the width of Patch (W)-

The width of the Microstrip patch antenna is given as

$$W = \frac{c}{2f_o\sqrt{\frac{(\varepsilon_r + 1)}{2}}}$$

For f_o=2.4GHz, ε_r=4.4

We get W=38.22 mm.

Cite this article as: Nilima Arun Bodhaye, Prasanna L Zade. "Design of Multiband Microstrip Patch antenna with I-shape slot for wireless applications". *International Conference on Innovative Trends in Electronics Communication and Applications (2015)*: 170-178. Print.

Step 2: Calculation of effective dielectric const-

Fringing makes the microstrip line look wider electrically compared to its physical dimensions. Since some of the waves travel in the substrate and some in air, an effective dielectric constant is introduced, given as:

$$\varepsilon_{reff} = \frac{\varepsilon_r + 1}{2} + \frac{\varepsilon_r - 1}{2}\left[1 + 12\frac{h}{W}\right]^{-\frac{1}{2}}$$

We get $\varepsilon reff = 3.99$

Step 3: Calculation of Length of Patch (L)-

The effective length due to fringing is given as:

$$L_{eff} = \frac{c}{2f_o\sqrt{\varepsilon_{reff}}}$$

For $\varepsilon reff = 3.99$, $fo = 2.4$GHz

We get $Leff = 30.25$ mm

Step 4: Calculation of ΔL -

Due to fringing the dimension of the patch as increased by ΔL on both the sides, given by:

$$\Delta L = 0.412h\frac{\left(\varepsilon_{reff} + 0.3\right)\left(\frac{W}{h} + 0.264\right)}{\left(\varepsilon_{reff} - 0.258\right)\left(\frac{W}{h} + 0.8\right)}$$

For W=36.4mm, h, =1.53mm, εreff=3.99

We get ΔL=0.70mm

Hence the length the of the patch is: L= Leff-2ΔL=28.4 mm

Step 5: Calculation of Substrate dimension-

For this design this substrate dimension would be

Ls=L+2*6h

Ws=W+2*6h

Ls = 2*6h + L = 2*6(1.6) + 39 = 59mm

Ws = 2*6h + W = 2*6(1.6) + 30 = 50 mm

Step 6: Calculation of feed length-

For this feed would be given-

lam/4*sqrt(4.4) distance.i.e 14.5mm.

Cite this article as: Nilima Arun Bodhaye, Prasanna L Zade. "Design of Multiband Microstrip Patch antenna with I-shape slot for wireless applications". *International Conference on Innovative Trends in Electronics Communication and Applications (2015)*: 170-178. Print.

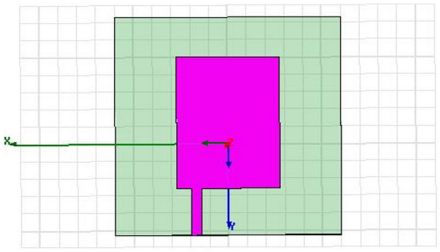

Figure 2: HFSS model of Rectangular microstrip patch antenna

After designing a simple rectangular microstrip patch antenna for 2.4 Ghz frequency band, a single H- shaped slot is inserted on the radiating patch. And for the proposed antenna a dual frequency band is achieved. The Hfss model for the I-shape slot is as shown in fig. below.

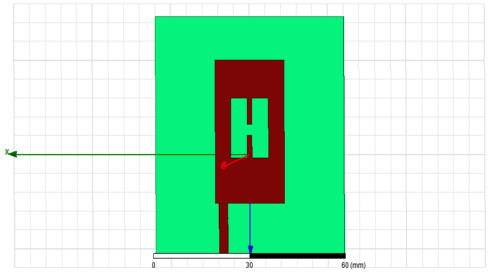

Fig3: Rectangular microstrip patch antenna with single H shape slot

MODIFIED DESIGN FOR TRI-BAND ANTENNA

Furthermore, to increase the number of frequency band the proposed microstrip patch antenna with H shaped slot is odified by inserting a double I-shape slot on the radiating patch.. The Hfss model for the I-shape slot is as shown in fig. below.

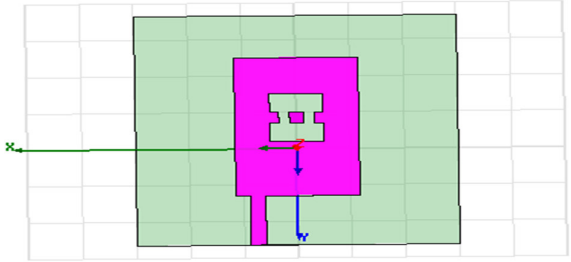

Fig4: Rectangular microstrip patch antenna with double I- shape slot

By introducing the Double I-shape slot in the antenna structure the number of frequency bands is increased and the frequency response of S11 parameter is improved which is described in the next section.

SIMULATION AND RESULTS

The software used to model and simulate the proposed and modified microstrip patch antenna is Hfss i.e.high frequency simulation software. It has been widely used in the design of tunable filters, patch antennas, wire antennas, and other RF/wireless antennas. It can be used to calculate and plot the S11 parameters, VSWR plot,directivity , smith chart, current distributions as well as the radiation pattern. The simulation is done for three cases. The first one is for simple rectangular microstrip patch antenna for 2.4 Ghz frequency band. Antenna structure with H-shaped slot as described in section II and third one is for modified antenna structure with double I-shaped slot described in section III.

Case-I Antenna structure with rectangular shape patch

The rectangular shape microstrip patch antenna is designed for 2.4 GHz. The return loss plot , VSWR plot , radiation pattern and current distribution for the antenna is as shown in figures below.

Cite this article as: Nilima Arun Bodhaye, Prasanna L Zade. "Design of Multiband Microstrip Patch antenna with I-shape slot for wireless applications". *International Conference on Innovative Trends in Electronics Communication and Applications (2015)*: 170-178. Print.

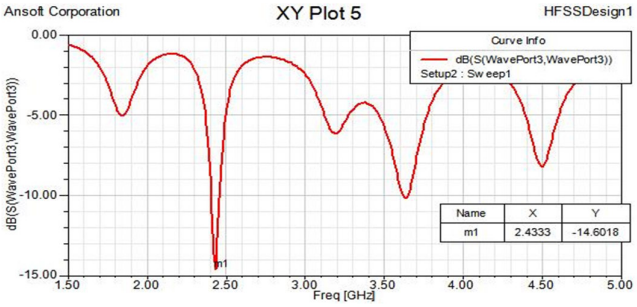

Fig5: s11 plot of rectangular microstrip patch antenna

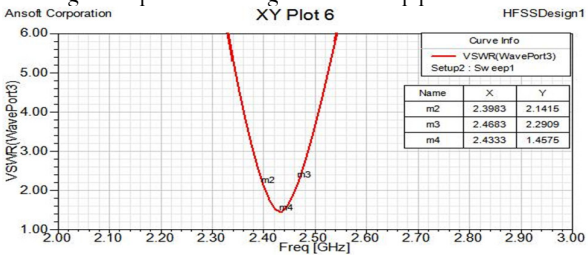

Fig6: VSWR plot of rectangular microstrip patch antenna

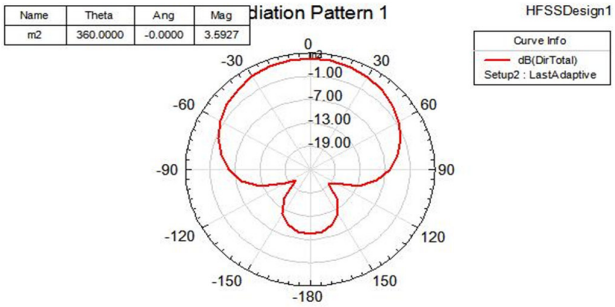

Fig7: Radiation pattern of rectangular microstrip patch antenna

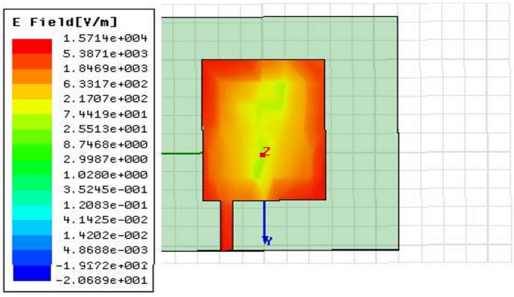

Fig8: current distribution of rectangular microstrip patch antenna

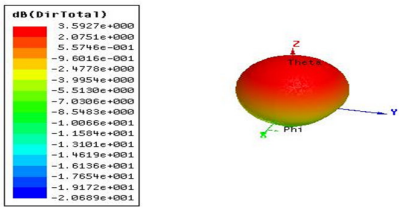

Fig9: directivityt of rectangular microstrip patch antenna

Cite this article as: Nilima Arun Bodhaye, Prasanna L Zade. "Design of Multiband Microstrip Patch antenna with I-shape slot for wireless applications". *International Conference on Innovative Trends in Electronics Communication and Applications (2015)*: 170-178. Print.

Case-II Antenna structure with H-shape slot on rectangular shape radiataing patch

The H-shape slot is introduced on the rectangular microstrip patch antenna structure. This antenna structure is covering 2.42-3.59GHz. This antenna structure has two distinct frequency bands, centered at 2.42 GHz, 3.59 GHz as shown in the Fig. 3. As shown in Fig.3 the return loss is less than -10 dB which showing that this antenna is workable on these two frequency bands. The radiation patterns of dual-band antenna of directivity at theta is 90 degree for three resonance frequencies are shown in Fig. 5, 6, 7. The directivity of antenna is described by the shape of the radiation pattern, so from the Fig.5, 6, and 7, it is clear that the radiation pattern is Omni-directional but it becomes directional when operating frequency band is increased.

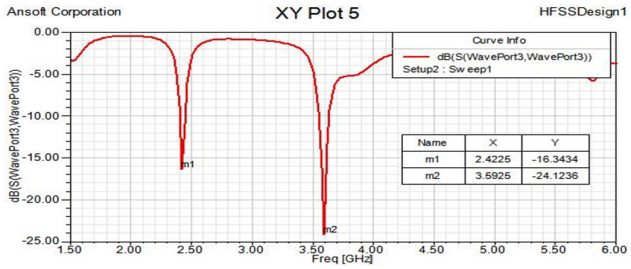

Fig10: s11 plot of microstrip patch antenna with single H shape slot

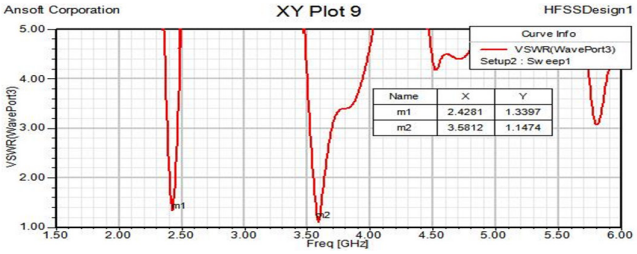

Fig11: VSWR plot of microstrip patch antenna with single H shape slot

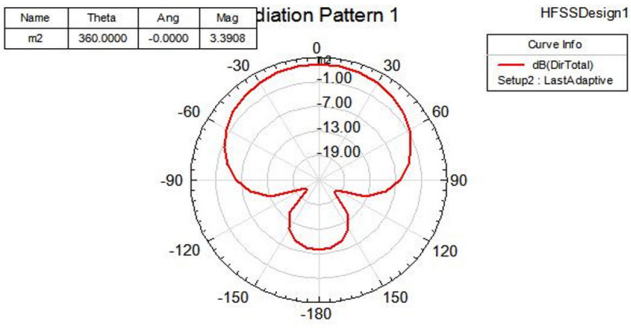

Fig12: Radiation pattern of microstrip patch antenna with H shape slot

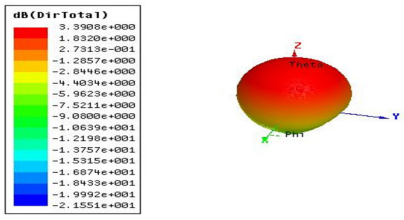

Fig13: Directivity of microstrip patch antenna with single H shape slot

Cite this article as: Nilima Arun Bodhaye, Prasanna L Zade. "Design of Multiband Microstrip Patch antenna with I-shape slot for wireless applications". *International Conference on Innovative Trends in Electronics Communication and Applications (2015)*: 170-178. Print.

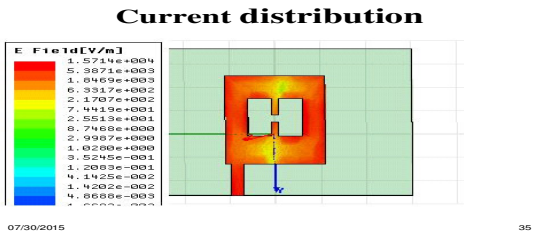

Fig14: current distribution of microstrip patch antenna with H shape slot

Case-III Antenna structure with Double I-shape slot on rectangular shape radiataing patch

As shown in Fig. 3, the return loss of basic antenna structure is tuned for two frequency bands. For improvement of the return loss and increment by one more frequency band, a double I-shaped slot is inserted in the proposed structure. Therefore, this structure works as a tri-band microstrip antenna. As shown in the Fig. 8, proposed structure has three distinct frequency bands centered at 2.44 GHz, 3.54 GHz, 5.37 GHz and 11.35GHz. and operating range from 2.44-5.37 GHz. So the proposed structure has more smooth and extra operating frequency band than the basic antenna structure.

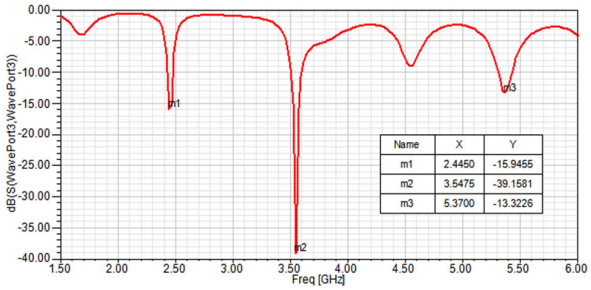

Fig15: s11 plot of microstrip patch antenna with double I- shape slot

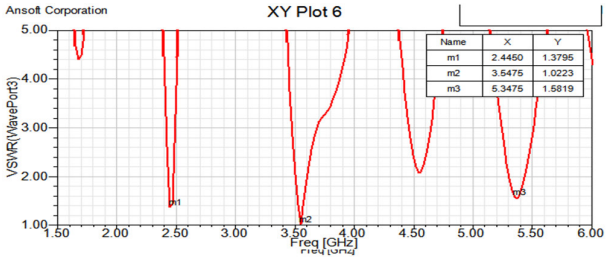

Fig 16: VSWR plot of microstrip patch antenna with double I- shape slot

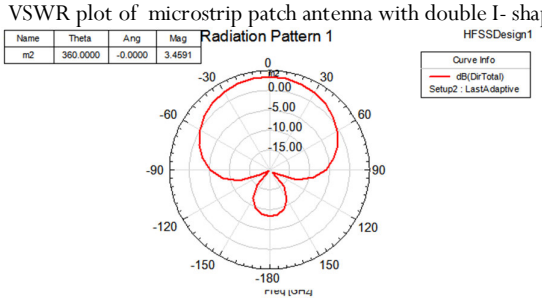

Fig 17: Radiation pattern of patch antenna with double I- shape slot

Cite this article as: Nilima Arun Bodhaye, Prasanna L Zade. "Design of Multiband Microstrip Patch antenna with I-shape slot for wireless applications". *International Conference on Innovative Trends in Electronics Communication and Applications (2015)*: 170-178. Print.

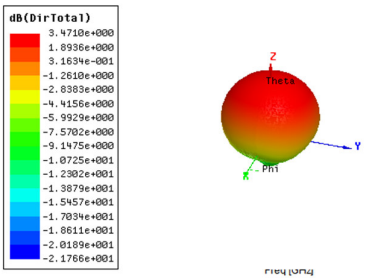

Fig18: Directivity of microstrip patch antenna with double I- shape slot

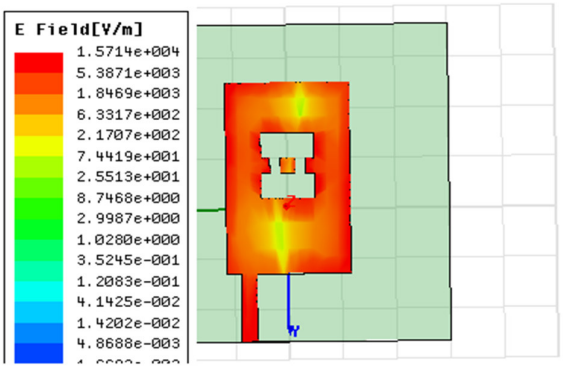

Fig 19: current distribution of patch antenna with double I- shape slot

Comparisons table of simple patch, patch H-shape slot and patch with double I-shaped slot

S.N.	Shape of MSA	Freq (GHZ)	Return Loss (dB)	VSWR	Bandwidth (MH)	Directivity (dB)
1.	Simple patch antenna	2.43	-14.60	1.45	68	**3.59**
2.	Patch with H shaped slot antenna	2.42	-16.34	1.33	53	**3.39**
		3.59	-21.12	1.14	90	
3.	Patch with double I shaped slot antenna	2.44	-15.94	1.37	54.76	**3.47**
		3.54	-39.15	1.02	51.10	
		5.37	-13.32	1.58	47.58	

CONCLUSION

In this paper, a new approach to multiband antenna structure is shown for increasing the number of operating frequency bands and improvement in return loss. The comparison between patch antenna with H-shape slot and with double I-shape slot is shown. From comparison table, the conclusion the future aspect of this work is to increase the number of operating frequency bands by made change using different shaped structures in place of H-slots and I-slots. This structure can be further modified by increasing the switch-ability

Cite this article as: Nilima Arun Bodhaye, Prasanna L Zade. "Design of Multiband Microstrip Patch antenna with I-shape slot for wireless applications". *International Conference on Innovative Trends in Electronics Communication and Applications (2015)*: 170-178. Print.

of radiating patch by connecting PIN diode or RF-MEMS switch in switchable slot. The modified antenna are very valuable for many modern wireless applications and radar system applications, such as object detection, secure communication, multi frequency communication and multi frequency communication These proposed antennas can be used for multiband wireless communication applications.

REFERENCES

[1] James, J.R. and Hall, P.S.: "Handbook of Microstrip Antennas" (Peter Peregrinus)

[2] Jigar M. Patel1, Shobhit K. Patel2, Falgun N. Thakkar, "Design of S-shape multiband microstrip patch antenna"

[3] Fan Yang, Student Member, IEEE, and Yahya Rahmat-Samii, Fellow, IEEE , "A econfigurable Patch Antenna Using Switchable Slots for Circular Polarization Diversity", IEEE MICROWAVE AND WIRELESS COMPONENTS LETTERS, VOL. 12, NO. 3, MARCH 2002.

[4] Y. J. Cho, K. H. Kim, D. H. Choi, S. S. Lee, and S. O. Park, "A iniature UWB planar monopole antenna with 5-GHz band-rejection filter and the time-omain characteristics," IEEE Trans. Antennas Propag., vol. 54, no. 5, pp. 1453–1460, May 2006.

[5] Y. C. Lin and K. J. Hung, "Compact ultra-wideband rectangular aperture antenna and band-notched designs," IEEE Trans Antennas Propag., vol.54, no. 11, pp. 3075–3081, Nov. 2006.

[6] J. Liu, S. Gong, Y.Xu,X. Zhang, C. Feng, and N.Qi, "Compact printed ultra-wideband monopole antenna with dual band-notched characteristics," Electron. Lett., vol. 44, no. 12, pp. 710–711, Jun. 2008.

[7] James Sor, Student Member, IEEE, Chin-Chang Chang, Student Member, IEEE, Yongxi Qian, enior Member, IEEE,and Tatsuo Itoh, Fellow, IEEE, "A Reconfigurable Leaky-Wave/Patch MicrostripAperture for Phased-Array Applications" IEEE TRANSACTIONS *ON MICROWAVE THEORY AND TECHNIQUES, VOL. 50, NO. 8, AUGUST 2002 1877.*

[8] Q. X. Chu and Y. Y. Yang, "A compact ultrawideband antenna with 3.4/5.5 GHz dual band-notched characteristics," IEEE Trans. Antennas Propag., vol. 56, no. 12, pp. 3637–3644, Dec. 2008.

[9] J.-C. Langer, J. Zou, C. Liu, Senior Member, IEEE, and J. T. Bernhard, Senior Member, IEEE "Micromachined Reconfigurable Out-of-Plane Microstrip Patch Antenna Using Plastic Deformation Magnetic Actuation" EEE MICROWAVE AND WIRELESS COMPONENTS LETTERS, VOL. 13, NO. 3, MARCH 2003

[10] Y. J. Sung, T. U. Jang, and Y.-S. Kim "A Reconfigurable Microstrip Antenna for Switchable Polarization" IEEE MICROWAVE AND WIRELESS COMPONENTS LETTERS, VOL. 14, NO. 11, NOVEMBER 2004

[11] Dimitrios Peroulis, Member, IEEE, Kamal Sarabandi, Fellow, IEEE, and Linda P. B. Katehi, Fellow, IEEE "Design of Reconfigurable Slot Antennas" IEEE TRANSACTIONS ON ANTENNAS AND PROPAGATION, VOL. 53, NO. 2, FEBRUARY 2005

[12] Shing-Lung Steven Yang and Kwai-Man Luk "A Wideband L-Probes Fed Circularly-Polarized Reconfigurable Microstrip Patch Antenna" IEEE TRANSACTIONS ON ANTENNAS AND PROPAGATION, VOL. 56, NO. 2, FEBRUARY 2008

[13] Joseph Costan tine, "New Multi-Band Microstrip Antenna Design for Wireless Communications" IEEE Antennas and Propagation Magazine, Vol. 49, No. 6, December 2007.

[14] Mukesh Arora, Shubhi Jain, Abha Sharma, "Multi Band Circularly Polarized Microstrip Patch Antennas for Mobile Communication" International Journal of Soft Computing and Engineering (IJSCE) ISSN: 2231-2307, Volume-2, Issue-3, July 2012

[15] V. Anitha " Characterization of Multi-band Rectangular-Triangular Slotted Antenna" International Journal of Modern Engineering Research (IJMER) www.ijmer.com Vol.2, Issue.2, Mar-Apr 2012 pp-483-486 ISSN: 2249-6645

[16] C. A. Balanis, Antenna Theory Analysis and Design, Second Edition, New York, Wiley, 1997.

[17] S. Xiao, B. Z. Wang, and X. S. Yang, "A Novel Frequency **382** Kyungho Chung et al. TRI Journal, Volume 28, Number 3, June 2006Reconfigurable Patch Antenna," Microwave Opt. and Technol.Lett. 36, Feb. 2003, pp. 295-297.

[18] F. Yang and Y. Rahmat-Samii, "Patch Antenna with Switchable Slot (PASS): Dual - frequency Operation," Microwave Opt. and Technol. Lett., 31, Nov. 2001, pp. 165-168.

[19] F. Yang and Y. Rahmat-Samii, "Switchable Dual-Band Circularly Polarized Patch Antenna with Single Feed," Electron. Lett., vol.37, no. 16, Aug. 2001, pp. 1002-1003. Ghanshyam singh and Mithilesh Kumar, member IEEE "Design of frquency reconfigurable microstrip patch antenna"6th international conference on industrial and information system ICIIS 2011, Sri Lanka.

Cite this article as: Nilima Arun Bodhaye, Prasanna L Zade. "Design of Multiband Microstrip Patch antenna with I-shape slot for wireless applications". *International Conference on Innovative Trends in Electronics Communication and Applications (2015)*: 170-178. Print.

International Conference on Innovative Trends in Electronics Communication and Applications 2015 [ICIECA 2015]

ISBN	978-81-929742-6-2
Website	icieca.in
Received	02 - April - 2015
Article ID	ICIECA026

VOL	01
eMail	icieca@asdf.res.in
Accepted	15 - November - 2015
eAID	ICIECA.2015.026

Design of Artificial Intelligence Based Speed Control, Automation & Braking System For Cars Using Open Source Brain-Computer Interface Technology

Sibu C M[1], S Preethi[2], Bharath Kumar M R[3], K S Pradeesh[4], S Pragaspathy[5]

[1, 2, 4] UG Scholar, [3]PG Scholar, Dept., of EEE, Dept., of Mechatronics, Dept., of Aeronautical Engineering

[5]Asst.Professor, Department of EEE

Nehru Institute of Engineering and Technology

Abstract: *A new design of speed control, automation and braking system for cars incorporating open source Brain-Computer Interface technology is proposed in this paper. In traditional cruise control system, accidents may occur, if there exist any lack of concentration. To overcome this automated system controlled by brain waves is proposed. In the open source BCI, Brain waves are obtained as voltage fluctuations and Ionic current through high sensitivity electrodes from which they are categorizes based on its frequency limit. The signal acquisition part conditions the extremely low frequency radio waves. By employing machine learning algorithm, a signal is converted into codes- machine language and is transmitted. The received signals after error detection and filtration process is compared with the actual value determined by the Hall sensor fixed at the rear wheel of the car. The output of the comparator is fed to decision device which controls the mechanical system and performs the operation. Along with this automated system, additional guidance is provided to the user by means of Voice Guidance based Bluetooth module. The proposed mind reader section is in the form of a head set.*

Keywords: Open source Brain-Computer Interface (BCI), Duemilanove Arduino board, Machine Learning algorithm, automated control, Integrated Computer System, Bluetooth module.

INTRODUCTION

Road fatalities are one of the major problems faced in today's world. From the Bibliometric statement of World Health Organisation (WHO), India leads in road fatality rate of about 20.1 percent. Whereas from the another analysis of Economic Times about 13 people die per hour in road accidents in India, that results in annual mortality of about 1,19,860 per year. Among this death rate, car accidents stands top of about 54%. The major reason for car accidents is due to lack of concentration of the driver. Every year about 78.5% of car accidents occur due to this lack of concentration. The road fatality rate for last five years is shown in Fig 1.

Cite this article as: Sibu C M, S.Preethi, Bharath Kumar M R, K S Pradeesh, S Pragaspathy. "Design of Artificial Intelligence Based Speed Control, Automation & Braking System For Cars Using Open Source Brain-Computer Interface Technology". *International Conference on Innovative Trends in Electronics Communication and Applications (2015)*: 179-188. Print.

Artificial Intelligence has become a tremendously growing technology for production, Instrumentation and automated Control systems. In this current state of artmost cars uses the ordinary speed control technology, in which the pedal pressure is to be maintained.

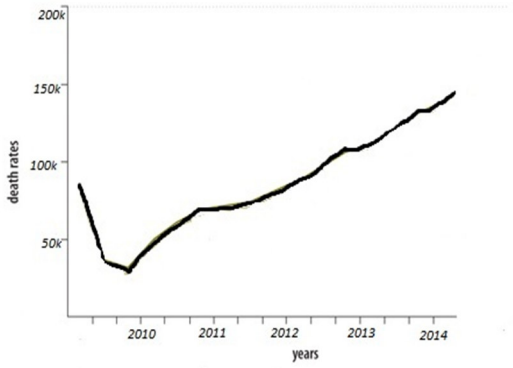

Fig 1: Statistical Death Rate In India

For this high degree of concentration is required, hence by this method road accidents cannot be completely eliminated. By taking the above factor in consideration a speed control system that results in higher efficiency and reduced mechanical stresses even in case of rash driving is proposed. The major theoretical background of this proposal is from Electroencephalography. Brain- it is the most complex system ever existed in this world with greater speed of response and higher degree of accuracy. Human- Brain produces different responses as waves for various situations; these responses are tracked as voltage fluctuations and ionic current from which the frequency limits of z the response can be easily determined.

Open source Brain-Computer Interface is a fully customizable optimum device that is available to track brain wave at a faster rate with better accuracy. In particular, the waves are obtained through the scalp region by high sensitivity electrodes. By employing "Reducing Electrode" concept, the number of electrodes required for analysation is reduced to half such that the complexity is reduced [section IV-A]. From the potential difference and ionic current the frequency of wave is calculated and is injected to the signal acquisition part. The signal is amplified with Gain factor (i.e.) signal with poor characteristics is converted into a better characteristics signal [section IV-B]. Translation part converts the signal into codes by employing machine learning algorithm and is transmitted. Signal is transferred at the rate of 120 signals/minute. The receiver section receives the BPSK code and is filtered and processed to retrieve the original signal. In order to remove noisy interferences a band-pass filter is introduced at processing unit [section VI]. The original retrieved signal is assigned previously, for a specified speed limit, this value is compared with the original speed calculated from the digital hall sensor fixed to rear wheel of the car. The comparator output is fed into a decision device which is normally an integrated computer system. Based on the output, computer system controls the mechanical system and performs the desired operation [section VII]. An efficient operation is only possible when the comparator continuously compares the original speed with the reference speed. In addition guidance is provided by APR9600 microcontroller, to which voice guidance's system (bluetooth module) is connected. For different mind state, different guidance are played which are pre-recorded. The method proposed in this paper is an initial step to avoid the limitations posed by the traditional speed control strategy, and incorporate open source BCI making the system more stable, feasible, reliable and economical. The proposed control system is independent and does not require high degree of concentration level. This is achieved with a simple BCI circuit without adding complexity to the system.

LITERATURE SURVEY

[1] Arelene Ducao, a post graduate student of MIT has designed a prototype model of helmet that can read the brain waves to determine the current status of mind of the cyclist. She has used coloured LED lights to show alert for various moods. Prototype model works on electroencephalography technique, that tracks and analyse the brain waves from the specified frequency limit is calculated and with respect to that instruction LED will glow. The main shortcoming of her proposal model is that it acts only as a mood detector helmet with alert guidance, in visual mode.

[2] Joel Murphy and Conor Russomanno designed a fully integrated and customizable device that performs the action of an EEG with reduced size thus forming an interface between Human and computer. This design comprises both hardware and software

Cite this article as: Sibu C M, S.Preethi, Bharath Kumar M R, K S Pradeesh, S Pragaspathy. "Design of Artificial Intelligence Based Speed Control, Automation & Braking System For Cars Using Open Source Brain-Computer Interface Technology". *International Conference on Innovative Trends in Electronics Communication and Applications (2015)*: 179-188. Print.

toolkits thus eliminating long lines of codes and circuit diagrams. This design led to the development of next generation technology.

[3] Ankita Mishra and Pranav paranjpe proposed a paper on RF based speed control system for cars. The system runs on embedded programming. The major drawback of the system is that it includes only the speed control operation. Moreover the efficiency of the system is limited and in certain cases of rash driving accidents is unavoidable.

PROPOSED SPEED CONTROL & BRAKING SYSTEM

The block diagram of the proposed speed control and braking system is illustrated in fig.2. The proposed system consists of the Brain Wave analysation, wave amplification (EEG hardware amplifier), transmission and operational stages connected through a wireless medium. The wave analysation stage consists of high sensitivity active electrodes, to convert the physical vibrations in the scalp regions to its respective voltage fluctuations (V_f) and Ionic current (i_c). The amplification stage amplifies the extremely Low frequency Radio Signals with a high gain factor, along with signal processing unit. The transmission stage performs the code conversion by employing machine learning algorithm along with BPSK transmission and reception. The receiver end converts the binary codes to retrieve original signal. The output signal is filtered with the help of a band pass filter before sending it to the computer automated system. The corresponding reference speed of the signal is compared with original speed of the vehicle, based on comparator output decision device performs the operation in stages. The measurement of quantities of voltage and current from the analysation stage is very important for guidance system.

BRAINWAVE PROCESSING UNIT

It is something exclusive and impressive to define about the organ- human brain. Brain is the complex system ever existed in this universe with most complicated structure with higher degree of consciousness. Brain- the complex machine system capable to response for emotions, thoughts and memories. It is capable to transfer data between neurons at a rate of hundred terabytes. When a human brain thinks or responds, it transfers information as spontaneous electrical activity between lakhs and lakhs of neurons, which can be tracked and analysed by implementing an interface. EEG processor plays a major role in detecting the status of brain such as sleep disorder, coma or condition of agitation. No wonder that every minute section of brain can dictate and target disease in whole body.

Table 2
Brain Wave Analysis & its Parameters

Brain wave	Status	Frequency pulse/second	Amp (μV)
Beta β	Consciously alert	13-16	5-10
Alpha α	Mental relaxation	7-13	20-200
Delta δ	Reduced Consciousness	4-7	10
Theta θ	Deep sleep or Catalepsy	0.1-4	20-200

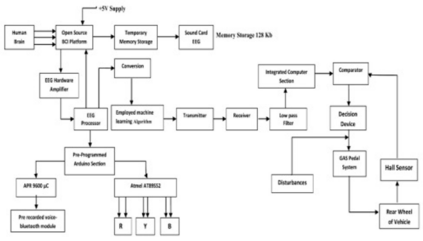

Fig 2: Block Diagram of Proposed System

Cite this article as: Sibu C M, S.Preethi, Bharath Kumar M R, K S Pradeesh, S Pragaspathy. "Design of Artificial Intelligence Based Speed Control, Automation & Braking System For Cars Using Open Source Brain-Computer Interface Technology". *International Conference on Innovative Trends in Electronics Communication and Applications (2015)*: 179-188. Print.

BRAINWAVE CLASSIFICATION:

Human brain produces four distinct types of pulses for various responses. The description of the pulses are as follows:

(i). **Beta**: human brain produces beta (β) pulse under conscious alert stage, with a frequency range of 13-16 pulses/second

(ii). **Alpha**: it is produced under relaxation stage. It is further classified into two short pulses

a). μu Wave: Relaxed Mental state

b). REM wave: Sleep stage

The frequency range is between 7-13 pulses/second

(iii). **Delta**: these waves are analysed when human brain faces reduced consciousness level with a frequency limit of 4-7 pulses/second.

(iv). **Theta**: It is the state of deep sleep or catalepsy with extremely low frequency of 0.1-4 pulse/second.

BRAIN WAVE TRACKING USING ACTIVE ELECTRODES:

One square millimetre of cerebral cortex has more than 100,000 neurons. When electrical activity takes place on scalp surfaces can be tracked by using high sensitivity active metal electrodes. Large quantities of neurons are present in the scalp regions of frontal, sulcus, temporal,

Parietal and occipital. Hence, a configuration with 64 pair of electrodes is to be placed in these regions with a ground electrode placed in ear. Potential difference action majorly takes place in soma and dendrites. This results in ionic current flow consisting of Na^{+}, K^{+}, Ca^{++} and Cl^{-}ions that can be obtained by metal electrodes.

Mostly, seven sets of electrodes have predefined activity that can never be altered.

F7- rational activity of brain (Delta wave)

F8- Emotional activity impulses (Alpha wave)

C3, C4 & Cz- Sensory and motor functions

P3, P4- Perceptional activity (μu wave)

T3, T4- processor unit for alpha waves

O1, O2- Bellow points

Various types of electrodes are there, for this proposal the electrode should meet the following specifications:

1). Reusability Behaviour

2). Metal electrode [Au, Ag, tin]

3). Active material- Should eliminate need of gel and needle

4) Thickness of electrode: imm-1.5mm

5). Diameter of electrode 1-3mm

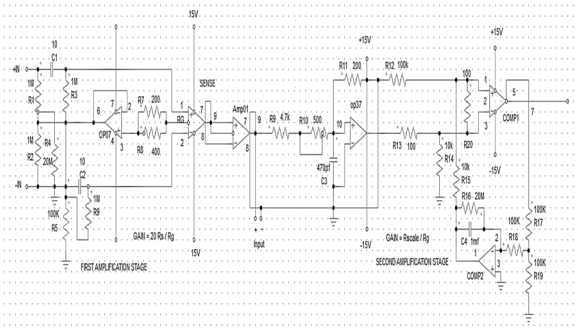

Fig 3: Amplification Circuit for Brain Wave Processing Stage

Cite this article as: Sibu C M, S.Preethi, Bharath Kumar M R, K S Pradeesh, S Pragaspathy. "Design of Artificial Intelligence Based Speed Control, Automation & Braking System For Cars Using Open Source Brain-Computer Interface Technology". *International Conference on Innovative Trends in Electronics Communication and Applications (2015)*: 179-188. Print.

BRAIN WAVE CONDITIONING UNIT:

The obtained weak electrical signals are massively amplified for next stage process and also stored in SCEEG for future analysis. The received signal is of 100μV, but for next stage analog to digital process the signal should be of 0 to 10V. Hence the signal requires a gain of about 10,000 or more. The next major issue is the frequency range, with 0.1 to 64 Hz creates a large noise levels. To reduce the complexity level and for better performance two stage amplification with a gain inverter is proposed here. MC34084- 'Instrumentation amplifier' overcomes the basic issues and produce balanced output with a very low noise characteristics. The above fig. shows the first stage amplification of brain wave coupled with second stage through a gain inverter.

$$\text{Gain} = 20[R_S / R_G]$$

The selection of Rs and Rg depends on that the first stage amplification should produce a gain of 1000. Error may occur due to the improper pattern aligned of brain wave analysation electrodes which leads to the development of Offset voltages. To remove this a non-polarised capacitor is coupled with amplifier. The unity gain inverter removes the common mode signal. The operational amplifier Op-37 removes the noise signal and eliminate the effect of phase shift. The second amplification stage is configured for variable gain described as

$$\text{Gain} = \text{Rscale} / \text{Rg}$$

AF-100 filters are employed as an anti-aliasing filter. The phase shift applied by this filter is linear, maintaining composite waveform. Thus the total gain of $1x10^4$ is achieved.

MACHINE LEARNING ALGORITHM

Machine Learning Algorithm is one of the popular Artificial Intelligence technique employed to manage conversion of ELF radio waves to binary codes. A specified Minimum Redundancy Maximum Relevance (mRMR) with accurately identified subset of data constraints are used. The supervised mRMR type algorithm automatically identifies the data subset relevant to the initial parameters already employed. The next feature of the mRMR algorithm is the sequential selection behaviour. This type of heuristic algorithm reduces the dependency of the system.

Step 1: **P**roblem **d**escription: At the very first stage the problem statement is defined and observed. From that the formal constraints of data and initial design of the solution is found.
Step 2: **A**nalysation **o**f **D**ata: This stage involves summarise the structure of data and visualization of data.
Step 3: **P**reparation **o**f **D**ata: here the pre-processing of data along with transformation is carried out.
Step 4: Evaluation of result: For this specified application supervised linear formal Machine learning algorithm.
Step 5: Improvement of Data: Final stage content, problem, solution, limitations and conclusion are considered for improvement and the process is again carried out for better performance.

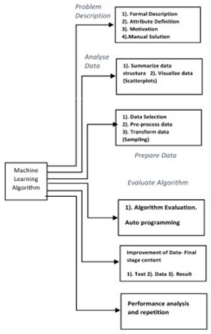

Fig 4: STRUCTURE OF APPLIED MACHINE LEARNING ALGORITHM

TRANSMISSION OF CODES

The signal is converted into code with a carrier signal to a balanced modulator. Redundancy is a major problem faced in bit conversion which is easily reduced by employing minimum redundancy technique. The model includes the square law device and band pass filter that removes the noisy interferences. The transmission and reception of the code sequence is manipulated by the Binary Phase Shift Keying methodology.

Cite this article as: Sibu C M, S.Preethi, Bharath Kumar M R, K S Pradeesh, S Pragaspathy. "Design of Artificial Intelligence Based Speed Control, Automation & Braking System For Cars Using Open Source Brain-Computer Interface Technology". *International Conference on Innovative Trends in Electronics Communication and Applications (2015)*: 179-188. Print.

Let the signal is represented as

$f(x) = \mathrm{A}\cos(\omega t)\ldots$ *(1)*

A is the peak value of the sinusoidal wave. ω = 2πf; Where 'f' corresponds to the frequency of the analysed wave. The continuous signal is converted into a discrete one with a phase shift of 180 degree, when the value of the symbol is changed. The phase shift depends on the time delay between the transmitter and the receiver. The received BPSK signal is passed into a square law device and then to a band pass filter for filtering process. After this the frequency of the halved and compared with the received signal. The bit synchroniser controls the switch s1 and s2 of the integrator system by which the phase

For symbol '0' $\longrightarrow f_1(x) = A\ Cos\ (\omega_o t)$ *… (2)*

For symbol '1' $\longrightarrow f_2(x) = A\ Cos\ (\omega_o t + \pi)$ *… (3)*

Then the signal from the square law device will be

$$Cos^2\ (2\pi ft + \theta) = \frac{1+Cos\ 2\ (2\pi ft+\theta)}{22}\ldots (4)$$

$$= \left(\frac{1}{2}\right) + \left(\frac{1}{2}\right) Cos\ 2\ (2\pi ft + \theta)$$

Here (1/2) represents the DC voltage level, hence it can be neglected.

$$S(kT) = b(kT)^2\sqrt{\frac{p}{2}}\int_{(k-1)T}^{kT}[1 + Cos\ 2\ (2\pi ft + \theta)]dt\ldots (5)$$

By expanding and substituting the limits

$$S(kT) = b(kT)^2\sqrt{\frac{p}{2}}\int_{(k-1)T}^{kT}[1]dt\ldots (6)$$

From the above integration process the original signal is retrieved at the receiver end section. The important issue is to determine the distance 'd' between the symbols, by.

$d = +\sqrt{E_b} - (-\sqrt{E_b})$

'E_b' is termed as bit energy.

AUTOMATION &CONTROLLOOP

In the propose system, automated operations are performed based on the analysed output of the decision chamber. The lookup table provides the status of the brain and its corresponding binary value. The original signal is compared with the reference signal obtained by the digital Hall sensor that is fixed to the rear wheel of the vehicle.

Table 2:
LIST OF OPERATIONS FOR BRAIN WAVES

Binary Sequence	Pulse	Specified operation
00	Theta	Brake
01	Delta	Speed=30Km
10	Alpha	Speed=40Km
11	Beta	No change

Cite this article as: Sibu C M, S.Preethi, Bharath Kumar M R, K S Pradeesh, S Pragaspathy. "Design of Artificial Intelligence Based Speed Control, Automation & Braking System For Cars Using Open Source Brain-Computer Interface Technology". *International Conference on Innovative Trends in Electronics Communication and Applications (2015)*: 179-188. Print.

DETERMINATION OF SPEED FROM HALL SENSOR

For better accuracy DRV5013 digital hall sensor is fixed at the rear wheel of the car. This hall sensor determines the accurate and current RPM status of the car. But for comparison speed is required, so it is converted into speed using the following relation.

$$Actual\ rpm\ of\ wheel = N\ revolutions/minute$$

$$Drive\ shaft\ speed = \frac{[N]}{[X1]}\ revolutions/minute$$

$$Drive\ shaft\ speed = \frac{[N]}{[X1]}\ revolutions/minute$$

$$Actual\ rpm\ of\ wheel = N\ revolutions/minute$$

For speed (i.e. Km conversion);
1 mile = 5280 feet =63,630 inches
1 hour = 60 minutes = 3600 seconds

X2 = Rear axle speed
R = Radius of Wheel
From the above equation the speed of the vehicle is determined.

CONDITIONS FOR OPERATIONS:

Condition 00: Here the reversal order of the wave is used. Binary sequence '00' represents the Delta wave. Since the pulse produced per second is in order of 0.1 to 4, the response rate is low. So the speed control of the system takes place in a faster manner. Suppose the car is running at a rate of 3000 RPM, the RPM rate is reduced in steps at the rate of 1000 rotations/minute. Finally the speed is completely reduced and braking is applied for safety purpose.

Condition 01: Condition '01' stands for Theta wave. Along with the guidance measure provided by the LED blinking and the Bluetooth module the speed is also reduced in two steps. Suppose the speed of the car is 60km/hour. The speed is reduced in three steps. This is done that the final speed of the car will be equal to 30Km/hour.

Formula used: [(Current speed – 30) km/hour] / 3

Step actions: from the above analysis when the current speed is 60Km/hour. Then [60-30]/3 = 10Km. So, in each step 10Km speed is reduced. In the decision device the time can be altered within which the speed of the system want to reduce in one step. For better performance and to reduce the accident occurrence rate. The time should be less than 60 seconds for a step.

Condition '10': Condition '10' is used for the Alpha pulses, at this time the user is in relaxation stage, also aware of what is happening around him. But when a sudden change occur in surrounding may make the brain to change its response, accidents may occur. So in this stage the speed is maintained at 40Km/hour (Maximum City Speed limit in India). The speed is reduced in a single step.

Formula used: [(current speed)-40]/1

Example: suppose when the speed of the car is 60Km/hour. Then it is reduced to 40Km/hour in a single step.

Cite this article as: Sibu C M, S.Preethi, Bharath Kumar M R, K S Pradeesh, S Pragaspathy. "Design of Artificial Intelligence Based Speed Control, Automation & Braking System For Cars Using Open Source Brain-Computer Interface Technology". *International Conference on Innovative Trends in Electronics Communication and Applications (2015)*: 179-188. Print.

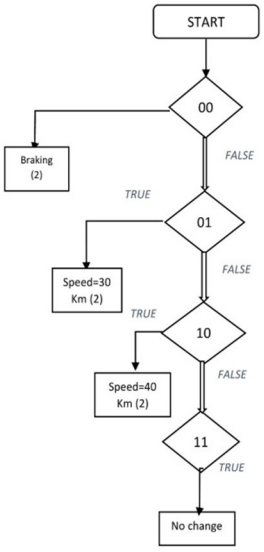

Fig 5: CONTROL FLOW STRUCTURE

Condition '11': Binary sequence '11' represents the Beta wave. At this state the human brain is completely aware about what is happening around it. So in this the speed control action is not performed and the speed is maintained and can be controlled by the driving person. So based upon the output of the decision device the speed of the system can be controlled.

WORKING OF COMPUTER AUTOMATED OPERATIONAL SYSTEM:

The control scheme of car controls the speed by adjusting the throttle. The car will maintain the desired speed by adjusting throttle value cable with a solenoid. This runs a vacuum driven servomechanism completely controlled by a microcontroller, built electronic section. The original speed which is to be maintained is compared with the reference internal speed pulses produced by the speed sensor and the difference in speed is calculated. Let the actual speed of the car is 70km/hour. The original speed is to be maintained at 40km/hour calculated from the automated system. The difference in speed is about 30km/hour. Hence the microcontroller controls throttle cable that drives the vacuum driven servomechanism and alters the pressure of the braking pedal. Thus when the actual speed equals to reference speed then the movement of throttle cable is stopped and maintained throttle is majorly controlled and operated by a actuator; stepper motor.

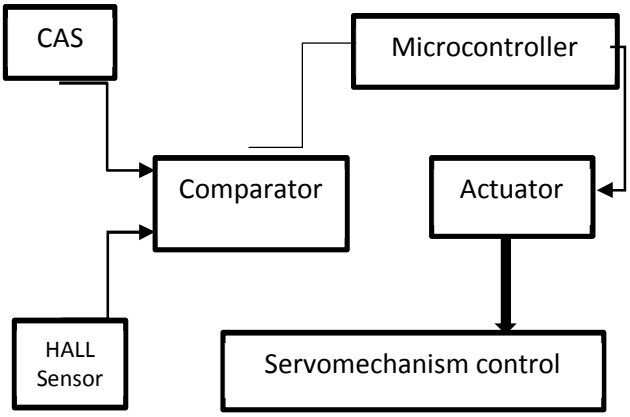

Fig 6: MECHANICAL CONTROL OF SYSTEM

Cite this article as: Sibu C M, S.Preethi, Bharath Kumar M R, K S Pradeesh, S Pragaspathy. "Design of Artificial Intelligence Based Speed Control, Automation & Braking System For Cars Using Open Source Brain-Computer Interface Technology". *International Conference on Innovative Trends in Electronics Communication and Applications (2015)*: 179-188. Print.

DECISION DEVICE:

Here Decision device includes a main computer which compares the input from Hall sensor (which continuously monitors the velocity of the vehicle) and the reference speed which is already predefined for each concentration level or mood. This classification is done with the signal received. Then the decision device compares and by employing the formula the speed of the vehicle is altered with the help of the throttle.

BRAKING SYSTEM:

The brake action is the most critical, since it must be able to stop the car in case of a failure of the autonomous system. For safety purpose electro hydraulic braking is used. Two shuttle valves are connected to the input of the braking system in order to keep the system independent. Each valve permits flow from either of two inlet ports to a common outlet by means of a free-floating metal ball that shuttles backend-forth according to the relative pressures at the two inlets.

BLUETOOTH BASED VOICE GUIDANCE MODULE:

The signal from open source BCI is transmitted to the microcontroller through serial port using RS-232 protocols. Corresponding to the string received, the microcontroller places data on the pin activates, which transmits a string of 0's and 1's to the **APR9600 IC**. A LOW signal placed on the pin activates it and voice stored in that memory location is played back through the headphone.

RESULT

Here, the graphical representation of the brain wave scatter plots (i.e.) sudden change in mind set is shown in figure (7). It is plotted by taking Time (in second) versus Frequency of the Brain wave in Hertz.

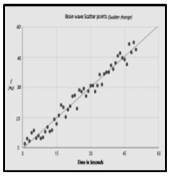

Fig 7: BRAIN WAVE SCATTER PLOTS.

The major aim of this proposal is to provide an initial stage design of an automated speed control and braking system that should be much efficient to overcome the limitations of ordinary cruise speed control system. Thus the speed control strategies are yet to be standardized for the brain wave responses. In reality, concentration level of human brain varies and this may lead to inaccuracies and accidents, if the ordinary cruise control system is not efficient. To overcome this problem, four different brain response characteristics are analysed and these data is provided as input for further operation. The brain wave pattern and arrangement characteristics used in this design is based on the real data measured by EEG. Brain is the high speed system which commands and controls all the other parts of body. Here, the brain is direct the way connected to the automated system. So, the system will function with high accuracy and speed.

CONCLUSION

The automated speed control system and braking system using an open source Brain-Computer interface Technology and Arduino section has been discussed in this paper and the control, operation conditions was proposed. The system reduces the complexity and the shortcoming of the normal Cruise control scheme. The Machine Learning Algorithm for conversion is very simple, that completely overcomes the limitations in transmission of the extremely low frequency radio waves. The proposed system has been developed for the real time access application to limits the road accidents due to lack of concentration.

REFERENCES

[1] M.Teplan, Institute of Measurement Science; "Fundamentals of EEG Measurement", Volume 2- Section 2, 2002- Measurement Science Review

Cite this article as: Sibu C M, S.Preethi, Bharath Kumar M R, K S Pradeesh, S Pragaspathy. "Design of Artificial Intelligence Based Speed Control, Automation & Braking System For Cars Using Open Source Brain-Computer Interface Technology". *International Conference on Innovative Trends in Electronics Communication and Applications (2015)*: 179-188. Print.

[2] Chris Ding and HanchuanPeng," Minimum Redundency Feature Selection from Microarray Gene Expression Data"- IEEE Computer Society Bioinformatics Conference, Aug 2003
[3] O'Regan, S.Faul and S.MArnane."2010 Annual International Conference in Engineering Medicine and Biology"-IEEE
[4] Klein.S; Thorne B M, Biological psycology. Newyork. ISBN 7167-9922-7
[5] Millet David (2002)- "International Society for the History of Neurosciences"
[6] Horovitz.G.Silva; SkudlarskiPawel (2002)." Correlations and the dissociations between BOLD signals and P300 amplitude in an auditory oddball task; A parametric approach to combining FMRI and ERP". Magnetic Resonance Imaging: 319-25
[7] G.Buzsaki. Rhytms of the brain (2006). Oxford University Press. ISBN 0-19-530106-4
[8] A.UlsoyGalip; HueiPeng; MElihCakmakci (2012); Automotive Control Systems"- Cambridge University Press: ISBN:9781107010116
[9] E.S.Lohan and M.Renfors,"On the Performance of Multiplexed- BOC Modulation for future GNSS Signal"- European Wireless Conference-2007, France
[10] Avila-Rodriguez, Issler J L, Irsigler M." A Vision on New Frequencies, Signals and Concept for Future GNSS Systems":, ISBN: GNSS 2007, Texas USA.
[11] Raghavan S H, Holmes J K."Modelling and Simulation of Mixed Modulation formats for improved CDMA Bandwidth Efficiency". ISBN:4290-4295-Vehiular Technology Conference
[12] Magariyama Y, Sugiyama S. Muramota K; Maekawa Y, Kawagishi I. (1994)-"Very Fast Flagellor Rotation".
[13] KAseem N, Microsoft Corp, VRF-Based Vehicle Detection and Speed Estimation Vehicular Technology. IEEE (2012).
[14] PL Nunez- Neocortical Dynamics and Human EEG Rhythms- Oxford University, Newyork-1995
[15] Arelene Ducao, MIT has designed a prototype model- helmet that can read the brain waves to determine the mind of the cyclist.
[16] Joel Murphy and Conor Russomanno's design comprises both hardware and software toolkits thus eliminating long lines of codes.
[17] Ankita Mishra and Pranav paranjpe- "RF based speed control system for cars".
[18] Documents and Hardware descriptions collected from www.openbci.com
[19] [10]Assessment research study- Margot Anderson Brain Restoration Foundation
[20] [11] http://www.mc.uky.edu/neurobiology
[21] http://openbci.myshoify.com/collections/frontpage/products
[22] http://hyperphysics.phy-astr.gsu.edu/
[23] http://www.mc.uky.edu/neurobiology
[24] www.openbci.com

Cite this article as: Sibu C M, S.Preethi, Bharath Kumar M R, K S Pradeesh, S Pragaspathy. "Design of Artificial Intelligence Based Speed Control, Automation & Braking System For Cars Using Open Source Brain-Computer Interface Technology". *International Conference on Innovative Trends in Electronics Communication and Applications (2015)*: 179-188. Print.

International Conference on Innovative Trends in Electronics Communication and Applications 2015 [ICIECA 2015]

ISBN	978-81-929742-6-2
Website	icieca.in
Received	02 - April - 2015
Article ID	ICIECA027

VOL	01
eMail	icieca@asdf.res.in
Accepted	15 - November - 2015
eAID	ICIECA.2015.027

A Review on Novel Design Method for Compact UWB Bandpass Filters

Long CAI[1], Kokula Krishna Hari K[2], Prithiv Rajan S[3]

[1]Research Scholar, HKUST, [2]Secretary General, ASDF, [3]Global President, Techno Forum Group

Abstract: *This paper presents a brief review of Ultra wide band (UWB) Bandpass filter (BPF) using multiple mode resonator (MMR).The Bandpass filters are designed for the frequency range of 3.1-10.6 GHz. The brief history of the multiple mode resonators and the evolution of the filter by adding different techniques to enhance the filter performance and also the techniques which are used for miniaturization of the filter size are studied. With the help of these techniques the performance and size have increased and decreased resp. The outputs of various filters are compared with each other for proper analysis of the filter design to study the limitations of the previously proposed techniques.*

Keywords: Bandpass filter (BPF), multiple-mode resonator (MMR, stepped impedance stub load resonator (SISLR, ultra wideband (UWB)

INTRODUCTION

SINCE the Federal Communications Committee (FCC) authorized the unlicensed use of the ultra-wideband (UWB) frequency spectrum for short-range and high-speed wireless communication in 2002, tremendous interests in both academic and industrial fields have been attracted to explore various UWB devices, antennas, and systems. To meet the required UWB frequency mask (3.1 to 10.6 GHz), it has been commonly recognized that UWB Bandpass filters (BPFs) with good in-band transmission and out-of-band rejection performances are highly demanded. So far, several prototype UWB filters have been reportedly developed based on varied principles, such as dual-stopband features , composite lowpass-Highpass filter topology , cascaded broad- side-coupled structure and resonance characteristics of Stepped-impedance multiple-mode resonator (MMR).

In a filter with tightened coupling extent via a three-line coupling section originally showed its capacity in realizing a wide passband of 40% to 70%. A wideband passband of 49.3% was achieved in terms of two Stopbands of a filter block with the two tuning stubs on a ring resonator. However, this filter configuration was found theoretically difficult to be directly employed for the design of such a UWB filter with a bandwidth of about 110.0%.UWB passband. A Microstrip ring filter with the dual Stopbands below 3.1 GHz and above 10.6 GHz was constructed to make up the most initial UWB filter. However, this filter in fact has many problematic issues, such as unexpected Passband below 3.1 GHz, narrow lower/upper Stopbands, and large size.

Cite this article as: Long CAI, Kokula Krishna Hari K, Prithiv Rajan S. "A Review on Novel Design Method for Compact UWB Bandpass Filters". *International Conference on Innovative Trends in Electronics Communication and Applications (2015)*: 189-196. Print.

It was initially exhibited in that the first two resonant modes of the constituted MMR could be utilized together with the input/output parallel-coupled lines to achieve a 70% wide passband with four transmission poles. The first three resonant modes of an improved MMR were newly constructed to realize five transmission poles with lowered return loss in the whole passband. Then, an improved Microstrip line UWB BPF was presented by forming an alternative MMR with proper loading of three open-ended stubs. The open-ended stubs are introduced at the center of a stepped-impedance resonator to allocate the first two resonant modes more closely with each other. By feeding this resonator with two parallel-coupled lines at two sides, a class of wideband filters with a fractional bandwidth of 60% to 80% were constructed. Open ended stub, placed at center, to a great extent. However, with the use of only a single loaded stub or paired stubs at the central position, these filters have been found to hardly achieve the FCC defined UWB passband with a fractional bandwidth of 110% at 6.85 GHz. Following this work, two identical stubs were in addition introduced at the two symmetrical positions with respect to the central plane. It provided us with an additional degree of freedom to relocate the first four resonant modes within the UWB band while pushing up fifth mode, aiming at achieving sharpened out-of-band rejection skirts and widened upper stopband. All the above mentioned SIR-type UWB BPFs showed good passband performance except the Stopbands suffer the slow increase in attenuation and there were no longer enough degrees of freedom for effective control of resonant frequencies and also suffered from large size. Then the MMR increasing the degree of freedom and miniaturizing the size of the filter were developed in [4], [5].

DIFFERENT DESIGN TECHNIQUES FOR DESIGNING UWB BANDPASS FILTER USING MMR.

In [1], the initially proposed UWB Bandpass filter using a Microstrip line multiple-mode resonator (MMR) was presented. Here the MMR has been properly modified in configuration so as to reallocate its first three resonant modes close to lower-end, center, and upper-end of the targeted UWB passband. Also, the coupling degree of the input/output parallel-coupled line sections is largely raised. At the central frequency of the UWB passband, i.e., 6.85 GHz, the MMR consists of one half-wavelength low-impedance line section in the center and two identical $\lambda/4$ high-impedance line sections at the two sides.

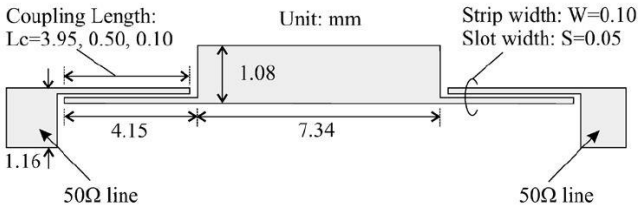

Fig. 1. Schematic of the compact Microstrip-line UWB Bandpass filter

With respect to the configuration, the proposed MMR was categorized as a so-called stepped-impedance resonator (SIR). As a non-uniform transmission line resonator, the SIR was proposed in to enlarge the frequency spacing between the first and second-order resonant modes so as to effectively widen the upper stopband above the dominant passband of a Bandpass filter. Here, all the first three resonant modes are taken into account together and they are applied to make up a wide dominant passband. In this case, the first and third-order resonant frequencies basically determine the lower and upper cutoff frequencies of a wide passband. Further the two additional transmission poles in the $\lambda/4$ parallel-coupled lines, a UWB filter can be built up with good insertion and return loss in the entire passband of concern.

Then in [2], the Microstrip line stepped impedance stub loaded MMR was proposed. As discussed in [1], the first three resonant modes in the stepped-impedance MMR can be quasi-equally allocated within the concerned UWB passband by adjusting width/length ratios of central-to-side sections. However, this MMR-based filter usually suffers from a high insertion loss of about 2.0 dB in the upper UWB passband and a narrow upper stopband of 11.0 to 14.0 GHz. The former is mainly caused by parasitic radiation from the central part with wide strip conductor at high frequencies, while the latter is due to the 4th resonant mode in this stepped-impedance MMR.

Cite this article as: Long CAI, Kokula Krishna Hari K, Prithiv Rajan S. "A Review on Novel Design Method for Compact UWB Bandpass Filters". *International Conference on Innovative Trends in Electronics Communication and Applications (2015)*: 189-196. Print.

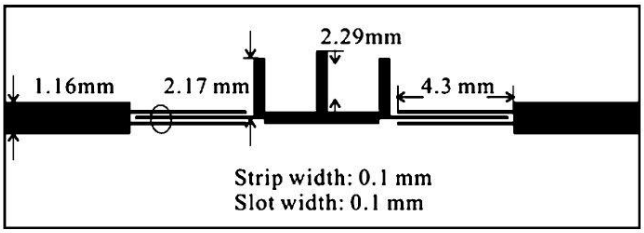

Fig no 2 Configuration of the proposed UWB BPF based on stub-loaded MMR in ref [2].

As shown in Fig.2, the proposed stub-loaded MMR is formed by properly attaching one single open-ended stub in the middle and two identical ones in the two symmetrical positions. The lengths of the central stub and side stubs are indicated by Lc and Ls, respectively. In this way, the first four resonant modes expect to be relocated within the UWB passband while pushing up the fifth mode to make up a wide upper stopband.

Now the novel stepped impedance stub loaded resonator (SISLR) was proposed in [3] to design UWB BPF. The previously mentioned SIR type UWB BPF showed good performance in passband except the Stopbands suffer the slow increase in attenuation and there were no longer enough degree of freedom for effective control of resonant frequencies.

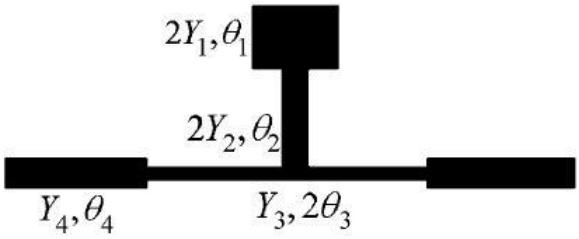

Fig no 3 Basic structure of SISLR in ref [3]

This resonator has more degrees of adjusting freedom to control its resonant frequencies, which results in conveniently relocating the required resonant modes within the UWB band. The basic structure of the proposed SISLR is shown in Fig no 3.It consists of a traditional SIR with the characteristic admittance, and electrical lengths and, which is tapped-connected to a stepped-impedance stub (SIS) in the center. The SIS is also made of transmission-line sections of characteristic admittance, and electrical length. Since the SISLR is symmetrical in structure, odd- and even-mode analysis can be adopted to characterize it.

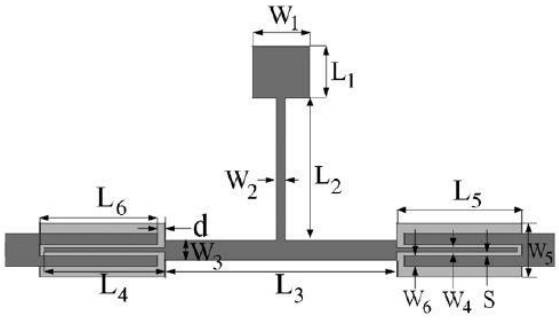

Fig no 3: Configuration of the UWB SISLR in ref [3]

Compared with the conventional multi-mode resonator in [1], this filter design had an extra stepped-impedance stub loaded in the center. The performance of the filter was good but was large in size.

Cite this article as: Long CAI, Kokula Krishna Hari K, Prithiv Rajan S. "A Review on Novel Design Method for Compact UWB Bandpass Filters". *International Conference on Innovative Trends in Electronics Communication and Applications (2015)*: 189-196. Print.

Now the filter size miniaturization was the major challenge faced by the design engineers so the Novel UWB Bandpass filter using stub load multiple mode resonator was proposed in [4] .this paper has the filter size less as compared to the filter proposed in ref [3]. This filter used a uniform impedance resonator and consisted of the SIS at the center and two extra added open stubs at the side of the center stub placed symmetrically around the center. The MMR consists of three open stubs in a uniform impedance resonator, and five modes, including two odd modes and three even modes within the desired band are combined to realize UWB passband.

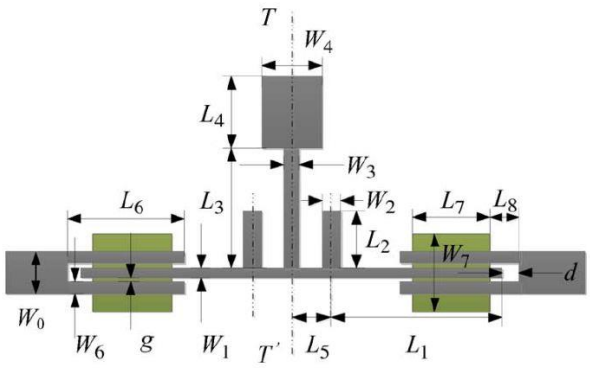

Fig no 4 - Structure of the SISLR in ref [4].

There are five modes, including two odd modes and three even modes within the desired band, and two transmission zeros generated by the stepped-impedance stub are at the lower and upper cutoff frequencies. The two odd modes could be located within the UWB band by properly designing the horizontal uniform-impedance resonator and the two side stubs. Otherwise, the even modes could be flexibly tuned by the stepped-impedance stub while the odd modes are fixed.

In this design method mentioned in ref [5], the size of the filter is further reduced improving the performance of the filter in the passband as well as in stopband.

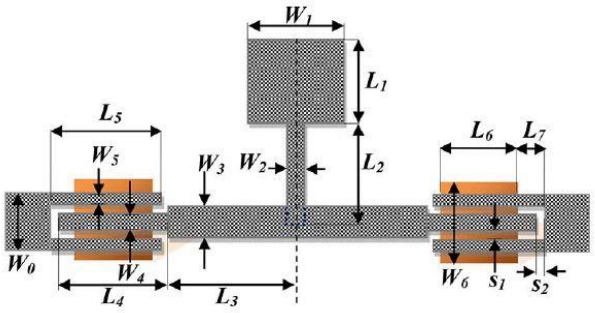

Fig no 5 UWB Bandpass filter in ref [5]

The size of the filter is further reduced as compared to the filter designed in ref [4]. Also the technique uses only a single SIS connected at the center of the uniform impedance transmission line and an aperture-backed beneath three inter-digital parallel coupled lines at connected at each side of the filter for coupling enhancement. The adopted method leads to a simplified objective function with a minimum number of variables to avoid convergence and implementation problems.

COMPARATIVE PERFORMANCE ANALYSIS OF VARIOUS UWB BANDPASS FILTER

In the ref [1], the structure of the filter is shown in the figure no 1 the performance obtained good as compared to the previously designed filters without MMR. The MMR design had good performance in the passband but slow attenuation in the stop band. The figure no 6 shows the varying effect of the length of parallel coupled line on the gain and the insertion loss varied with frequency. The attenuation obtained is about -30 dB at 1 GHz and less than 30 till 13 GHz from the upper cutoff frequency.

Cite this article as: Long CAI, Kokula Krishna Hari K, Prithiv Rajan S. "A Review on Novel Design Method for Compact UWB Bandpass Filters". *International Conference on Innovative Trends in Electronics Communication and Applications (2015)*: 189-196. Print.

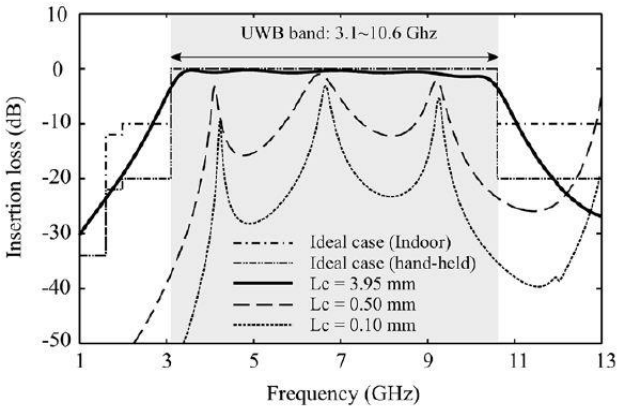

Fig. 6. Insertion loss of the Microstrip-line UWB Bandpass filter with different parallel Coupled line lengths (Lc).

The figure no 6 shows the varying effect of the length of parallel coupled line on the gain and the insertion loss varied with frequency. The attenuation obtained is about -30 dB at 1 GHz and less than 30 till 13 GHz from the upper cutoff frequency. The slope or the roll off of the filter is less so the transition band is more. The filter is fabricated and measured using the substrate dielectric of ε_r=10.8 and height =1.27mm. In the measurement, the lower and higher cutoff frequencies of the fabricated filter are equal to 2.96 GHz and 10.67 GHz. This shows that the relevant fractional bandwidth achieved is about 113%. At the central frequency of 6.85 GHz, the measured insertion loss is found as 0.55 dB. The fabricated and the simulated results are in the good agreement with each other.

The performance of the filter designed in ref [2] is comparatively better as compared to the ref [1]. The filter designed as shown in fig no 2 is fabricated using the substrate RogersRT/Duriod 6010 with the relative permittivity ε_r= 10.8 and the substrate thickness h=1.27. The tool used here for simulation is the Agilent Momentum software and the fabricated filter is measured with universal test fixture and Agilent network analyzer.

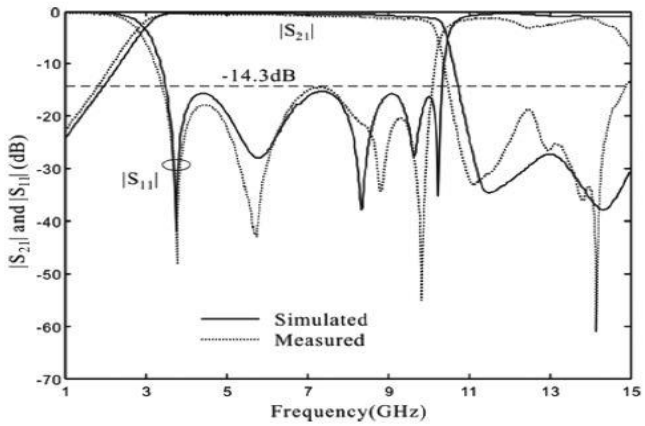

Fig. 7- Simulated and measured frequency responses of the optimized UWB BPF in ref [2]

Here compared to the initially designed UWB filter in ref [1] the insertion loss is more that is that is -23 dB at 1 GHz where as in ref [1] it is -30 dB. The performance of the filter is increased by increasing the roll off in the upper cutoff frequency i.e. we can observe the attenuation of -35 degree at 11.5GHz in ref[1] the attenuation is -25 dB at 13 GHz. The size of the filter is also reduced in this design to 13.80mm from 15.64mm from design shown in ref [1]. This designed helped to increase the roll-off and also to reduce the size of the filter.

The filter designed in ref [3] as shown in the figure 3 the filter performance is the best compared to the earlier designs. Two transmission zeros at the edge of both the passband results in the sharper roll-off as compared to the ref [2]. The selectivity factor

Cite this article as: Long CAI, Kokula Krishna Hari K, Prithiv Rajan S. "A Review on Novel Design Method for Compact UWB Bandpass Filters". *International Conference on Innovative Trends in Electronics Communication and Applications (2015)*: 189-196. Print.

of this design is more as compared to the previous designs in ref [1] and [2].compared to the conventional multimode resonator MMR in ref [1] the substrate used in this design has a dielectric constant of $\varepsilon_r = 2.55$ and the substrate thickness as h= 0.8mm.

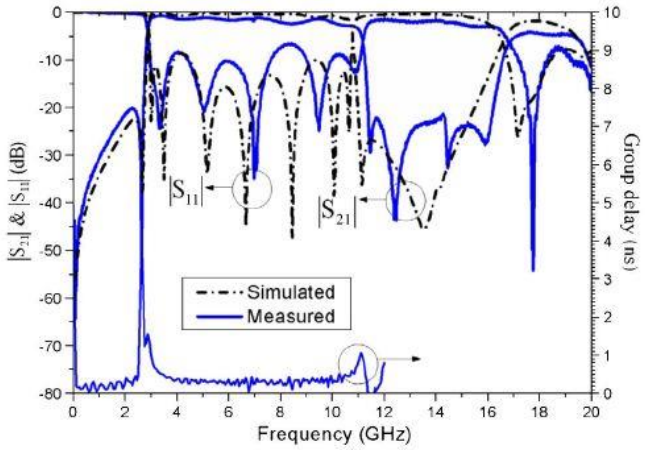

Fig. 8. Simulated and measured results of proposed UWB BPF in ref [3].

The measured passband of the measured filter is from 2.90 to 10.90 GHz against the simulated frequency range of passband as 2.92 to 10.72 GHz. The measured return loss is lower than -10 dB for most of the passband of the filter. The major drawback of the design was its large size. The filter designed by this techniques has the best performance compared to the ref [1],[2] but also had the largest size of 24.14 mm as compared with the size of 15.64 in ref [1] and 13.80 mm in ref [2].

The filter structure shown in fig 4 shows the filter design of ref [4] the filter has two extra open stubs in the designs as compared to the ref [3] design structure. The filter is fabricated and simulated using the substrate dielectric constant as er=2.55 and substrate thickness of h=0.8 mm. This filter design has the same filter performance as compared to ref [3] but has the reduction in size of about 33.6 %. The size of the filter structure in ref [3] was 24.14 mm and that of this filter is 16.1 mm. The simulated and the measured results are in the good agreement with each other. The passband covered is from the frequency range of 3.1 - 11.1 GHz which 117 % which is more than in the ref [3] which has fractional bandwidth of 114 %. The measured return loss is less than -10 dB for most part of the passband. The attenuation of the upper stopband is less than -20 dB up-to 17GHz which means the design has an extended stopband as compared to the design results of ref [3]. The selectivity factor of ref [3] is 0.926 and that of this design is 0.921 which means they have the same performance.

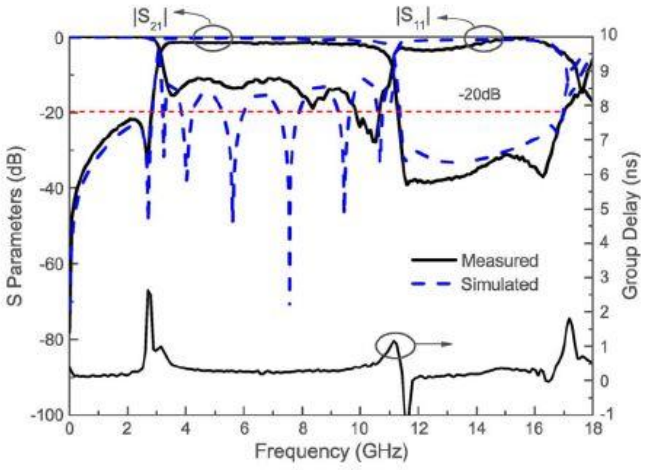

Fig. 9. Simulated and measured frequency responses of fabricated UWB BPF.

Cite this article as: Long CAI, Kokula Krishna Hari K, Prithiv Rajan S. "A Review on Novel Design Method for Compact UWB Bandpass Filters". *International Conference on Innovative Trends in Electronics Communication and Applications (2015)*: 189-196. Print.

In ref [5] design structure shown in fig 5 the filter is simulated using the momentum simulation software and the filter used RT Duriod 5870 substrate having the relative dielectric constant of ε_r=2.33 and substrate height of h= 0.5 mm. The substrates used in the ref [3] and [4] used the substrate having ε_r=2.55 and the substrate height of h= 0.8 mm.

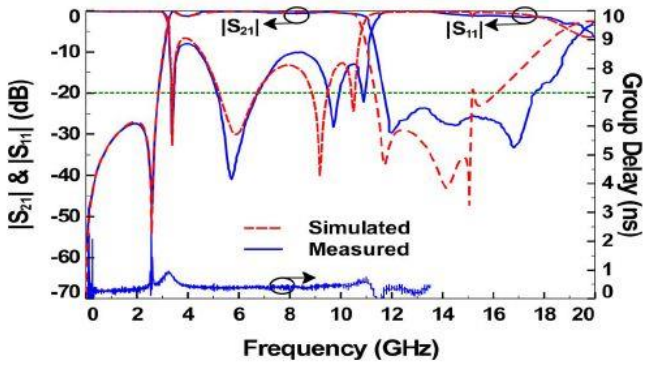

Fig. 10. Measured and simulated results of the UWB BPF in ref [5].

The measured passband extents from 3.2 to 11.1 GHz covering a fractional bandwidth of 115 % as compared to 117 % of that of the filter designed in the ref [4]. In addition to good performance of the filter the filter design has the least size amongst all the filter designed earlier. This design has the filter size of 11.72 mm as compared to the filters having size 15.64 mm, 13.80 mm, 24.14 mm and 16 mm in the ref [1], [2], [3] and [4] respectively. The filter has the size reduction of 54.12 % and 27 % compared to the ref [3] and [4]. This design focuses on the compactness and the good performance of the filter.

TABLE I

Reference	Dielectric	S.F	-3 dB FBW	Size in $\lambda_0 \times \lambda_0$	Size in (mm)
[1]	10.8/1.27	0.642	116 %	0.371× 0. 043	15.64
[2]	10.8/1.27	0.594	114 %	0.315×0.061	13.80
[3]	2.55/0.8	0.926	114 %	0.73×0.35	24.14
[4]	2.55/0.8	0.921	117%	0.514×0.312	16.1
[5]	2.33/0.5	0.861	115 %	0.382×0.307	11.72

λ_0 is the free space wavelength at 6.85 GHz. The selectivity factor or skirt factor ref [4] is defined by the ratio $\Delta f|_{-3dB}/\Delta f|_{-30dB}$ at -3 dB and -30 dB of bandwidth of filter.

CONCLUSION

The various design structures using the MMR for the design of UWB BPF are discussed in this paper. The comparative analysis of the various structures and their respective outputs are done. The filters from the conventional MMR to the latest MMR developed recently are seen and their comparison table is carried out to study the various advantages and limitations of the design. The paper properly explains about the evolution of the MMR in UWB BPF and its benefits in terms of performance and the size of the filter. The study has revealed that the design developed in the ref [5] is the best design in terms of the performance and size of the filter compared to the various other designs developed earlier. The design has good performance in the passband as well as an extended stopband till 18 GHz after the upper cutoff frequency also the filter is very compact i.e. 11.72 mm in size.

REFERENCES

[1] L. Zhu, S. Sun, and W. Menzel, "Ultra-wideband (UWB) Bandpass filters using multiple-mode resonator," IEEE Microwave. Wireless Component, Letter, vol. 15, no. 11, pp. 796–798, Nov. 2005.

[2] R. Li and L. Zhu, "Compact UWB Bandpass filter using stub-loaded multiple-mode resonator," IEEE Microwave. Wireless Component. Letter, vol.17, no. 1, pp. 40–42, Jan. 2007.

Cite this article as: Long CAI, Kokula Krishna Hari K, Prithiv Rajan S. "A Review on Novel Design Method for Compact UWB Bandpass Filters". *International Conference on Innovative Trends in Electronics Communication and Applications (2015)*: 189-196. Print.

[3] Q.-X. Chu and X.-K. Tian, "Design of UWB Bandpass filter using stepped-impedance stub-loaded resonator," IEEE Microwave. Wireless, Component. Letter, vol. 20, no. 9, pp. 501–503, Sep. 2010.

[4] Q.-X. Chu, X.-H. Wu, and X.-K. Tian, "Novel UWB Bandpass filterUsing stub-loaded multiple-mode resonator," IEEE Microwave.Wireless Component. Letter, vol. 21, no. 8, pp. 403–405, Aug. 2011.

[5] Abdelkader Taibi, Mohamed Trabelsi, Abdelhalim Slimane, Mohand Tahar Belaroussi, Member, IEEE, and Jean-Pierre Raskin, Fellow, IEEE"A Novel Design Method for Compact UWB Bandpass Filters" IEEE microwave and wireless component letters .2014.

[6] Q. X. Chu and S. T. Li, "Compact UWB Bandpass filter with improved Upper-stopband performance," Electron Letter., vol. 44, no. 12, pp.742–743, Jun. 2008.

[7] B. Y. Yao, Y. G. Zhou, Q. S. Cao, and Y. C. Chen, "Compact UWB Bandpass filter with improved upper-stopband performance," IEEE Microwave. Wireless Component. Letter, vol. 19, no. 1, pp. 27–29, Jan. 2009.

[8] L. Zhu and W. Menzel, "Compact Microtrip Bandpass filter with two transmission zeros using a stub-tapped half-wavelength line resonator," IEEE Microwave. Wireless Component. Letter, vol. 10, no. 1, pp. 16–18, Jan. 2003.

[9] L. Zhu, H. Bu, and K. Wu, "Aperture compensation technique for innovative design of ultra-broadband Microstrip Bandpass filter," in IEEE MTT-S Int. Dig., Jun. 2000, vol. 1, pp. 315–318, vol. 1.

[10] L. Zhu, H. Bu, K. Wu, and M. S. Leong, "Miniaturized multi-pole broad-band Microstrip Bandpass filter: concept and verification," in Proc. 30th Eur. Microwave. Conf., Paris, France, Oct. 2000, vol. 3, pp.334–337.

[11] L. Zhu, H. Bu, and K. Wu, "Broadband and compact multi-pole Microstrip Bandpass filters using ground plane aperture technique," Proc. Inst. Elect. Eng., vol. 147, no. 1, pp. 71–77, 2002.

[12] S. W. Wong and L. Zhu, "Quadruple-mode UWB Bandpass filter with improved out-of-band rejection," IEEE Microwave. Wireless Component. Letter, vol. 19, no. 3, pp. 152–154, Mar. 2009.

[13] H. W. Deng, Y. J. Zhao, L. Zhang, X. S. Zhang, and S. P. Gao "Compact quintuple-mode stub-loaded resonator and UWB filter," IEEE Microwave. Wireless Component. Letter, vol. 20, no. 8, pp. 438–440, Aug. 2010.

[14] M. Z. Ji and Q. X. Chu, "Compact UWB Bandpass filter using pseudo Inter-digital stepped-impedance resonators," in Proc.China Micro. Millimeter-Wave Conf., Ningbo, China, Oct. 2007, pp. 1096–1098.

[15] J.-S. Hong and M. J. Lancaster, "Chapter 10 advanced RF/microwave filters," in Microwave Filters for RF/Microwave Applications. New York: Wiley, 2001.

Cite this article as: Long CAI, Kokula Krishna Hari K, Prithiv Rajan S. "A Review on Novel Design Method for Compact UWB Bandpass Filters". *International Conference on Innovative Trends in Electronics Communication and Applications (2015)*: 189-196. Print.